Development of the visual pathway in Xenopus laevis (Daudin)

Bertram P. Payne

Development of the visual pathway in Xenopus laevis (Daudin)

by

Bertram P. PAYNE, B.Sc. (Dunelm)

Being a thesis submitted for the degree of Doctor of Philosophy of the University of Durham, December 1977

University College
University of Durham

ACKNOWLEDGEMENTS

I would like to thank Mr. D. Hyde for his supervision during the course of the work produced in this thesis and I am grateful for his critical reading of the manuscript. I would like to thank Professor D. Barker for making the facilities of the Department of Zoology available to me and the Science Research Council for the tenure of a research grant.

I am indebted to Helen Pearson for her constant encouragement and unfailing support during the period of these studies and for making this thesis possible. This thesis is dedicated to her.

CONTENTS

ABSTRACT

Aspects of the development and distribution of the primary retinal afferent projection to the contralateral optic tectum were studied by light microscopy, electron microscopy, and microelectrode recording from adult and tadpole optic nerves and optic tecta of the toad Xenopus laevis (Daudin). The adult tectum was found to be innervated by four populations of optic nerve afferents with different conduction velocities and retinal receptive field properties. Current source density analysis of the postsynaptic potentials recorded extracellularly from tectal cell populations revealed the spatial distribution of optic nerve afferent synapses. The dendrites of cells that constitute tectal cell layer 8 were found to receive the majority of retinal afferent fibre input. The earliest time at which ganglion cell terminal activity was recorded in the tectum was tadpole Stage 46, at which time the optic nerve was entirely composed of unmyelinated fibres. The excitatory receptive fields of these units were large, and these units were easily habituated. Stage 46 was also the earliest time at which postsynaptic field potentials ('u' waves) could be recorded in the tectum and synapses observed morphologically. Evoked potentials ('m' waves), characteristic of a myelinated fibre

innervation of the tectum, were first seen at tadpole Stage 59, as was the appearance and development of optic nerve myelination. No obvious correlations, other than the division of optic nerve axons into myelinated and unmyelinated fibre populations, could be made between optic nerve fibre conduction velocity groups and fibre diameter histograms. However, an obvious correlation between optic nerve conduction velocity groups and postsynaptic field potentials recorded in the tectum was observed. In addition, a clear correlation was discovered between the distributions of the current sinks of postsynaptic activity and the location of recording sites of ganglion cell axon terminals having known receptive field properties. A gradual emergence of the adult pattern of tectal innervation by optic nerve afferents, during the time at which the tadpole undergoes metamorphosis, was observed.

INTRODUCTION

GENERAL INTRODUCTION

The retinotectal pathway in adult amphibians has received much interest in recent years, from both a physiological and a morphological viewpoint. The responses of frog retinal ganglion cells were first investigated by Hartline (1938, 1940 a, b) and Barlow (1953). Responses to visual stimuli were recorded from presumed retinal ganglion cell terminals in the optic tectum by Andrew (1955). These ganglion cell terminal responses were characterized into five types, using "natural" visual stimuli (Lettvin et al, 1959, 1961; Maturana et al, 1960). Four of these response types have been reported regularly since, and are represented diagrammatically in figure 4:1. Numerous physiological studies have been carried out on the retinotectal visual system in anurans (reviewed by Grüsser and Grüsser-Cornehls, 1976). The responses of tectal neurons have also been recorded (Lettvin et al, 1959; Fite, 1969; Ewert and Borchers, 1971; Ewert and von Wietersheim, 1974 b, c; Ewert et al, 1974; Grüsser and Grüsser-Cornehls, 1976), as have responses from the caudal

thalamus (Ewert, 1971; Brown, 1973; Brown and Ingle, 1973) and from the anterior thalamus (Muntz, 1962; Keating and Kennard, 1976; Kicliter and Chino, 1976; Fite et al, 1977).

These locations of the recordings of visual stimuli correspond to the locations of the primary projections of retinal ganglion cells (Knapp et al, 1965).

The structure of the optic tectum was first studied over eighty years ago by Ramon (1890) and later by Wlassak (1893), Gaupp (1899), Herrick (1925) and Larsell (1931). The rapidly accumulating data from recent physiological studies, however, demands a better understanding of the structure of the optic centres.

Orthograde degeneration and the transport of radioactive tracers and horseradish peroxidase indicate that there are six primary projection areas of the retinal ganglion cells (Knapp et al, 1965; Scalia et al, 1968; Lázár and Székely, 1969; Scalia and Gregory, 1970; Scalia, 1973; Scalia and Colman, 1974); bilaterally to the "nucleus" of Bellonci, the "corpus" geniculatum thalamicum and the posterior thalamic "nucleus", and contralaterally to the pretectal nucleus, the basal optic nucleus and the optic tectum. These projections have been shown morphologically to be organized retinotopically (Lázár, 1971; Scalia and Fite, 1974). However, recent evidence (Neary, 1976), from autoradiographic tracing methods, suggests that a

direct ipsilateral retinotectal pathway exists in Bombina, Xenopus, Rana and Bufo. Picouet and Clairambault (1976) obtained evidence for an ipsilateral pathway in Discoglossus. More recently, Gaillard and Galand (1977) believe that they have recorded responses from the terminals of this direct ipsilateral retinotectal projection in Rana.

Lettvin et al (1959) presented evidence to indicate that the terminals of the five types of retinal ganglion responses were located in four distinct layers in the tectum. Ewert and von Wietersheim (1974) have obtained results in the toad Bufo bufo which correlate the location of the three classes of ganglion cell terminals with three layers of degeneration in the optic tectum following the nucleation. Similar studies in frogs attempting to correlate the layering of the classes of ganglion orthograde transported materials have not been so successful (see Scalia, 1976, for review).

The retinotectal pathway of amphibia has been studied for over thirty years. This work has been of interest to neuroembryologists concerned mainly with the formation of neuronal connexions. It is only in recent years that these problems have come to occupy a central position in neurobiology. Since the field was reviewed by Gaze (1970) and Jacobson (1970) there have been a plethora of new experiments reported. These studies have largely been on the development of the surgically manipulated visual system

of Xenopus. This non-normal development has been studied to elucidate the phenomenon and mechanisms of neuronal specificity (Straznicky, Gaze and Keating, 1971, 1974; Hunt and Jacobson, 1972 a, b, 1973 a, b, 1974 a, b; Straznicky, 1973, 1976; Feldman and Gaze, 1975; Berman and Hunt, 1975; Hunt, 1975 a, b; Hunt and Berman, 1975).

The effects of visual experience on development have also been investigated in Xenopus (Feldman et al, 1971; Keating, 1974, 1975 a, b, 1977; Keating and Feldman, 1975; Keating et al, 1975) and in Rana (Jacobson, 1971; Hirsch and Jacobson, 1973; Jacobson and Hirsch, 1973; Skarf, 1973; Skarf and Jacobson, 1974). These experiments have dealt with the abnormal development of the system produced by surgical intervention or under conditions of abnormal visual experience. Considering the ease of access to the developing visual system in amphibian tadpoles, it is surprising that the normal morphogenesis and physiogenesis has not been examined in greater detail.

A number of studies have been carried out on the normal morphological development of the retinotectal visual system in Xenopus (Jacobson, 1968 a, b, 1976; Hollyfield, 1971; Straznicky and Gaze, 1971, 1972; Lázár 1973; Fisher, 1976; Scott and Lázár, 1976; Straznicky and Tay, 1977) and in Rana (Hollyfield, 1968; Fisher, 1972; Currie, 1974; Currie and Cowan 1974 a, b, 1975).

Fig. 1 Coronal section of Xenopus midbrain

(a) Outline to show that the tectum (T) forms the roof to the midbrain. The ventricle (Vent) has outpushings which form a non-neuronal space below the tectum. The area in the rectangle is shown in more detail in (b). Calibration bar is as indicated.

(b) Light micrograph to show the thickness (350 μm) and lamination of the tectum, the numbering of these layers is indicated on the left. Layer 1 contains ependymoglial elements which ascend to the surface. Layers 2, 4 and 6 are cellular laminae which are not well delimited from the intermediate plexiform layers 3 and 5. Layer 6 contains the most number of neurons of any lamina. Note the 4 large neurons situated in layers 3-5 (V), these form part of the mesencephalic nucleus of the trigeminal nerve. Layer 7 contains the efferent fibres of the tectum and occasional neurons and is 50 μm thick. Layer 8 is a band of cells which separates layer 7 from layer 9. Layer 9 is the main recipient area of optic afferents, and is 100 μm thick. Dendrites of most cells in the tectum ascend to layer 9. Calibration bar is as indicated.

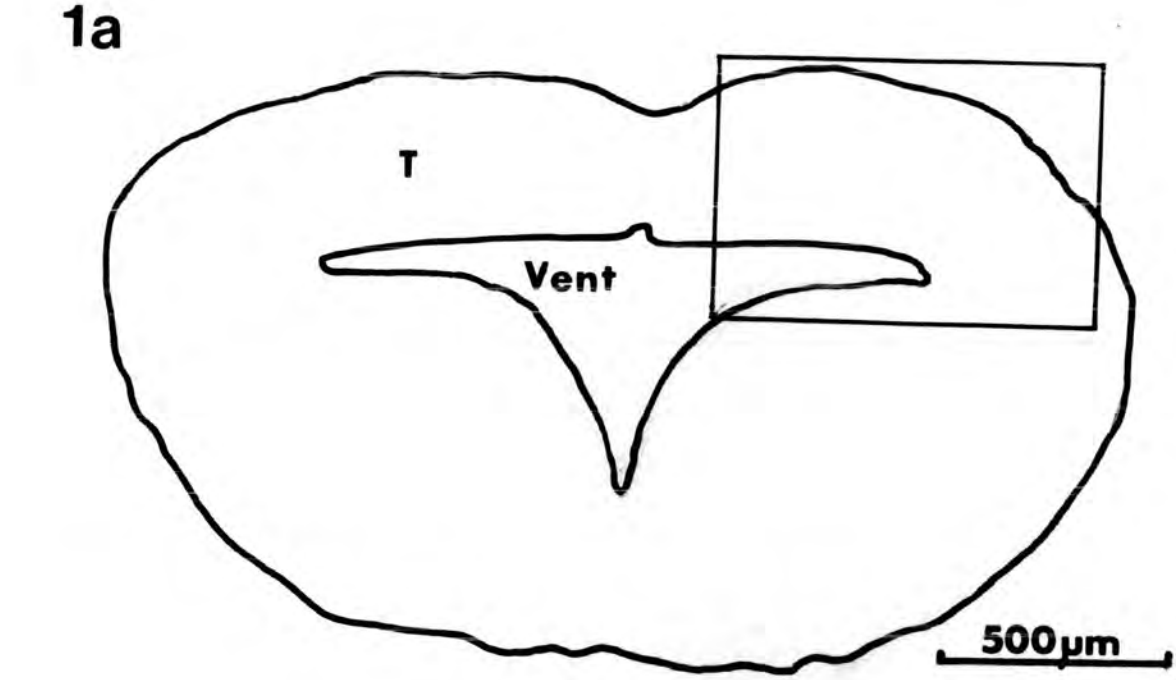
1a
T
Vent
500µm

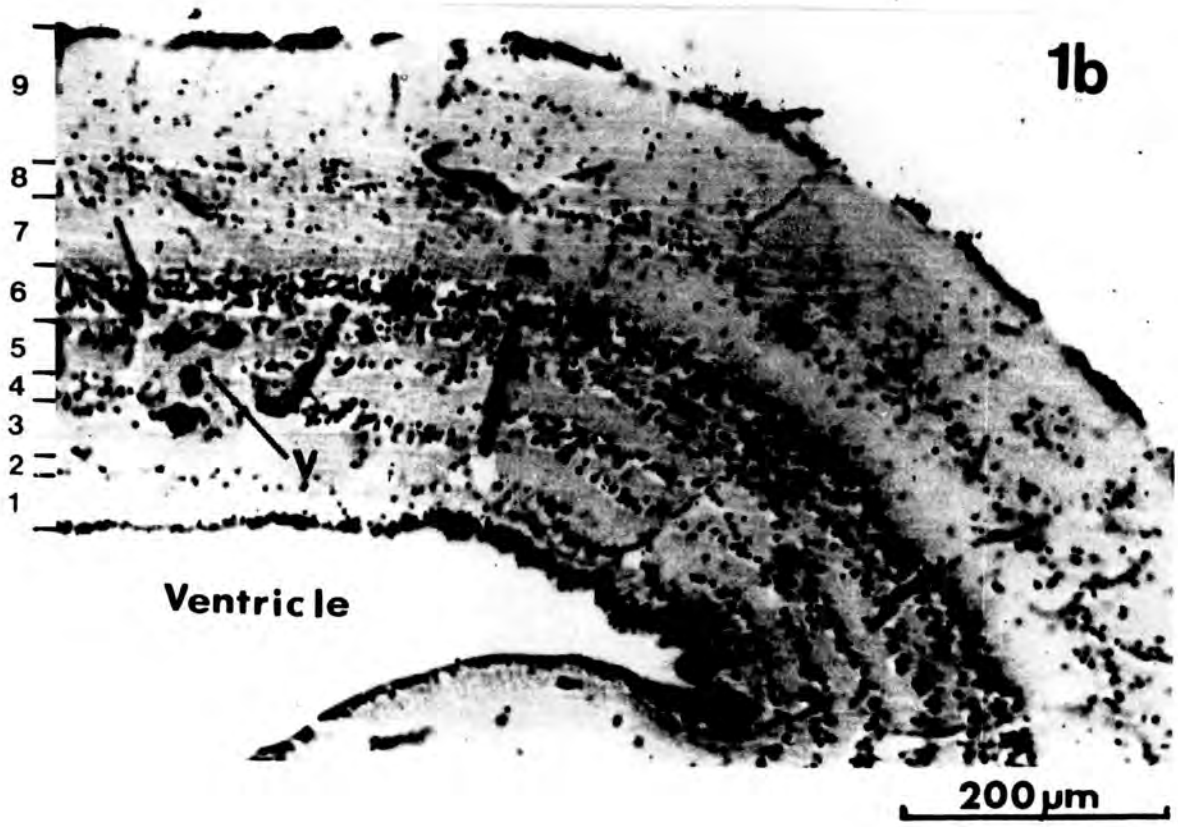
1b
9
8
7
6
5
4
3
2
1
Ventricle
200µm

The optic tectum is a prominent feature of the adult Xenopus brain when viewed from the dorsal aspect. In low power coronal sections, the optic tectum forms the roof to the mesencephalon, with ventricular outpushings (fig. 1 a). The tectal roof is thin (350 μm) and is not as well laminated as the thicker (600 - 700 μm) tectum of the frog (Székely and Lázár, 1976). Nine alternating cellular and plexiform laminae are present and are described as follows using the terminology of Székely (1973).

The ventricle is bordered by ependymoglial cells which constitute layer 1. The cells are the supporting elements of the neurons in the optic tectum. They have a single main process which reaches to the pia forming the glia limitans. Along the sides of the process are small glial processes which interdigitate with the neuronal elements.

Layers 2, 4 and 6 are cellular layers and constitute the stratum periventriculare. The neurons are compact in the much thicker layer 6, but more dispersed in layers 2 and 4 (Fig. 1 b). The uniformity of layer 6 is interrupted by axonal fibres. At the anterior margin of the tectum, large (15 - 20 μm) unipolar neurons often form groups (fig. 1 b). These neurons belong to the mesencephalic nucleus of the trigeminal nerve.

Layers 3 and 5 are plexiform layers which contain axons and their synapses which terminate on the dendrites of the neurons of the stratum periventriculare. Layer 7,

the stratum album centrale, is a thick (50 μm) plexiform layer which comprises thick myelinated efferent fibres of the tectum and a few scattered neurons. More superficially is layer 8, the stratum album centrale, which consists of loosely packed cells and, in common with the deeper layers of the stratum periventriculare, is not well delimited. The neurons of this layer are somewhat smaller than deep neurons.

Layer 9, the stratum fibrosum et griseum superficiale, is the thickest plexiform layer (100 μm) and occupies about a quarter of the thickness of the tectum. This layer is the main recipient area for retinal afferents, which form synapses principally with ascending apical dendrites of deeper located neurons. Amacrine and stellate cells are intermingled with the axons and dendrites of this layer.

Potter (1972) has been able to discern four sub-layers of afferent fibres in layer 9 of the optic tectum of Rana catesbeiana and a fifth fibrous layer immediately below the neuronal somata of layer 8. Laminae such as these are not discernable in the tectum of Xenopus, nor is a stratum zonale.

Golgi impregnation methods are useful for determining the morphology of neurons. In such studies the cells in the Xenopus optic tectum can be seen to be similar to those in the optic tectum of the frog. Larger neurons are located in the stratum periventriculare. The form of the dendrites of the majority of tectal cells is a single apical process

which divides near the end to form a number of branches, or they may branch once or extensively prior to reaching layer 9 having the form of candelabra cells described by Potter (1969). Cells of layer 8 have single or multiple radially oriented dendrites. Within layer 8, the upper part of layer 6 and scattered in layer 7 are the large ganglionic neurons (Székely and Lázár, 1976). The scattered neurons in layer 9 are amacrine and stellate cells. (Full details of the neuronal types in the frog optic tectum have been reviewed by Székely and Lázár (1976)).

The synaptology of the optic afferent terminals with the tectal neurons in the frog has been reported by Székely et al (1973). The significant features of this work relevant to the study that follows are that optic afferents synapse on to the upper reaches of tectal cell dendrites, their dendritic shafts and the cell bodies of layer 8.

Amphibia are a phylogenetically older vertebrate group than the primates. The brain is much smaller, but the determination of interconnexions of the component neurons is by no means easier. It is of considerable interest how such a complex pattern of elements interconnects so intricately to produce the mature state found in the adult.

The developing visual system in fish has been studied using anatomical techniques (Hollyfield, 1972; Schmatolla, 1972; Schmatolla and Fischer, 1972; Schmatolla and Erdman, 1973; Kennedy and Rubinson, 1977) but there does not appear to have been any comparable physiological work carried out.

To my knowledge no reports have been published on either the morphological or physiological development of the visual system in reptiles.

The morphological development of the chick visual system has been studied extensively by Cowan and his colleagues (LaVail and Cowan, 1971 a, b; Crossland, Cowan and Kelly, 1973; Kahn, 1973, 1974; Crossland, Cowan, Rogers and Kelly, 1974), by De Long and Coulombre (1965) and Cantino and Daneo (1973).

Rager (1976 a, b) has studied the morphological and physiological development of the retinotectal pathway in the chick. Although electrical stimuli evoked postsynaptic potentials from day 11 of incubation, visual stimuli could not elicit responses, since this must await the development of the photoreceptor outer segements. These results indicate that the connexions in the visual system are completed prior to the onset of vision, as appears to be the case for mammals.

The morphological development of the visual system in mammals is somewhat easier than the physiology to study since the foetus may be removed from the uterus for histological processing to determine the location and morphology of neurons. The time of origin of neurons may be determined by autoradiography.

A somewhat more complex approach to the study of the developing visual system is to determine the projections of the neurons at a given time. This may be done by various methods, such as degeneration (Fink and Heimer, 1967), orthograde transport of tritiated amino acids and sugars (Cowan et al, 1972) or the retrograde transport of horseradish peroxidase (Graham and Karnovsky, 1966). Lund and Bunt (1976) have carried out experiments on foetal rats to determine the time of innervation and synapse formation in the dorsal lateral geniculate nucleus and in the superior colliculus, using degeneration methods and retrograde horseradish peroxidase transport.

Rakic (1976, 1977) carried out similar experiments in foetal rhesus monkeys to determine the time of origin and the pattern of migration of neurons in the visual system using autoradiographic methods. He also studied the time of innervation of these structures using orthograde transport of labelled amino acids and sugars. However, the properties of the afferent inputs and their connexions cannot be determined since physiological studies are precluded in foetal mammals.

Physiological work of the developing visual systems that has been reported (see reviews by Blakemore (1974) and Barlow (1975)) was prompted largely by the effects of visual deprivation on the visual system of the cat (Hubel and Wiesel, 1963; Wiesel and Hubel, 1963 a, b). Similar studies using visual deprivation have been carried out on rhesus monkeys (Wiesel and Hubel, 1974). However, mammals are highly unsuitable for an investigation into the developing visual system, since physiological recordings cannot be undertaken prenatally.

Amphibians are relatively easy to keep and Xenopus are extremely easy to breed. Their developmental stages are readily available for study. This animal was chosen for these qualities and because the studies on the development of surgically induced abnormalities could not be compared with the normal pattern of development. The mode of life of Xenopus changes at metamorphosis and hence any changes which occur during development are likely to be most evident at this time.

Autoradiographic studies of the time of development of the elements of the retina and tectum have been carried out (Gaze and Straznicky, 1971, 1972; Hollyfield, 1971; Jacobson, 1976). The development of the connexions of the inner plexiform layer of the retina have been studied by Fisher (1976). The morphological development of the optic nerve, the development of the retinotopic innervation of the tectum and the responses of developing

ganglion cells have been reported (Wilson, 1971; Gaze et al, 1974; Chung et al, 1975). One report has appeared on the development of physiological interaction of ganglion cell terminals and tectal cells (Chung, Keating and Bliss, 1974).

The studies reported here are on the morphological development of both glial cells and axons in the optic nerve. The range of conduction velocities of retinal ganglion cell axons were examined and compared with the axon diameter distributions and with the postsynaptic events recorded in the tectum during development. Recordings of responses from retinal ganglion cells to visual stimuli were recorded throughout development and compared with the responses which could be evoked in the adult. Responses to electric stimuli applied to the optic nerve of both adult and tadpole Xenopus were used to determine the properties and location of optic afferent synapses and the location of the postsynaptic neurons in both adult and tadpole optic tectum.

GENERAL METHODS

GENERAL METHODS

A. ANIMAL CARE, BREEDING AND STAGING OF TADPOLES

Mature adult Xenopus laevis (Daudin) were obtained from T. Gerrard and Co., East Preston, Sussex. These animals were caught in the wild and imported from South Africa rather than being bred in the laboratory. They were kept in about 80 litres of water contained in stainless steel tanks which measured 90 x 45 x 60 cm. The tank room was well lit by natural light and heated by convection to $22^{o}C \pm 2^{o}C$.

Breeding

Mature adults were induced to breed by injection of Chorionic gonadotrophin (Billett and Wild, 1975; Nieuwkoop and Faber, 1956; Wilt and Wessells, 1967). The animals were first primed by an injection of 100 i.μ.s. "Chorulon" chorionic gonadotrophin (Intervet Laboratories Ltd.) in 0.5 ml of water for the male and 150 i.μ.s. for the female. Two days later in the evening, supplementary doses were given consisting of 150 i.μ.s. Chorulon for the male and 500 i.μ.s. for the female. The pair was then placed in a plastic tank containing water to a depth of four inches and a few pieces of muslin to which the eggs could adhere. The tank was covered by a lid and placed in a dark, quiet corner of the tank room.

The next morning any eggs which had been produced were transferred to metal framed glass tanks, containing aerated tap water which had been allowed to stand for a few days to dechlorinate. The tanks contained submersible aquarium heaters which maintained the temperature of the water at a minimum of 23°C (Nieuwkoop and Faber, 1956). When the tadpoles hatched, their numbers were regulated to give a density of about two tadpoles per litre. Any infertile eggs were removed. The tadpoles were fed on an unstrained suspension of nettle powder (Nieuwkoop and Faber, 1956) every three days. On the intervening days, any excess food was stirred up from the bottom of the tanks.

These conditions proved adequate for all tadpole stages up to stage 59 (Nieuwkoop and Faber, 1956) after which metamorphosis proceeded rapidly. At stage 59 the tadpoles were transferred to stainless steel tanks which measured 60 x 60 x 30 cm and were half-filled with water. At this time, the tadpoles would no longer eat nettle powder, and were provided with an ample supply of live Tubifex worms.

From the age of two months onwards, the toads were treated in the same way as the adults. They were fed on Heinz strained baby food (Gaze et al, 1974), 'Steak and Kidney dinner' being the most suitable. The toads were found to eat not only pieces of food dropped into the water, but also stationary food on the bottom of the tank. Any excess food remaining after feeding was removed by siphoning.

At six months of age, the toads were transferred to the larger tanks in which the adults were housed.

The water from the tanks containing toads was changed twice a week and all tanks were cleaned thoroughly with hot water and potassium permanganate once a week.

Staging

All tadpoles were staged according to external characteristics (Nieuwkoop and Faber, 1956). The age of toads is given with reference to the last day of metamorphosis (Day 0).

A number of Rana temporaria and R. pipiens were also used. These animals were obtained from the same suppliers, and were maintained at room temperature. All frogs were used within three weeks of purchase.

B. SURGICAL PROCEDURE

One year or older adult Xenopus were anaesthetized either by placing the animal in a closed vessel containing ether, or by an injection of 0.3 mg/gm of an aqueous solution of MS 222 (methane tricaine sulphonate, Sandoz) into the dorsal lymph sac. After the animal had become reflexively immobile for at least two minutes, it was placed on a cork board. A piece of wet Kleenex medical

wipe tissue was draped over all the body except for the head. A small black cardboard cutout was placed over the front of the head, positioned so as to protect the eyes from the bright dissecting light but not to interfere with the region for surgery. The whole operation was carried out with the aid of a Zeiss stereo-dissecting microscope.

A small flap of skin overlying the skull was removed. Any minor bleeding of the cut skin was stopped by squeezing and holding the affected region with forceps for a few seconds. The muscles which are attached to the dorsal and lateral parts of the skull were gently cut from their insertion with a scalpel. The skull of adult Xenopus has two large blood vessels running over the dorsal surface and adequate access to the midbrain could not be achieved unless these vessels were removed. The blood vessels were sutured caudal to the position of the tectum using a 7 mm Vogt Corneal suture needle. The blood vessels and underlying muscles were removed rostral to the suture, to gain access along the whole length of the skull on both sides.

The dorsal surface of the skull was removed by erosion with a Hager and Meisinger 0.5 mm dental burr in order to expose the entire brain.

The Rana species used in this study were prepared in the same manner, except neither blood vessel sutures nor muscle removal was required.

Individuals from two months to one year of age were prepared in the same manner. However, blood vessel sutures were not required since the blood vessels pass on either side of the skull.

Anaesthesia was attained for animals aged between post-metamorphosis and two months of age by placing them either in an ether atmosphere or in a 1 : 1000 (w/v) aqueous solution of MS 222. These animals only required a gentle burring to thin the skull cartilage and a Swan-Morton No. 11 scalpel blade was used to cut through the remainder of the skull.

All tadpoles were anaesthetized by immersion in a 1 : 3000 (w/v) solution of MS 222. They were then partially immersed in Niu-Twitty (1953) solution and the skin and cartilage overlying the brain were incised and removed using insect scissors. From all animals meninges were removed with insect forceps and a sharpened stainless steel needle.

C. HISTOLOGY

Animals were prepared as described in Section B above.

All postmetamorphic toads were decapitated rapidly and the lower jaw was removed. The head was then submerged in 0.9% saline in 10% formalin. Tadpoles were fixed whole.

After one to three days the brains were removed from the skulls of individuals older than two months of age and the tails and lower jaws were removed from the tadpoles. The brains of these animals and toads up to two months of age remained *in situ*. The tissue was left in fixative for up to five days.

The tissue was dehydrated and infiltrated using an automatic tissue processor, as Table I.

Cresyl Violet Staining

The slides were treated according to the following method:

(i) Dewaxed in two changes of xylene for ten minutes each.

(ii) Hydrated to distilled water through a graded series of alcohols (absolute, 95%, 70%) for five minutes each.

(iii) Stained for five to ten minutes in a 0.1% solution of cresyl violet. The duration of the staining was increased for increasing age of the tissue and increasing section thickness.

(iv) Differentiated in 95% alcohol for one to two minutes. The degree of staining was controlled microscopically.

(v) Dehydrated in three changes of absolute alcohol for five minutes each.

TABLE I

(i) 70% alcohol (1½ hours)

(ii) 95% alcohol (1½ hours)

(iii) Absolute alcohol (1½ hours)

(iv) Absolute alcohol (1½ hours)

(v) 50% Absolute alcohol/chloroform (v/v) (1½ hours)

(vi) Chloroform (1½ hours)

(vii) Chloroform (1½ hours)

(viii) Paramat plasticised paraffin wax (Gurr) (2 hours)

(ix) Paraffin wax (2 hours)

After embedding, the tissue blocks were trimmed and sectioned at 10, 15 or 20 μm in the three principal planes on a Spencer A20 microtome. All sections were mounted on acid alcohol cleaned, albumin coated glass slides, and the sections were dried onto the slide overnight in an oven at 37°C.

(vi) Cleared in three changes of xylene.

(vii) Mounted in DePeX (Gurr).

(viii) Placed in an oven at 37°C for five days for the DePeX to harden.

A 0.1% solution of Cresylecht Violet was made up by dissolving one gram of cresylecht violet in one litre of a solution of 0.5 M acetic acid and 0.5 M sodium acetate, which were mixed in the ratio of 18.7 : 1.3. This produced a solution of pH 3.5. Each time, prior to use, five drops of glacial acetic acid were added to the solution. This solution did not appear to deteriorate with time, but it did require filtering occasionally.

Klüver-Barrera Staining

The material was prepared as described in 'B' above and processed as in Table I as far as mounting the sections onto the slides. The slides were then treated according to the following modified Klüver-Barrera (1953) method:

(i) Dewaxed in two changes of xylene for ten minutes each.

(ii) Hydrated through absolute alcohol to 95% alcohol for five minutes each.

(iii) Stained in Luxol fast blue in 95% alcohol, containing 5 ml of 10% acetic acid per litre, for 16 hours at 57°C.

(iv) Washed in 95% alcohol to remove the excess stain.

(v) Hydrated in distilled water for two minutes.

(vi) Differentiated in 0.05% lithium carbonate, until the stain started to be released from the tissue.

(vii) Further differentiated in 70% alcohol. If the results were not satisfactory the tissue was rehydrated in distilled water and the differentiation was repeated until a sharp contrast was obtained between the greenish-blue of the white matter and the colourless grey matter.

(viii) Hydrated in distilled water for three minutes.

(ix) Stained, differentiated, cleared and mounted as described in 'A' above.

The location of cell bodies and the course of axons in the optic tectum have been described extensively elsewhere (Straznicky and Gaze, 1972; Lázár, 1973) for both developmental and mature tissue from normal and experimental animals. The material stained by the methods described above were used mainly for comparison and reference to Golgi impregnated cells and tissue prepared for electron microscopy.

D. GOLGI IMPREGNATION

112 animals were prepared for Golgi staining. 80 were successful, of which 14 were postmetamorphic frogs. Three methods were used to impregnate neurons by the Golgi method. They are described in their order of use.

Both adult and tadpole tissue for impregnation was prepared as described in 'B' above. The material was immersed in a fixative made up of one part 25% glutaraldehyde and four parts 2.5% potassium dichromate (Colonnier, 1964). After overnight fixation the brains were removed and left in fixative for a further six days. The tissue was rinsed in 0.75% silver nitrate solution and immersed in a fresh silver nitrate solution for seven days. Five brains were kept in this solution for one year.

The second method employed the fixative recommended by Valverde (1965; 1970); an aqueous solution of 2.33% (w/w) potassium dichromate and 0.19% (w/w) osmium tetroxide. This solution was made up by dissolving 12 gms of potassium dichromate and one gram of osmium tetroxide in 500 ml of distilled water. The fixative was freshly prepared prior to use.

The brains were exposed as described in 'B' above and immersed in fixative at 0-4^{o}C. The following day, the brains were removed and left in a large excess (at least 50 tissue volumes) of fixative for a further period at room temperature (Morest, 1965). After fixation, the

tissue was rinsed in several changes of 0.75% silver nitrate solution and left in this impregnating solution until it was dehydrated, or transferred back to the same fixative solution in the case of double and triple impregnations.

The duration of each different stage was as suggested by Lázár (personal communication) and is tabulated in Table II.

The third method of Golgi impregnation was based on the above method. However, the tissue was prefixed in 1% glutaraldehyde, 1% paraformaldehyde in 0.12 M phosphate buffer as in Table III.

This fixative was made up as follows:
The distilled water was heated until it steamed but did not boil and the paraformaldehyde was added while the solution was stirred. Solid paraformaldehyde was used to avoid the impurities in commercially available solutions (Peters, 1970). Four to six drops of 1 M sodium hydroxide were added until the solution became clear. It was allowed to cool and then 150 ml of buffer and 20 ml of glutaraldehyde were added. The solution was made up to almost final volume before 2 ml of 0.5% calcium chloride were added. The dilution was completed and the solution was filtered.

The 0.4 M phosphate buffer contained 5.3 gms $NaH_2PO_4.H_2O$ and 28 gms K_2HPO_4 made up to 500 ml with distilled water.

TABLE II

	Impregnation (in days)			
	Single	Double	Triple	
Initial fixation $K_2Cr_2O_7/OsO_4$	6	5	5	1st impregnation
$AgNO_3$	4	1	1	
$K_2Cr_2O_7/OsO_4$	-	4	4	2nd impregnation
$AgNO_3$	-	3	3	
$K_2Cr_2O_7/OsO_4$	-	-	4	3rd impregnation
$AgNO_3$	-	-	3	

TABLE III

Paraformaldehyde	5 gm
Distilled water	200 ml
1 M sodium hydroxide	4-6 drops
25% glutaraldehyde	20 ml
0.4 M phosphate buffer	150 ml
0.5% calcium chloride	2 ml
made up to	500 ml

The brains were exposed as described in 'B' above and were fixed by immersion in a large excess of ice cold 1% glutaraldehyde - 1% paraformaldehyde fixative. The tissue was left in this fixative in a refridgerator overnight. The next morning the brains were removed, except in the smallest tadpoles of stage 50 or younger which were left *in situ*, and the tissue was placed in fresh aldehyde fixative. After a further twelve hours the tissue was transferred to the chromating solution of 2.33% (w/w) potassium chromate and 0.19% (w/w) osmium tetroxide at room temperature. The tissue remained in this solution for varying times depending on whether the tissue was processed according to the single or double impregnation method. Prior to the transfer to 0.75% silver nitrate, the tissue was placed on filter paper to remove any excess dichromate solution. Only two time variants were used for this method and are given in Table IV.

All solutions were in a 50-fold excess of tissue volume.

The material impregnated by all three methods was embedded according to the schedule in Table V.

Sections were cut at 80 μm or 100 μm on a horizontal sliding microtome and were mounted on warm slides using DePeX and coverslips. The slides were left on a hotplate at 60°C for at least two days for the DePeX to harden.

TABLE IV

	Impregnation (days)		
	Single	Double	
Aldehyde fixation	1	1	1st impregnation
$K_2Cr_2O_7/OsO_4$	7	5	
Silver Nitrate	8	1	
$K_2Cr_2O_7/OsO_4$	-	4	2nd impregnation
Silver Nitrate	-	3	

TABLE V

(i) Wash in distilled water for one hour.

(ii) Dehydrate in a graded series of alcohols of 70%, 90%, absolute and absolute for one hour each.

(iii) Transfer to a 50% (v/v) solution of absolute alcohol and propylene oxide for one hour.

(iv) Transfer to propylene oxide for one hour.

(v) Infiltrate with a 50% (v/v) solution of propylene oxide and soft epon overnight at room temperature.

(vi) Infiltrate with soft epon at room temperature for one day.

(vii) Infiltrate further with fresh epon for one day at room temperature. The soft epon is polymerised at 60°C for two days.

The soft epon is prepared from the following by volume:

Dodecasuccinic anhydride (DDSA)	22 parts
Epon 812	13 parts
DMP 30 catalyst	0.7 parts

Each is warmed at 60°C for five minutes prior to measuring to facilitate mixing.

Cells were drawn with the aid of a Zeiss drawing tube on a Zeiss GFL microscope, and linear dimensions were calibrated with a micrometer slide. The final magnification of the drawings was x 1018.

Photographs of Golgi impregnated cells were taken on a Zeiss Ultraphot II microscope using 35 mm Kodak-Panatomic-x film at magnifications ranging from x 16 to x 250.

The details of impregnated cells often extended through several planes of focus, and therefore it was often necessary to compose a single montage from several photomicrographs taken at different focal levels. To facilitate this films were contact-printed and suitable representatives were selected for enlargement and subsequent montage construction.

E. ELECTRON MICROSCOPY

42 individuals from Stage 45 to mature adults were prepared for electron microscopy. The brains were exposed as described in 'B' above, and were fixed in 1% glutaraldehyde 1% paraformaldehyde solution in 0.12 M phosphate buffer at $4^{o}C$. This was done by immersion of the whole tadpole or the upper part of the head of postmetamorphic individuals. After three hours, the brains were excised and left in the same fixative in a refridgerator overnight. The tissue was then processed according to the Schedule in Table VI (Palay and Chan-Palay, 1974).

TABLE VI

(i) Rinse in 0.12 M phosphate, 0.02 mM calcium chloride and 8% dextrose solution for 15 minutes with two changes of solution.

(ii) Postfix in 2% osmium tetroxide in 0.12 M phosphate buffer containing 7% dextrose for two hours.

(iii) Rinse in 0.1 M sodium acetate for four minutes with one change of solution on ice.

(iv) Stain in 0.5% (w/v) aqueous uranyl acetate for 30 minutes.

(v) Rinse in 0.1 M sodium acetate for 4 minutes with one change of solution.

(vi) Dehydrate on ice with the following grades of methanol for 15 minutes each: 50%, 70%, 80%, 95%, 100%, 100%.

(vii) Dehydrate in propylene oxide with two rinses each of 15 minutes.

(viii) Infiltrate with a 50% (v/v) mixture of propylene oxide and Epon for three hours.

(ix) Infiltrate with a fresh change of 50% (v/v) propylene oxide and Epon.

(x) Infiltrate with freshly made Epon for six hours.

(xi) Embed in Epon (Palay and Chan-Palay, 1974) at 37°C overnight. Embedding is continued at 48°C for eight hours and completed at 60°C for two days.

After embedding sections were cut using glass knives on a Reichert OMU III ultramicrotome. Semi-thin (1-2 μm) sections were collected from the knife and were transferred to a drop of water on a clean glass slide. The slide was placed on a warm (60°C) hotplate and allowed to dry. The sections were stained in 0.1% Toluidine Blue in 1% sodium borate solution for 1½ minutes, after which the excess stain was removed by rinsing with distilled water. The slides were dried and mounted using DePeX and a coverslip. These sections were scanned under a light microscope to determine the area of the brain being sectioned. Occasionally, these sections were photographed on a Zeiss Ultraphot II for correlative purposes.

Thin (silver to gold) sections were collected on 200 mesh copper grids and stained with uranyl acetate (four minutes) and lead citrate (three minutes) which were prepared according to Palay and Chan-Palay (1974). Sections were examined and photographed in an A.E.I. EM 801 electron microscope at an accelerating voltage of 80 KV.

CHAPTER I

Morphology of the developing optic nerve

INTRODUCTION

The fact that the optic nerve is still undergoing development, in the tadpole and during the time of metamorphosis, has implications for the organization and function of the whole of the visual system and visually guided behaviour.

Little work has been carried out on the optic nerve in comparison to other regions of the amphibian visual system. Gaze and Peters (1961) and Wilson (1971) have studied the ultrastructure of normal Xenopus optic nerves with respect to fibre diameter distributions during development. The method of myelination in Xenopus tadpole optic nerve has been described (Peters 1960 a, b).

The present study of the optic nerve structure was carried out in order to determine the morphology of the developing optic nerve in tadpole and adult Xenopus with special emphasis on the time of metamorphosis, since this is the period at which the whole body of the tadpole is reorganized and the adult form is attained.

METHOD

Optic nerves were exposed by one of two surgical methods, depending on the age of the animal.

A. TWO MONTHS OF AGE AND OLDER

The brains were exposed as described in section 'B' of the General Methods. However, after suture of the two principal dorsal blood vessels, the underlying muscle was removed to expose the optic nerve from the eye to the point of entry into the cranium. The eye was punctured and the upper half of the head was immersed in ice cold 1% glutaraldehyde-1% paraformaldehyde fixative in 0.12 M phosphate buffer. The tissue was left in this fixative overnight in a refridgerator. Extraneous tissue surrounding the nerve, including the bone of the skull, was removed. The eye was released from the surrounding skin and remained attached to the nerve to enable determination of the nerve's orientation. The tissue was left in the fixative for a further twelve hours and was then washed in a solution of 0.12 M phosphate, 0.02 mM calcium chloride and 8% dextrose. The tissue was processed for electron microscopy as detailed in section 'E' of the General Methods.

B. TADPOLES AND JUVENILE TOADS UP TO TWO MONTHS OF AGE

The brains of these animals were exposed as described in section 'B' of the General Methods. The skin from the cranium to the eye and the ocular muscles in young toads were also removed. In tadpoles, the optic nerve is visible through the transparent skin. The skin was incised and the tissue either side of the optic nerve was dislodged, care being taken not to affect the blood supply. The upper part of the head was removed rapidly and transferred to the mixture of aldehyde fixatives and processed as described for adults above.

Some nerves were also prepared for electron microscopy by fixing in 5% glutaraldehyde in 0.1 M cacodylate buffer. They were washed in 0.1 M cacodylate buffer and 0.2 M sucrose, post-fixed in 1% (w/v) osmium tetroxide in 0.1 M sodium cacodylate, washed in buffer, dehydrated and embedded in Epon at 60^{o}C for two days (Mercer and Birbeck, 1966).

One micron thick sections were cut and were stained for 50 seconds in Toluidine Blue. They were scanned under a light microscope to determine the orientation of the optic nerve. Once a circular (transverse) profile was obtained at a level approximately 1 mm behind the eyeball, thin sections were cut and stained for two minutes in uranyl acetate and one and a half minutes in lead citrate, prior to viewing in the electron microscope. Any interesting features were photographed.

RESULTS

Twenty-seven optic nerves from tadpole and adult Xenopus were studied using conventional light and electron microscopy. Eight of these nerves were also used to produce whole nerve montages from which axon diameters were measured (see Chapter 2). The end point of development, the adult optic nerve, will be described first.

A. THE STRUCTURE OF THE ADULT XENOPUS OPTIC NERVE

The following results were derived from mature adults caught in the wild and from six month old postmetamorphic adults bred in the laboratory.

The optic nerve of Xenopus is a compact, slightly flattened cylindrical tract, measuring 250 to 350 μm in internal diameter (fig. 1:1). It is surrounded by a thick connective tissue and meningeal sheath consisting of the dura mater, arachnoid and pia mater (figs. 1:1 and 1:3). The sheath carries the ophthalmic artery, and three blood vessels, although none were found within the neuronal space, in contrast to the observations of Maturana (1960) on other Anuran species.

Fig. 1:1 A light micrograph of part of an adult optic nerve

The nerve consists of thick meninges (m) which are surrounded by large amounts of connective tissue (CON). Just above the meninges is a blood vessel (BV). Myelinated fibres and glial cells (g) are distributed throughout the nerve. Unmyelinated fibres occupy the remaining spaces.

Fig. 1:2 Electron micrographs to show the ultrastructure of the adult Xenopus optic nerve

a) An axon (A) bound by a myelin sheath (M) 0.5 μm in thickness. Also present is a glial cytoplasmic process containing microfilaments (mf)

b) A typical glial cell soma from an adult optic nerve. Note the unevenly distributed heterochromatin of the nucleus (Nuc). The glial cell is surrounded by both myelinated and unmyelinated (U) fibres. Within the glial cytoplasm, rosettes of free ribosomes (R) are evident. Microfilaments are present (mf) in the soma along a cytoplasmic process (see fig. 1:2 a)

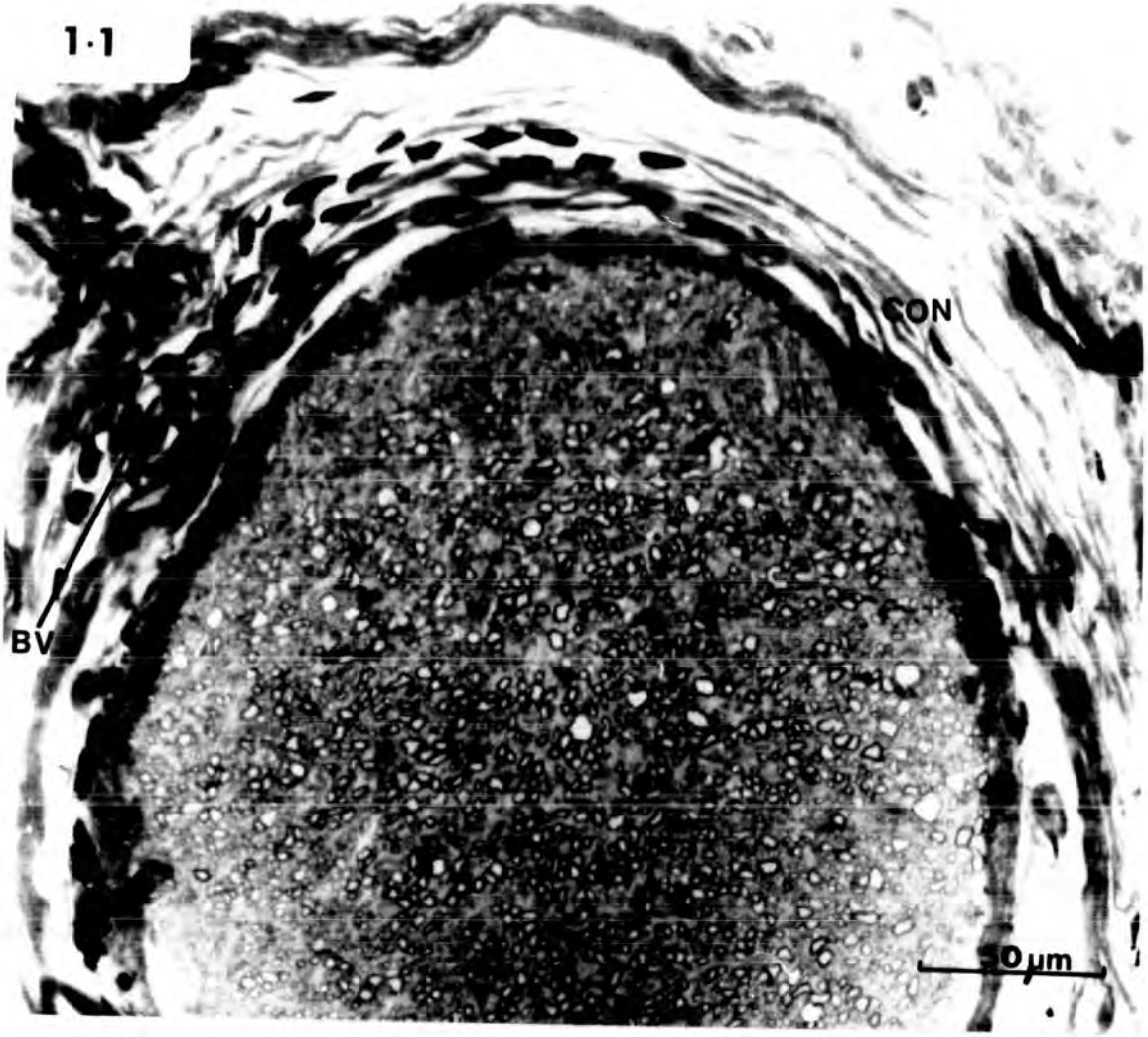
1·1
CON
BV
50µm

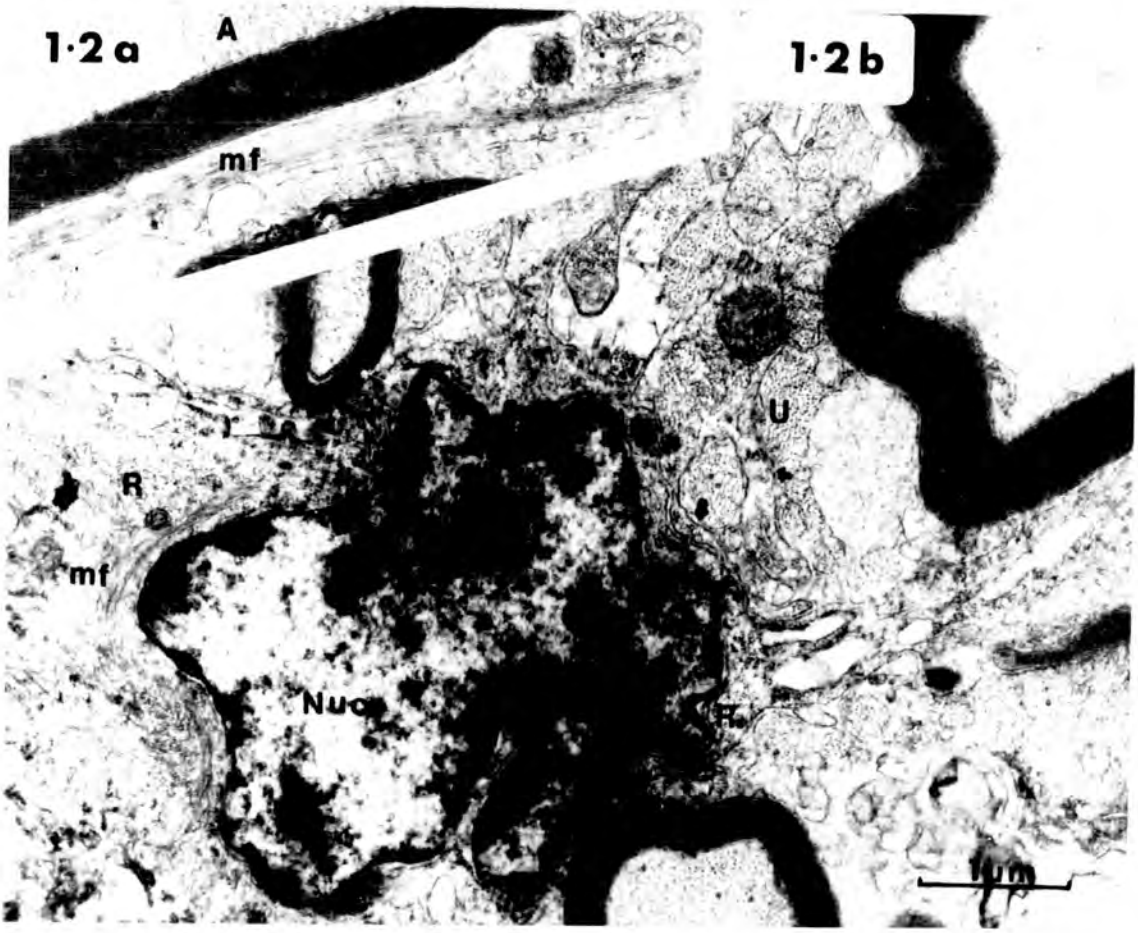
1·2a
A
mf
1·2b
U
R
mf
Nuc
1µm

Electron micrographs of the optic nerve show a highly compact structure with little intercellular space (fig. 1:2 a, b). The nerve is not sub-divided into fascicles, the nervous elements being distributed homogeneously. Myelinated fibres extend to the periphery and are interspersed with unmyelinated fibres and glial cell processes.

Glial cells

In transverse section only one type of glial cell is observed and is characterized by a darkly staining nucleus and cytoplasm. This glial cell type resembles that described by Maturana (1960). The glial cells have small somata (6 - 10 μm) and a large number of processes. The nuclei are also small (mostly 4 - 5 μm in diameter) and are irregular with numerous indentations (fig. 1:2 b). The densely stained heterochromatin is located towards the periphery (fig. 1:2 b). The perikaryon consists of a moderate to dense cytoplasmic matrix containing mitochondria; a few cisternae of predominantly smooth endoplasmic reticulum; small vesicles; and rosettes of free ribosomes (fig. 1:2 b). Glycogen granules are not evident. The perikaryal cytoplasm is usually characterized by the presence of microtubules and numerous microfilaments. Microfilaments may also be observed to accumulate in a concentrated band within the periphery of the glial perikaryon and extend into cytoplasmic processes (fig. 1:2).

In sections of adult optic nerves glial cell processes can be distinguished readily from axons by the concentrated bundles of microfilaments in comparison to the more distributed nature of the microfilaments and microtubules in axons (fig. 1:3). Many glial processes reach the surface of the nerve to terminate as elongated 'end-feet', which spread out over the outer surface of the nerve (fig. 1:3). However, these structures are more apparent in tadpole optic nerves and will be described in more detail later. Glial cell processes may be observed to be joined at "close junctions" (Peters et al, 1970) (fig. 1:4).

In the adult nerve, there appears to be no special morphological relationship between the glial processes and unmyelinated axons except where the individual processes and axons are in close proximity (figs. 1:3 and 1:4). However, a more intimate relationship exists between glial processes and myelinated axons. Branches of the processes surround part or all of the myelin sheath and are continuous with the myelin lamellae (fig. 1:5). The myelin lamellae are separated by a space of 100 - 200 Å (fig. 1:5). The glial cells cannot be identified categorically as astrocytes or oligodendrocytes and this point will be taken up further in the discussion.

Fig. 1:3 The structure of glial end feet and the optic nerve sheath in the adult

Endfeet (E) arise from a radially oriented glial process (GI) which contains micro-filaments. Profile G2 is a transverse section of a similar glial process. The endfeet can be seen to stop abruptly below the Pia matter (P) which is seen to contain longitudinally and transversely sectioned collagen (C). Between the glia and the pia lies a dense basement membrane (BM). External to the pia is the arachnoid (A) and dura matter (D). No relationship between the glial process and the unmyelinated fibres (U) is apparent except that the radial processes produce fascicles.

Fig. 1:4 Newly myelinating fibres in the adult

Newly myelinating fibres can be observed in three situations: on the side of a fibrous glial shaft (Ax1); encircled a number of times by glia (Ax2); or adjacent to a previously myelinated fibre (Ax3). Mesaxons (Mx) can be observed in all three cases. Close junctions (CJ) between glial cells are common.

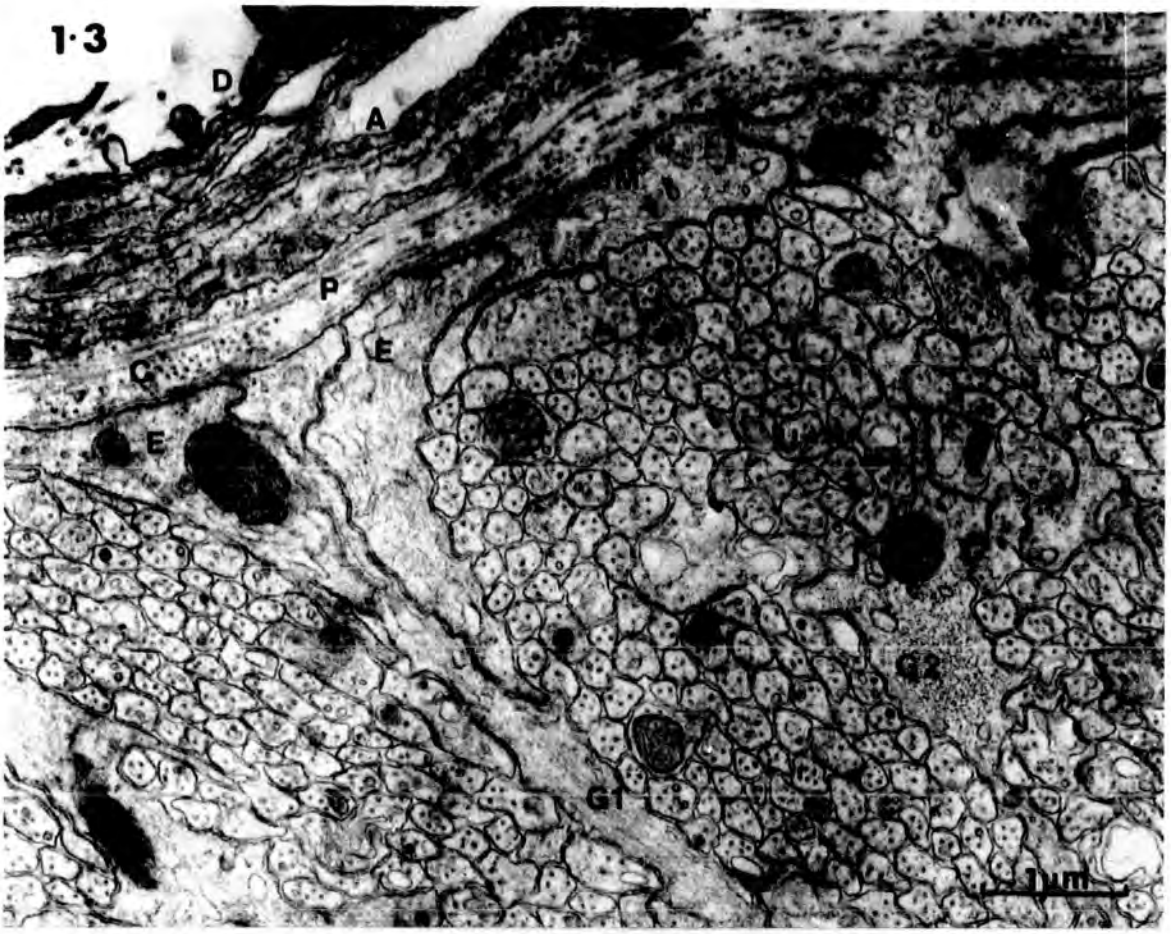
1·3
D
A
P
E
E
G2
G1
1µm

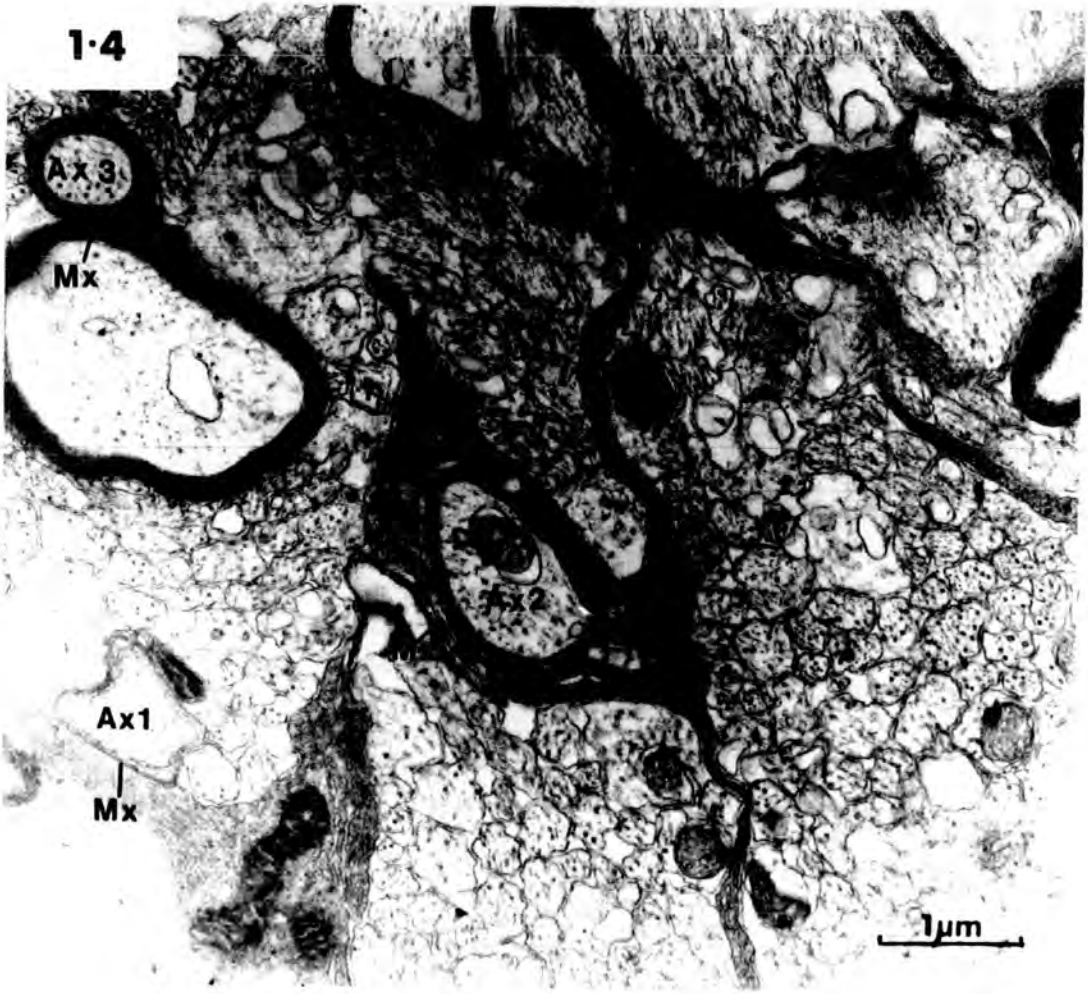
1·4
Ax3
Mx
Ax2
Ax1
Mx
1µm

Fig. 1:5 The continuity of glial cell membranes with myelin in an adult optic nerve

An axon (AX) is surrounded by loose (LM) and compact (CM) myelin, which have periods of 200 Å and 100 Å respectively. Glial cytoplasm (G) can be seen both internal and external to the myelin with their respective inner (IMx) and outer (OMx) mesaxons. Unmyelinated fibres (U) contain principally microtubules, although microfilaments are occasionally present. One unmyelinated fibre is swollen by the presence of a mitochondrion (mit).

Fig. 1:6 Typical myelinated fibres within an adult optic nerve

Microfilaments (Mf) continuously change orientation within the glial process, so that sections show both longitudinal and transverse profiles. No intervening cytoplasm is present between the adjoining myelinated fibres A1 and A2 and an intraperiod line of typical width is present. Axons A2 and A3 and possibly A1 are invested by a common glial (G) process. Many of the myelinated fibres have angular profiles.

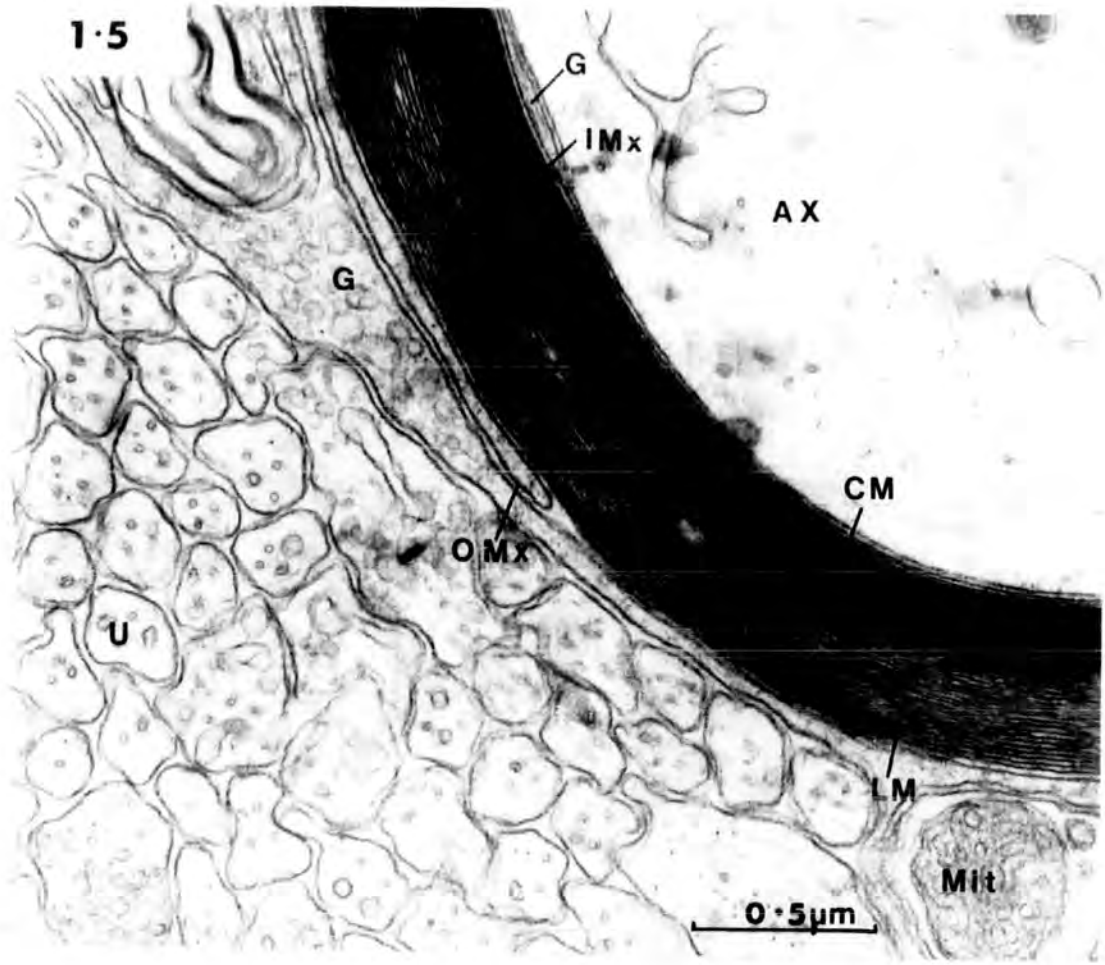
1·5
G
IMx
AX
G
CM
OMx
U
LM
Mit
0·5µm

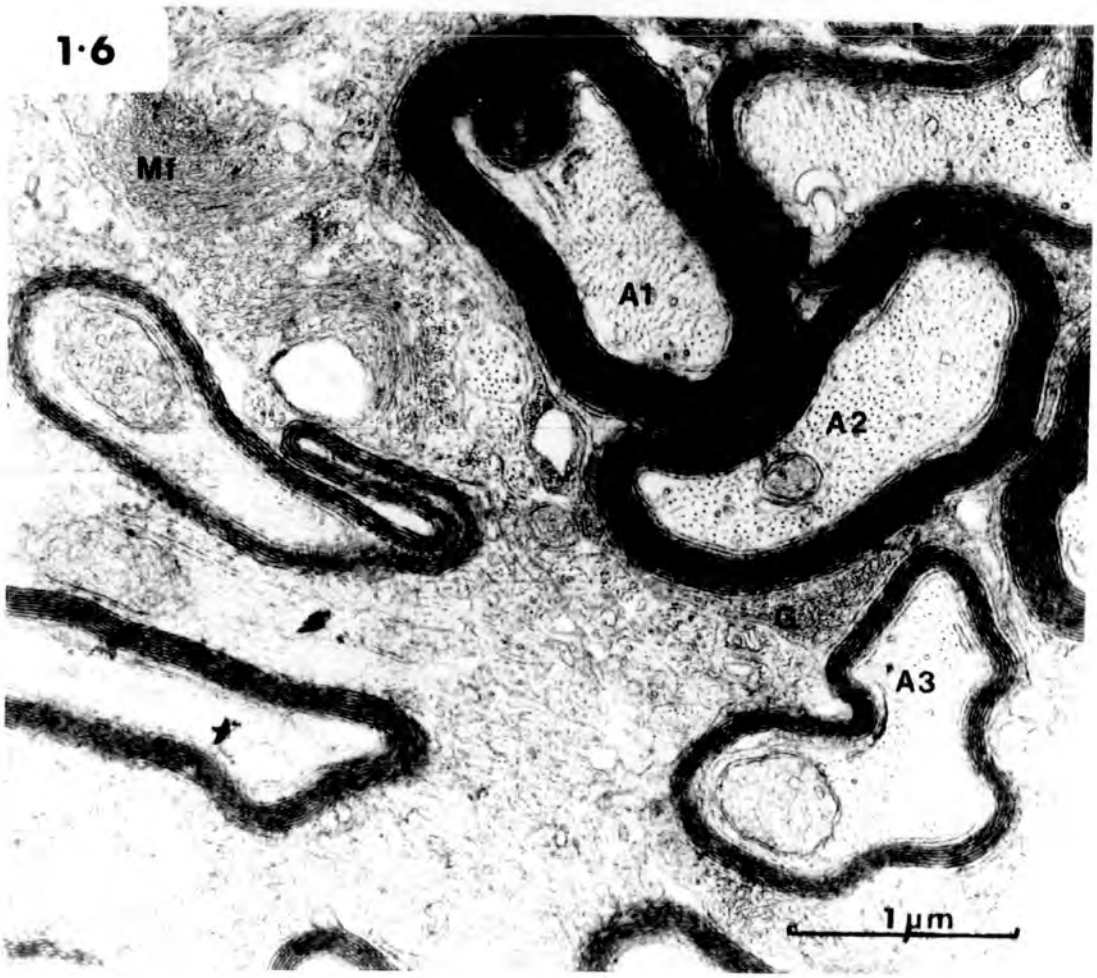
1·6
Mt
A1
A2
A3
1µm

Unmyelinated fibres

Unmyelinated fibres are distributed evenly throughout the nerve and have a diameter range of 0.1 - 2.0 μm. Larger axons are few in number. The axonal cytoplasm is typically agranular. Microtubules, microfilaments and mitochondria are present, the latter usually being associated with an increased axon diameter (fig. 1:5).

Myelinated fibres

The myelin sheath may be loose, compact or both and possess between 4 and 40 lamellae (fig. 1:5). The compact myelin sheath has a thickness of 0.03 - 0.5 μm in the internodal region. Glial cytoplasm is visible internal to the myelin sheath in some cases (fig. 1:5). Occasionally, 'flocculent' material may be found within the myelin in addition to the axon and glia (fig. 1:7). Schmitt-Lantemann clefts were never observed.

Myelinated fibres are usually scattered singly or in groups, although often chains of fibres occur. In the case of groups or chains, the myelin sheaths of adjacent fibres are in close proximity, often without any intervening glial cytoplasm (fig. 1:6). A group of axons may share a common fibrous glial process.

Adult myelinated fibres vary in diameter from 0.16 to 8.6 μm. The axoplasm is agranular and contains numerous microfilaments, microtubules and a small number of mitochondria (figs. 1:4 and 1:6).

Fig. 1:7 Abnormal adult myelinated fibre profiles

A long finger-like process (F) arises from a myelinated fibre and for part of its distance contains an axonal process. Within another myelin sheath, flocculent material (F1) is situated adaxonally.

Fig. 1:8 A newly myelinating axon within an adult optic nerve

An enlarged part of fig. 1:4, showing the early stages of myelination (A2) adjacent to a fibre with compact myelin (A1). Both fibres are invested by a common glial process.

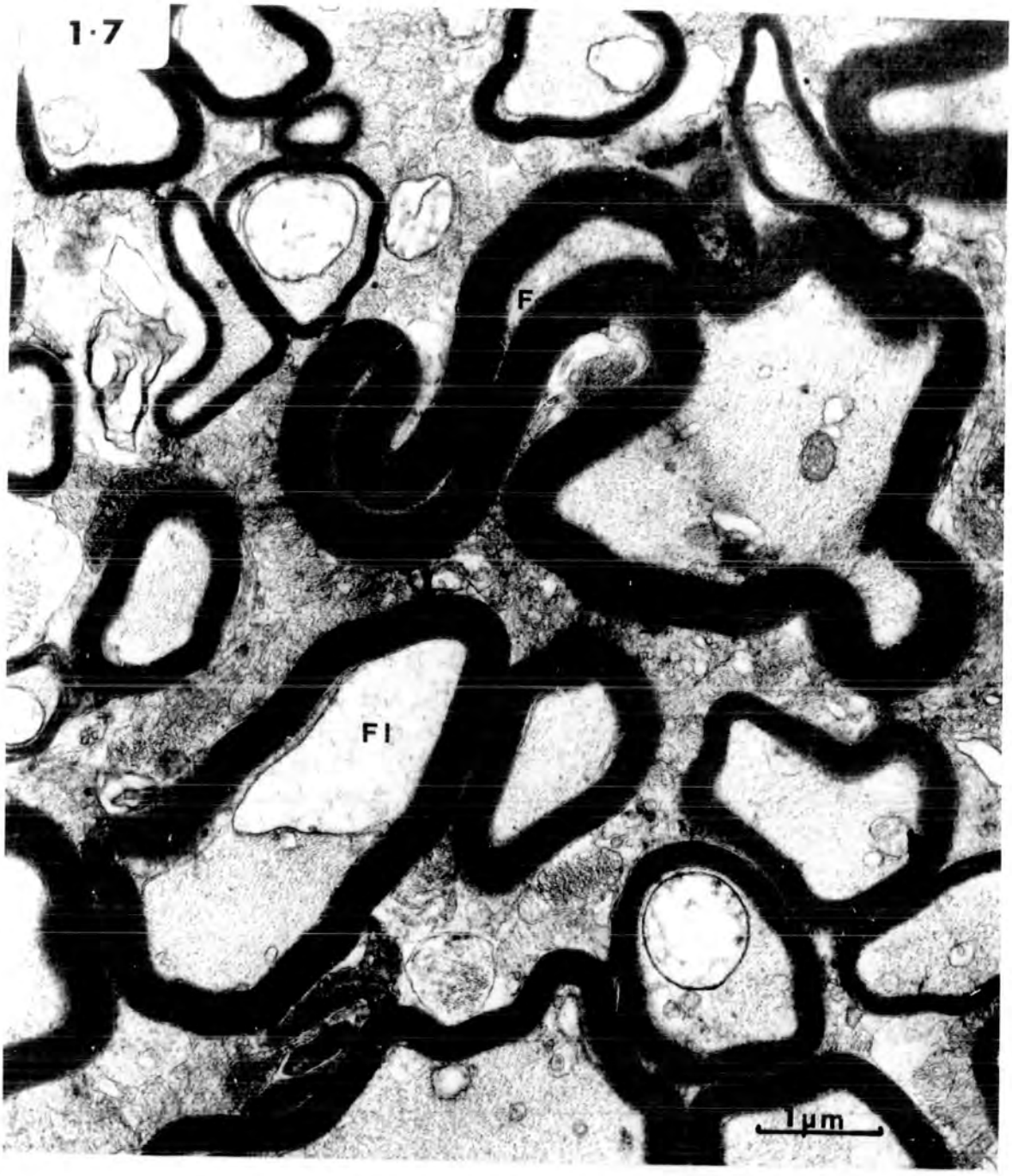
1·7
F
FI
1 µm

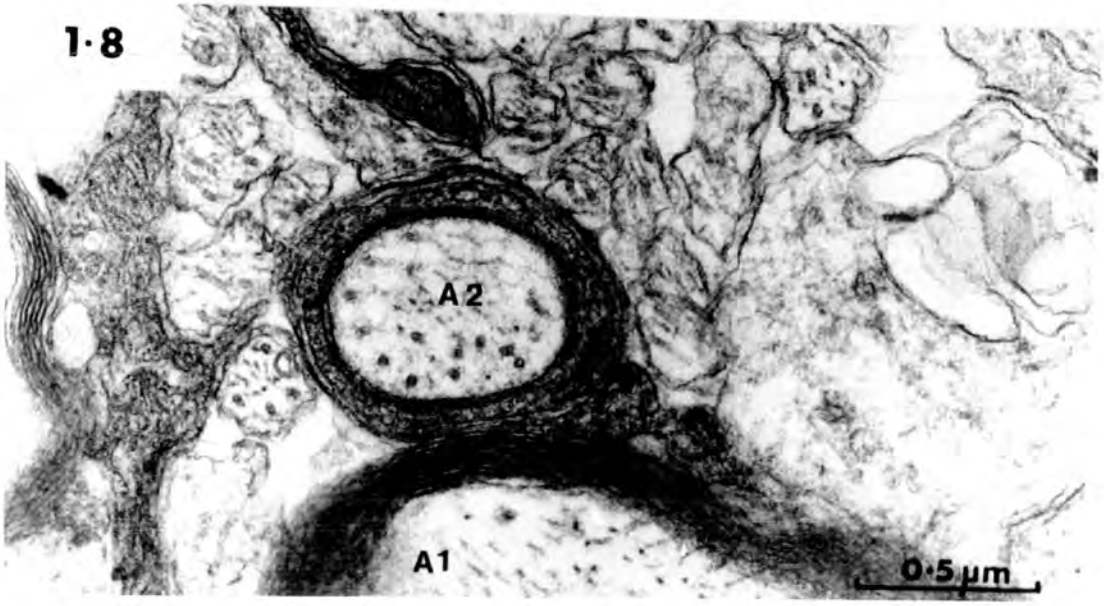
1·8
A2
A1
0·5 µm

Newly myelinating fibres

Careful study revealed that even in the adult optic nerve myelination of ganglion cell axons was continuing (figs. 1:4 and 1:5). A small number of axons were found to be completely encircled by glial cytoplasm, with a few loose wrappings of glial membranes present. New myelination may involve fibres adjacent to a previously myelinated fibre (figs. 1:4 and 1:8) or fibres situated within a group of unmyelinated fibres (fig. 1:4). Myelination may be carried out either on the side of the main shaft of glial cytoplasm (Axon 1, fig. 1:4) or within a bulkier part of the glial cytoplasm (Axon 2, fig. 1:4) or adjacent to a previously myelinated fibre (Axon 3, fig. 1:4). These observations were more apparent in six month old adults than in those adults caught in the wild, which were probably much older. The rate of myelination in adult animals must be at a low level considering the small number of myelinated fibres present.

Aberrant myelin

A small proportion of aberrant myelin profiles were detected in the adult optic nerve and these were more abundant in six months old adults than in individuals caught in the wild.

Aberrant myelin took the form of long finger-like outpushings, away from the main axon cylinder (fig. 1:7,

1:9 and 1:10). In some cases, the axon and glial cytoplasm are highly contorted (figs. 1:7 and 1:9). Occasionally, profiles suggest the presence of either two axons within one myelin sheath or one axon folded back on itself (fig. 1:10). A more common form of aberrant myelin usually took the form of a ring of myelin within a larger ring, with the inner cylinder containing glial, rather than axonal, cytoplasm (figs. 1:13 and 1:14). This myelin could be destined for removal and degradation, and possibly is caused by an inpushing of a glial cell near to the node of Ranvier. In fig. 1:14, the axon in this region has decreased in size considerably to a diameter of 0.7 μm as a result of the myelin inpushing.

B. THE DEVELOPMENT OF XENOPUS OPTIC NERVE

These observations were derived from a developmental series of optic nerves from Stage 46 tadpoles to postmetamorphic toads. This age range was chosen since it is at Stage 46 that the first neuronal responses can be recorded consistently in the optic tectum in response to visual or electrical stimuli (Gaze et al, 1974; Chung et al, 1975).

The essential features of the developing optic nerve are similar to those of the adult. All nerves which were studied contained fibrous astrocytes and unmyelinated nerve fibres. Myelinated axons were absent from tadpoles younger than Stage 49.

Abnormal myelinated fibre profiles

Fig. 1:9 A mis-shapen axon (A) is surrounded by aberrant myelin, with a prominant finger-like process (F). Adaxonal inclusions (In), myelin leaflets (ML) and a myelin body (M) are present.

Fig. 1:10 A large myelinated fibre (AX) with a large finger-like process (F) and myelin inclusions (In) is present. There is also a smaller myelinated fibre with what appears to be a double axon (A) or, alternatively, an axon which has folded back on itself.

Fig. 1:11 An axon (A) is surrounded by aberrant myelin, myelin invagination (I) and contains glial cytoplasm (G).

Fig. 1:12 A thick myelin invagination (I) surrounding flocculent material is present. The axon (A) is situated to one side of the myelin sheath and is small compared to the myelin invagination.

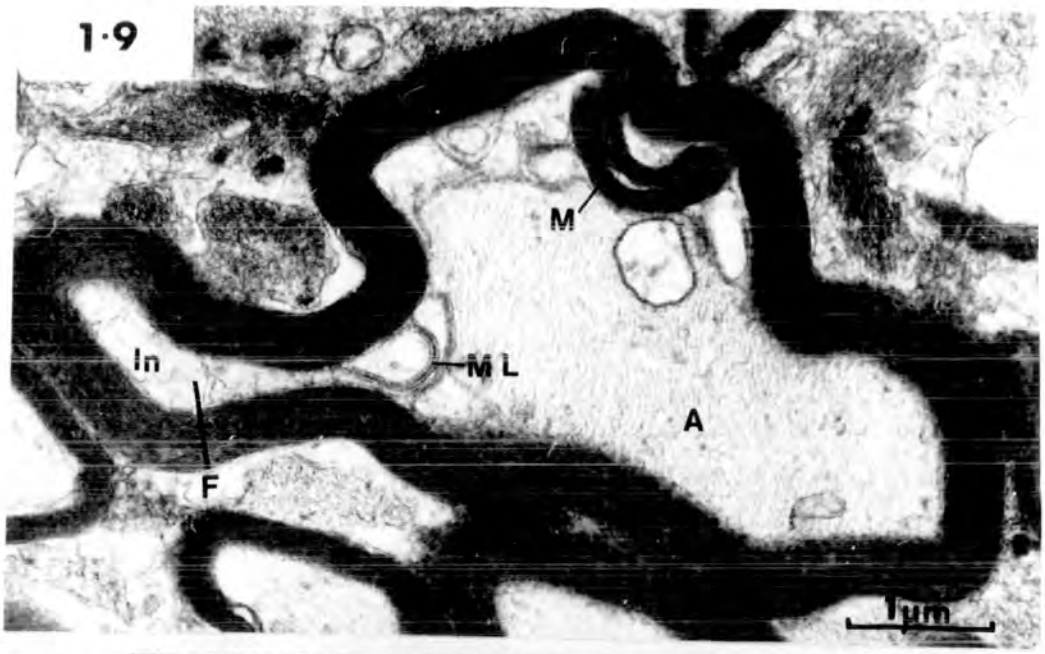
1·9
M
In
M L
A
F
1μm

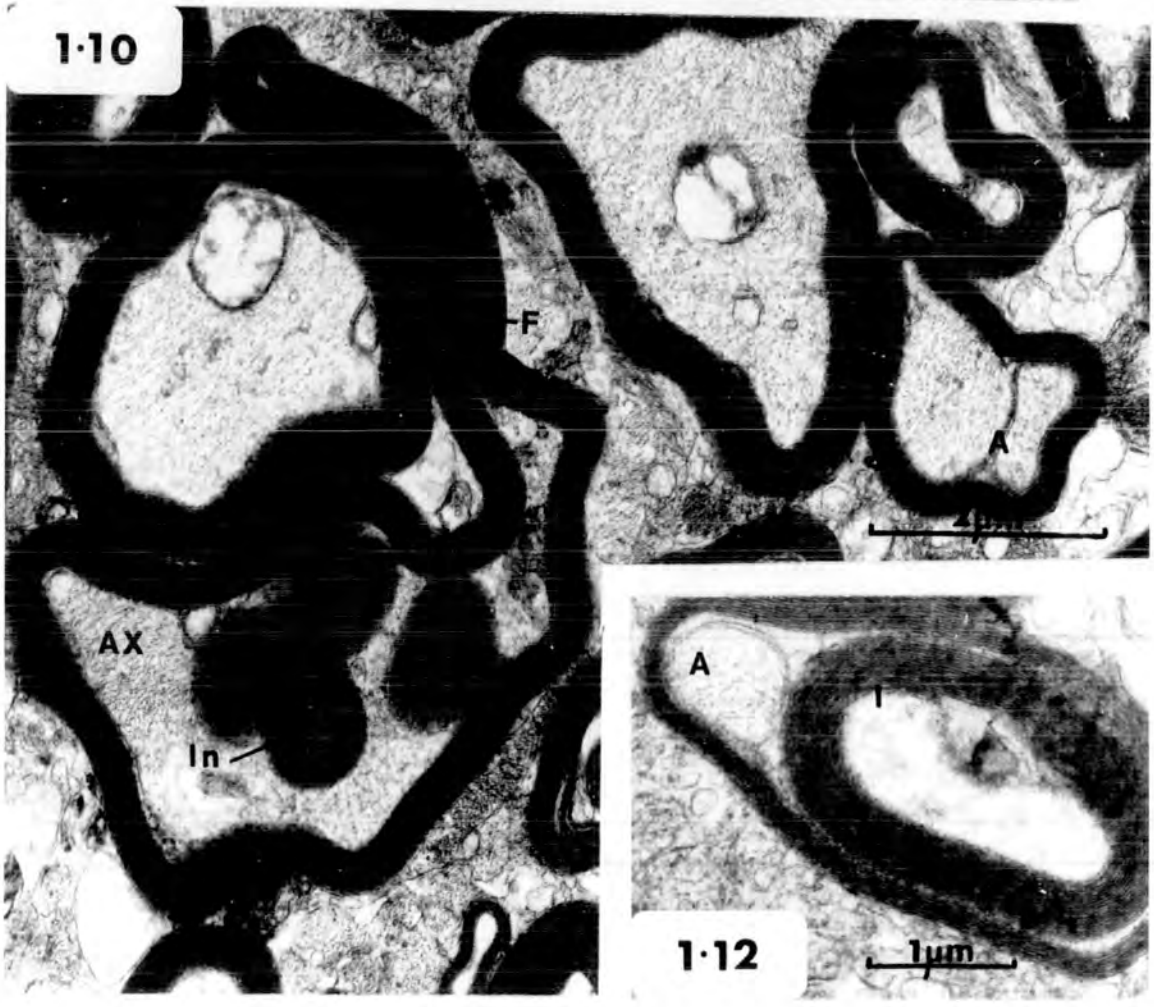
1·10
F
A
AX
In

A
I
1·12
1μm

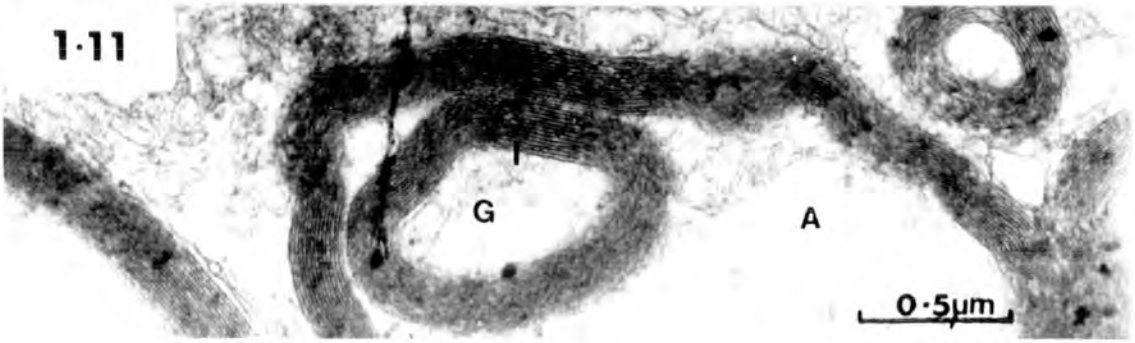
1·11
I
G
A
0·5μm

Light microscopy revealed that the optic nerve of tadpoles (fig. 1:13) comprises a large core region containing predominantly glial cell bodies and myelinated fibres and a peripheral region containing the processes of those cell bodies and predominantly unmyelinated fibres. During development there is an increasing number of myelinated fibres in the peripheral region and the relationships between the components change to produce the adult pattern. However, in tadpoles younger than Stage 49, myelinated fibres are absent and the glial cells are located in a bundle at the centre of the nerve.

Surrounding the nerve are the meninges and the thick protective coat of connective tissue. Attached to the meninges is the ophthalmic artery and within the meninges are three blood vessels (fig. 1:13).

The electron microscope reveals a highly compact structure with little intercellular space (figs. 1:14 and 1:5) as in the adult. The tissue is divided into fascicles by the glial cell processes which originate from centrally located cells which move more peripherally with time. These fascicles may include both myelinated and unmyelinated fibres or unmyelinated fibres alone (fig. 1:14 and 1:15).

Fig. 1:13 A light micrograph of a 1 μm.Toluidine Blue stained section of a plastic embedded nerve from a Stage 58 tadpole. Note the meninges (m), which contain a blood vessel (bv). Within the nerve, myelinated fibres are present, but there is a band of predominantly unmyelinated fibres towards the periphery. Oligodendrocytes (o) are darker than the spidery astrocytes (a). Glial cells are absent from the periphery.

Fig. 1:14 Note the compact structure with very little intercellular space. The light astrocytic (AST) glial cell contrasts with the much darker oligodendrocyte (OLIGO) but both nuclei are uniformily chromatic. The astrocytic cell soma contains numerous microfilaments (mf), whereas the oligodendrocyte has very few microfilaments but is filled with rough endoplasmic reticulum (RER) and mitochondria (mit). Some axons are in the process of myelination (nmf) and the dark glial cytoplasm which surrounds the axon is typical of oligodendroglia. Note the eccentricity of the nucleus of the oligodendrocyte.

Fig. 1:15 Note the compact structure ond the fascicles of unmyelinated (U) and myelinated fibres produced by the radiating astrocytic processes. These processes are packed with microfilaments (mf), which collect in the cell soma prior to leaving in a cytoplasmic process. Note the abundance of smooth endoplasmic reticulum (ER) in astrocyte 'ast 1' and its almost total absence in astrocyte 'ast 2'. Newly myelinating fibres (nmf) are present.

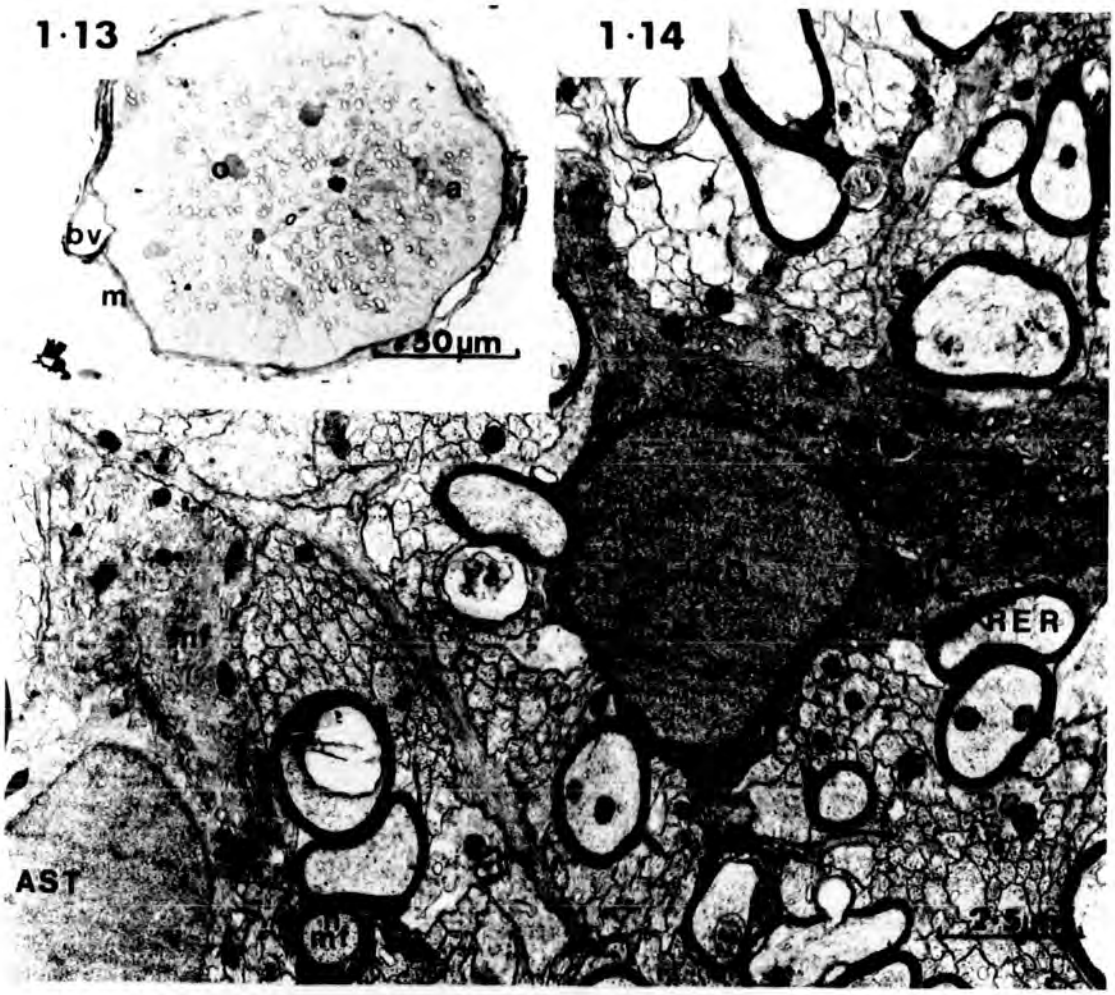
1·13
bv
m
50µm
1·14
mf
RER
AST
2·5µm

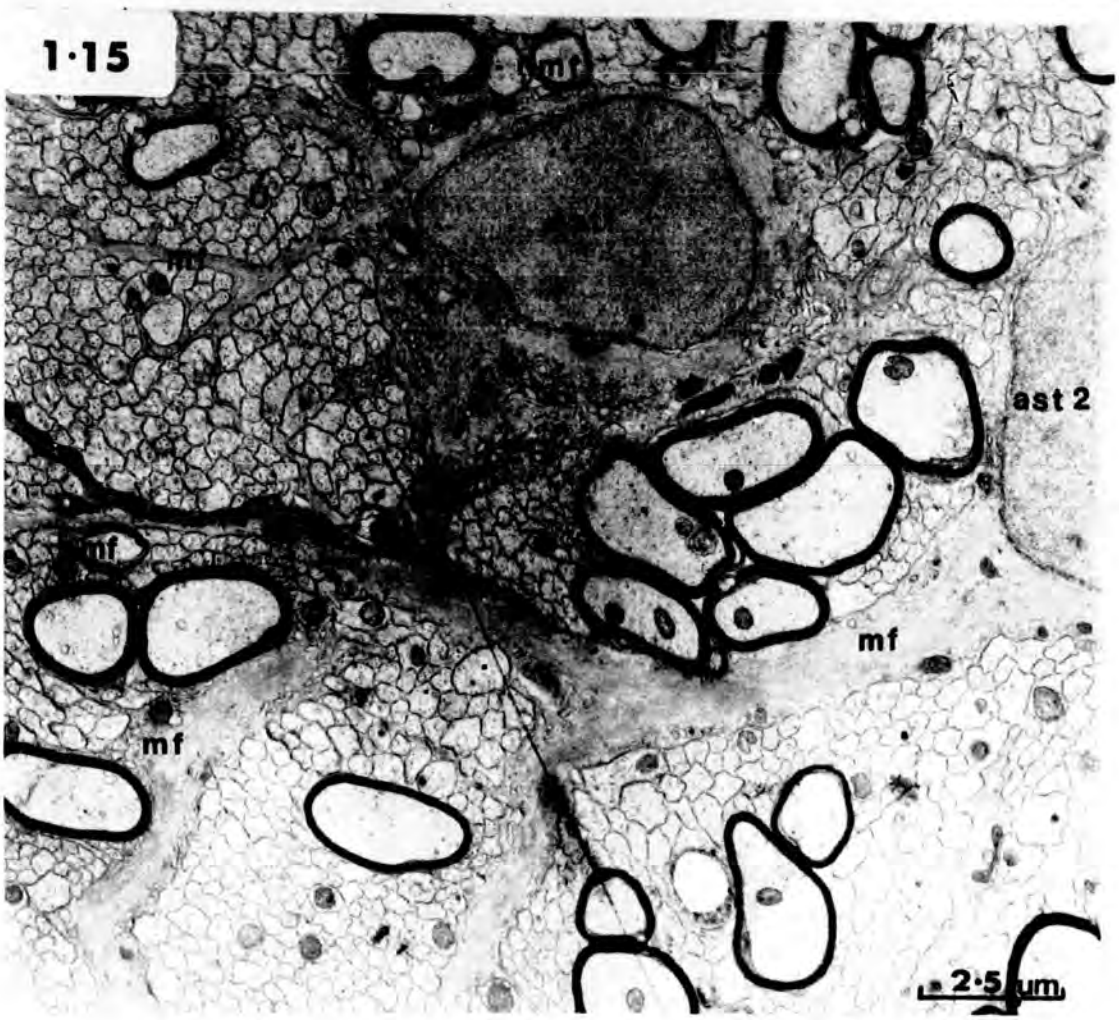
1·15
mf
mf
ast 2
mf
mf
mf
2·5µm

Glial Cells

In the Xenopus tadpole optic nerve there appear to be two types of glial cell, whereas in the adult there is only one type. Tadpole glial cells are not large (approximately 8 μm in diameter), and they have correspondingly small nuclei (approximately 5 μm in diameter) which sometimes have indentations. The karyoplasm generally has a fairly even density (figs. 1:14 and 1:15) unlike the heterochromatic nuclei in adult glial cells (fig. 1:2). The perikarya contain 80 Å microfilaments, mitochondria, endoplasmic reticulum, few rosettes of free ribosomes some smooth vesicles and Golgi-like complexes (figs. 1:14, 1:15 and 1:16).

Two cells are shown in figure 1:14, one being more osmiophilic and hence darker than the other. Both types have the contents mentioned above, but the more osmiophilic cell has a greater abundance of organelles, although fewer microfilaments are present. These light and dark cells often occur in pairs. Bundles of tightly packed microfilaments give the light cells the characteristic appearance of astrocytic glial cells, whereas the cytology of the dark cells corresponds to the characteristics of oligodendrocytes (Peters et al, 1970). Both types of glial cell are found in close contact with myelinated fibres, though in the case of oligodendrocytes, this is by means of long cytoplasmic processes. The membranes of oligo-

Fig. 1:16 Ultrastructure of tadpole glial cells

Note the light cytoplasm of the two astrocytes (AST) which contrasts with the darker cytoplasm of the oligodendrocyte (OLIGO). The nuclei of these two types of cells are uniformily chromatic. Note the presence of endoplasmic reticulum (ER) and a greater number of mitochondria (mit) in the oligodendrocyte and the presence of microfilaments (mf), smooth vesicles (sv) and a Golgi apparatus in one of the astrocytes.

1·16

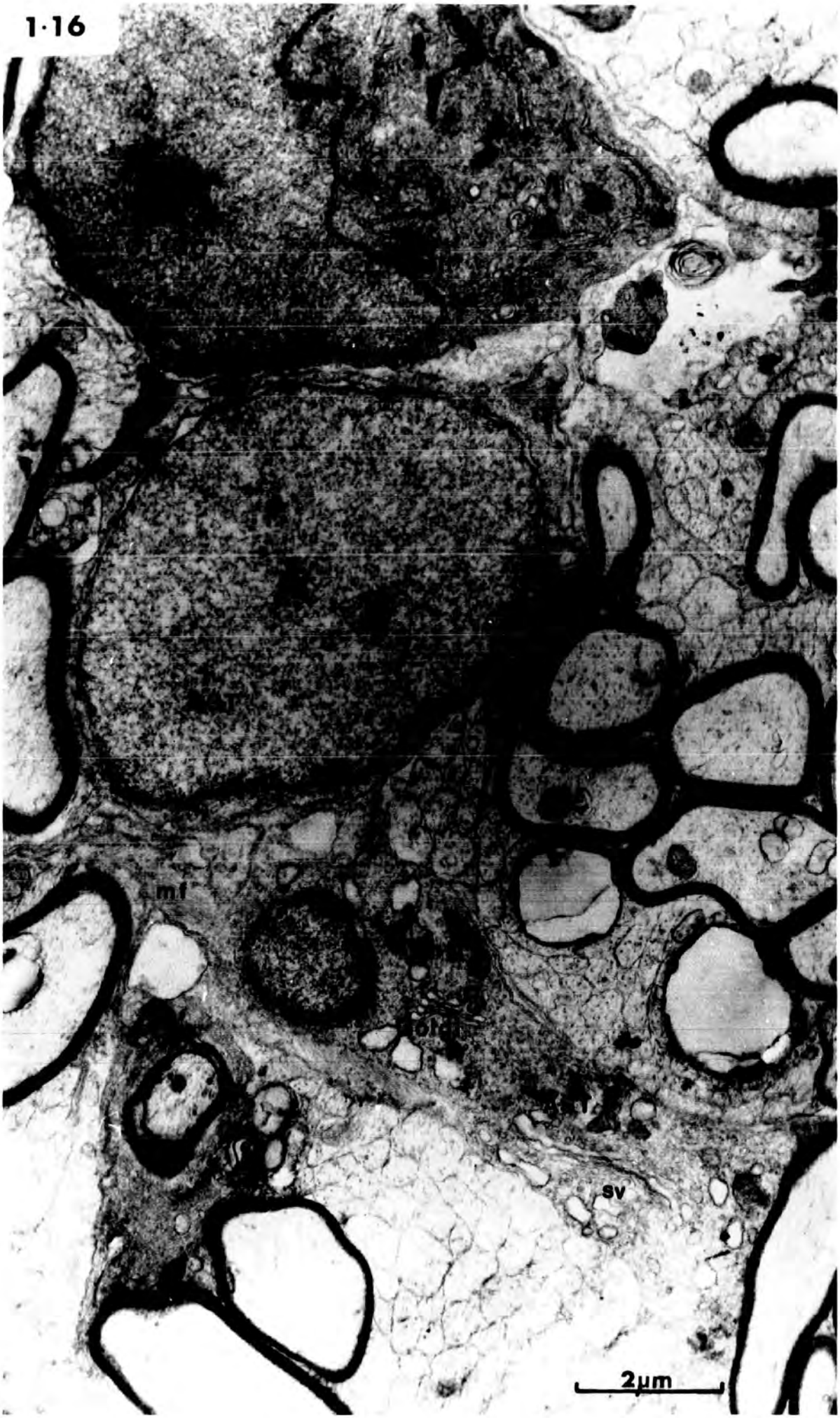

dendrocytes were found to be in direct continuity with the myelin lamellae, and often similar dark cytoplasm was found adaxonally (fig. 1:17 a,b). Reier and Webster (1974) have estimated the ratio of astrocytes to oligodendrocytes in Xenopus tadpole optic nerve to be 4 : 1.

The endoplasmic reticulum of glial cells usually does not extend far beyond the bases of the cytoplasmic processes which arise from the perikaryon. However, some isolated regions of oligodendroglial cytoplasm far removed from the soma were found to contain large amounts of rough endoplasmic reticulum (fig. 1:18). These regions are associated with myelinated fibres, and are present usually in areas of myelination (figs. 1:18 and 1:26) or myelin degradation (see below).

As described for the adult optic nerve, the glial cell processes form end-feet at the surface of the tadpole nerve (figs. 1:3 and 1:19). These astrocytic end-feet form a complete layer that is interposed between the nervous tissue and the endothelial cells. The thickness of the astrocytic layer varies, sometimes being several processes in extent, but more frequently it is formed by only a single layer of processes. Beyond the end-feet are numerous layers of collagen fibres (figs. 1:3 and 1:19) and these are surrounded by pericytes (fig. 1:19) and connective tissue. A thick basement membrane occurs between the glia and the collagenous pia (fig. 1:19).

Fig. 1:17 Myelinated axons in tadpole optic nerve

Myelinated axons (A) are shown with oligodendrocyte cytoplasm (O) both internal and external to the myelin.

a) The myelin is partially invested by astrocytic cytoplasm (Ast).

b) The oligodendrocyte can be seen to be producing myelin around two axons (A). The inner (IMX) and outer (OMX) mesaxons are clearly depicted. The myelin is almost totally invested by astrocytic cytoplasm (Ast).

Fig. 1:18 Part of an oligodendrocytic glial cell

Part of an oligodendrocyte (OLIGO) is filled with large amounts of rough endoplasmic reticulum (RER). Note the intimate relationship between the oligodendrocyte and the three axons (A1, A2, A3). Glial cytoplasm of a similar structure is common in regions where myelination or degeneration is taking place.

Fig. 1:19 The tadpole optic nerve sheath

Astrocytic glial cytoplasm (G) containing microfilaments (mf) fasciculates the unmyelinated fibres (U) of the tadpole optic nerve, and forms endfeet (E). At least one layer of glia separates the neuronal components of the nerve from the Pia, which contains collagen fibres (Col). Between the glial boundary and the pia is a thickened basement membrane (BM). The supporting pericyte cytoplasm (Peri) of the Arachnoid (Ar) invests the optic nerve and abuts onto a blood vessel (BV). The external layer is the dura mater (Dura).

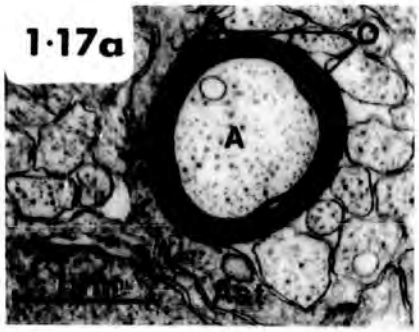
1·17a
O
A

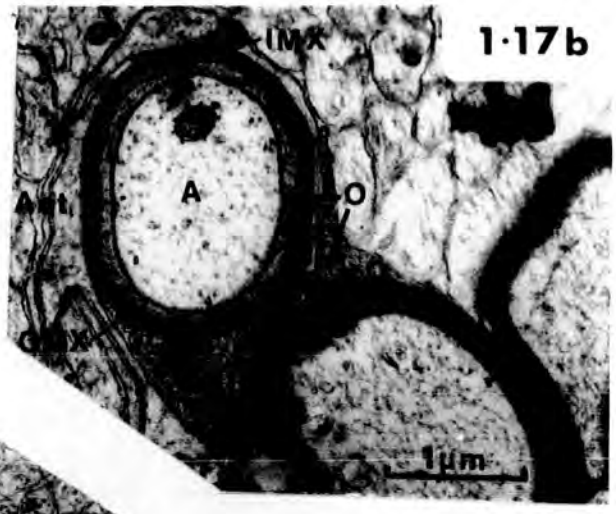
1·17b
IMX
A
O
1µm

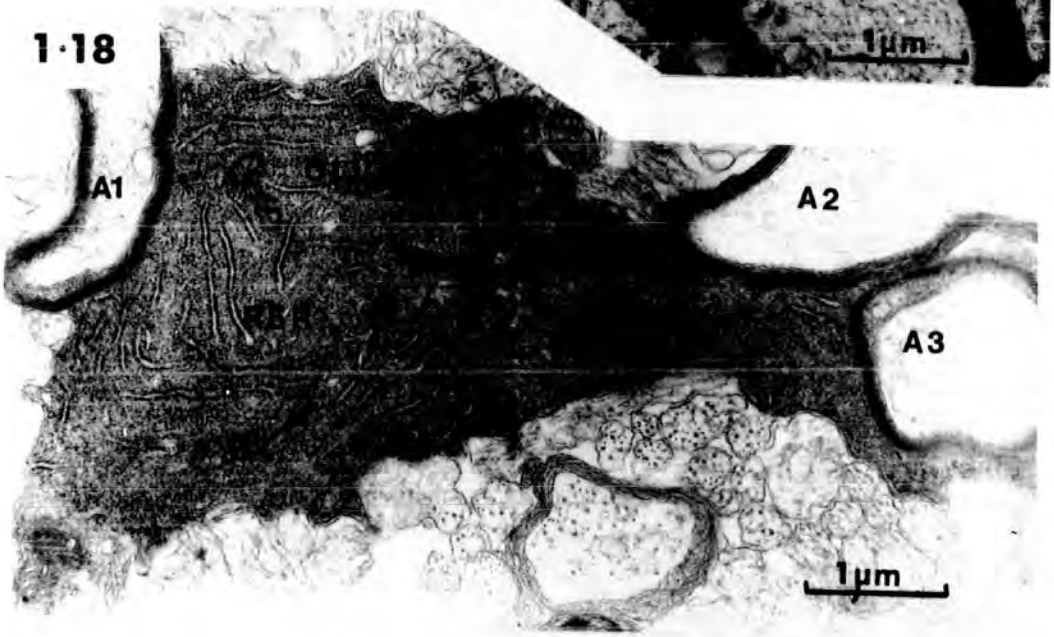
1·18
A1
A2
A3
1µm

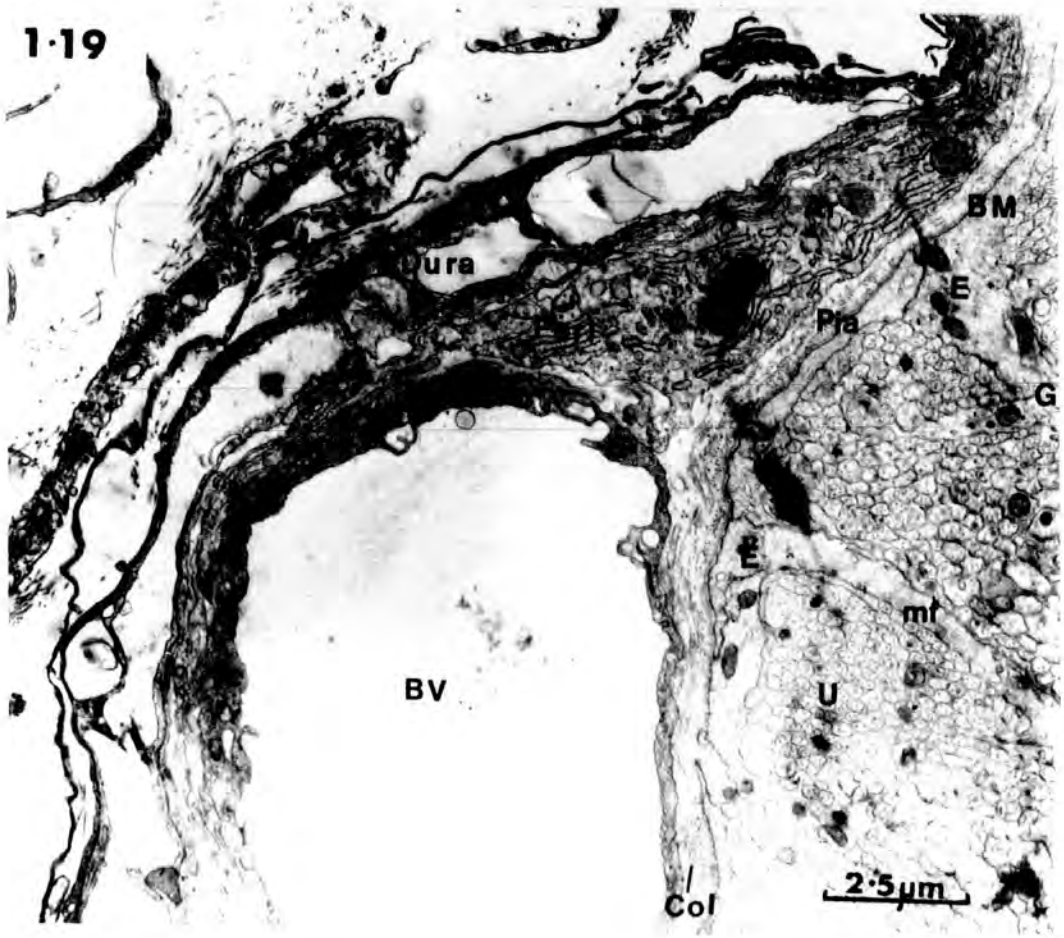
1·19
Dura
BM
E
Pia
G
E
mf
BV
U
Col
2·5µm

Within the meninges are three blood vessels (fig. 1:19) and attached to the meninges is the ophthalmic artery.

Unmyelinated fibres

Within the fascicles produced by the glial cell processes the naked axons of unmyelinated fibres are closely apposed to each other with little intercellular space (figs. 1:14, 1:15 and 1:19). The axons are small, the majority falling within the range of 0.1 - 0.4 μm diameter (see Quantitative Results in Chapter 2). There is often a gradient of axon size within the nerve with the larger axons towards the centre. The axonal cytoplasm contains mitochondria, microfilaments, microtubles and agranular endoplasmic reticulum.

Myelinated fibres

Myelinated fibres are found in ever increasing numbers in the tadpole optic nerve from Stage 49 onwards. They are always in contact with glial cell processes and, apart from newly myelinating fibres, always show compact myelin (figs. 1:14, 1:15, 1:16 and 1:17 a, b). Adaxonal glial cytoplasm is dark (fig. 1:17 a, b) and, in mature tadpole myelinated fibres, forms a thin sheet surrounding the axon (figs. 1:17 a, b, 1:23 and 1:24). There is usually a well defined mesaxon (figs. 1:17 a, b and 1:24). The oligodendrocytic process is wrapped around the axon three to seven times.

Optic nerve myelinated fibres are usually more scattered in tadpoles, than in adults (fig. 1:13). They occur singly or in groups and generally have a circular or oval shape in well fixed preparations (figs. 1:14, 1:15, 1:17 and 1:20). Groups of fibres often share a common glial process. The axonal cytoplasm of myelinated fibres contains microtubules and microfilaments, but those are fewer in number than those within the axoplasm of adult myelinated fibres (fig. 1:17 a, b).

Myelination

Myelination in the central nervous system has been well described elsewhere (Peters, 1960 b; Hirano, 1972) and will only be summarized briefly here. The first stage of myelination involves a process from an oligodendrocyte coming into contact with a nerve fibre approximately 1 μm in diameter (fig. 1:12) and then enveloping the axon by means of many turns (figs. 1:20 and 1:21). The glial membranes start to become apposed to produce compact myelin, leaving glial cytoplasm adaxonally (figs. 1:22 and 1:23). Apposition of the cytoplasmic surfaces leads to the formation of the major dense line, which in compact myelin alternates with the intraperiod line arising from the mesaxon (fig. 1:5). Throughout this process, the axon increases in diameter.

Fig. 1:20 The structure of the non-cellular part of the tadpole optic nerve

Both unmyelinated (U) and myelinated (MA) fibres are present, with oligodendrocytes (Oligo) and supporting astrocytes (Ast). The oligodendrocytes are continuous with the myelin, and similar cytoplasm is present adaxonally (MA1, MA2, MA3). MA1 and MA2 share a common oligodendrocyte, as evidenced by the glial bridge (arrow). Axons A1, A2 and A3 show aspects of the sequential process of myelination. A1 is partially encircled, A2 is invested in oligodendrocyte cytoplasm, and in A3, myelin is partially compact. Unmyelinated fibres (U) contain microfilaments, microtubules and mitochondria (Mit). Note the close association between the astrocytic and oligodendrocytic cytoplasm.

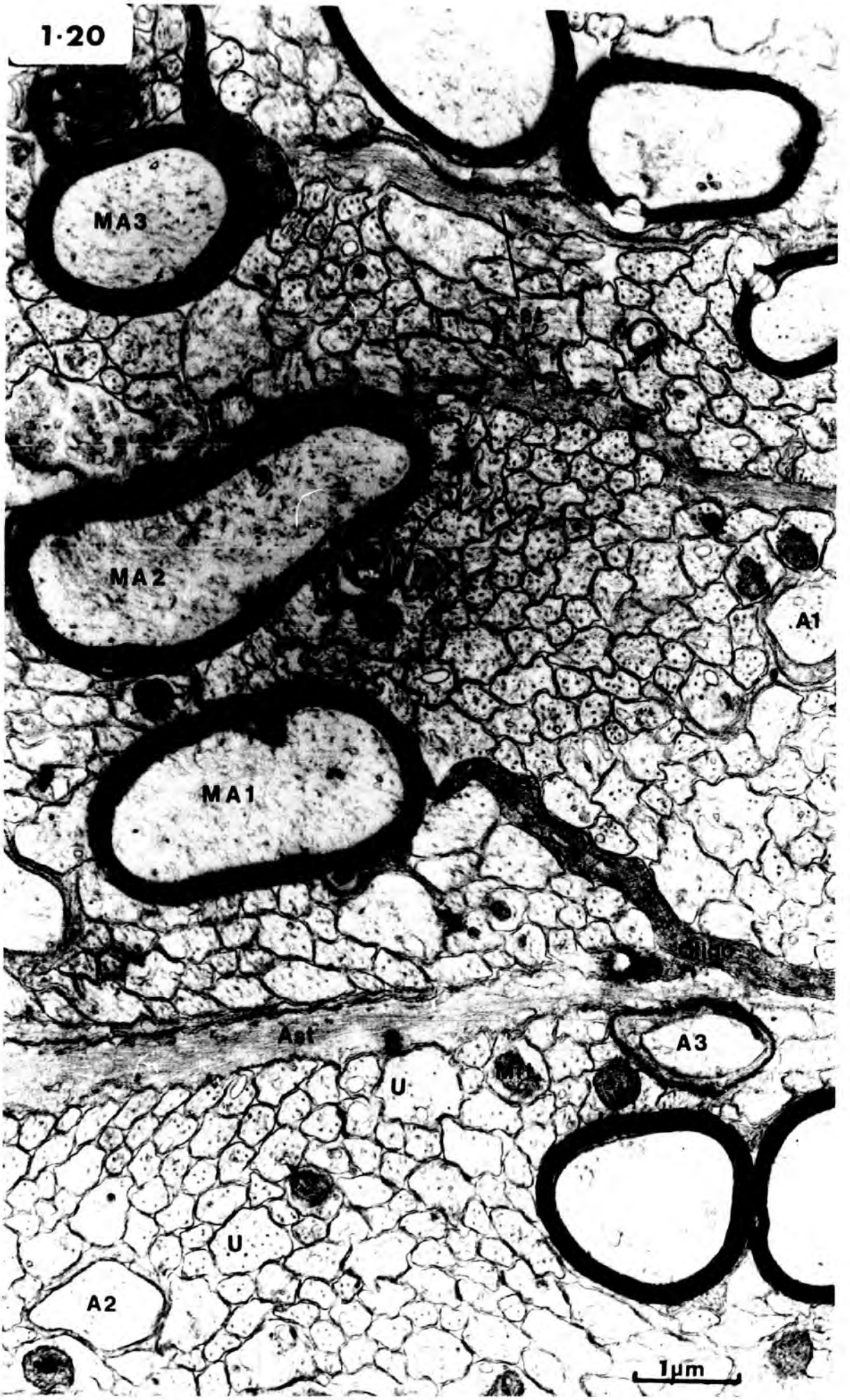
1·20
MA3
MA2
MA1
A1
A3
A2
Ast
U
U
1µm

Fig. 1:21 Multiple wrappings of an oligodendrocyte process (OLIGO) surround axon A1. This "myelin" is loosely apposed. The myelin of axon A2 is also derived from the same oligodendrocyte.

Fig. 1:22 Two wrappings of oligodendrocyte (OLIGO) membrane about the axon A are compact and a thin layer of myelin is seen. Clear inner (IM) and outer (OM) mesaxons are present. Note the abundance of rough endoplasmic reticulum (RER) in an oligodendrocyte in the vicinity of myelination.

1·21

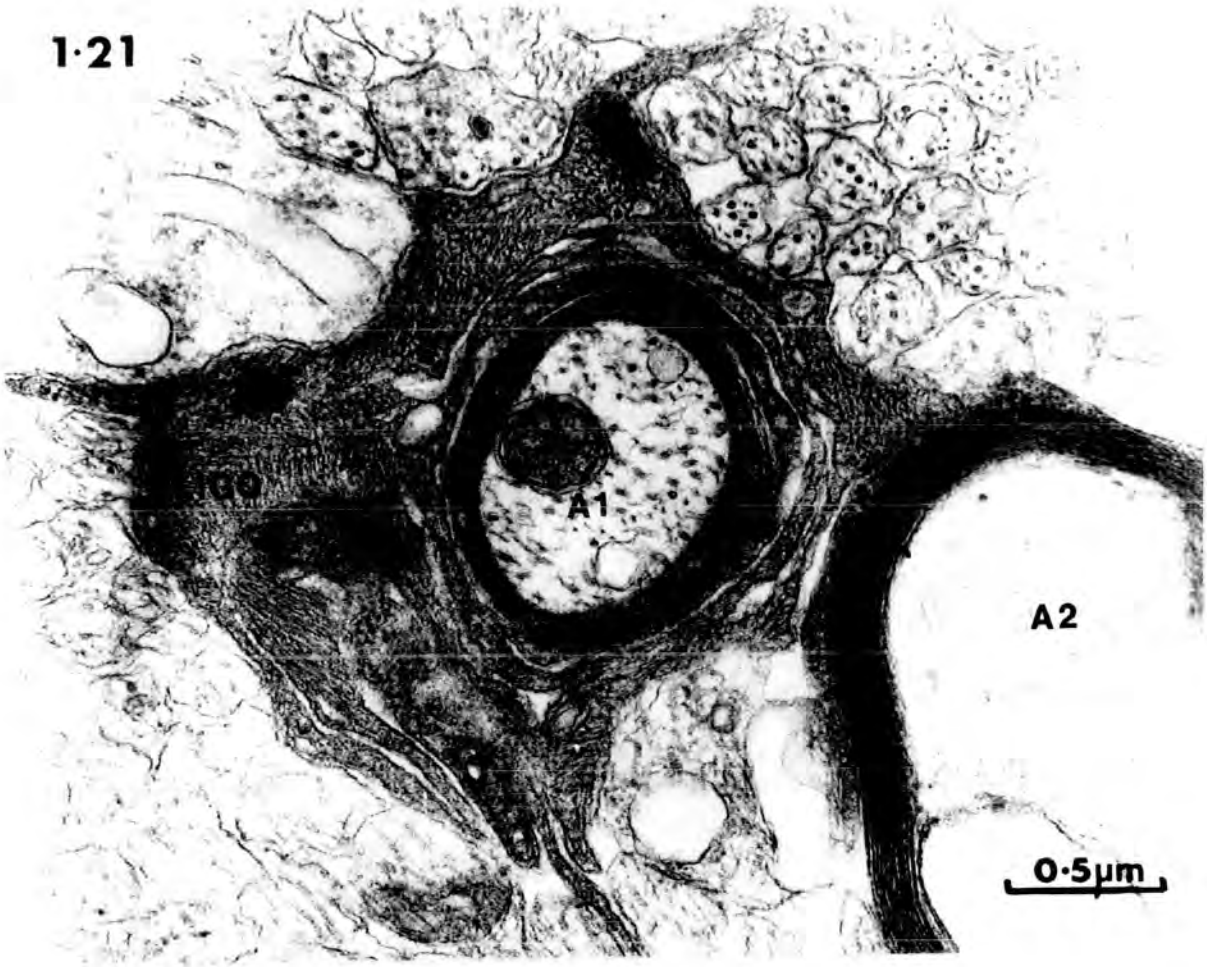

1·22

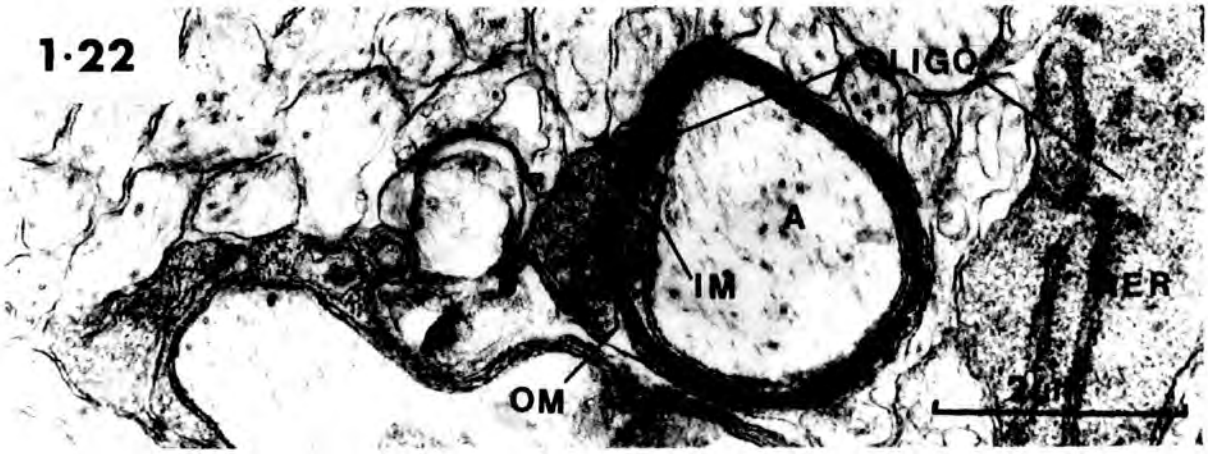

Fig. 1:23 Fibres at different stages of myelination

A number of fibres in the process of myelination are present and in conjunction with those in figures 1:20, 1:21 and 1:22, show different stages in the process of myelogenesis. Axon A1 is encircled a number of times by oligodendroglial cytoplasm. The glial membranes of axon A2 are more compact and the first dense lines of myelin are formed. Axon A3 shows a more consolidated picture with a clear inner mesaxon (IMX). Axon A4 appears to be at a similar stage of myelination as axon A3. Axon A5 is slightly more advanced, with removal of the oligodendroglial cytoplasm taking place. Axon A6 is ensheathed by myelin which is almost mature. Axon A7 is somewhat atypical in that its myelin is partially derived from that of axon A6 and only partially surrounds the axon.

1·23

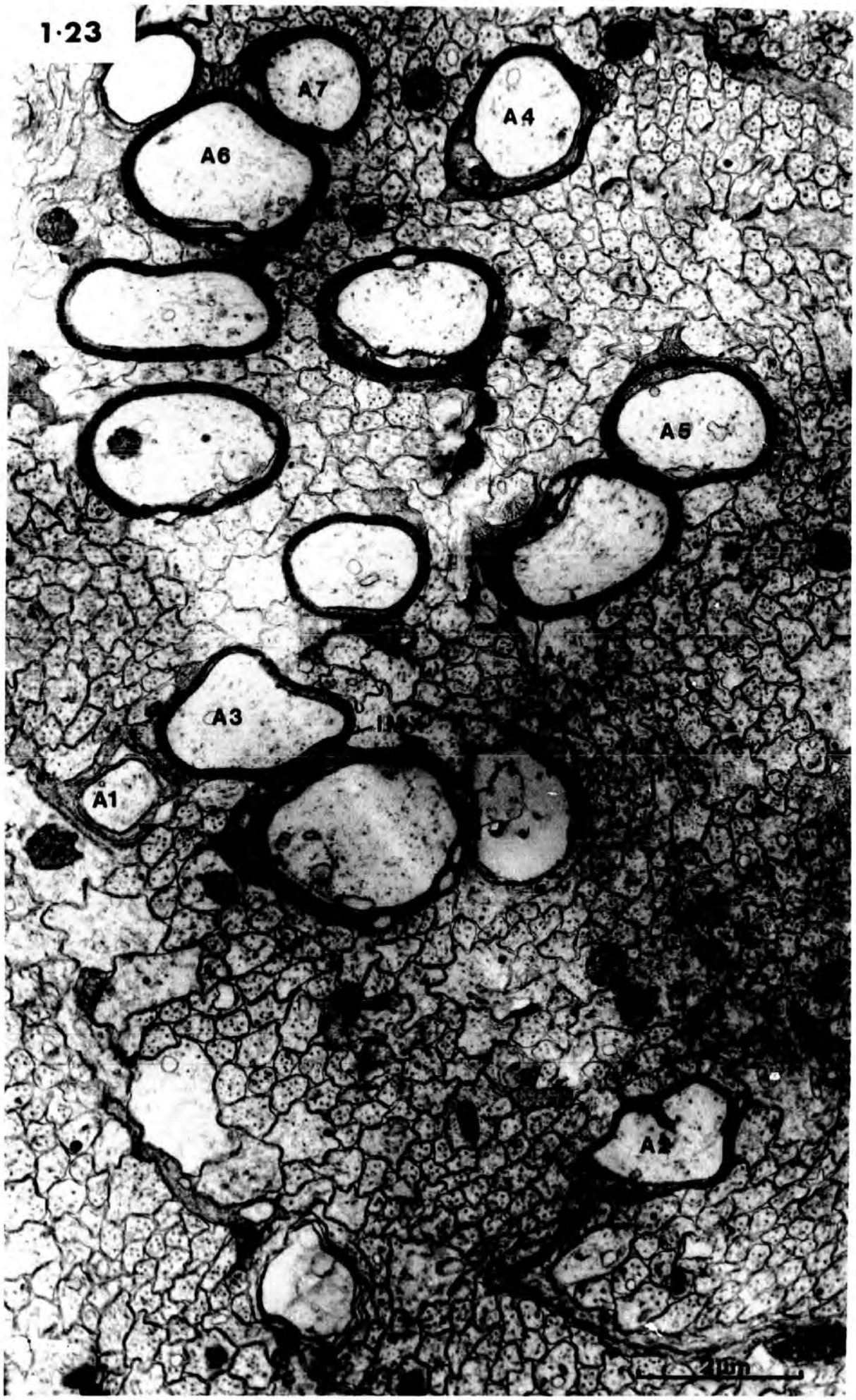

The process of myelination, beginning at Stage 49, is carried out by oligodendrocytes in the central region of the optic nerve. Myelination in the tadpole optic nerve continues until six or seven turns of the glial process round the axon have been completed and most of the adaxonal glial cytoplasm has been removed. The external glial cytoplasm surrounding the myelin sheath is usually minimal, enabling myelin from adjacent fibres to become apposed (fig. 1:24). The structure of the myelinated axon is then typically mature (figs. 1:14, 1:15, 1:20 and 1:24). However, the presence of mature myelin does not preclude the myelination of other fibres in the same locality (fig. 1:24). After Stage 58, a greater number of fibres at the periphery become myelinated and, as discussed earlier, myelination continues in the adult. The majority of fibres which become myelinated do so by the age of one month postmetamorphosis. After this, myelination principally consists of an increase in thickness of the myelin already present.

Aberrant myelin

In Xenopus tadpoles younger than Stage 57, myelin usually has a circular or oval profile with a smooth outline (figs. 1:14, 1:15, 1:17 a, b, 1:20 and 1:24). However, in the adult Xenopus optic nerve irregular, somewhat angular profiles (fig. 1:6) with finger-like outpushings (figs. 1:7, 1:9 and 1:10) and profiles containing

Fig. 1:24 The ultrastructure of tadpole glial cells

An astrocyte (AST) containing microfilaments (mf) with radiating processes. Both the astrocyte and the oligodendrocyte (OLIGO) have a uniformily chromatic nucleus. The oligodendrocyte perikaryon is rich in mitochondria (Mit), rough endoplasmic reticulum (RER), has a large Golgi apparatus (GOLGI) and is darker than the astrocyte. The myelinated axons (A) are typical for a tadpole optic nerve with six or seven wrappings of myelin. Axons A1 and A2 are in the process of myelination, and indicate that myelin production is not inhibited by the presence of 'mature' myelin. Note the close association between the astrocyte and axons A1 and A2. In the case of axon A2, the astrocyte almost engulfs the oligodendroglial component producing the myelin. Vesiculations (V) have been observed occasionally in tadpole optic nerves.


1·24
A2
A
A1
AST
A
A
A
A
mf
2µm

concentric rings of myelin (figs. 1:11 and 1:12) are present. Abnormal myelinated fibres start to appear in the developing optic nerve of tadpoles at Stage 58 and they can be observed until about one month after metamorphosis. Their number then drops to approximately that found in the adult.

Aberrant and degenerating myelin can be observed together in the optic nerve. Very little new degeneration appears beyond one week after metamorphosis, and debris is finally lost at one month postmetamorphosis. Degeneration of the myelin appears to be associated with the following:

(i) Inpushing of myelin by glial cells. The myelin and axon distort to produce the irregular profiles at Stage 58. This distortion is accentuated by the glial cells which invade the myelin folds (fig. 1:25). Glial cells may also be seen to distort the myelin of an intact fibre (fig. 1:26). In later stages, the myelin appears as concentric rings with oligodendrocytic cytoplasm within the inner myelin (fig. 1:25). Glial cytoplasm which has protruded into the myelin appears to be very rich in endoplasmic reticulum (fig. 1:25). The action of the glial cell within the inpushing of myelin is to peel off the myelin membranes into the invagination (fig. 1:25, 1:27 and 1:28). A common occurrence with myelin degradation is the appearance of presumably oligodendroglial organelles in the adaxonal glial cytoplasm (figs. 1:27 and 1:28). The rate of myelin destruction increases and by Stage 60

Abnormal myelin profiles

Fig. 1:25 Irregular myelin profiles (1, 2, 3) can be seen clearly. Profiles 1 and 3 contain axons in which the axoplasm appears normal. The myelin (m) in 1 appears normal and is continuous (arrow, my) with the membrane of the oligodendrocyte (OLIGO). Fibre 2 clearly shows the concentric nature of some of the abnormal myelin (cm), and the space so created is invaginated by oligodendrocytic cytoplasm which appears to contain rows of endoplasmic reticulum. Between the invaginated myelin and oligodendrocyte, membranous fragments (arrow) appear to be peeling away. The axon of fibre 2 has an abnormal flocculent appearance. (Stage 60)

Fig. 1:26 Both an astrocytic (AST) and an oligodendrocytic (OLIGO) glial process are present. The astrocytic process does not appear to be involved with the deformed myelin (dm) of the finger process of axon (A1). However, the oligodendrocyte is probably intimately related with the myelin sheath of axon 1. The finger-like process (1) and the loop of myelin (2) are derived from the same parent axon, since membranes linking the loop 2 with fibre 1 can be seen (arrow). Within the finger-like process, double membrane vesicles (v) are commonly found associated with abnormal myelin. Within the axoplasm of A2, vasicular membranes (vm) are present. The astrocyte is densely filled with microfilaments (mf). (Stage 58)

1·25

1·26

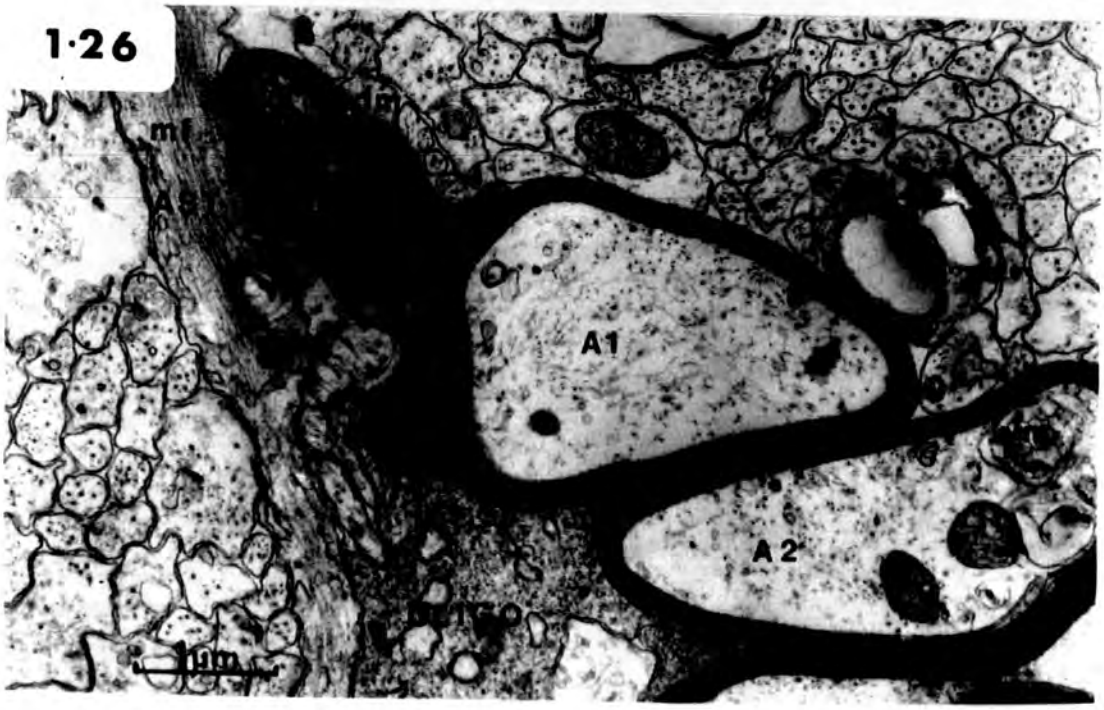

Degenerating myelin

Fig. 1:27 A myelinated fibre completely encircles an extracellular space (s), and within this space the myelin membranes appear to be peeling away (arrow). The myelin appears to have fused or become continuous (fm). Adaxonally double membrane vesicles (v) are present in the oligodendrocyte cytoplasm. Most of the myelin and the axoplasm appears to be normal. (Stage 58)

Fig. 1:28 There is an abnormally myelinated axon (A) present, although the axon and myelin adjacent to the axon are essentially normal in appearance. At the invagination (in), no glial cell is present. The space is filled with membrane fragments which have peeled away from the invaginated myelin to produce sheets or vesicular fragments of membrane (arrow). Adaxonally, a membranous vesicle (v) is present. (Stage 60).

Fig. 1:29 A dark oligodendrocyte (OLIGO) is present and there are four myelinated fibres with abnormal myelin (A1-A4). Axon A1 is enclosed by apparently healthy myelin, although adaxonally a large amount of degenerating myelin (DM) is present. Within this region of degeneration is an extracellular space. The breakdown of the myelin deforms the myelin sheath considerably. Axon A2 is wrapped around A1 almost completely, except for the intervention of A4. Axon A3 is only slightly irregular in comparison. No glial cell appears to be involved with the degeneration, although the fibres do appear to have been drawn together. (Stage 63)

1·27

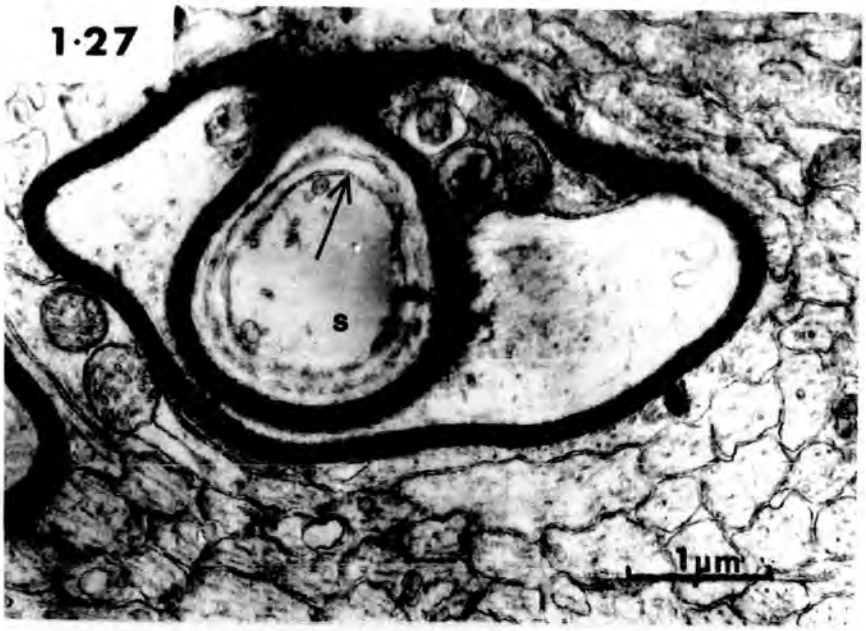

1·28

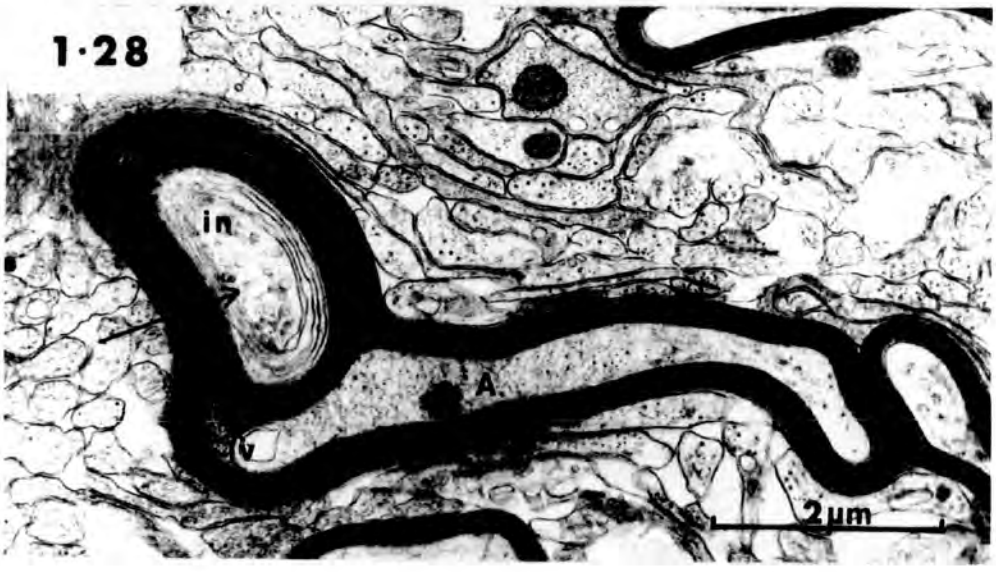

1·29

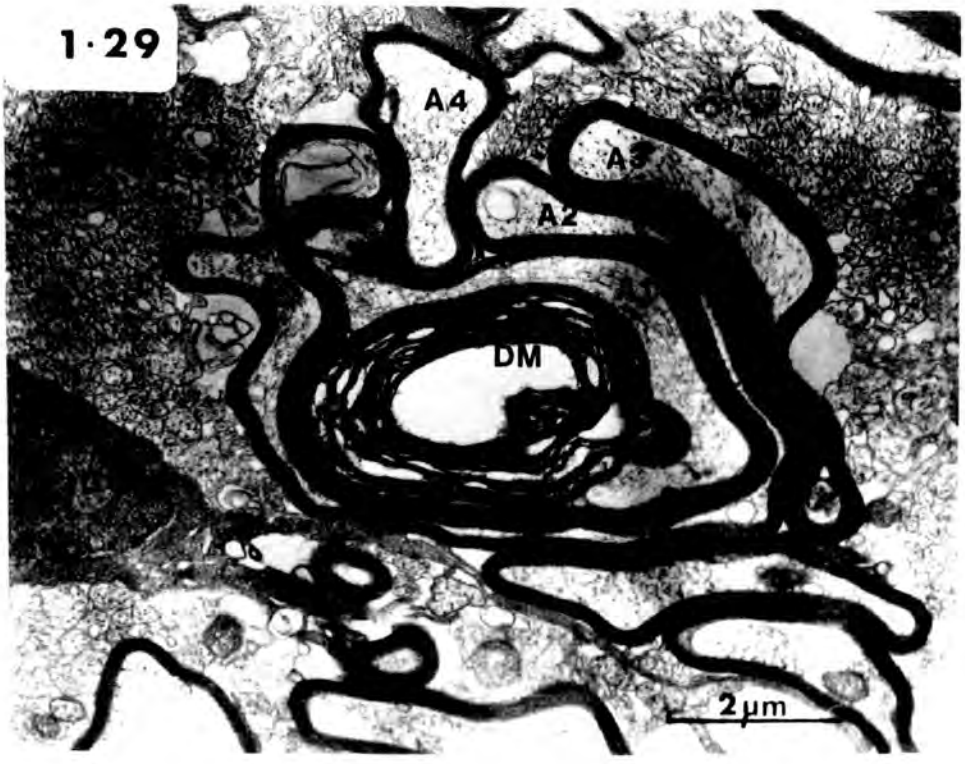

degenerating myelin profiles (fig. 1:29) are common. In many cases, two or more myelinated fibres together may be involved in this degeneration (figs.1:29, 1:30 and 1:31) as if drawn together by common oligodendrocyte. Two common features of myelin degeneration are firstly, the intact nature of the myelin which is not directly associated with the area of degradation (figs. 1:27, 1:28, 1:29 and 1:31) and secondly, the normality of the contents of the axonal cytoplasm with its usual complement of microfilaments, microtubules and mitochondria (figs. 1:25, 1:26, 1:28, 1:29 and 1:31).

(ii) Outpushing of the myelin. Myelinated fibres also have a tendency to become flattened in cross-section and to produce long finger-like protrusions of myelin from which the axoplasm receeds. Often myelin protrusions from adjacent fibres curl around one another (figs. 1:30, 1:32 and 1:33) and may form large aggregates and whorls (fig. 1:34). These are in contact with oligodendrocytic glial cells (fig. 1:35) and the more centrally located myelin is degraded. The fibres involved in this process have all the usual characteristics of myelinated fibres except that occasionally a myelin sheath may contain no axon (fig. 1:35) or be fragmented (fig. 1:34). In Stage 66 animals extensive degeneration of the myelin is very common, with large lipid droplets and myelin figures present within the glial cytoplasm (figs. 1:36 and 1:37).

Fig. 1:30 The astrocyte (AST) with radiating processes filled with microfilaments (mf) does not seem to be involved with the observed aberrant myelin profiles. A number of myelinated fibres (A) have been drawn together by an oligodendrocytic process (O). Glial cell membrane invaginations may be present which in some cases are completely isolated from the axon (arrow). Note the long lateral processes of the myelin and fibre B which is completely flattened. In general, the axoplasm and myelin appear normal. (Stage 59).

Fig. 1:31 The axons (A1-A3) are atypical in shape. Fibre A1 has a long finger-like outpushing, which divides (OP). The axon almost totally fills the intramyelin space. Fibre A2 contains dark glial cytoplasm which is indicative of an oligodendrocyte. Fibre A3 is markedly abnormal, with three concentric rings of myelin, the second of which also contains oligodendrocytic cytoplasm (OLI). Note the normal appearance of the axoplasm and of the majority of the myelin. An astrocytic process (AST) is also present. (Stage 60).

Fig. 1:32 Two myelinated fibres (A1, A2) with apparently normal axoplasm and myelin are present. Fibre A1 is aberrant in shape, whereas in fibre A2 there is a long finger-like outpushing. Part of the axoplasm (a) has become isolated from the remainder of the axon cylinder (A2) but much of this evagination contains no axoplasm (between the two lines) and the aberrant myelin has completely collapsed. Note the small vesicle (arrow) which is situated adaxonally. (Stage 60)

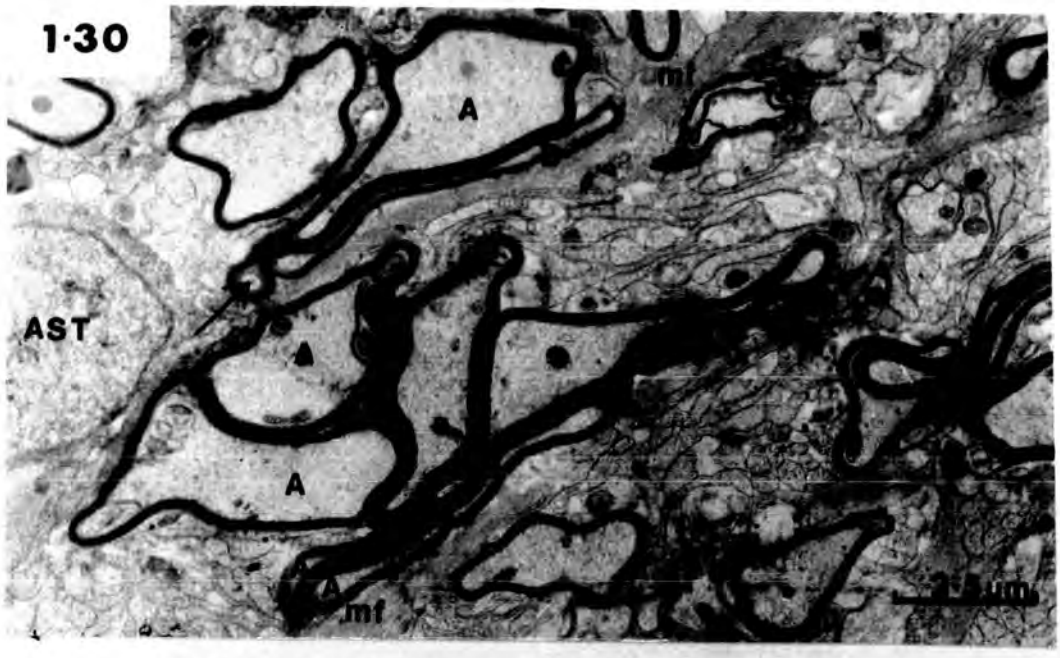
1·30
A
mf
AST
A
A
mf

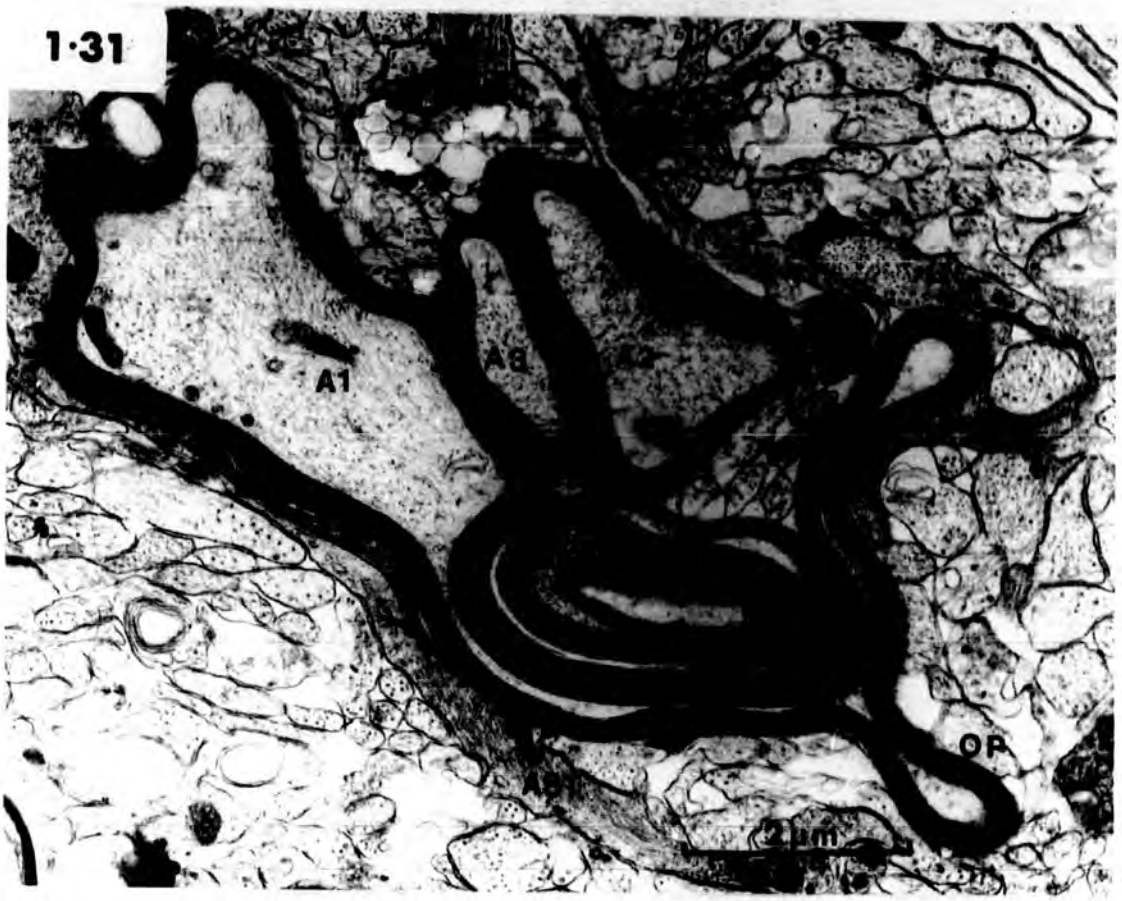
1·31
A1
A2
OP
2µm

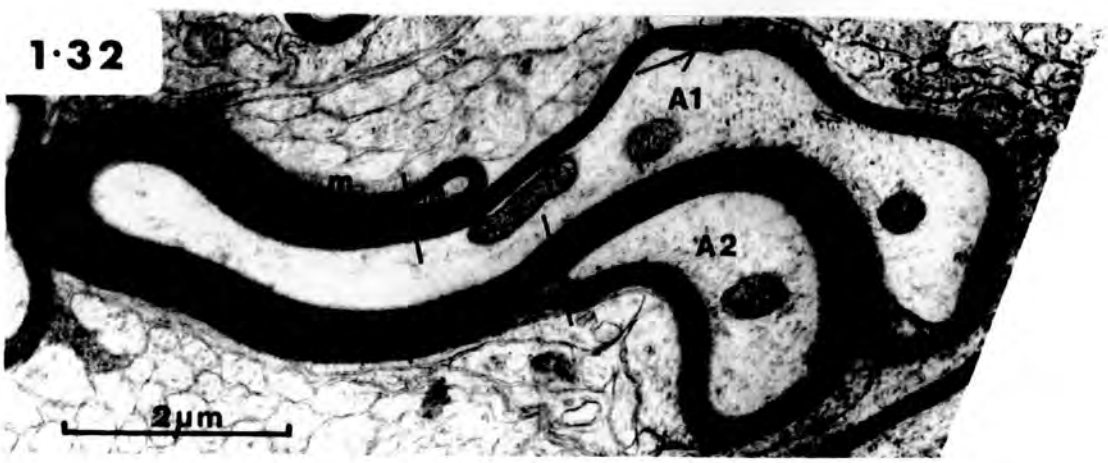
1·32
A1
A2
2µm

Fig. 1:33 Myelinated and unmyelinated axons

The figure shows both unmyelinated (U) and myelinated (A1-A3) fibres, astrocytic (AST) and oligodendrocytic (O) processes. The oligodendrocytes can be seen to be continuous with the myelin, with the inner (IM) and outer (OM) mesaxons clearly evident in fibre A2. The myelin and axoplasm appear to be structurally normal. Vesicular fragments (V) are present both outside the myelin and within the axoplasm of fibre A1. Fibre A2 is curled partially around fibre A1, and the axon has receeded from a major portion of the aberrant loop, although at one end a small swelling is present, which contains a portion of axoplasm (a). Note the four small vesicular components (arrow) which are situated within the myelin. These are possibly indicative of the first stages of degeneration. (Stage 58)


1·33
AST
OM
A1
A2
IM
OM
U
A3
1um

Aberrant myelin profiles

Fig. 1:34 A large aggregate of myelinated fibres (A1-A6) is present in which the fibres are associated with an oligodendrocyte (O). The fibres have extensive aberrant loops. Fibre A1 has an almost normal axon cylinder (C) although the long loop of myelin has no axonal contents in places (X). In other regions (Y and A1) the axon and glial axoplasm extensively interdigitate with vesicular membranes (V). Axons A2, A4 and A6 show invaginations involving the adaxonal glia (arrows). Fibre A5 shows a large myelin figure (M) which is presumably part of a myelin invagination. This fibre also contains smooth vesicles (sv), but it cannot be determined whether these are intra- or extra-axonal. In Fibre A2, the axon has receded from a large region of the myelin. More distally a number of myelin fragments (fm) are apparent within the myelin sheath. Fibre A3 has a finger-like process. Note the normality of most of the myelin and axons apart from A1. (Stage 60)

Fig. 1:35 An oligodendrocyte (OLIGO) is almost totally surrounded by myelinated fibres. Fibre A1 has two evaginations. The major one contains axoplasm for part of its course, but the remainder of the loop is either completely accluded by two regions of myelin coming together (X) or is filled with fragmenting myelin (fm). Fibre A2 also has an outpushing of myelin which contains part of the axon. The axon is slightly deformed by vesicle-like membranes (vm) which are positioned adaxonally. Fibre A3 has an axon barely visible and at one end is slightly swollen so as to contain a space (s). An astrocyte (ast) abuts onto fibre A4 which is partially wrapped around fibre A5. Both these fibres have long finger-like processes. Fibre A6 seems to be devoid of axoplasm. Some fibres contain large myelin bodies (M) which are presumably regions of invaginated myelin. One fibre, which abuts onto the oligodendrocyte (arrow) is devoid of contents including axoplasm and the myelin membranes have become apposed. Another fibre contains a myelin invagination (in). (Stage 60)

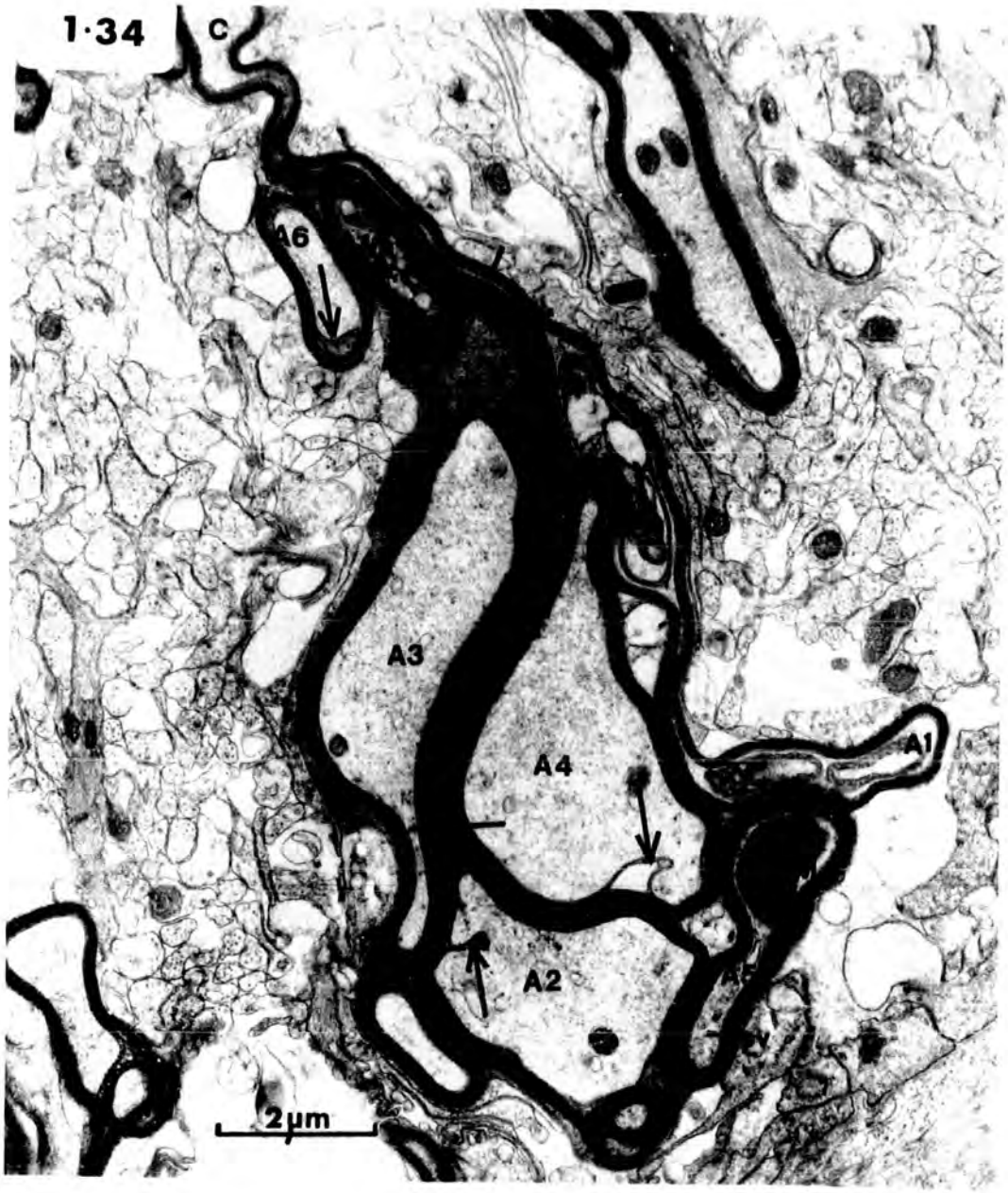
1·34
C
A6
A3
A4
A1
A2
2µm

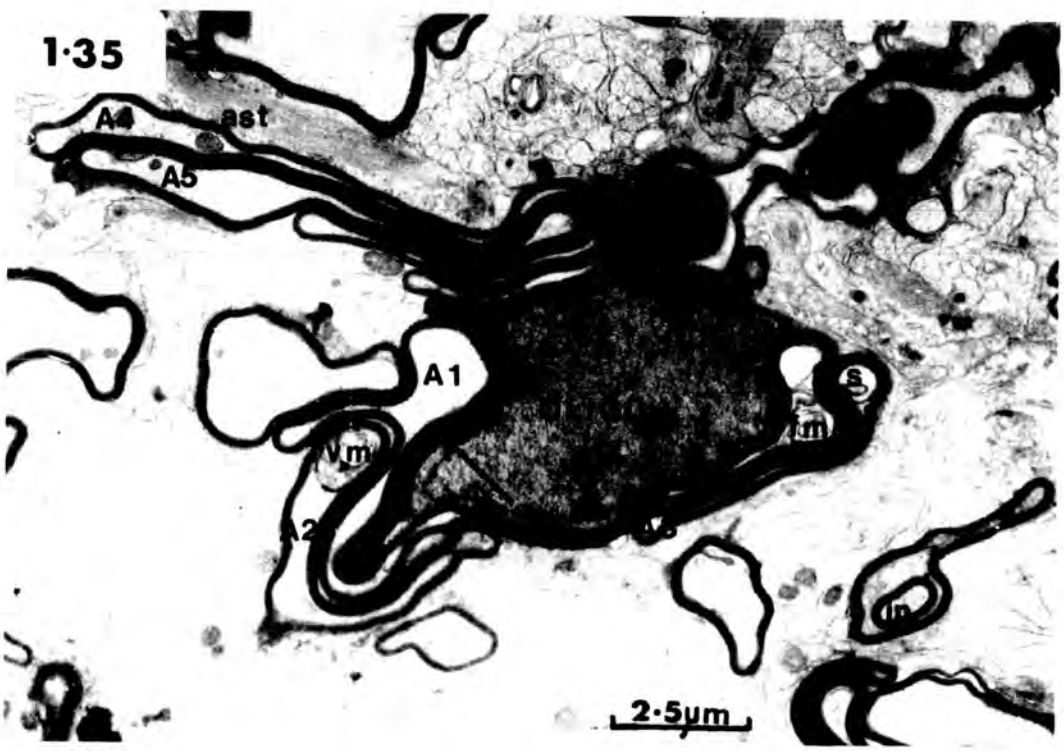
1·35
A4
ast
A5
A1
Vm
2·5µm

Intact fibres may be in association with degenerating areas (figs. 1:29, 1:34 and 1:35), although in some cases no axon is present in any of the myelinated profiles which are actively involved in the degeneration (fig. 1:35 and 1:36). On occasions, the finger-like outpushings may fold back and come into contact with the main myelin sheath (fig. 1:27).

Degeneration of myelin occurs by the glial cells pinching off small amounts of myelin and the myelin figures produced are degraded within the glial cell soma (fig. 1:38). Glial cells involved in myelin degeneration have also been observed to be able to construct new myelin sheaths around other fibres (fig. 1:38). These glial cells contain extensive microfilaments. Degradation and myelination can also occur at glial processes which are some distance from the soma (fig. 1:39).

Two to three weeks after metamorphosis the number of myelin figures and lipid droplets in the glial cells decreases and some glial cells consequently take on a lighter appearance.

(iii) Axonal degeneration. In degenerating optic nerve fibres, adaxonal vesicles are present within the myelin sheath (figs. 1:27, 1:32 and 1:33). The presence of small adaxonal vesicles as in figures 1:27, 1:32 and 1:33, are indicative of ensuing degeneration, since Turner and Glaze (1977) found similar vesicles in newt optic nerve within hours of nerve section. Some axons contain

Degenerating myelin

Fig. 1:36 A large amount of degenerating myelin (DM) is present in an extracellular space which is completely surrounded by myelin. A collapsed myelin loop (CM) is present, which partly surrounds the degenerative space and other myelinated fibres in the vicinity. The outer mesaxon (OM) of the collapsed myelin is present. The nucleus of the glial cell (G) is slightly heterochromatic, and microfilaments (mf) are present within a cytoplasmic process. It is clear that the glial cells are in the process of changing their morphologiaal properties (compare with fig. 1:24). The glial cell (G) also produces myelin around axon A1. Fibre A2 is clearly aberrant with a long loop of myelin which is devoid of axoplasm. In a second glial process, large lipid droplets (L) are present. An astrocyte (AST) is also present which contains degenerating myelin figures (myf). (Stage 64)

Fig. 1:37 Portions of two glial cells are present, an oligodendrocyte soma (OLIGO) and a dark astrocytic process (AST). Two myelinated fibres (A1, A2) abut against the oligodendrocyte and fibre A1 has a clear outer mesaxon (OM). The astrocytic process contains microfilaments (mf) and a large number of myelin figures (myf) which are in the process of degradation. Fibre A3 appears to be intimately associated with the astrocytic process and it is possible that phagocytosis (P) of redundant myelin may be in progress. (Stage 60)

1·36

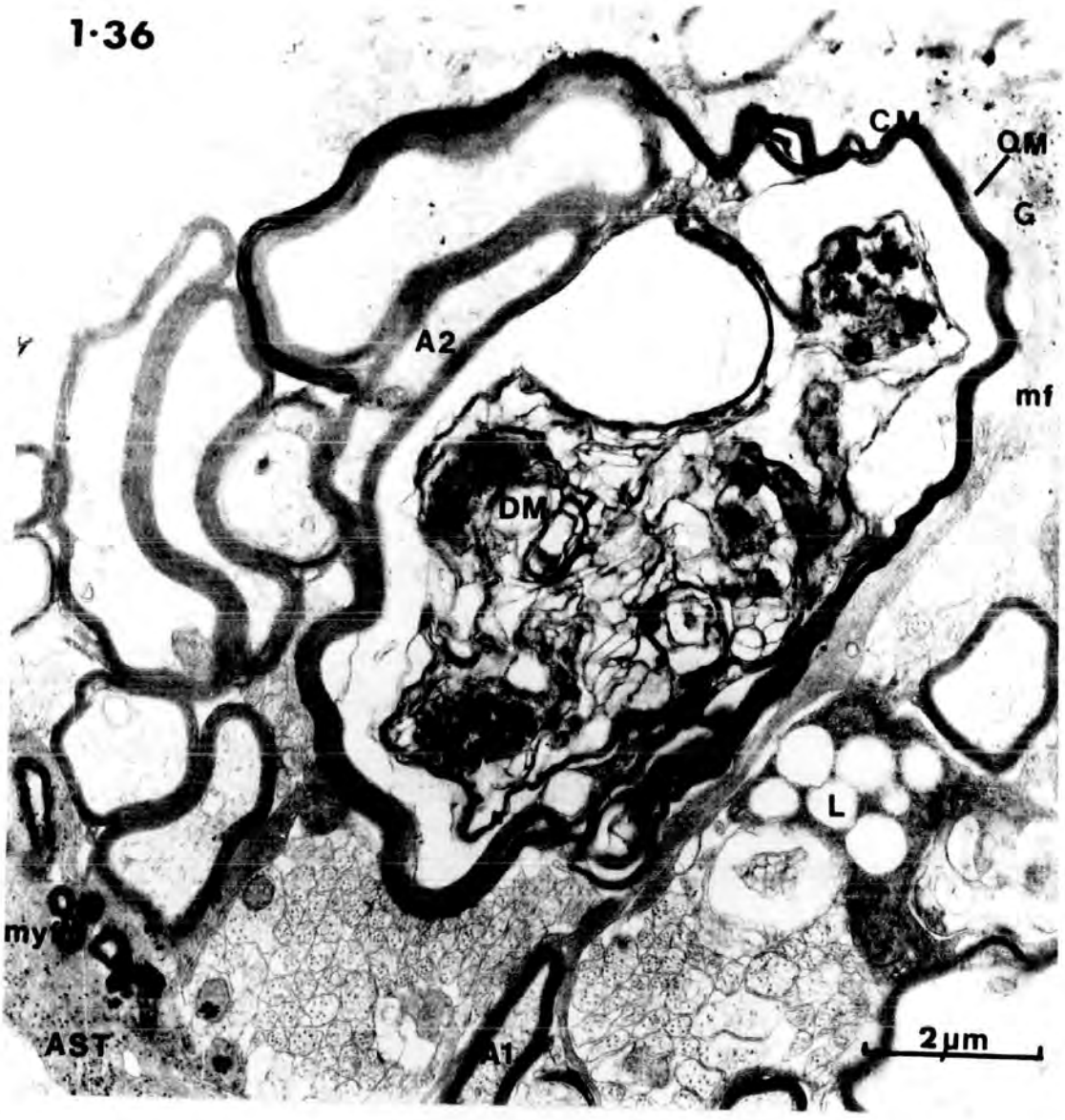

1·37

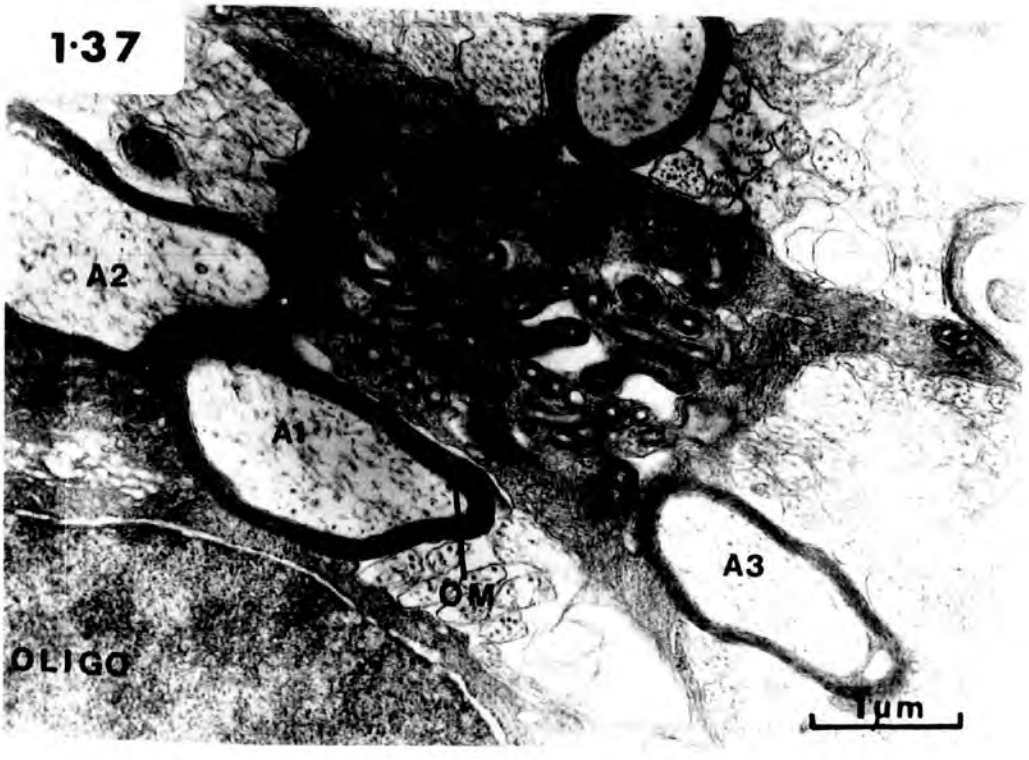

Fig. 1:38 Degenerating myelin and the glial cell involvement

Two major regions of degeneration (DM) are present. Fibre A1 appears to have surrounded a region of degeneration and the two abutting axonal membranes are separated by a thin glial process, since four membranes are present at A1. Within fibre A1, a glial process (GL) is associated with the breakdown of the myelin. The glial cell soma (G) contains microfilaments (mf) and ribosomes (R). It appears to be involved in the myelination of axon A3 and an outer mesaxon (OM) can be seen. The cell is also intimately related with the myelinated fibre A2. An outer mesaxon (OM) is present and the myelin of this fibre is partially invested with glial cytoplasm. Two myelin figures (myf) which are being degraded are visible. At P, myelin debris appears to have been removed from the myelin sheath of fibre A2 by phagocytosis. The glial cell (G) is involved in myelination and also contains microfilaments. Compared with the oligodendrocyte (OLIGO) and the two types of glial cell in figure 1:16, this cell contains a slightly darker cytoplasm, less endoplasmic reticulum (ER) and an excessively indented nucleus. (3 days postmetamorphosis)


1·38
AT
DM
A2
OM
OM
A3
OM
2μm

Fig. 1:39 Degenerating myelin

A number of abnormal myelinated fibres are present (A1, A2), which are adjacent to newly myelinating fibres (nmf). Also evident are major regions of degeneration; either of concentric degrading myelin lamellae (DM) or of large amounts of degenerative debris (DD) within glial cytoplasm juxtaposed to an abnormally shaped myelinated fibre (A1). Note the three close-junctions (CJ) between glial cell processes. (Stage 66)

Fig. 1:40 Axonal degeneration

Two astrocytic glial processes (AST) encircle a degenerating profile. The axon contains microtubules (mt), microfilaments (mf) and a number of mitochondria (mit). Within the axoplasm are large numbers of myelin figures (myf) and myelin debris (D). The myelin (M) surrounding the axon consists of only six lamellae at the most, and the axon is partially encircled by glial cytoplasm (GL). This in turn is surrounded by double myelin membranes. At X, both the axon and glial membranes have ruptured and the contents are starting to mix. At this junction, vesicular membranes (vm) are in abundance. Note the normality of the unmyelinated fibres (U). (Stage 58)

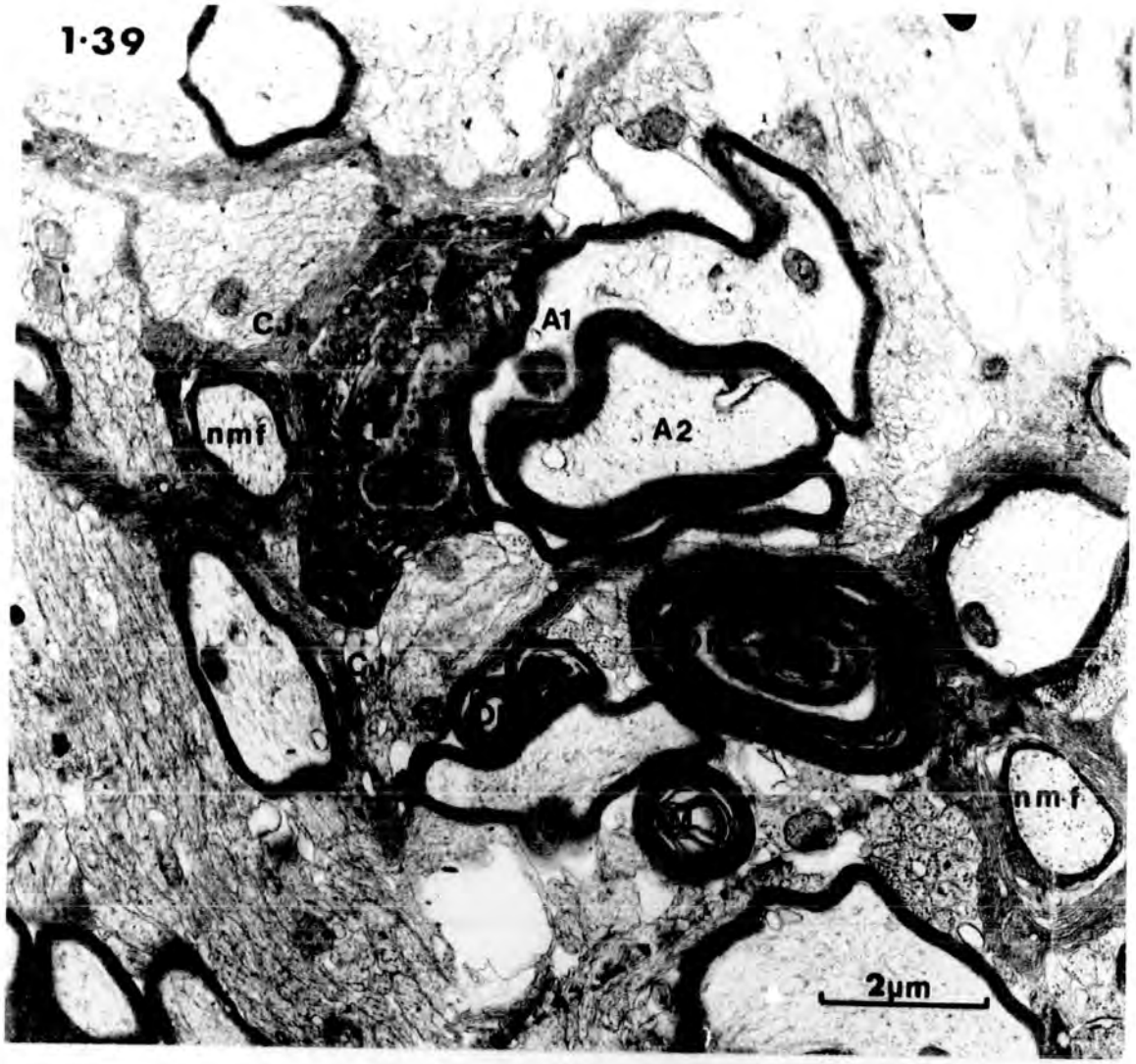
1·39
CJ
A1
nmf
A2
CJ
nmf
2µm

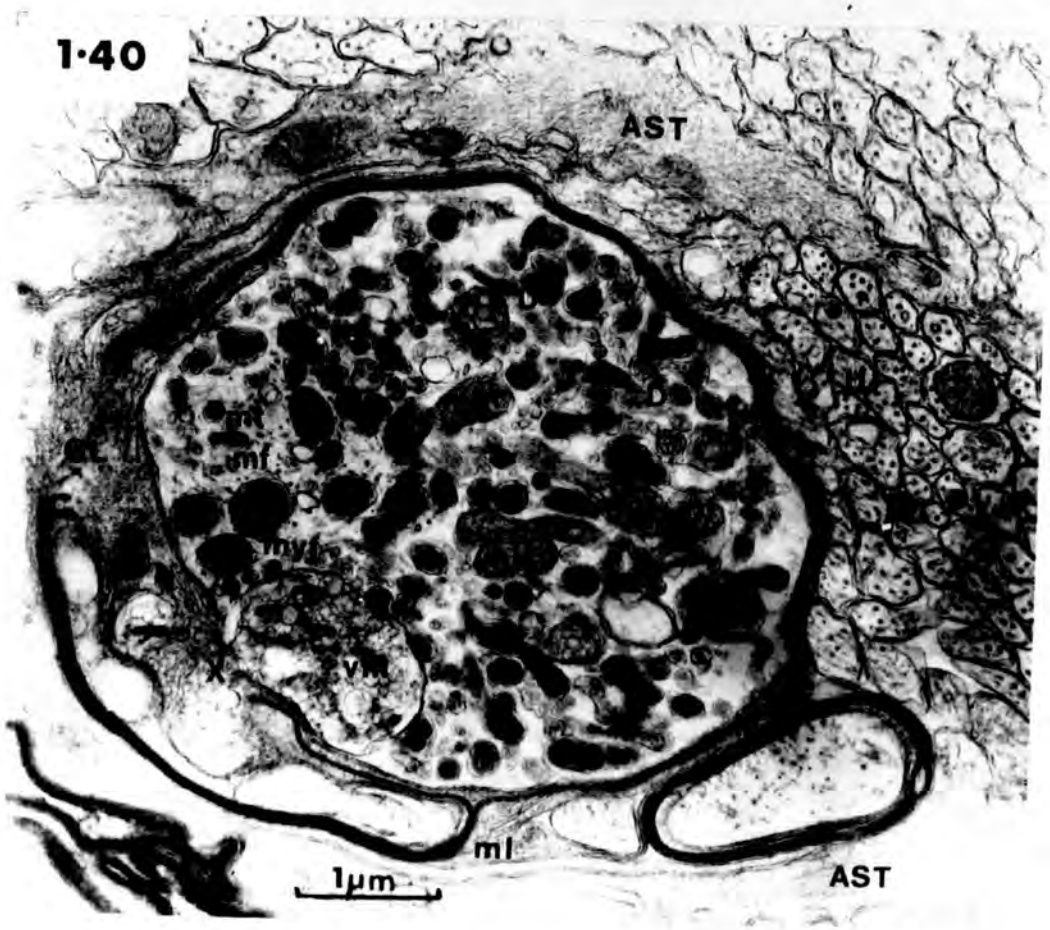
1·40
AST
mf
myl
ml
1µm
AST

increased numbers of mitochondria (fig. 1:40), degenerative products (figs. 1:40 and 1:41) and multivesicular areas may also be found (figs. 1:24, 1:33 and 1:40). Only three axons were observed to be degenerating and were swollen with degenerating material (fig. 1:40) which is present with typical axonal contents such as microtubules, microfilaments and mitochondria. The swollen axon in figure 1:40 has a ruptured axonal membrane and appears to be in a more advanced state of degeneration than the axon in figure 1:41. This is apparent from the increased contents of the axoplasm and the thinner myelin which is absent in places.

During the process of myelin degradation, the characteristic features of the glial cells change. The fibrils which are normally found only in astrocytic processes are present in oligodendrocytes, and there is a decrease in the number of mitochondria present in the somata of both glial cell types. The nuclei become more convoluted and the nucleoplasm and cytoplasm darken as they become laden with lipid droplets, rough endoplasmic reticulum, myelin debris and microfilaments (fig. 1:38). The two types of glial cell take on a uniform appearance at the end of the degenerative period, and remain in this form throughout life.

Fig. 1:41 Axonal degeneration

A myelinated axon (A) contains microfilaments (mf) and mitochondria (mit) but microtubules are not apparent. Within the axoplasm are myelin figures (myf) and large dense lysosomes (LY). The fibre has two outpushings (OP) one of which contains a part of the axon which has separated from the main axon cylinder at X. Within this arm, smooth vesicles (v) can be seen. Aberrant myelin lamellae (AL) are present, surrounded by dark glial cytoplasm, but no axon is evident. (Stage 62)

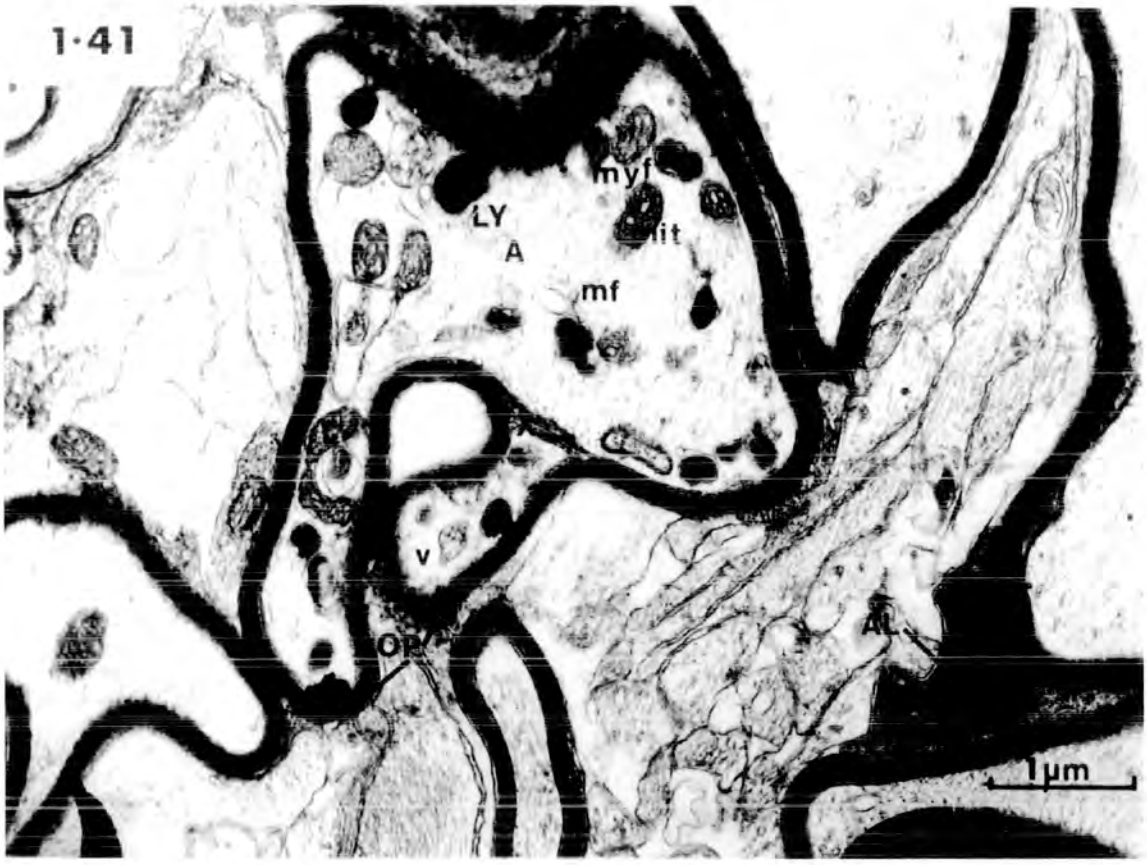
1·41
myf
LY
A
lit
mf
v
OP
1μm

DISCUSSION

The ultrastructure of the adult Xenopus optic nerve resembles that of the optic nerves of other Anuran species, Hyla cinerea, Rana pipiens, Bufo americanus and Bufo terrestris (Maturana, 1960) and of the alligator (Kruger and Maxwell, 1969), the tiger salamander (Gruberg, 1973) and the newt (Turner and Singer, 1974), with a single type of glial cell randomly distributed throughout the nerve. However, Maturana (1960) found capillaries within the optic nerve tissue whereas in Xenopus there is no evidence for their presence. The Xenopus optic nerve is not partitioned by the meninges as in the teleost Eugerres (Tapp, 1973) or human (Cohen, 1967).

A single type of glial cell has also been found in the lamina cribosa and prelamina regions of the cat optic nerve (Wendell-Smith et al, 1966; Blunt et al, 1972) and in the intraorbital portion of the human eye (Yamamoto, 1966; Cohen, 1967; Anderson et al, 1968). Other regions of the cat and human optic nerve contain two types of glial cell, astrocytes and oligodendrocytes. However, the glial cells observed in Xenopus adult optic nerve do not show characteristics which permit them to be identified unequivocally as either of these forms. Peters et al (1970) have characterized

extensively the properties of astrocytes and oligodendrocytes found within the central nervous sytem. The three major criteria used for identification of glial cells were (i) the greater electron-density of both the cytoplasm and nucleus of the oligodendrocytes, (ii) the absence of microfilaments from oligodendrocytes and (iii) the role of oligodendrocytes in myelination and that of astrocytes in support.

The characteristics of the glial cells seen in adult Xenopus optic nerves are a mixture of the properties described above. The presence of microfilaments and occasional microtubules, mainly smooth endoplasmic reticulum, small Golgi apparatus and processes ending as end-feet adjacent to the pia indicate an affinity to astrocytes. However, the presence of irregular heterochromatic nuclei, moderate to dense cytoplasm, absence of glycogen granules and the involvement in myelination indicate oligodendroglial cells.

Anderson and Hoyt (1969) and Cohen (1967) have found in the human optic nerve that the intraocular region, where only unmyelinated nerve fibres occur, contains only astrocytic glial cells. However, in the optic nerve proper where all nerve fibres are myelinated, both types of glial cell are present. They conclude, therefore, that oligodendrocytes are involved in the production of myelin. Some glial cells in the human optic nerve possess characteristics intermediate between astrocytes and oligodendrocytes. These cells contain

a dense cytoplasm, rich in endoplasmic reticulum and with microfilaments in the cytoplasmic processes. On this evidence, Cohen (1967) concludes that astrocytes and oligodendrocytes may represent the two extremes of a spectrum of different glial cell types, rather than two distinct populations. Cohen found similar results in macaque monkeys and mice.

In the premetamorphic tadpole the situation is quite different, with two easily discernable cell types, known as astrocytes and oligodendrocytes (Gaze and Peters, 1960; Reier and Webster, 1974). However, in tadpoles younger than Stage 46 only one type of glial cell is apparent. This glial cell type is located only at the centre of the nerve, and has a uniformly chromatic nucleus, moderate to dense cytoplasm and processes containing microfilaments. Glial cells with similar properties have been described in the newt (Öhman, 1977) and rat (Skoff et al, 1976 a, b). Turner and Singer (1974) have termed these cells ependymoglial cells on the basis of their ultrastructure and the fact that they have been shown to be continuous with the ventricular lining. They also show characteristics of both astrocytes and oligodendrocytes.

In studies of the developing optic nerves of rat Skoff et al (1976 a, b) and cat Blunt et al (1972) have shown the presence of glial cells which contain endo-

plasmic reticulum, Golgi apparatus, and microfilaments. These organelle-rich cells are termed astroblasts. Later in development, they become more electron lucent after a final mitotic division.

In Xenopus, at the time when abnormal myelin profiles are present, the characteristics of the glial cells change. The predominant change is the darkening of the astrocytic cytoplasm during myelin degeneration, with the presence of more organelles and increasing amounts of degenerative debris, so there is little distinction between the two types. This lack of distinction is maintained into adult life.

Similar changes in glial cells have been observed by Blunt et al (1972) in the developing cat optic nerve. Glioblasts give rise to astroblasts and oligodendroblasts and hence to astrocytes and oligodendrocytes. The characteristics of these cells change during development and some astrocytes were observed to be darkening and becoming involved in myelination. They postulate that astroblasts may differentiate to give oligodendroblasts. This has also been suggested by Skoff et al (1976 a, b) who note that although this may be unlikely, a precedent for this concept may be found in the newt Triturus viridescens. In the optic nerve of this amphibian, ependymal-like cells function as both astrocytes and oligodendrocytes (Turner and Singer, 1974). They send end-feet to the surface of the nerve and

also produce myelin. In the spinal cord of the same species, however, both astrocytes and oligodendrocytes are present (Schönbach, 1969).

It is relevant to note that the glial cells which predominate in tissue culture (Bunge et al, 1965) which are responsible for myelination (Ross et al, 1962) and the cells which predominate in developing kitten spinal cord (Bunge et al, 1965) are described as combining dense matrices with filaments and glycogen particles normally distinctive of astrocytes. However, Blunt et al (1972) suggest that these cells should be termed astrocytoblasts. Sturrock (1975) describes cells with a similar appearance from human embryos as astroblasts.

In Xenopus, the evidence from the present study suggests that the glial cells are still immature in the optic nerve of a Stage 46 tadpole, corresponding in character to the astroblast of Blunt et al (1972) and Skoff et al (1976 a, b) or to the ependymoglial cell of Turner and Singer (1974). At Stage 50, two glial cell types are present, the dark oligodendrocyte which is involved in myelination and the lighter structural astrocyte. These two cell types differentiate prior to the period of most rapid myelin production and remain until metamorphosis.

This feature has been described in the rat (Vaughn, 1969; Hirose and Bass, 1973) and reviewed by Davison and Dobbing (1966) where myelination is preceeded by oligodendrocytic differentiation. In both the cat (Moore et al, 1976) and rat (Skoff et al, 1976 a, b) there is an increase in glial cell numbers and an explosive increase in glial cell numbers prior to myelination. Skoff et al (1976 a, b) found that oligodendrocytes start to differentiate about two days prior to the start of myelination in the rat optic nerve, although the vast majority differentiate after myelination has commenced. They also found that these oligodendrocytes were generated well before myelination and those which differentiated late in development were markedly uncharacteristic, having fewer organelles. This they attribute to a lower metabolic activity resulting from a lack of axons for myelination.

During metamorphosis in Xenopus both oligodendrocytes and astrocytes become engaged in the degradation of aberrant myelin, but only the oligodendrocytes are involved in myelination. Both types of glia have high metabolic activities, indicated by the increase in numbers of organelles particularly mitochondria and Golgi cisternae, whereas prior to metamorphosis, only oligodendrocytes have the typical organelle characterisitics that indicate a high metabolic activity. The glial cytoplasm consequently becomes darker, and the two types of glia take on a similar appearance.

After metamorphosis, the main functions of the glia include the maintenance of the myelin and support of the nerve, with an additional low level of myelination. The glial cells then become refractory and appear to dedifferentiate to a form which may be termed an astroblast (Blunt et al, 1972). Astroblasts show morphological characteristics similar to those of either the oligodendrocytes in cat optic nerve (Wendell-Smith et al, 1966) but with more microfilaments, or the less differentiated ependymoglial structure in the newt (Turner and Singer, 1974). To summarise, during embryonic life a single precursor cell is present in the tadpole optic nerve. During larval life, two glial cell types, oligodendrocytes and astrocytes, are present which dedifferentiate to give an ependymoglial cell at metamorphosis.

An interesting feature of the Xenopus tadpole optic nerve is the common occurrence of oligodendrocytes and astrocytes in pairs. This not only includes the glial somata, but also the cytoplasmic processes. The presence of glial processes fasciculating the nerve in all the Xenopus individuals studied suggests that astrocytic processes must be sheet like, rather than cylindrical.

Although the function of astrocytes is unknown, it is possible that the radial sheets guide developing retinal ganglion cell axons to the brain. Their role in the optic nerve may be analagous to the postulated function of astrocytes (Bergmann glia) in the cerebellum,

to provide a pathway for granule cell migration (Rakic, 1971; Rakic and Sidman, 1973). However, this role has been disputed by Das et al (1974) since the astrocytes have not differentiated by the time granule cell migration takes place. Since Skoff et al (1976 a, b) have shown that the origin and the final cell division of glia are not necessarily coincidental, it is likely that the Bergmann astroglia are present for several days prior to their final mitotic division. Furthermore, in both the optic nerve and cerebellum, astroglial processes form the glia limitans before the appearance of microfilaments. Accordingly, their processes may be used as pathways for neuronal migration of axon growth before the glial cells are fully differentiated. In the cerebellum and the optic nerve, the formation of astroglia occurs shortly after the neurons have started to form axons, suggesting that neurons and glia interact very early in development. The first unmyelinated fibres appear in the Xenopus tadpole optic nerve at about Stage 35 (Wilson, 1971) and may induce the differentiation of the glial cells which occurs between Stages 46 and 50. The time interval between Stages 35 and 46 is 56 hours.

One unexpected feature of the adult optic nerve was the presence of newly myelinating fibres (fig. 1:4) even in adults which were large and mature. However, this is

not surprising in the light of the findings that retinal ganglion cells retain their ability to regenerate in adult amphibia (Sperry, 1943, 1944; Maturana et al, 1959; Gaze, 1959, 1970; Gaze and Jacobson, 1963; Jacobson, 1970; Freeman, 1977; Udin, 1977). This is probably due to the fact that amphibia and fish grow throughout life and hence retain some developmental characteristics. This point is accentuated by the ability of goldfish (Yoon, 1971; Schmidt, 1976) and amphibia (Keating, 1974, 1975 a, b, 1977; Keating and Feldman, 1975; Freeman, 1977; Udin, 1977) to retain the plasticity of the central visual connexions even after maturity has been reached. However, the rate of growth and hence plasticity are greatly reduced in the adult nerve, although recently this has been questioned (Freeman, 1977). The plasticity of intertectal connexions in Xenopus has been found to decrease with age (Keating, 1974, 1975 a, 1977).

The process of selection of axons for myelination is unknown, although in Xenopus newly myelinating axons are usually about 1 μm in diameter when observed within oligodendrocytic cytoplasm. The process of myelination in the central nervous system of immature animals has been the subject of several investigations (see review by Bunge, 1968) and experimental remyelination has also been studied (Reier and Webster, 1974; Turner and Singer, 1974).

In Xenopus tadpole optic nerve, myelin is formed only by oligodendrocytes. After a few turns about the axon, the membranes become apposed and the glial cytoplasm is gradually removed. Myelination of an axon may stop after the completion of six or seven turns. This may be due to the impending degeneration of myelin which occurs at metamorphosis. Myelinated fibres generally have an appearance of those within any central tract, although some fibres have aberrant profiles. This is not uncommon in the central nervous system and has already been reported in the acoustic ganglia of goldfish (Rosenbluth and Palay, 1961), the cerebellum of Bufo (Rosenbluth, 1965, 1966), the habenula nucleus of frogs (Kemali and Sada, 1973), rat optic nerve (Peters, 1968), cat spinal cord (Hildebrand, 1971 a, b, c; Hildebrand and Skoglund, 1971) monkey spinal cord (Bodian, 1966), monkey dorsal horn (Beal and Cooper, 1976), human optic nerve (Cohen, 1967) and in Xenopus tadpole optic nerves when the animals were cooled to artifically low temperatures (Cullen and Webster, 1976). Aberrant myelin has also been observed peripherally in guinea pig sciatic nerve (Webster and Spiro, 1960) and in the gastrocnemius and sural nerves of the cat (Berthold and Skoglund, 1968 a, b).

In the case of fibre tracts, large myelin processes have been found to leave one axon and to be engaged in the partial myelination of another (Cohen, 1967). However, in central grey regions the aberrant loops of myelin have been found to wrap around cell somata (Rosenbluth and Palay, 1961; Rosenbluth, 1965; Kemali and Sada, 1973) although the function of these loops is unknown.

Smaller myelin processes are more common in peripheral nerves where they are associated with Schwann cell inpushings and usually occur at a node of Ranvier (Webster and Spiro, 1960; Berthold and Skoglund, 1968 a, b). They are also found centrally in association with glial cell inpushings (Bodian, 1966; Hildebrand, 1971 a, b, c; Hildebrand and Skoglund, 1971). They are more common in developing nervous tissue (Berthold and Skoglund, 1968 a, b) and eventually become involved in degeneration (Berthold and Skoglund, 1968 a, b; Hildebrand, 1971 a, b, c; Hildebrand and Skoglund, 1971). There are numerous cases of cellular degeneration within the central nervous system. However, these cases are possibly genetically determined patterns of cell degeneration and are an important mechanism in vertebrate development (Glücksman, 1951; Saunders, 1966; Saunders and Fallon, 1966; Alley, 1974). These cellular deaths help to determine the final size and shape of organs and organ complexes (Alley, 1974).

Cell death has also been implicated as a morphogenetic mechanism in the developing nervous system. Dying cells free the early neural tube from the overlying ectoderm (Glücksman, 1951), assist in shaping the optic cup (Silver, 1972; Silver and Hughes, 1973) and determine the final size of various neural centres in the spinal cord and brain stem by producing competition within the synaptic field (Hughes, 1961; Prestige, 1965, 1967 a, b; Cowan and Wenger, 1967; Reier and Hughes, 1972; Rogers and Cowan, 1973; Alley, 1974; Clarke, Rogers and Cowan, 1976; Clarke and Cowan, 1976).

However, in Xenopus tadpole optic nerve described here, there is very sparse evidence for axonal degeneration. In fact only three cases were observed. In a preliminary study, no evidence of this or chromatolysis of ganglion cells was observed in the tadpole eye, using light and electron microscopic methods. At the stage of development when degenerative processes are involved, approximately 500 ganglion cells giving rise to myelinated fibres are present. A small number of ganglion cells, if degenerating, would be hard to detect among the 25,000 other ganglion cells present in the eyes of metamorphic tadpoles (Wilson, 1971). However, axonal degeneration may not imply ganglion cell soma death, since after experimental axotomy ganglion cells regenerate new axons (Gaze and Jacobson, 1963; Freeman, 1977). It is possible that the fibres in question may be centrifugal fibres. Rager and Rager (1976) have shown that in the embryonic chick there is an overproduction of axons in the optic nerve, and they postulate, as do Hughes and LaVelle (1975), that ganglion cells which do not make appropriate connexions in the optic tectum degenerate. This degeneration in the normal developing chick may amount to a decrease of nearly 50% (5.2 to 2.8 million, Rager and Rager, 1976).

The growth of the retina in tadpole Xenopus has been studied using multiple pulses of tritiated thymidine (Hunt, 1975; Jacobson, 1976; Straznicky and Tay, 1977). According to Hunt, the quantitative data obtained from this invest-

igation indicate extensive cell death prior to and during metamorphosis. However, he also states that ". . . cell death does occur among retinal ganglion cells, and the modest amount (5%) which occurs during the larval period may well function to eliminate the occasional ganglion cell whose fibre goes astray during tectal innervation." On the other hand, the results of Jacobson are in agreement with those of Straznicky and Gaze (1971) which indicate that the number of labelled cells did not alter significantly with time (1 to 200 days). They conclude that ganglion cell degeneration in the tadpole is insignificant, if it occurs at all. Axotomy without ganglion cell death is also unlikely in that, although contorted, the axons appear healthy in the late stages of myelin degeneration. In the newt, it has been found that Wallerian degeneration of myelinated fibres is completed within 10 days, when the animals are kept at 25°C (Turner and Singer, 1975; Turner and Glaze, 1977), and similarly for degenerating optic nerve myelinated axons in goldfish (Attardi and Sperry, 1963). The Xenopus in the present study were reared at 23°C. Reier and Webster (1974), using Xenopus tadpoles, found that after optic nerve crush myelinated fibres were completely removed within four days. They made no mention of their rearing temperature.

This evidence suggests that if natural axotomy were occurring, degenerating axons would not be in abundance at any given time due to the rapidity of the process. Contrary to this, Kruger and Maxwell (1969) found many axons with normal appearances in the alligator optic nerve nearly 100 days after enucleation. In kittens myelinated fibre degeneration is complete at four days (Cook et al, 1974). It has been suggested by Cook et al that the rapidity of the response in immature animals is due to the higher metabolic rate of immature glial cells.

It is possible that the degeneration observed here could be an artifact of fixation, However, this is unlikely for the following reasons. The nerves were fixed in situ and the preservation of the tissue was generally good, with organelles and their membranes intact, even in areas associated with the degeneration. Bad fixation cannot account for the presence of whole series of myelin figures within the glial cytoplasm. The most convincing piece of evidence against this possibility is the fact that the results are entirely reproducible, with aberrant myelin only ever found to any extent in individuals at a particular stage in development. An environmental effect may be important in this respect since all animals were reared under the same conditions (see General Methods). However, adult toads appear normal in both structural and physiological

respects and some of these laboratory reared toads are now three years old. On inspection of the fifth and seventh cranial nerves, no degeneration of myelin was observed, but this may be due to the fact that the nerves are still growing or that these nerves are part of the peripheral nervous system.

It is interesting to note other events which occur at the same time at this production of contorted axons, aberrant myelin sheaths and subsequent degeneration. Aberrant myelin is most frequently observed at the time of metamorphosis at which time the distance of the eyes from the brain decreases. This narrowing of the head starts at Stage 58-59. Both myelinated and unmyelinated ganglion cell axons are believed to project to the brain and form functional connexions (Chung, Keating and Bliss, 1974). In studies on the developing optic tectum at this time, neither degenerating fibres nor degenerating terminals were observed, and only one fibre with a redundant myelin sheath was found.

Davison and Dobbing (1966) believe that once formed, the myelin sheath is stable in terms of its contents and structure. If the amount of material in both the axon and the myelin sheath is to remain the same when the nerve shortens, the axon cylinder must increase in diameter, but because of the laminated nature of the myelin, it will necessarily be thrown into folds. This may be of the out-

pushing type where large finger-like lateral loops are formed, or by telescoping to produce concentric loops. In this way, these myelin sheaths will become redundant and therefore shortly after this time, myelin figures will appear in the cytoplasm of support cells. However, the evidence from fibre diameter distributions (see Chapter 2) suggests that axons do not increase in diameter to compensate for the decrease in length. An alternative hypothesis is that the nerve fibres could buckle during the shortening of the nerve. In this case, the myelinated fibres would tend to appear normal in cross-section, although the profiles would be elliptical rather than circular and the microtubules would be cut longitudinally.

Aberrant myelin loops and myelin droplets have been observed frequently in developing peripheral nervous system and were implicated by the early light microscopists in the mode of growth of the myelin (Vignal, 1883 a, b; Barden, 1903; Speidel, 1932, 1933; Gütner, 1936). However, these ideas are incompatible with the modern concepts of myelogenesis (Geren, 1954; Peters, 1960 a; Robertson, 1960). The ultrastructure of these loops and droplets has been investigated in the developing gastrocnemius and sural nerves of the kitten (Berthold and Skoglund, 1968 b) and in the kitten spinal cord (Hildebrand, 1971 a, b, c; Carlstedt, 1977 a, b; Berthold and Carlstedt, 1977 a, b).

Berthold and Skoglund considered the possible roles of these fragmenting bodies as (i) a myelin sheath precursor, (ii) myelin actually generated within the Schwann cell cytoplasm that would subsequently be added to the myelin sheath, or (iii) that these bodies represent myelin sheaths in different stages of disintegration. They considered the first role improbable and the second role unlikely, from the point of view that it would implicate a new method of myelination. They found the third possibility was acceptable. They suggested that the only obvious source of these sheath fragments were the aberrant myelin outgrowths that had lost contact with the main myelin sheath. In premetamorphic Xenopus tadpoles no myelin or lipid droplets appear prior to myelination. Neither do they occur in the adult where much additional myelination is continuing. The only time lipid droplets or myelin figures appear is during the period of myelin degradation about the time of metamorphosis and very occasionally in adults.

The hypothesis that degeneration is the source of the observed myelin figures is further supported by the high incidence of lamellated glial inclusions during Wallerian degeneration (Kruger and Maxwell, 1969; Cook and Wisniewski, 1973; Cook et al, 1974; Reier and Webster, 1974; Turner and Singer, 1975; Turner and Glaze, 1977) and chemically induced degeneration (Singer and Steinberg, 1972; Wisniewski and Raine, 1971; Prineas et al, 1969). It is well known that

injury to the nervous system by trauma or disease is accompanied by microglial proliferation (Blinzinger and Hager, 1964) and it is of interest to note the absence of microglial cells from Xenopus optic nerves even at a time of extensive degeneration. It has been suggested (Blinzinger and Hager, 1964) that because microglial phagocytes ingest necrotic cells the absence of microglia may be due to the absence of glial necrosis. The lack of glial cell death may be due to the fact that glial cells in the optic nerve have been observed to degrade and synthesise myelin simultaneously.

There appear to be three methods by which the myelin breakdown is brought about and these have been termed inpushing, outpushing and axonal, according to their basic appearance. The inpushing mode of degeneration appears to be very similar to the telescoping of myelin described by Kruger and Maxwell (1969) during Wallerian degeneration after enucleation in the alligator. These workers suggest that during Wallerian degeneration telescoping within an internode or between adjacent internodes occurs, thereby providing one axis cylinder with two or more sheaths of approximately equal thickness. The axon itself need not be in a central position. They also suggest that the sequestering of myelin into huge telescoped deposits could be a satisfactory mechanism for bringing this material closer to those cells capable of

manufacturing hydrolases for the degeneration and disposal of myelin. However, from the observations made of the inpushing type of degeneration in the present study, it appears as if the parent oligodendrocyte is the destructive element in this process. The myelin which is broken down is then translocated intracellularly to regions of myelin synthesis.

The outpushing mode of degradation appears to be mediated by astroglia, which have been reported to be involved in myelin degradation by attacking the nodal regions (Hildebrand, 1971 c). In a number of micrographs (figs. 1:25, 1:27, 1:28) it can be seen that the degradation of the myelin is such that the myelin membranes appear to be peeling away.

The presence of three axons showing signs of degeneration cannot easily be explained except in terms of axotomy or involvement of the ganglion cell itself in the degeneration. A more likely possibility is the case suggested by Singer and Steinberg (1972) that the glial cytoplasm, with its organelles, invades the myelin sheath adaxonally, as observed here, and erodes the axolemma. The contents fuse and degeneration ensues. It is important to keep in mind the continued presence of myelinated axons which appear healthy.

The simplest explanation for this degenerative process is the removal of whole internodes rather than small sections of myelin, as suggested by Berthold and Skoglund (1968 a, b) and also observed by Hildebrand (1971 c). However, in these cases, internodes are removed by the production and phagocytosis of aberrant myelin loops. The function of internode removal is to prepare the axon for its increase in size and conduction velocity, and the inextricably related increase in myelin thickness.

The degeneration observed in the tadpole optic nerve is clearly different from that of Wallerian degeneration produced by axotomy. In the instance discussed here, throughout the whole period of degeneration the axons within the myelin appear to be normal, whereas Wallerian degeneration usually ensues after signs of degradation in the axon are observed.

The inescapable conclusion regarding the function of myelin degeneration in the developing optic nerve is that linked to the requirement for the removal of excess myelin occurring as a consequence of the shortening of the optic nerve. The finding of insignificant axonal degeneration suggests that "programmed" axon degeneration during development is not a feature of the optic nerve afferent input to the tectum.

To determine whether the degeneration of myelin observed here can be linked to the movement of the eyes towards the brain with the shortening of the optic nerves, it may be useful to study other Anuran species such as Bufo or Rana during metamorphosis. Since their optic nerves do not shorten at this period, one would predict that no abnormal myelin would be present in these animals.

CHAPTER II

Fibre diameter distributions of myelinated and unmyelinated fibres in the developing optic nerve

INTRODUCTION

In addition to the qualitative study reported in the previous chapter, a quantitative analysis of the optic nerve components was carried out to determine the fibre diameter distributions and the relationship between axon diameter and the thickness of the myelin sheath. Compound action potentials could then be reconstructed from the data on fibre diameter distributions (Gasser and Erlanger, 1927).

Particular attention was given to the period of metamorphosis since abnormal myelin profiles occur at this time (Chapter 1) and this stage of development has been neglected by other workers (Gaze and Peters, 1961; Wilson, 1971).

METHOD

From the 27 optic nerves of tadpole and adult Xenopus used in Chapter 1, eight nerves from animals of different ages were used to determine the fibre diameter distributions. A single nerve was taken from representative stages of pre- and post-metamorphic Xenopus as follows: Stage 50, premetamorphosis; Stage 54, end of premetamorphosis; Stage 58, start of metamorphosis; Stage 60, during metamorphosis; Stage 66 end of metamorphic climax; six months of age and adult. Both nerves were taken from the Stage 58 animal to determine the variability within an individual. Adequate statistical comparison of the distributions would require fibre counts and measurements from at least ten nerves from each developmental stage. Such a study was prohibitive in terms of time and cost.

To overcome possible shrinkage effects, all nerves were prepared by the same method. Another nerve fixed in 1% glutaraldehyde in cacodylate buffer produced results which were markedly different from those derived from a nerve obtained from a comparable animal which had been fixed and prepared by the routine method. In the case of the cacodylate prepared nerve, the fibre diameter distribution was of a different shape, the fibres were larger and consequently the mean and mode were higher. However,

although the procedure of fixing, embedding and measuring was standardized, these facts do not exclude the differential effects of fixation and shrinkage of tissue. Any shrinkage which does occur is unlikely to have a differential effect on the axons within a given nerve, and so should only affect the absolute values of the distribution. However, differences between nerves may result from the differential effects of fixation on tissue from different aged animals.

Whole nerve montages were produced at a magnification of x 4,000, for axon measurement and counting. These micrographs were subsequently enlarged to a final magnification of x 20,000.

Identification Criteria

In similar studies, other workers have indicated that glial cell processes may be identified wrongly as axons (Gaze and Peters, 1961; Wilson, 1971). However, in the tadpole optic nerve two glial cell types are present, one containing dark cytoplasm (oligodendrocyte) and the other containing a ligher cytoplasm with dense bundles of microfilaments (astrocyte). Both of these types could be readily distinguished from each other and from axons in transverse sections. Similarly the presence of glial cell processes could be identified readily in the adult optic nerve, since only one type of glial cell is present. The glial cytoplasm in this case appears darker than that of the axons and also contains dense groups of microfilaments.

Axons could be identified readily by the presence of microfilaments and microtubules distributed within a light coloured cytoplasm and in some cases by the presence of a normal myelin sheath.

The criterion for a newly myelinating axon was that the unmyelinated axon in question was encircled by glial processes and possibly was surrounded by a few loose myelin wrappings. It is possible that these regions may have been nodes of Ranvier.

During the period of metamorphosis a number of myelinated fibres were degenerating and aberrant myelin profiles occurred. The assessment of the normality of these fibres was inevitably subjective. Fibres were measured only when the microfilaments and microtubules were circular in transverse section and when the myelin sheath, where present, had a regular periodicity.

Fibre Measurements and Counts

No attempt was made in this study to estimate the numbers of unmyelinated fibres present, since this seems to have been carried out quite successfully by Wilson (1971), who obtained a reasonable agreement between the number of axons present in the optic nerve and the number of ganglion cells in the eye. This data is plotted in Figure 2:8.

On the other hand, every myelinated fibre from each of the optic nerves studied, was counted.

Inaccuracies in measurement of the axonal profiles may occur when the profiles are not circular which was often the case. In the case of unmyelinated fibres two orthogonal diameters were measured, the mean taken and recorded in class intervals of 0.05 μm. At least 1,000 fibres were measured routinely except in the adult animal, where more than 2,000 unmyelinated fibres were measured. This data was then used to compile histograms.

Similarly, many myelinated fibres exhibited non-circular outlines (see fig. 1:6), and therefore diameters were difficult to measure. An attempt to avoid this problem was made by measuring the perimeter of the axon with an opisometer and converting this value to a diameter, had the periphery been circular. This strategy was employed since the conduction velocity of an axon is related to membrane area and hence diameter, and because most theoretical relationships between axon size and conduction velocity are associated with the diameter. The measurements were grouped into centimetre classes, which corresponded to 0.159 μm actual size.

The ratio of axon diameter (d) to fibre diameter (D) was also calculated, $p = {}^{d}/_{D}$ (Rushton, 1951), by measuring both axon and myelin peripheries, and these were measured to the nearest 1 mm (equivalent to a diameter of 0.0159 μm).

In the calculation of ρ errors can occur in measuring the periphery of the axon and the fibre, since the ratio strictly requires two concentric circles. Any part of the axon or fibre in which the cross-section is not circular will tend to make the two perimeter values for that portion of the fibre more similar and hence the value calculated for ρ will tend to be high. However, if the axons and fibres had been circular the method would be inapplicable, since it would be possible to measure the diameters directly.

Routinely at least 1,000 myelinated fibres were measured except in the cases where under 1,000 were present. A number of profiles were obviously abnormal or degenerating (see Chapter 1). These fibres were counted but not measured. Histograms were compiled with respect to the number of normal fibres measured.

The diameters of newly myelinating fibres were determined and the results were pooled in order to produce histograms.

However, the configuration of an axon and/or its sheath changes along its length (Meyer-Koenig et al, 1972; Treff et al, 1972) and this can be appreciated fully by viewing longitudinal sections of the nerve (Webster and Spiro, 1960; Berthold and Skoglund, 1968 b; Hildebrand, 1971 b, c). Therefore, fibres may appear normal when measured at one particular position in the nerve but may have aberrant processes at a different level. The diameters of the fibres may also vary along their length, but since it is a whole population that is under study, the general trends exhibited may be regarded as valid.

RESULTS

Axon diameter distributions of myelinated, unmyelinated and newly myelinating fibres were obtained from a developmental series of Xenopus tadpole and adult optic nerves. The ratio of the axonal and myelin sheath diameters $^{d}/_{D}$ was also determined for myelinated fibres.

In the nerves from metamorphic tadpoles and six months old and mature adult toads some irregular profiles were also present. These were counted but not measured. The axon diameter distribution of myelinated fibres at Stage 50 was not constructed since only eleven of these were present. In one Stage 54 optic nerve, the number of myelinated fibres only was determined.

Myelinated fibres

Myelinated fibres first appear at Stage 50 when eleven were present. They increase steadily in number to 229 at Stage 54 and to about 500 at Stage 58. There is a slight decrease at Stage 60 to 453. This decrease is likely to be peculiar to the individual used rather than a sign of general axon loss. From the end of metamorphosis the number increases once more to 594. After this period numbers

increase to 2,052 in a six month old toad and to 2,769 in a mature adult (Table 2:1 and fig. 2:8).

(i) Premetamorphosis

At both Stages 50 and 54 the numbers of myelinated fibres were only counted. No measurements were made since too few myelinated axons were present.

(ii) Metamorphosis

The diameter distributions of myelinated axons from nerve S58A is unimodal (fig. 2:2), nearly symmetrical, and distributed about a mean diameter of 1.97 μm. All 496 myelinated fibres present were measured. Nerve S58B is somewhat different (fig. 2:3). The distribution is again unimodal, with a slight positive skew. There is an increased number of larger fibres which results in the higher mean diameter value of 2.26 μm. The number of fibres present is greater by 67, more naked axons are becoming myelinated (Table 2:1) and there are also eight fibres present which have aberrant myelin profiles compared with none in S58A. The nerves S58A and S58B were obtained from the same animal and were used to determine the variability within one animal compared to the differences between animals of different stages. Figure 2:1 shows the change of the mean and the mode of myelinated axon diameters during development. From

TABLE 2:1

This table summarises the means and modes of the fibre diameter distributions of myelinated and unmyelinated fibres, the means and modes of the calculated values of ρ, and the total number of myelinated, newly myelinating and abnormal fibres in the eight nerves studied. Dashes indicate that no data was taken from these nerves.

TABLE 2:1

Stage	Myelin		$^{d}/_{D}$		Unmyelin		Total No. Myelin	No. new Myelin	No. Abnormal
	Mean	Mode	Mean	Mode	Mean	Mode			
S50	-	-	-	-	0.263	0.175	11	87	0
S54	-	-	-	-	-	-	229	-	-
S58A	1.97	1.67	0.845	0.885	0.328	0.275	496	27	0
S58B	2.26	1.83	0.858	0.885	0.343	0.300	563	41	8
S60	2.16	1.99	0.833	0.855	0.340	0.275	453	71	172
S66	1.57	1.51	0.768	0.755	0.288	0.275	594	59	49
6M	1.20	0.87	0.737	0.805	0.271	0.225	2052	-	-
Ad	1.63	1.11	0.702	0.725	0.357	0.275	2769	-	-

Fig. 2:1 Mean and modal diameters of myelinated axon populations in optic nerves of developmental tadpole stages and two adults. The two values (a and b) of means and modes plotted for a Stage 58 tadpole are the separate values obtained from both nerves in a single animal.

2·1

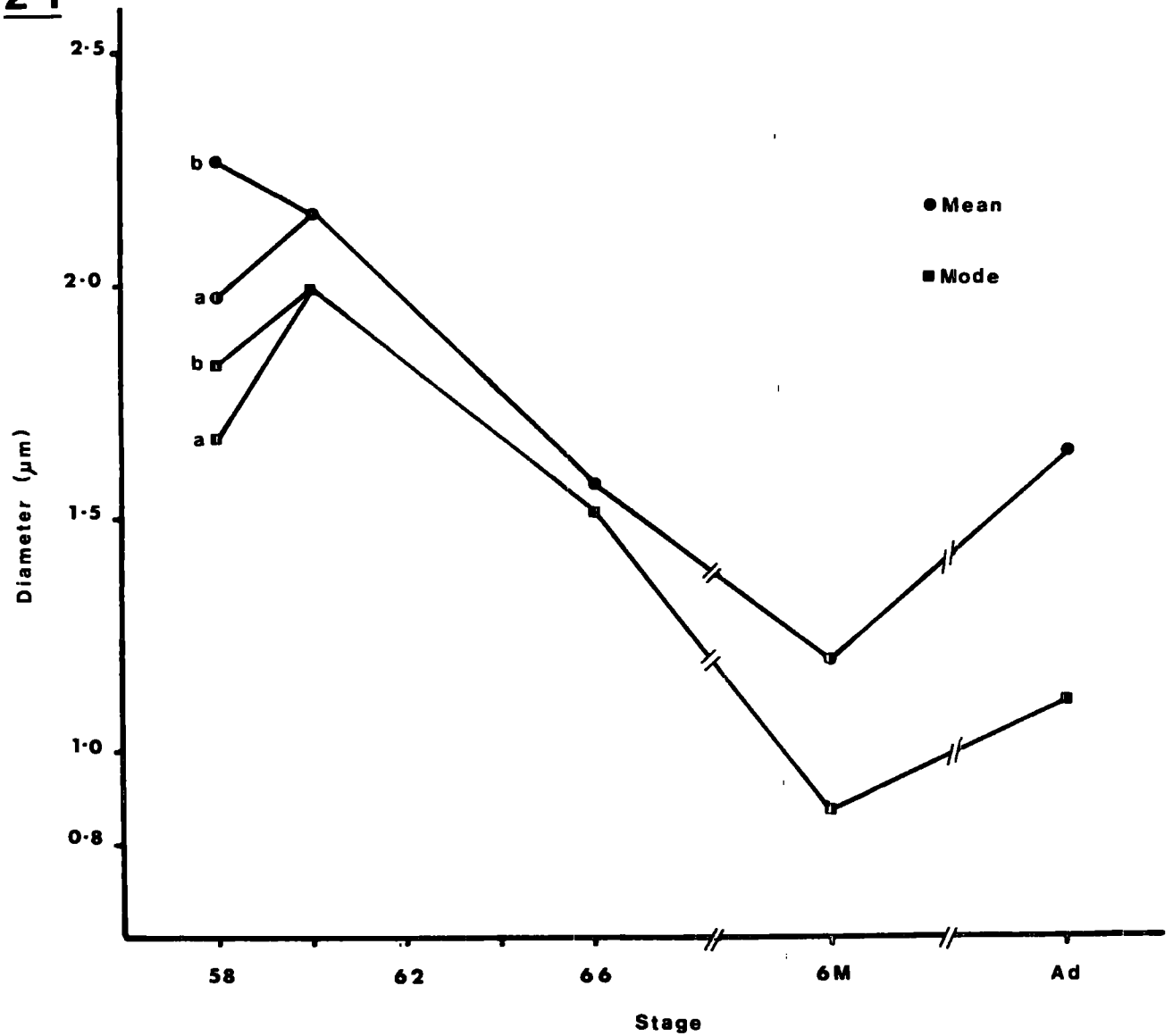

Fig. 2:2 Axon diameter histogram of myelinated axons measured from one optic nerve of a Stage 58 tadpole. The histogram is based on measurements of the total complement of myelinated axons (496). The mean diameter calculated for this unimodal distribution is 1.97 μm ± 0.025 S.E.

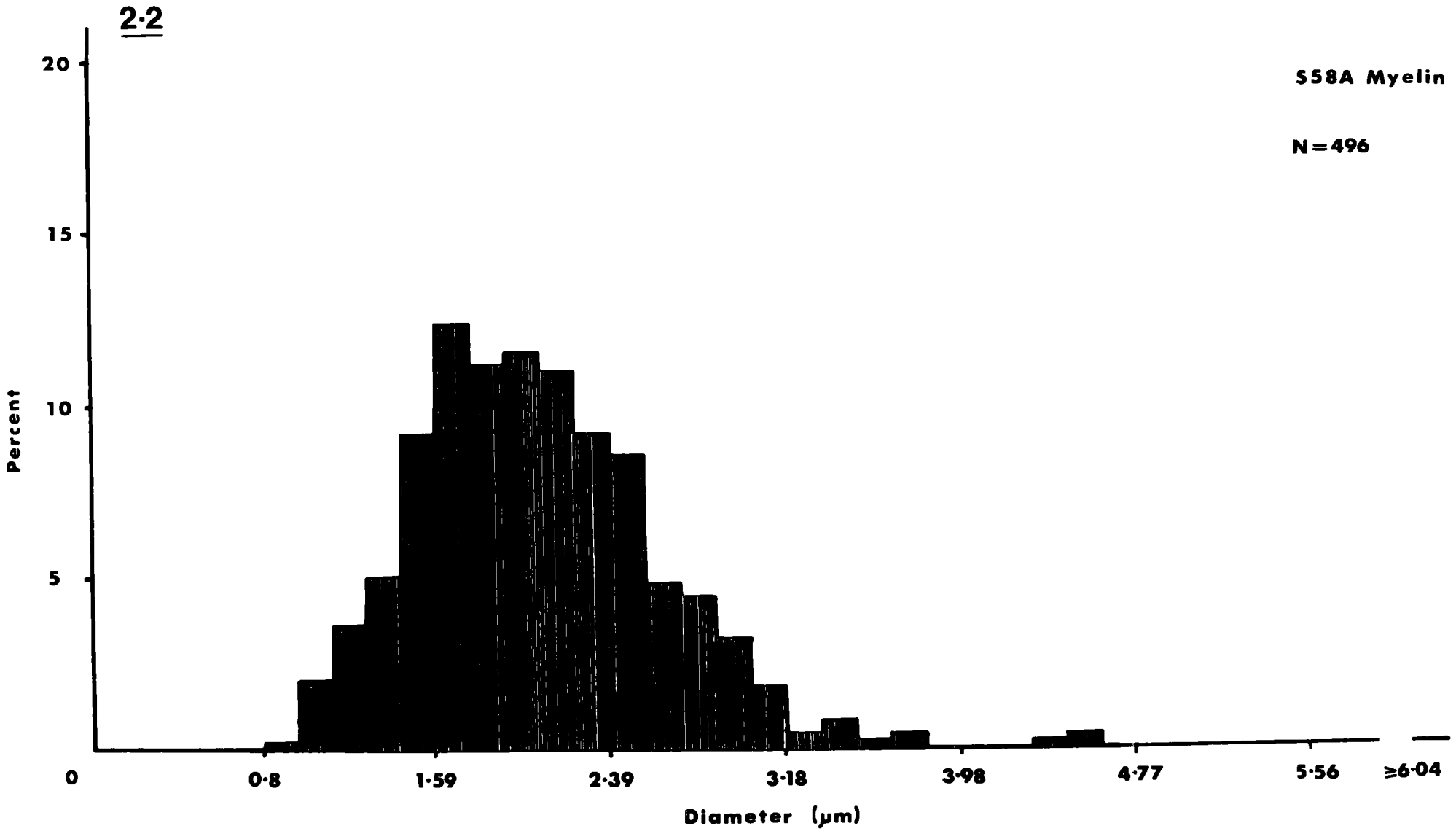
2·2
S58A Myelin
N=496
20
15
10
5
0
Percent
0·8
1·59
2·39
3·18
3·98
4·77
5·56
≥6·04
Diameter (μm)

Fig. 2:3 Axon diameter distribution of myelinated fibres of the second optic nerve taken from a Stage 58 tadpole. The mean axon diameter for this nerve is 2.26 μm ± 0.033 S.E. based on measurements of all 563 axons.

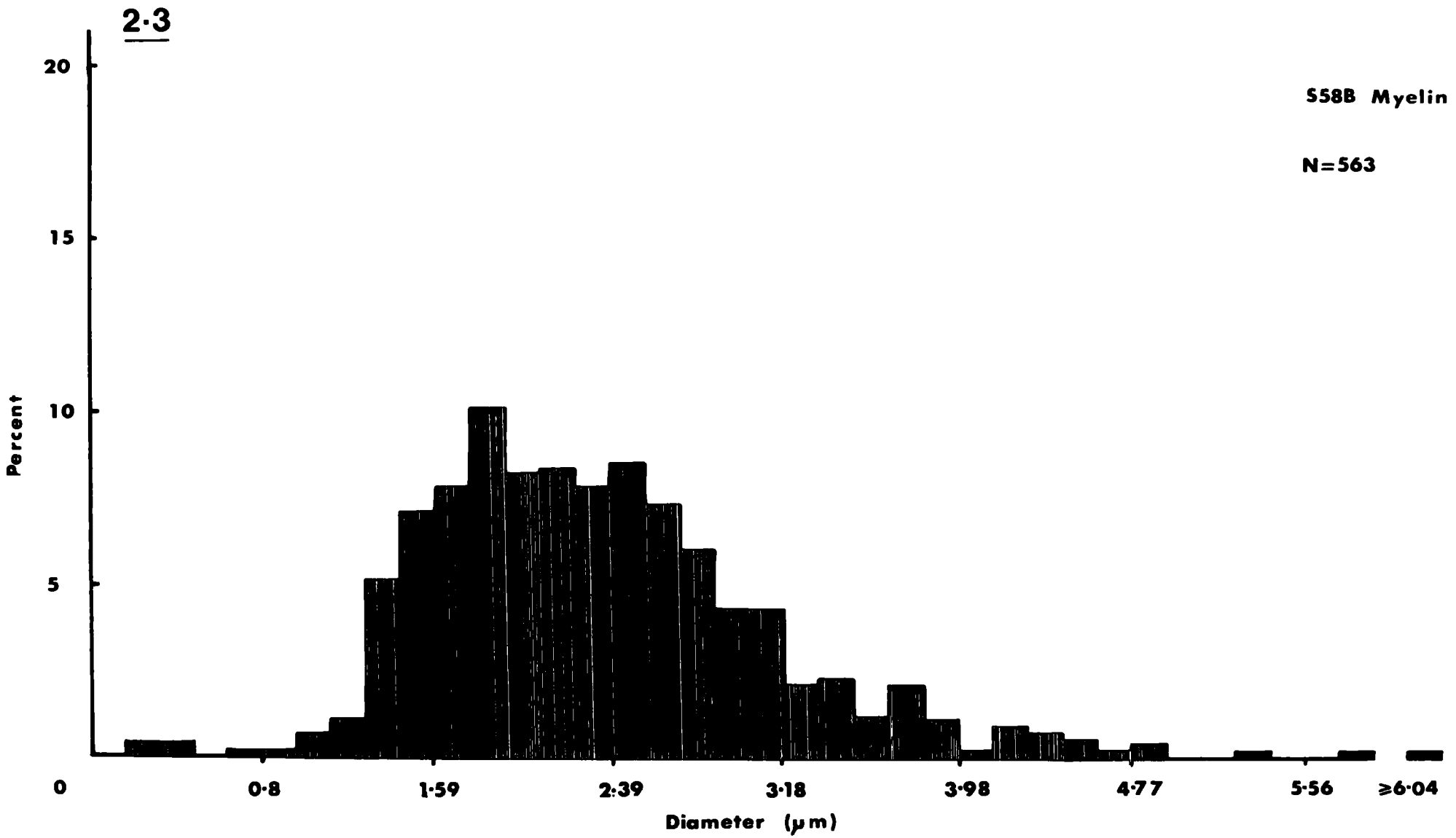
2·3
S58B Myelin
N=563
Percent
20
15
10
5
0
0·8
1·59
2·39
3·18
3·98
4·77
5·56
≥6·04
Diameter (μm)

this graph, it is clear that the values from the two nerves from the same Stage 58 animal differ. The mean diameter of fibres from S58A is some 20% less than that from S58B, and the mode of the distribution from S58A is also less than from S58B.

At Stage 60 (fig. 2:4) the myelinated axon diameters show a unimodal distribution although there are a number of smaller peaks also present. The mean diameter (2.16 μm) falls between the values obtained for the Stage 58 nerves, but the modal value is somewhat higher (Table 2:1, fig. 2:1). These results are based on 281 fibres measured out of a total of 453 myelinated fibres present. The remainder showed abnormal profiles or signs of degeneration and represent 38% of the total myelinated fibre population.

Figure 2:5 shows the histogram of the myelinated axon diameter distribution from an animal at the end of metamorphosis (Stage 66). The distribution is positively skewed with a mean value of 1.57 μm and a modal value of 1.51 μm (Table 2:1). The distribution is based on measurements from 535 fibres. In addition 49 fibres (approximately 8% of the total) showed degenerative profiles.

The values obtained for the mean and the mode are lower than those obtained from tadpole nerves (fig. 2:1 and Table 2:1). Inspection of the histogram (fig. 2:5) suggests that this decrease is concomitant with a reduction in the numbers of larger axons compared to S58A and S58B nerves (figs. 2:2 and 2:3). This reduction possibly begins at Stage 60 (fig. 2:4).

Fig. 2:4 Histogram of the axon diameter distribution of normal myelinated fibres (total 281) in an optic nerve of an animal during metamorphosis (Stage 60). The mean diameter calculated for this distribution is 2.16 μm ± 0.053 S.E. One hundred and seventy-two myelinated fibres in this nerve were not included in the distribution as they showed abnormal profiles or signs of degeneration.

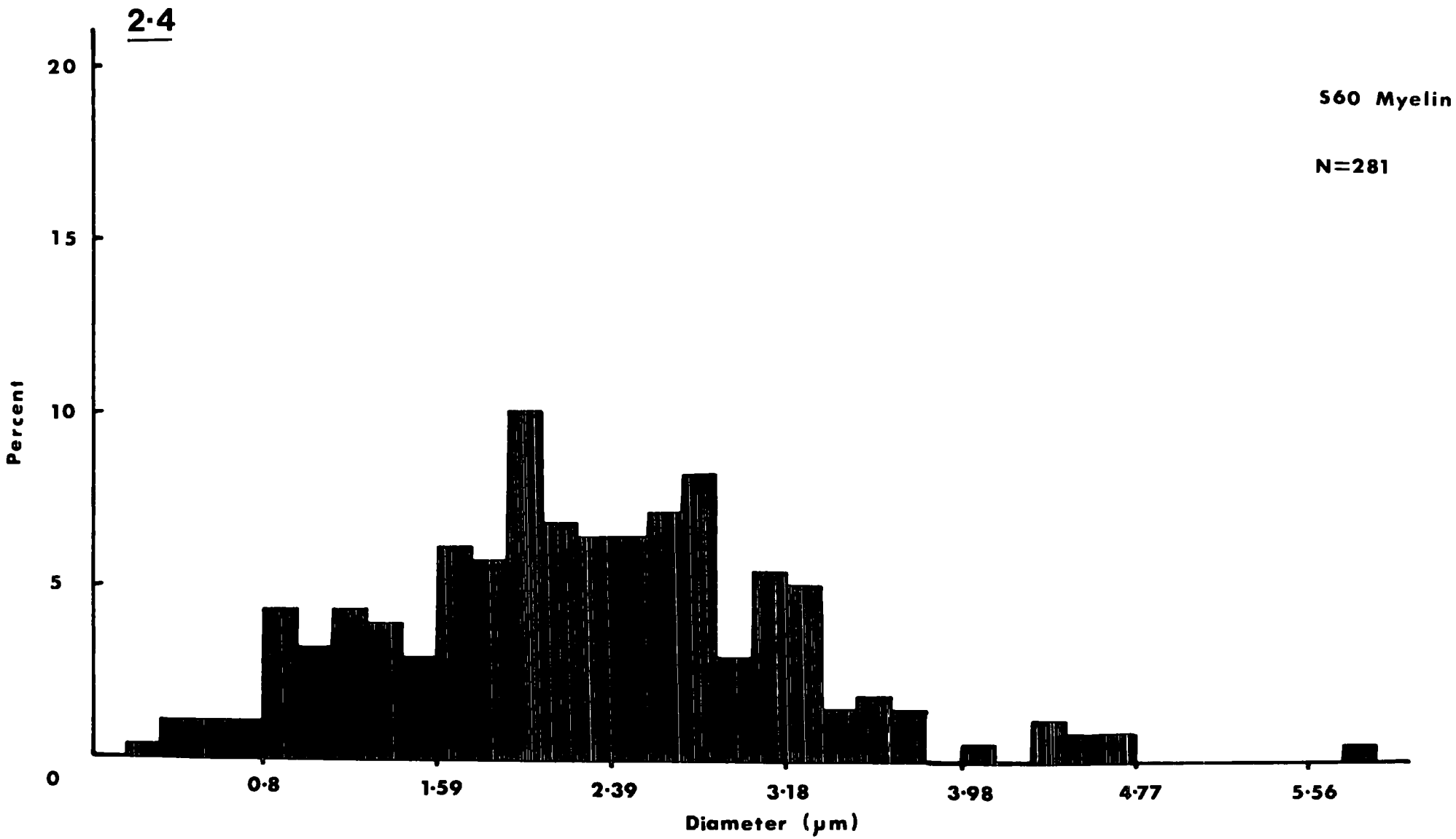
2·4
560 Myelin
N=281
Percent
20
15
10
5
0
0·8
1·59
2·39
3·18
3·98
4·77
5·56
Diameter (μm)

Fig. 2:5 Myelinated axon diameter distribution from an optic nerve of an animal at the end of metamorphosis (Stage 66). The distribution is based on measurements of 535 axons. Forty-nine fibres showing degenerating profiles were not included. The mean axon diameter for this distribution is 1.57 μm ± 0.060 S.E. A significant difference ($P < 1\%$) between the means of Stage 60 and Stage 66 was indicated by a 'Students' t-test ($t = 7.381$).

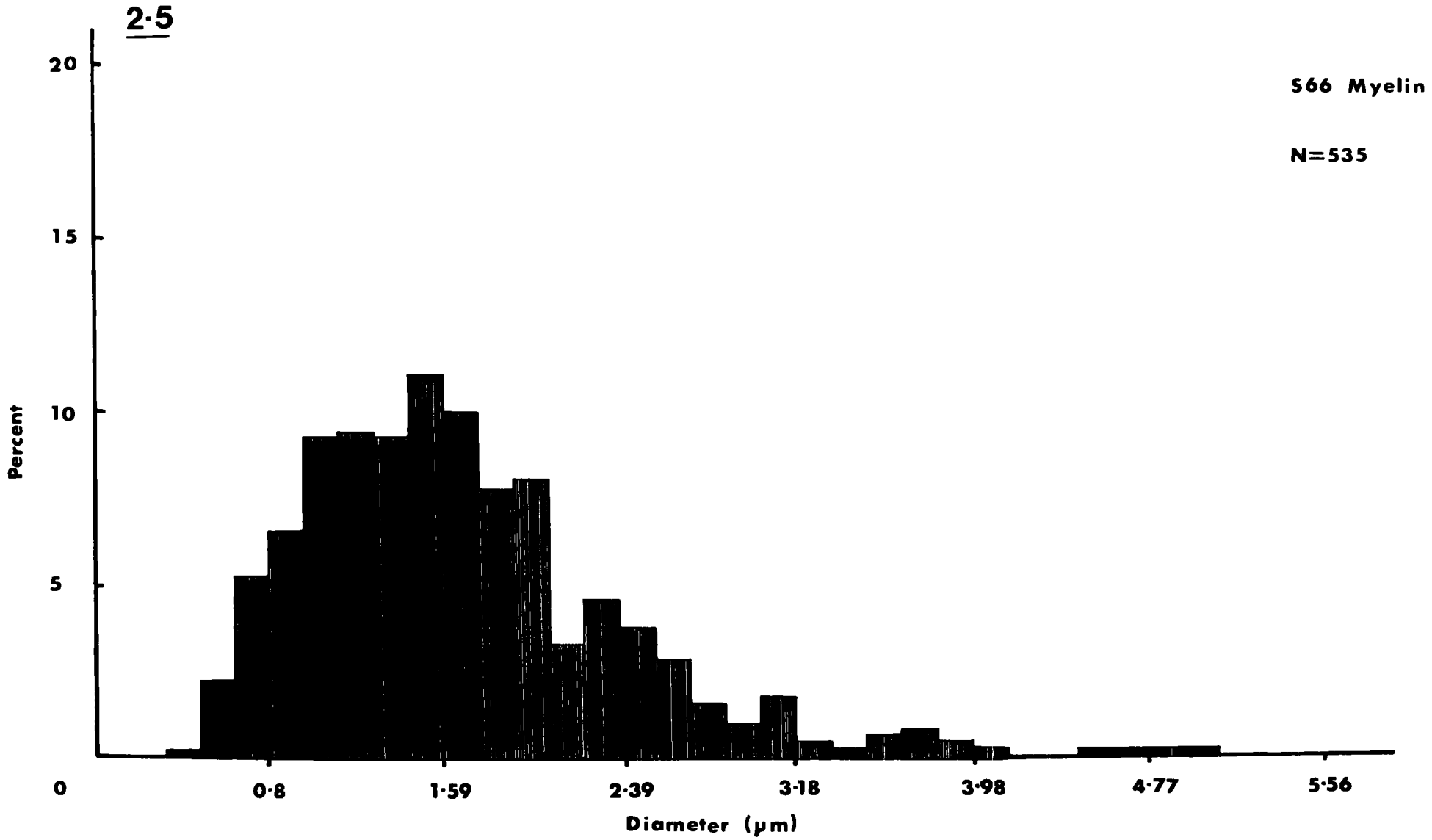
2·5
S66 Myelin
N=535
Percent
20
15
10
5
0
0·8
1·59
2·39
3·18
3·98
4·77
5·56
Diameter (μm)

(iii) Postmetamorphosis

The diameter distribution of myelinated axon diameters from a six months postmetamorphic toad, shown in figure 2:6 is produced by the measurement of 1,041 fibres out of a possible 2,052. The distribution is positively skewed and unimodal, with a mean diameter of 1.20 μm and a mode of 0.87 μm. Both these values are much lower than those from the Stage 66 animal and in conjunction with the histogram in figure 2:6 indicate a relative increase in the numbers of myelinated fibres in the small diameter range. The mode has decreased from a value of below 2 μm at Stage 58 to one below 1 μm at six months postmetamorphosis (fig. 2:1 and Table 2:1).

In the adult nerve the myelinated axon diameter distribution is positively skewed (fig. 2:7) and is derived from measurement of 1,132 fibres out of a total of 2,769 myelinated fibres present. The mean axon diameter has increased to 1.63 μm and reflects the presence of larger diameter fibres. However, the low modal value reflects the large numbers of fibres below 1 μm in diameter (fig. 2:7 and Table 2:1).

The distribution is similar to that obtained by ter Keurs (1970) for myelinated fibres in the optic nerve of Rana temporaria.

Fig. 2:6 Distribution of myelinated axon diameters from a six months postmetamorphic toad optic nerve. The mean axon diameter based on measurements of a sample of 1041 axons for this unimodal, skewed distribution is 1.20 μm ± 0.020 S.E. A significant difference ($P < 1\%$) between the means of Stage 66 and a six month old toad was indicated by a 'Students' t-test ($t = 5.85$).

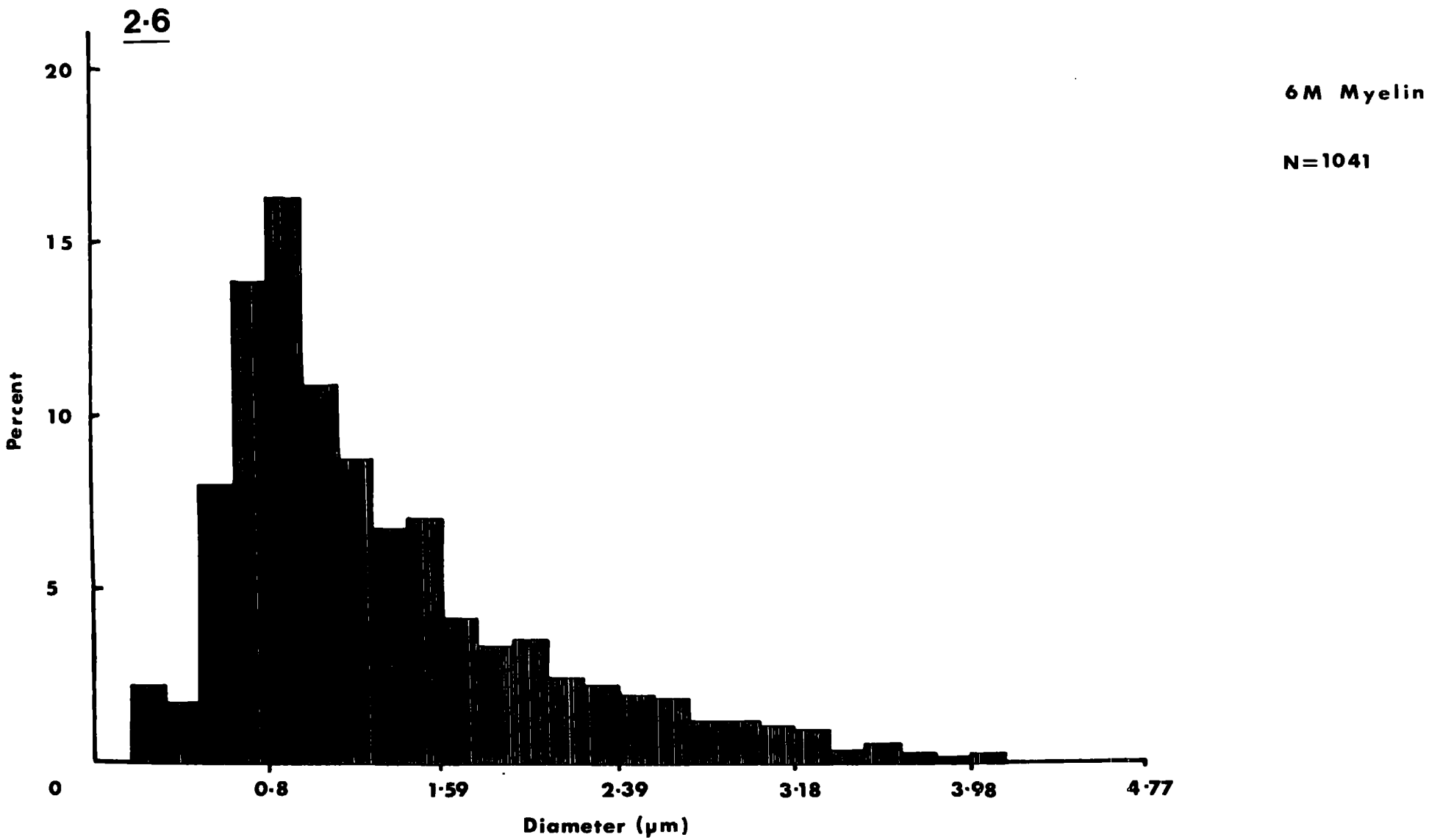
2·6
20
15
10
5
0
Percent
0·8
1·59
2·39
3·18
3·98
4·77
Diameter (μm)
6M Myelin
N=1041

Fig. 2:7 Myelinated axon diameter distribution in an optic nerve taken from an adult Xenopus. The histogram is based on a sample of 1132 axons from a total population of 2769 myelinated axons. The mean axonal diameter is 1.63 μm ± 0.032 S.E. Comparison of the mean with a six month old toad indicates a significant difference ($P<1\%$) by a 'Students' t-test ($t = 11.38$).

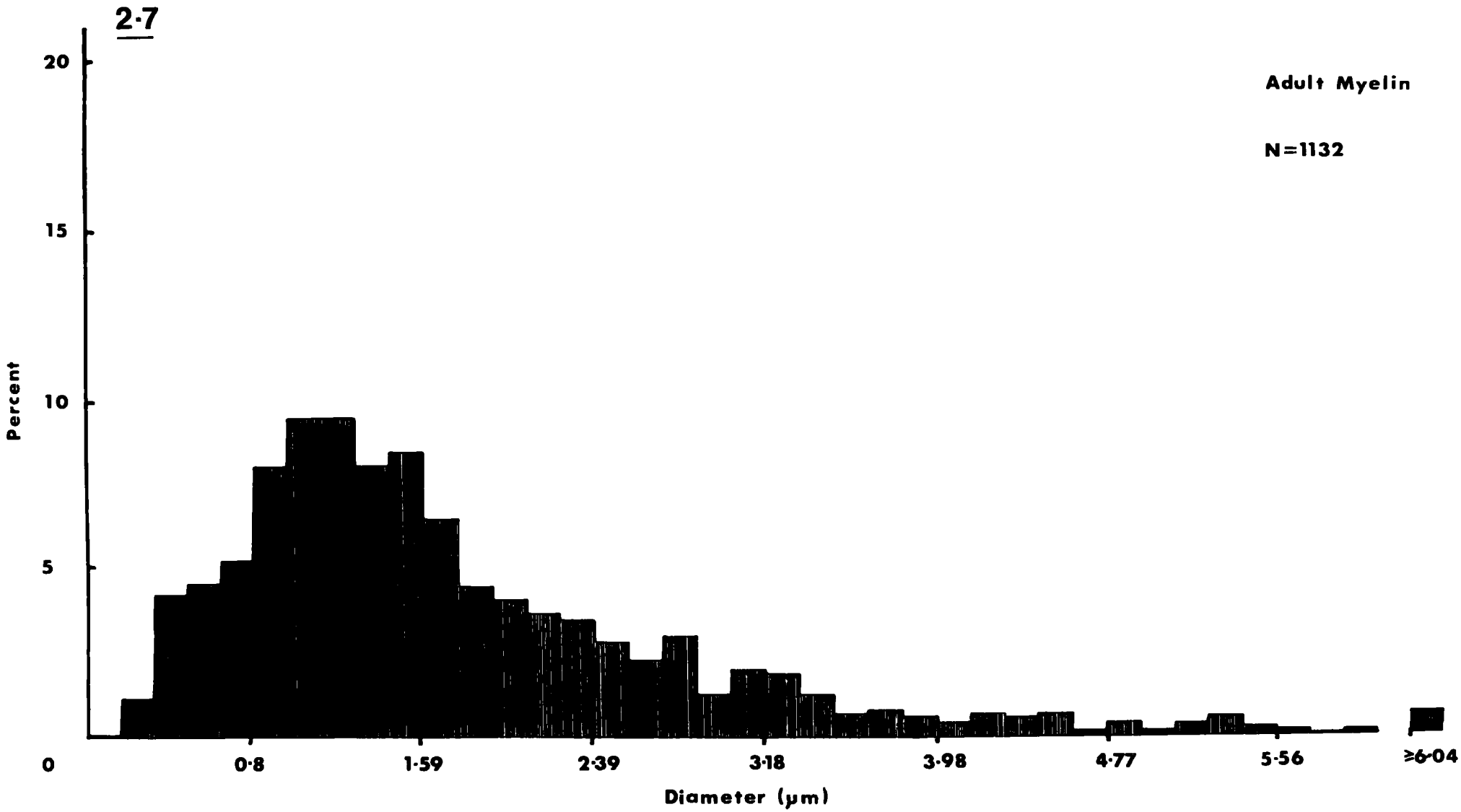
2·7
Adult Myelin
N=1132
Percent
20
15
10
5
0
0·8
1·59
2·39
3·18
3·98
4·77
5·56
≥6·04
Diameter (μm)

Fig. 2:8 Total numbers of normal myelinated fibres at different stages (from this study) of development compared with the numbers of unmyelinated fibres (Wilson, 1971).

2·8

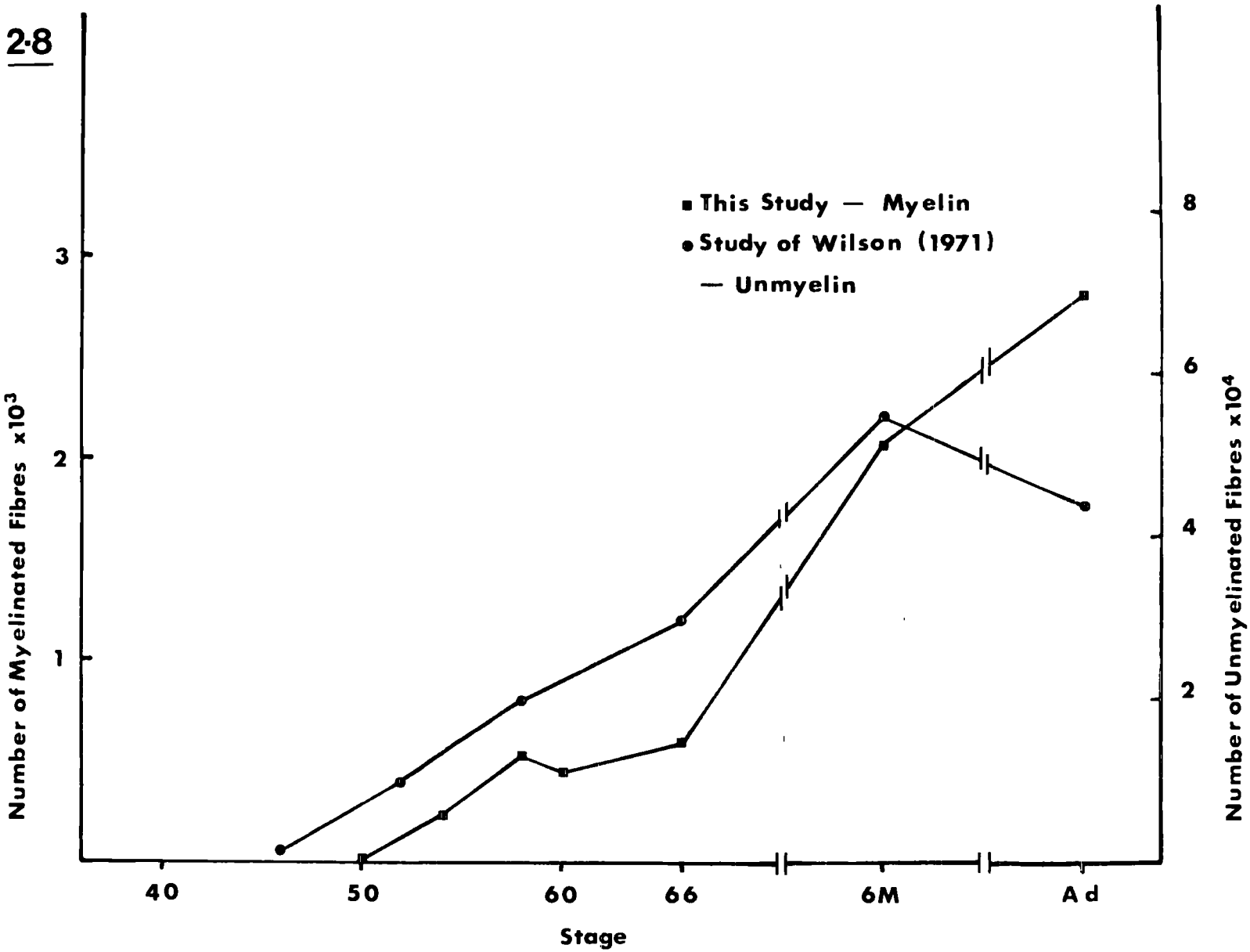
■ This Study — Myelin
● Study of Wilson (1971)
— Unmyelin
Number of Myelinated Fibres x10³
Number of Unmyelinated Fibres x10⁴
1
2
3
4
6
8
40
50
60
66
6M
Ad
Stage

The diameter of larger myelinated fibres is fairly constant in all stages of development, except that some fibres greater than 8 μm in diameter are present in the adult. The modal and mean diameters of the myelinated fibres in S58A, S58B and Stage 60 nerves (Table 2:1) and the shapes of the diameter histograms (figs. 2:2 and 2:3) are very similar. At Stage 60 the distribution of myelinated fibre diameters is not smooth (fig. 2:4). This may be a consequence of the abnormalities in shape of the fibres. Comparison of the histograms in figures 2:2; 2:3 and 2:4 indicates that no particular region of the distribution is affected especially by the changes occurring at this time.

Myelin Sheath Thickness

The ratio of axonal diameter to the fibre diameter was calculated by measuring the periphery of both the axon and the myelin sheath. Each value was converted into a diameter, assuming that the profile was circular. The ratio of the axon diameter (d) to the fibre diameter (D) is expressed as $^{d}/_{D} = \rho$ (Rushton, 1951).

The distributions of values from all of the nerves studied are skewed negatively, and the distributions derived from postmetamorphic animals are more irregular. Figure 2:9 shows that the mean values of decrease from Stage 58 onwards, which indicates a continuous increase in the relative thickness of the myelin sheaths.

Fig. 2:9 Trends of mean and modal values of ρ (ratio of axon diameter to fibre diameter d/D in myelinated fibres of metamorphic and adult animals. Decreasing values of ρ during development indicates an increase in the relative thickness of the myelin sheath.

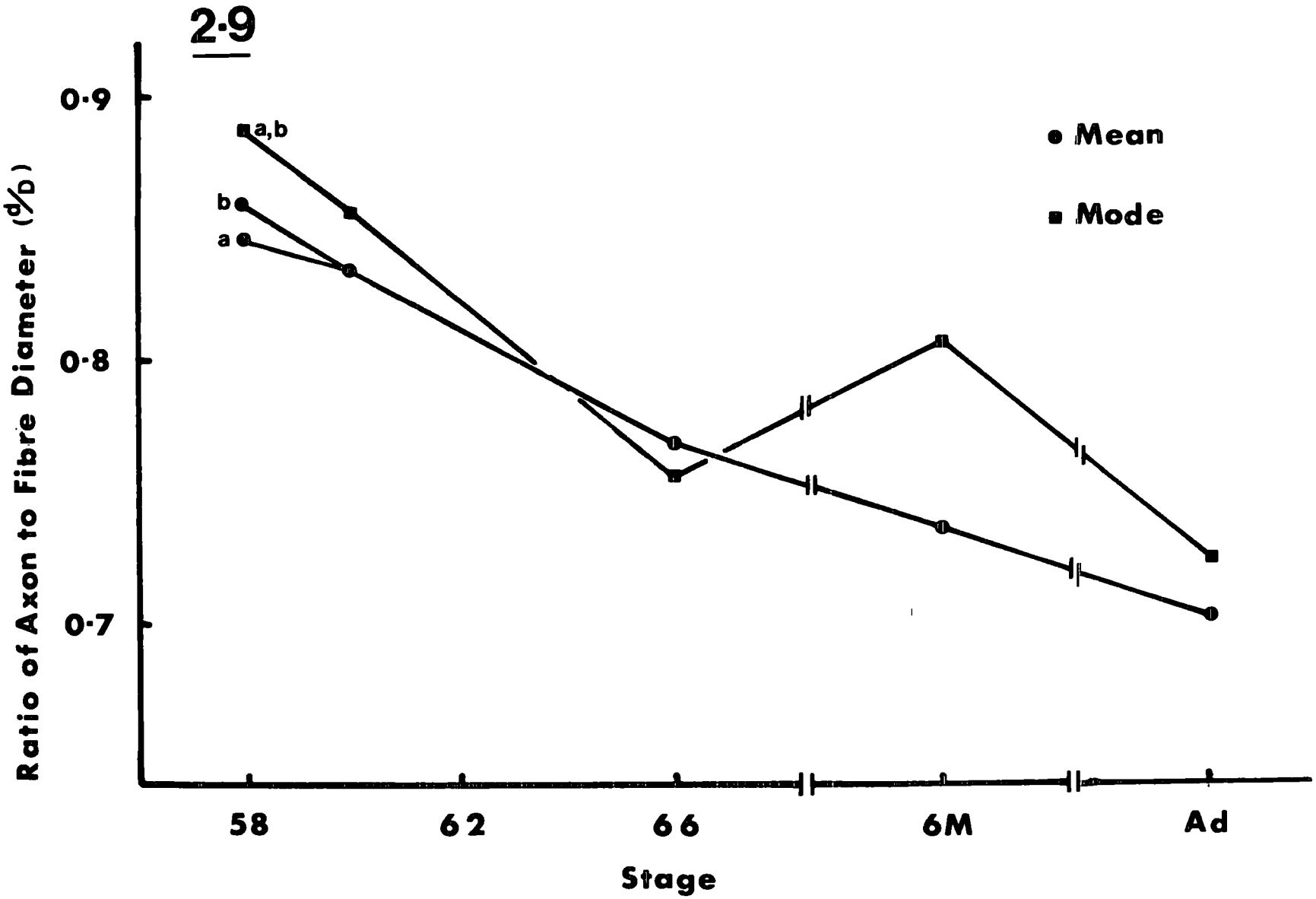
2·9
0·9
0·8
0·7
Ratio of Axon to Fibre Diameter (d/D)
a,b
b
a
Mean
Mode
58
62
66
6M
Ad
Stage

(i) Premetamorphosis

No myelinated fibres were measured from nerves derived from Stages 50 and 54.

(ii) Metamorphosis

The distribution of the values of ρ for the two nerves, S58A and S58B, from the same animal are very similar (figs. 2:10 and 2:11) with means of 0.845 and 0.858 respectively and identical modes (fig. 2:9 and Table 2:1).

At Stage 60, the mean and modal values decrease slightly (fig. 2:9 and Table 2:1) and there is an increase in the number of fibres with a ρ value below 0.7 (fig. 2:12).

The shift to lower values of ρ continues at Stage 66 (fig. 2:13) with 13.8% of the ρ values being below 0.7 compared with 5% at Stage 60. The decrease in the mean and mode to 0.768 and 0.755 respectively is a reflection of the relative increase in the number of smaller myelinated fibres.

(iii) Postmetamorphosis

The distribution of the values of ρ in the optic nerve from a six month old toad is much broader compared with tadpole stages (fig. 2:14). The trend to lower values indicated at Stage 60 and more evident at Stage 66 is continued, with 29.1% of the fibres in the six month old toad having values below 0.7.

Figs. 2:10 and 2:11 Distributions of the values of relative myelin thickness (ρ) of myelinated fibres in the two optic nerves from a Stage 58 tadpole. The mean values of for these two distributions are 0.845 ± 0.0017 S.E. and 0.858 ± 0.0017 S.E. respectively. Note particularly the small numbers of fibres (less than 1%) with values less than 0.7.

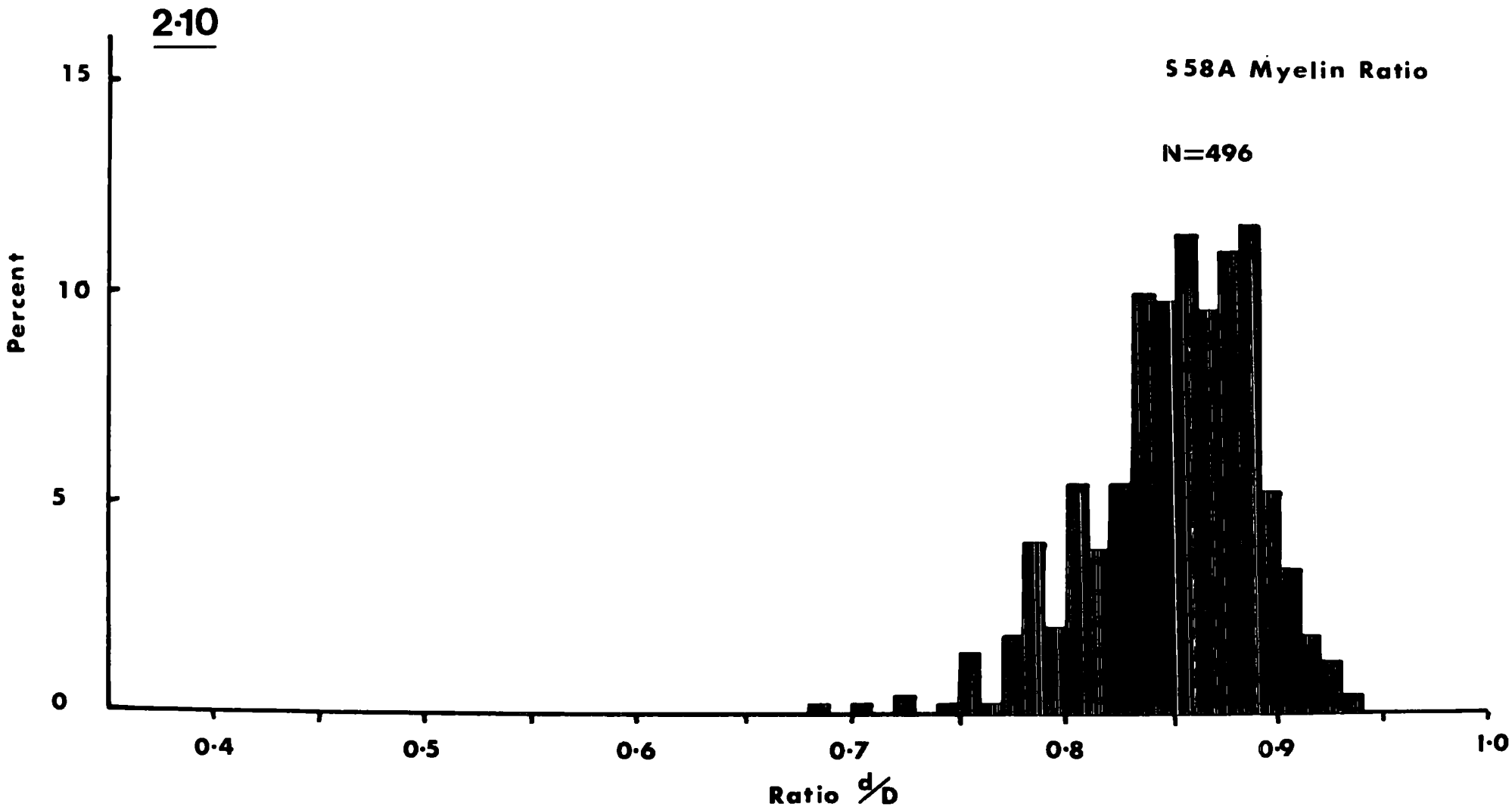
2·10
S58A Myelin Ratio
N=496
Percent
15
10
5
0
0·4
0·5
0·6
0·7
0·8
0·9
1·0
Ratio d/D

Fig. 2:11 See legend for figure 2:10.

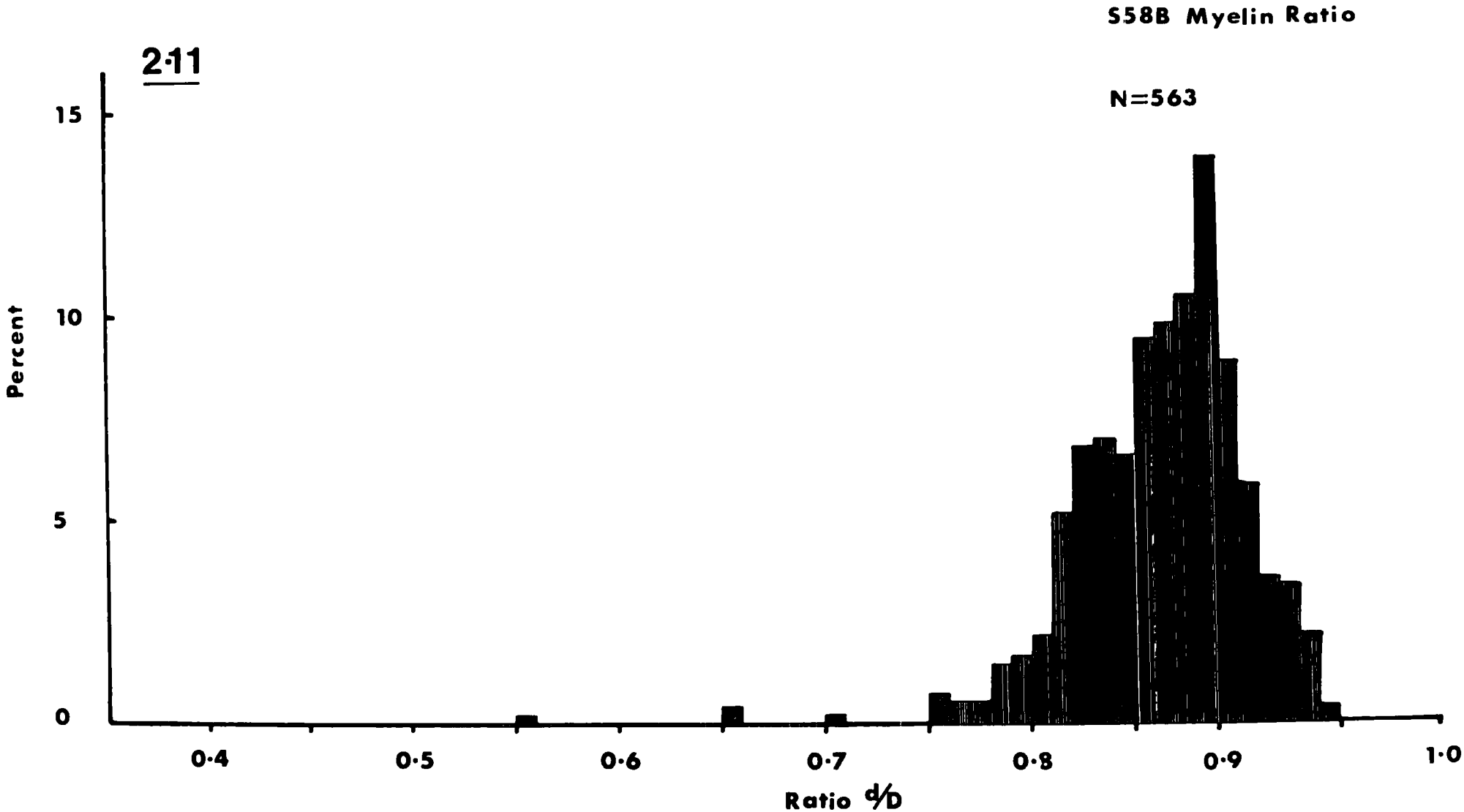
2·11
S58B Myelin Ratio
N=563
15
10
5
0
Percent
0·4
0·5
0·6
0·7
0·8
0·9
1·0
Ratio d/D

Fig. 2:12 Histogram of values of myelinated fibres in an optic nerve of a Stage 60 tadpole. The mean value for this distribution is 0.833 ± 0.004 S.E. with 5% of the myelinated fibres having a value of less than 0.7. A significant difference ($P < 1\%$) between the means of Stage 58 (0.845) and Stage 60 was indicated by a 'Students' t-test ($t = 2.79$).

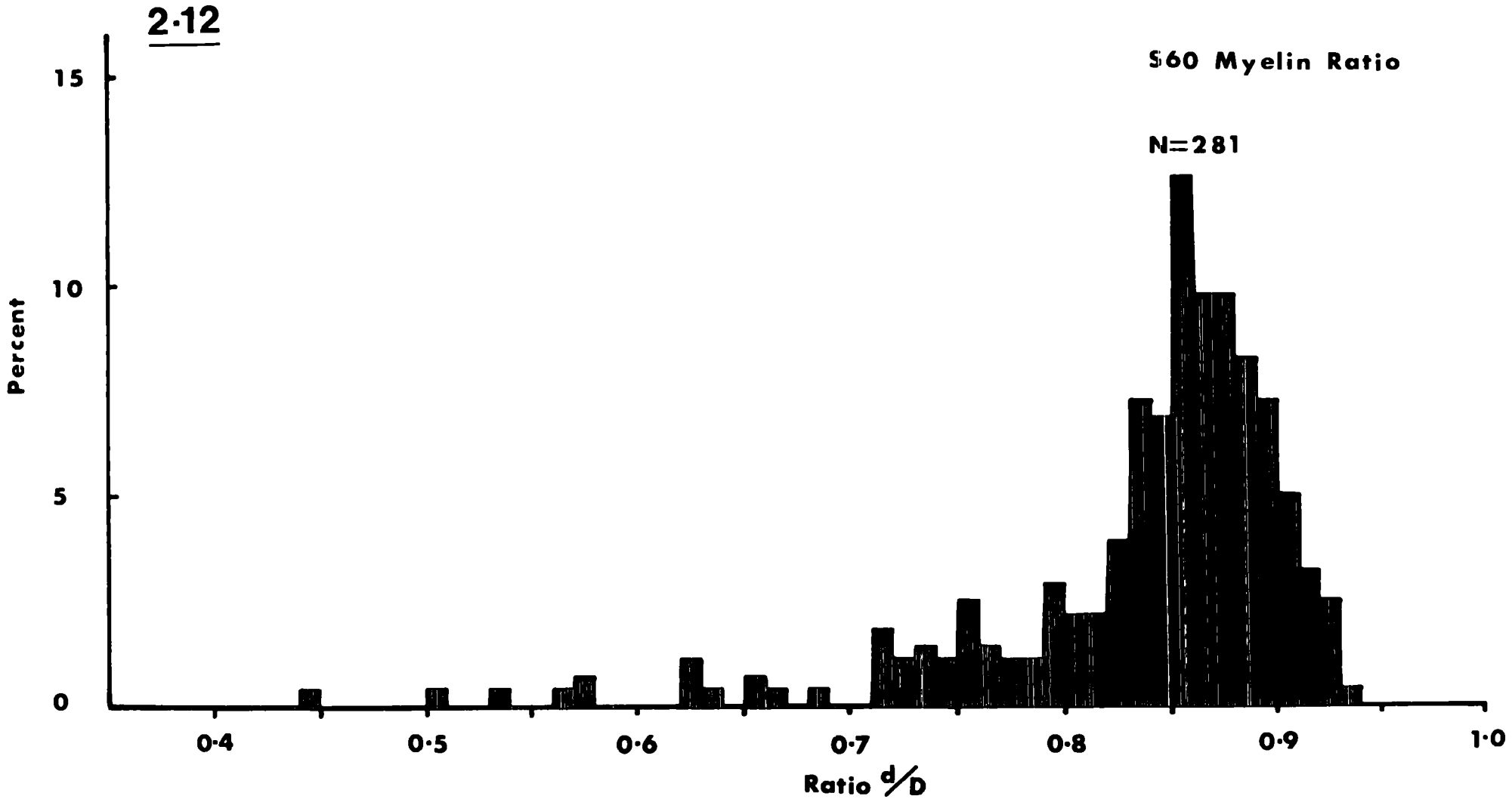
2·12
S60 Myelin Ratio
N=281
15
10
5
0
Percent
0·4
0·5
0·6
0·7
0·8
0·9
1·0
Ratio d/D

Fig. 2:13 Distribution of relative myelin thickness (ρ) in an optic nerve of a Stage 66 animal. The mean value of ρ is 0.768 $\pm$ 0.0035 S.E. The relative numbers of myelinated fibres with values of less than 0.7 is 13.8% and reflects that during the metamorphic period the relative numbers of small myelinated fibres increases. A significant difference ($P < 1\%$) between the means of Stage 60 and Stage 66 was indicated by a 'Students' t-test ($t = 12.16$).

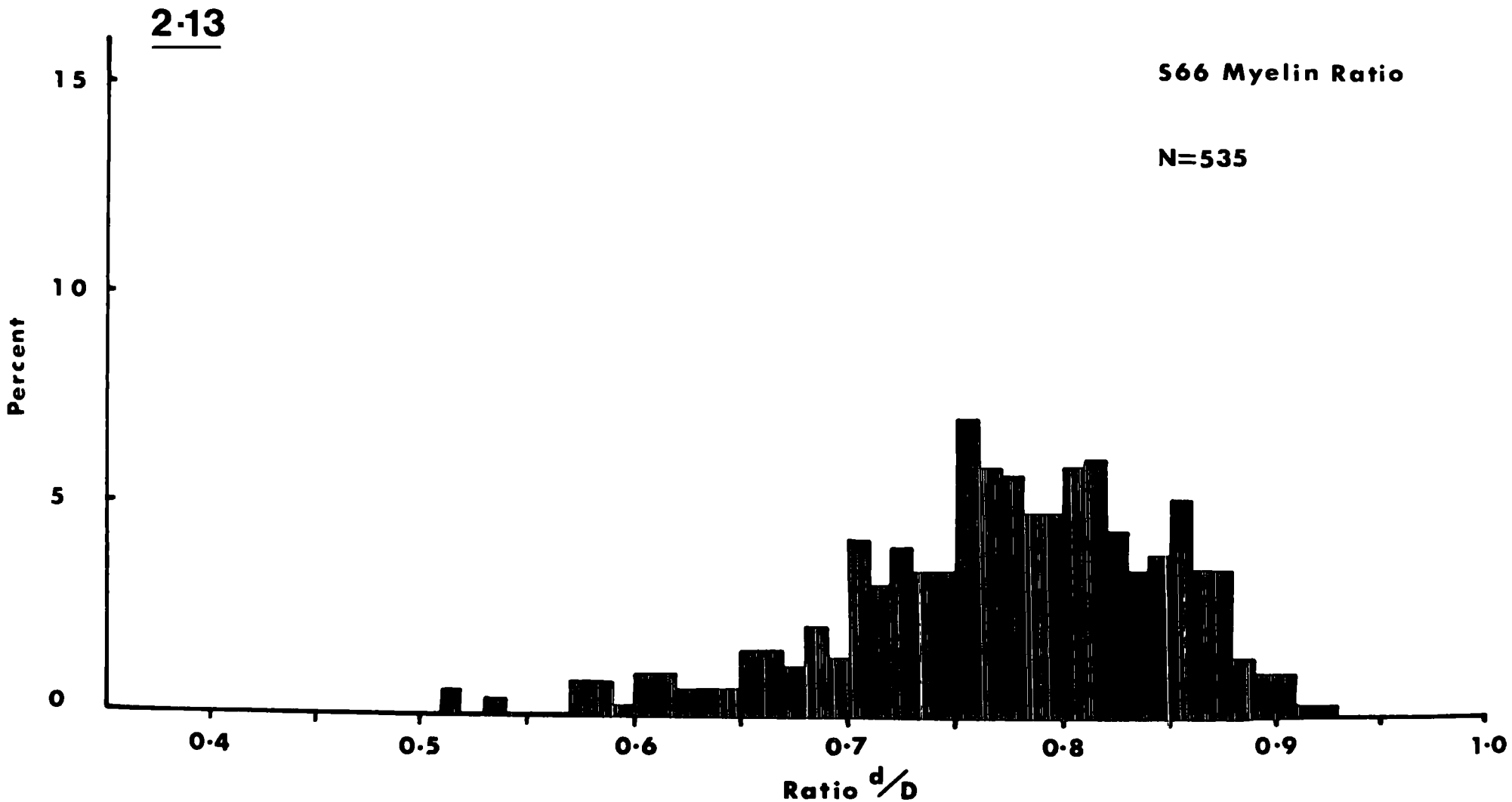
2·13
S66 Myelin Ratio
N=535
15
10
5
0
Percent
0·4
0·5
0·6
0·7
0·8
0·9
1·0
Ratio d/D

Fig. 2:14 Distribution of ρ values for myelinated optic nerve fibres in a six month old toad. The mean value for this distribution is $\rho = 0.737$. At this stage 29.1% of the fibres have ρ values below 0.7. A significant difference ($P < 1\%$) between the means of Stage 66 and six months old was indicated by a 'Students' t-test ($t = 6.739$).

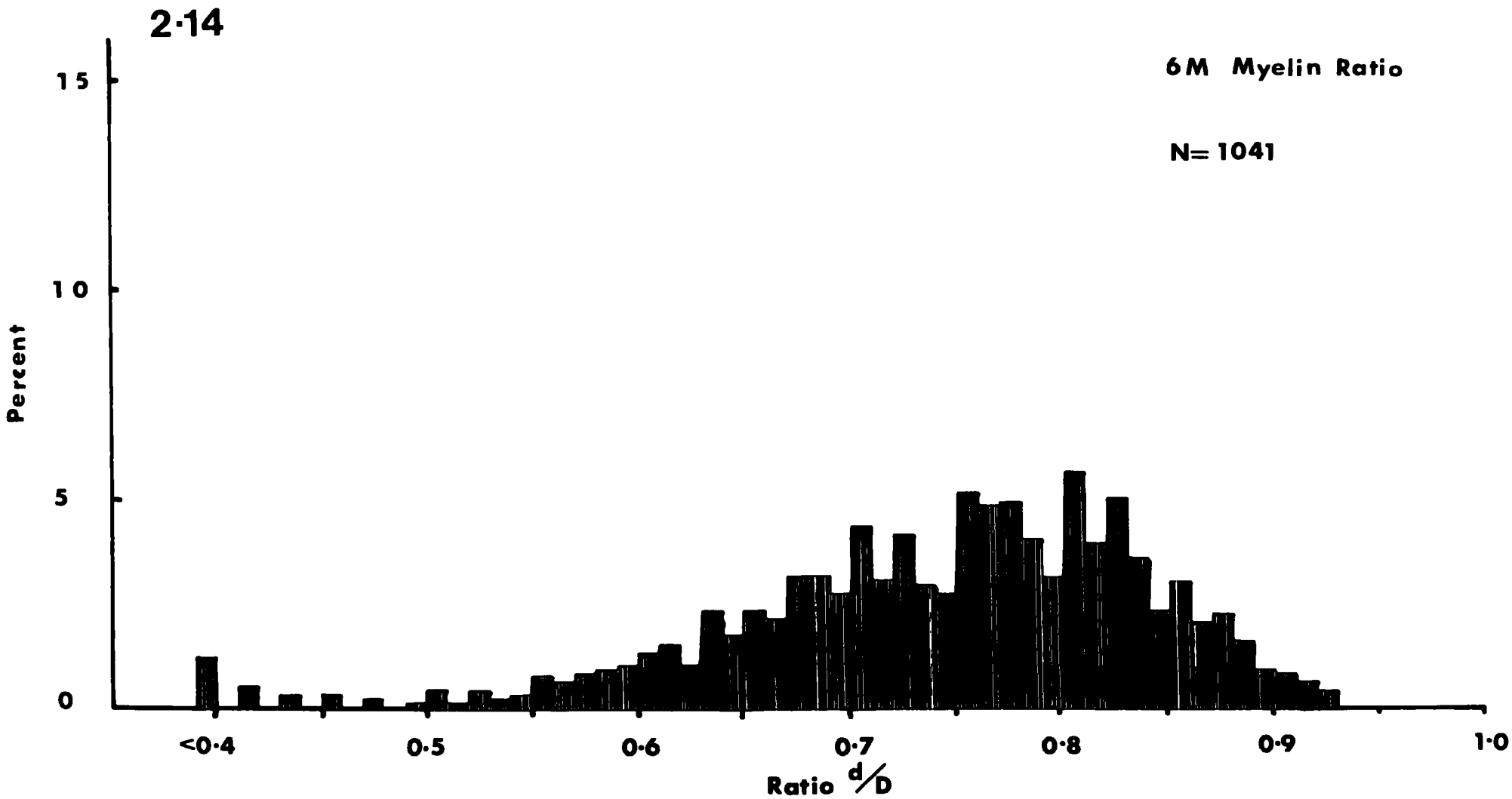
2·14
6M Myelin Ratio
N= 1041
15
10
5
0
Percent
<0·4
0·5
0·6
0·7
0·8
0·9
1·0
Ratio d/D

Fig. 2:15 Distribution of ratios of axon diameter to fibre diameter (ρ) of myelinated fibres in an optic nerve from an adult animal. The mean ratio for the distribution was found to be 0.702 with 33% of the fibres having ρ values less than 0.7. A significant difference ($P < 1\%$) between the means of a six month old toad and a mature adult was indicated by a 'Students' t-test ($t = 8.12$).

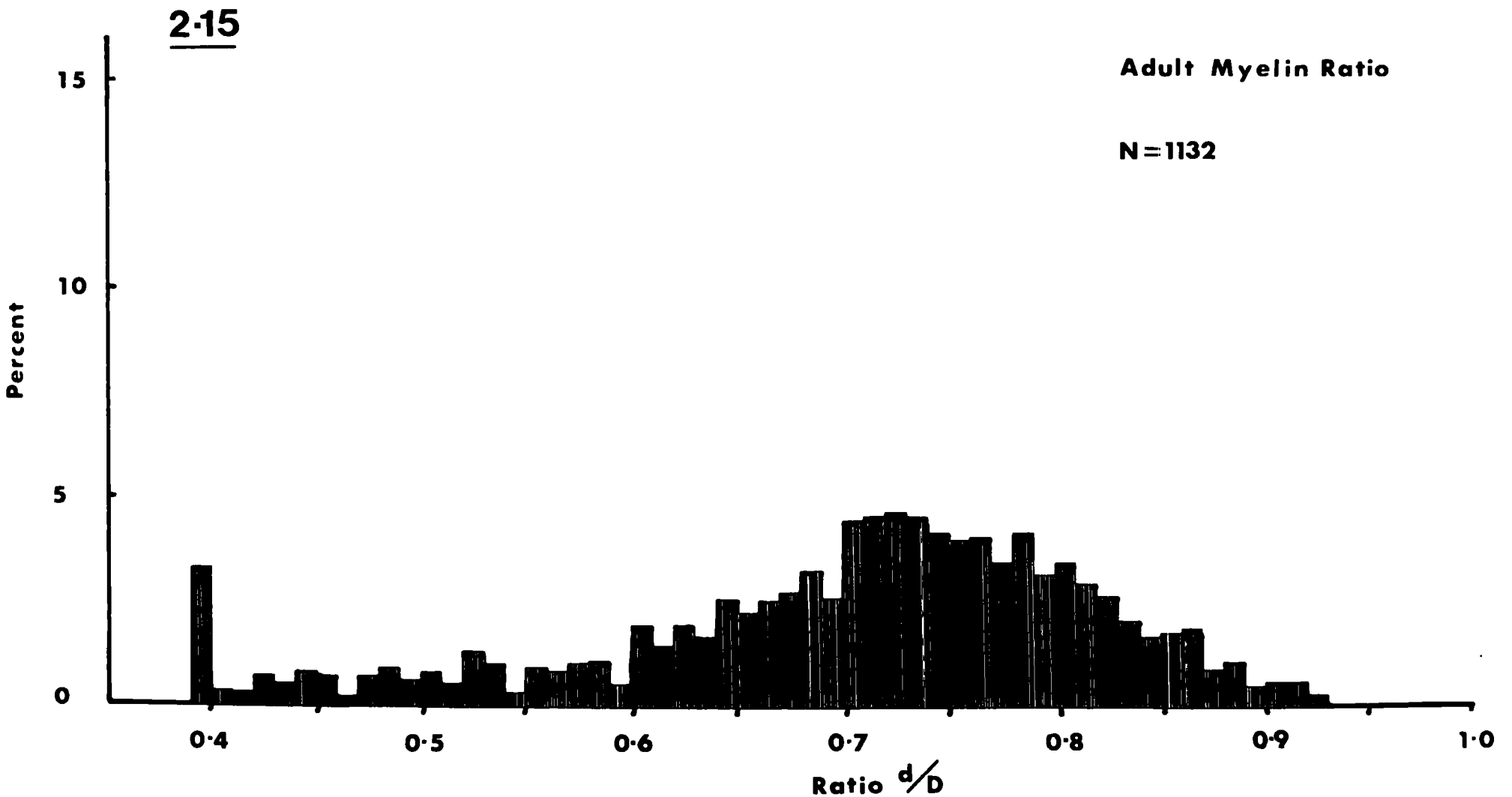
2·15
Adult Myelin Ratio
N=1132
15
10
5
0
Percent
0·4
0·5
0·6
0·7
0·8
0·9
1·0
Ratio d/D

Fig. 2:16 Mean and modal diameters of unmyelinated fibre populations from animals at different stages of development. The two points indicated a and b, for both the mean and mode of Stage 58 are the values for both optic nerves from a single animal.

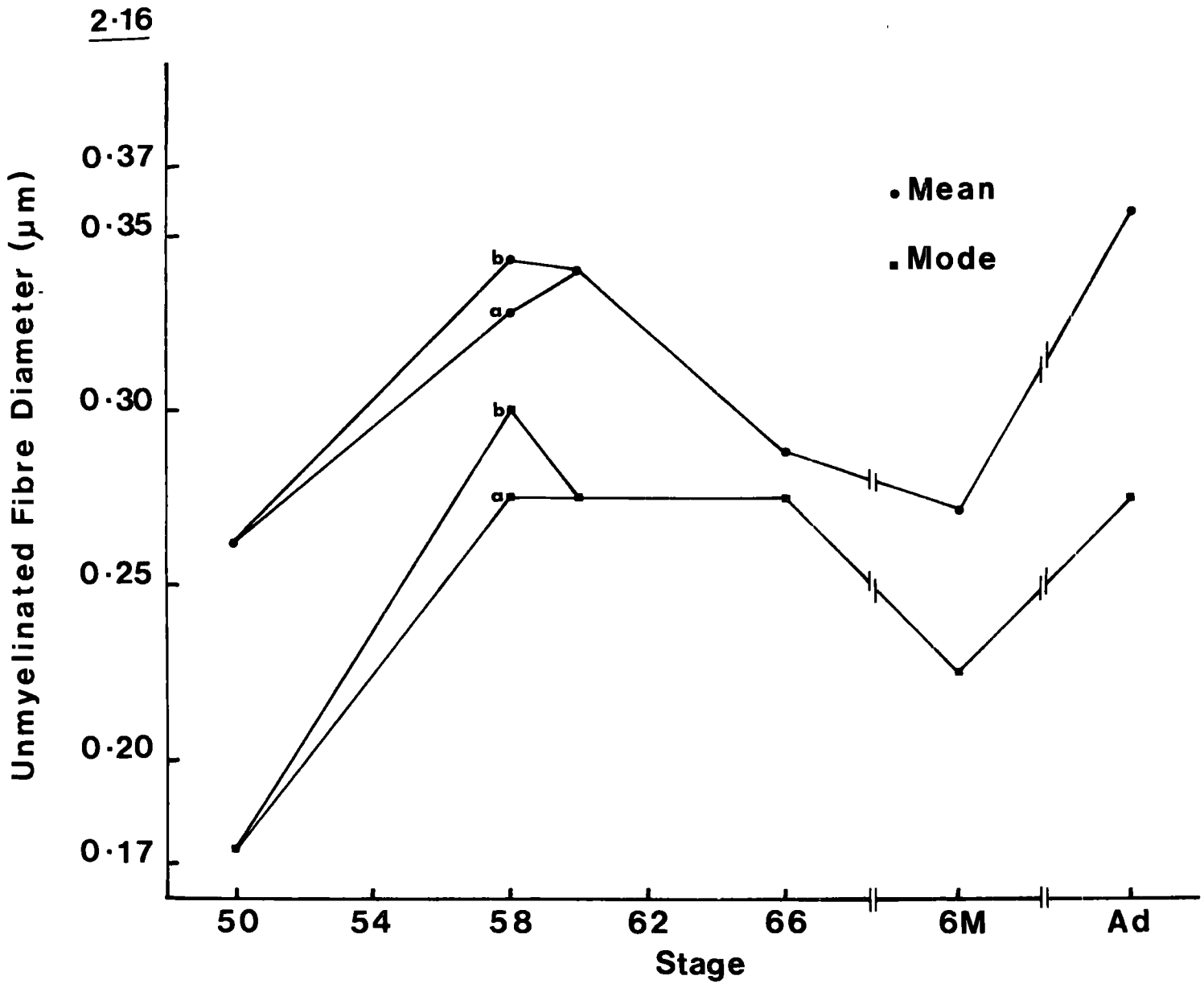
2·16
0·37
0·35
0·30
0·25
0·20
0·17
Unmyelinated Fibre Diameter (μm)
• Mean
▪ Mode
b
a
b
a
50
54
58
62
66
6M
Ad
Stage

Fig. 2:17 Distribution of unmyelinated fibre diameters in a sample (N = 1199) taken from the optic nerve of a Stage 50 tadpole. The mean diameter of this sample was found to be 0.26 μm.

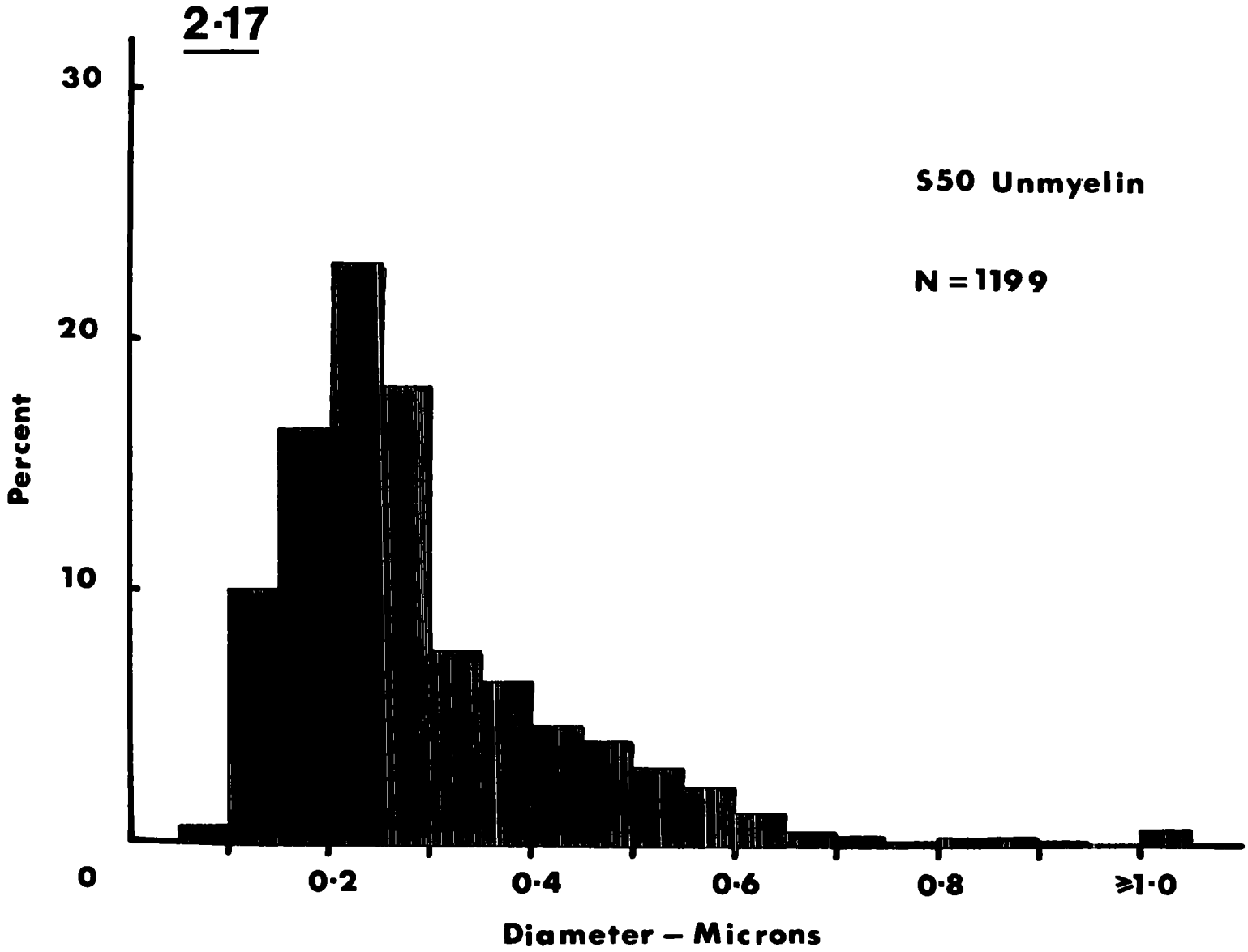
2·17
30
20
10
0
Percent
S50 Unmyelin
N = 1199
0·2
0·4
0·6
0·8
≥1·0
Diameter – Microns

Figs. 2:18 and 2:19 Diameter histograms of unmyelinated fibres in samples (of greater than 1000 fibres) from both optic nerves in a single Stage 58 tadpole. The mean diameters for the two nerves illustrated in figures 2:18 and 2:19 are 0.328 μm ± 0.0045 S.E. and 0.343 μm ± 0.0041 S.E. respectively.

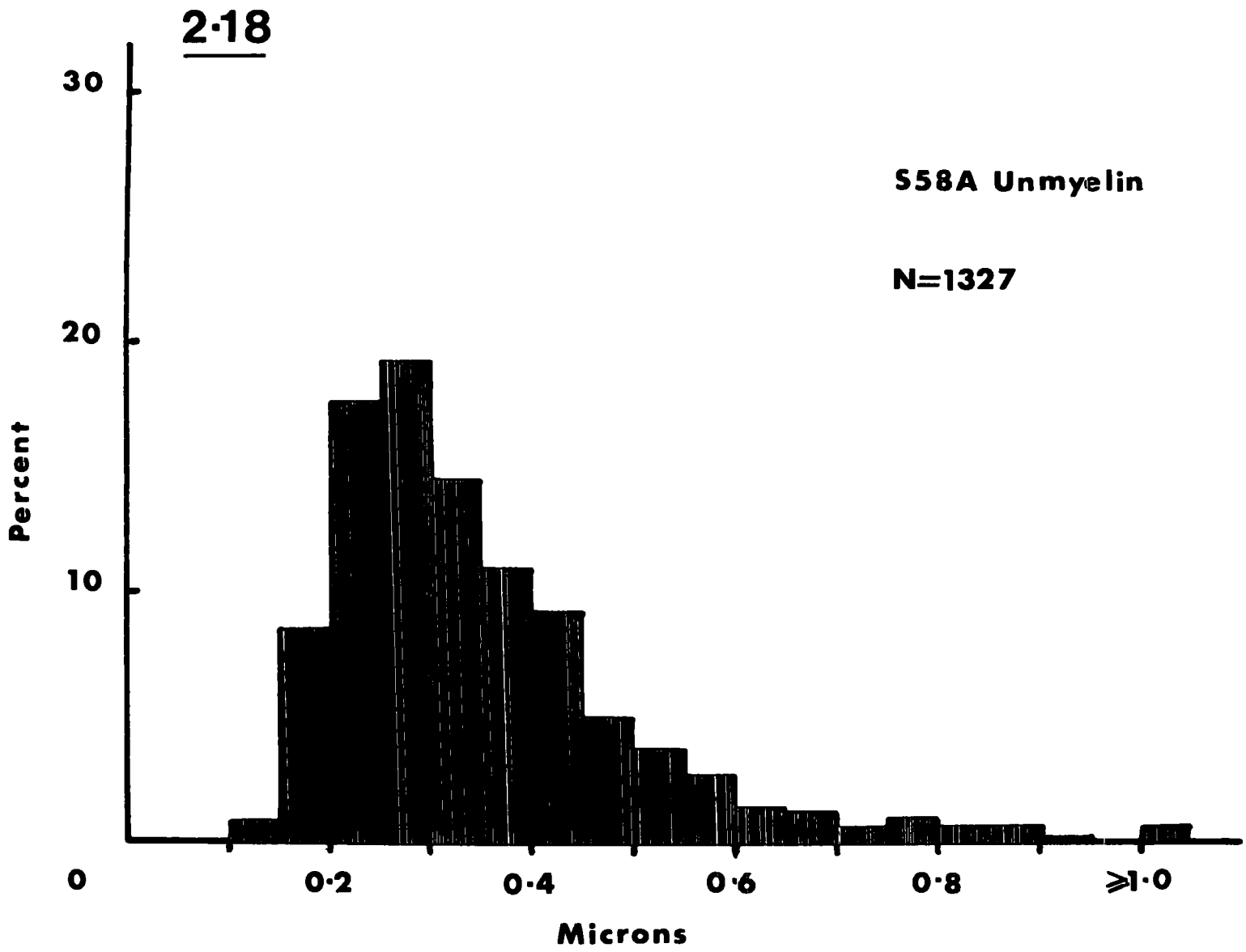
2·18
S58A Unmyelin
N=1327
Percent
30
20
10
0
0·2
0·4
0·6
0·8
≥1·0
Microns

Fig. 2:19 See legend to figure 2:18.

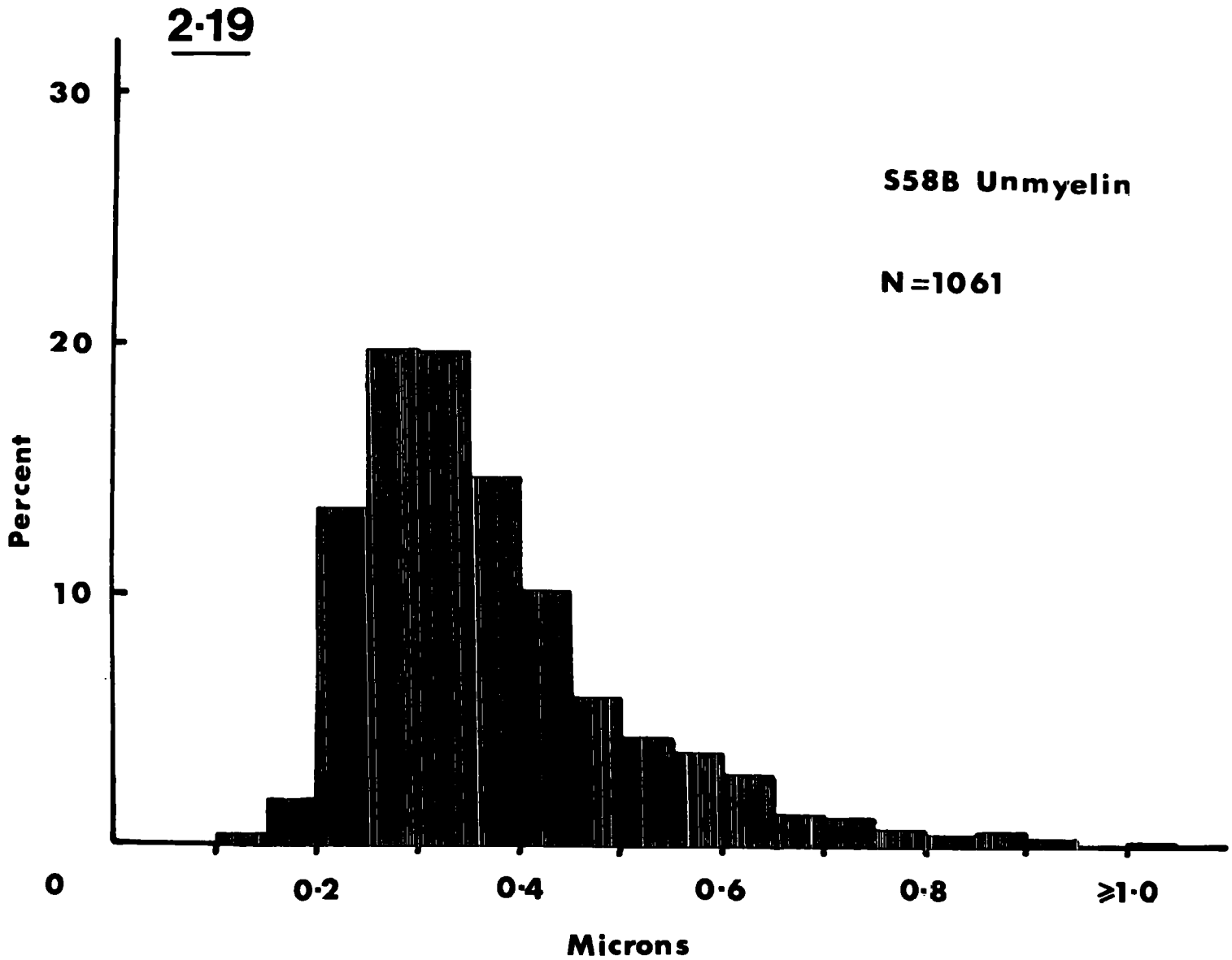
2·19
S58B Unmyelin
N=1061
Percent
30
20
10
0
0·2
0·4
0·6
0·8
≥1·0
Microns

The distribution in figure 2:15 is from an adult and has the broadest range of ρ values of the nerves measured, with values from below 0.4 to 0.92. The mean of the distribution is at 0.702 and the mode is at 0.725.

Unmyelinated fibres

Fibre diameters were measured from a sample of at least 1,000 unmyelinated fibres per nerve, and these results are summarized in Table 2:1 and figure 2:16. No attempt was made to estimate the total number of unmyelinated fibres present per nerve since this has already been carried out (Gaze and Peters, 1961; Wilson, 1971). The data of Wilson is plotted in figure 2:8.

(i) Premetamorphosis

Figure 2:17 shows that the distribution is skewed positively with the majority (97.2%) of the 1,199 fibres measured falling within the size range 0.1 - 0.6 μm. The mean and mode for this distribution is 0.26 μm and 0.175 μm respectively.

No axons were measured in the Stage 54 nerve.

(ii) Metamorphosis

At Stage 58 (figs. 2:18 and 2:19) both histograms are positively skewed. Not only have the means and modes increased (fig. 2:16 and Table 2:1) but the size range is

extended somewhat from that found at Stage 50 (figs. 2:17, 2:18 and 2:19).

The distribution of the fibre diameters of the Stage 60 nerve (fig. 2:20) is very similar to that of the Stage 58 nerves, although the peak is somewhat broader. The mean (0.340 μm) and modal (0.275 μm) values of the unmyelinated fibre distribution are similar to those derived from the Stage 58 animal.

At Stage 66 the unmyelinated fibre diameter distribution has a typical positive skew (fig. 2:21). The mean diameter has decreased from the values found at Stages 58 and 60, but the mode has remained the same (fig. 2:16 and Table 2:1). Most fibres (97.1%) fall within the size range 0.15 - 0.6 μm (fig. 2:21). No morphological changes have been noted in unmyelinated fibres at metamorphosis and the decrease in the mean diameter of the distribution must indicate the presence of newly developed ganglion cell axons, since at this stage only a small number of fibres are in the process of myelination.

(iii) Postmetamorphosis

The fibre diameter distribution of unmyelinated fibres derived from a six months old toad is positively skewed and is shown in figure 2:22. The distribution has a mean similar to that found at Stage 66. However, the mode of the distri-

Fig. 2:20 Distribution of unmyelinated fibre diameters in a sample of 1662 fibres from a Stage 60 tadpole. The mean diameter of this sample was found to be 0.340 μm ± 0.0043 S.E.

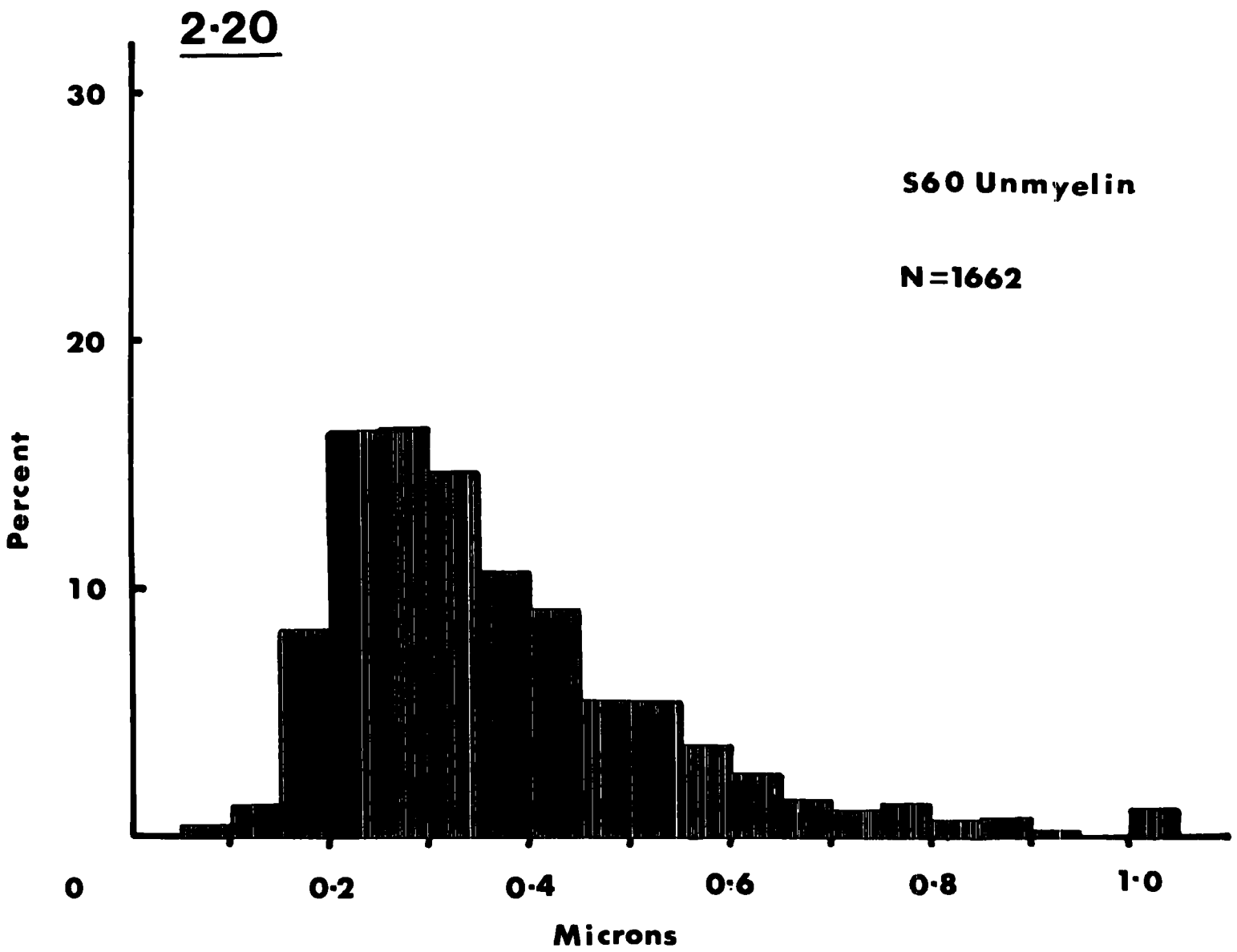
2·20
30
20
10
Percent
S60 Unmyelin
N=1662
0
0·2
0·4
0·6
0·8
1·0
Microns

Fig. 2:21 Unmyelinated fibre diameter distribution for a sample of 1334 axons in a Stage 66 animal. The mean diameter for this sample was found to be 0.288 μm ± 0.0042 S.E. A significant difference ($P < 1\%$) between the means of Stage 60 and Stage 66 was indicated by a 'Students' t-test ($t = 8.65$).

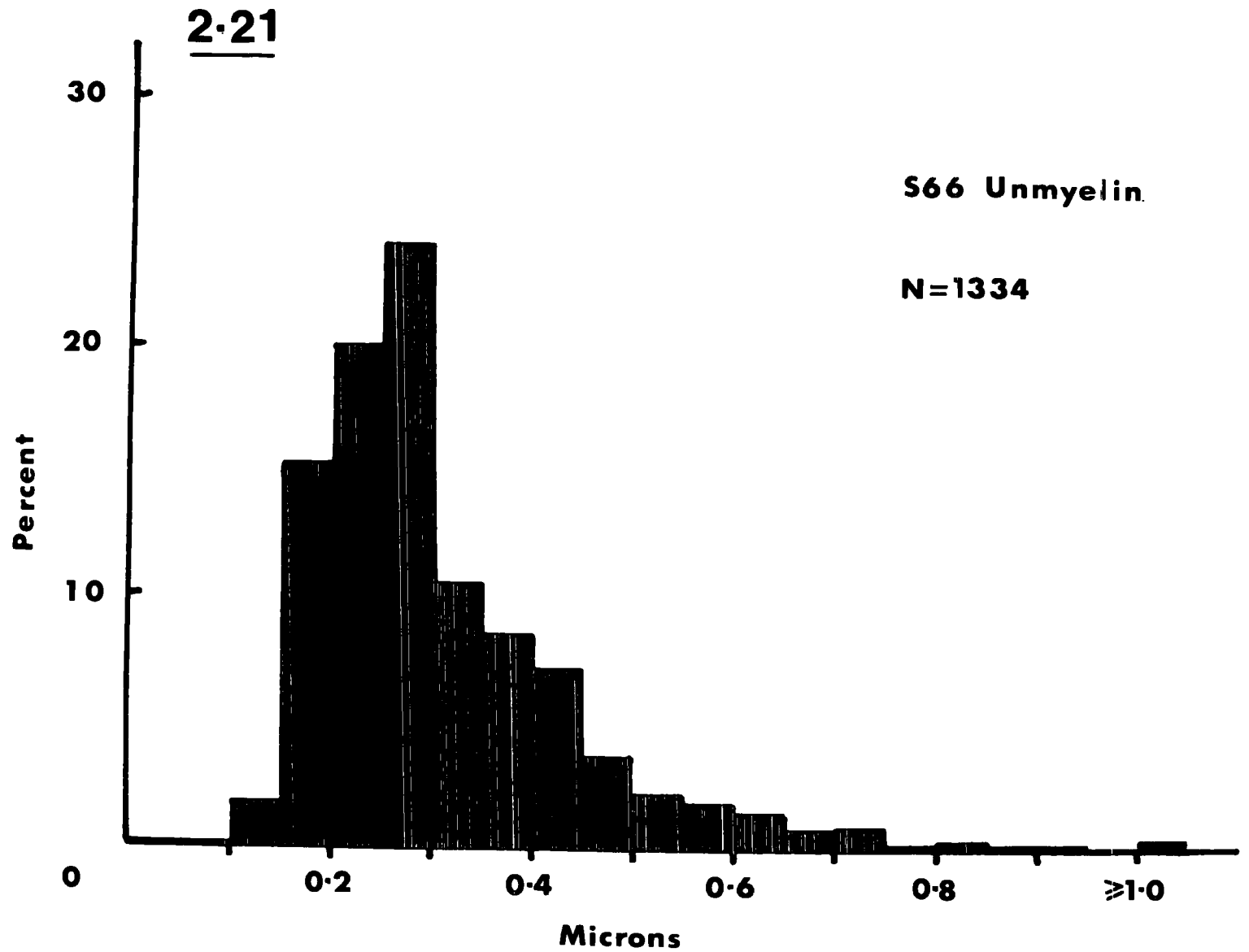
2·21
30
20
10
0
Percent
S66 Unmyelin
N=1334
0·2
0·4
0·6
0·8
≥1·0
Microns

Fig. 2:22 Histogram of unmyelinated fibre diameters in a sample of 1101 fibres from a six month old toad. The mean diameter for this sample was found to be 0.271 μm ± 0.0040 S.E. A significant difference ($P < 1\%$) between the means of Stage 66 and six months old was indicated by a 'Students' t-test ($t = 2.93$).

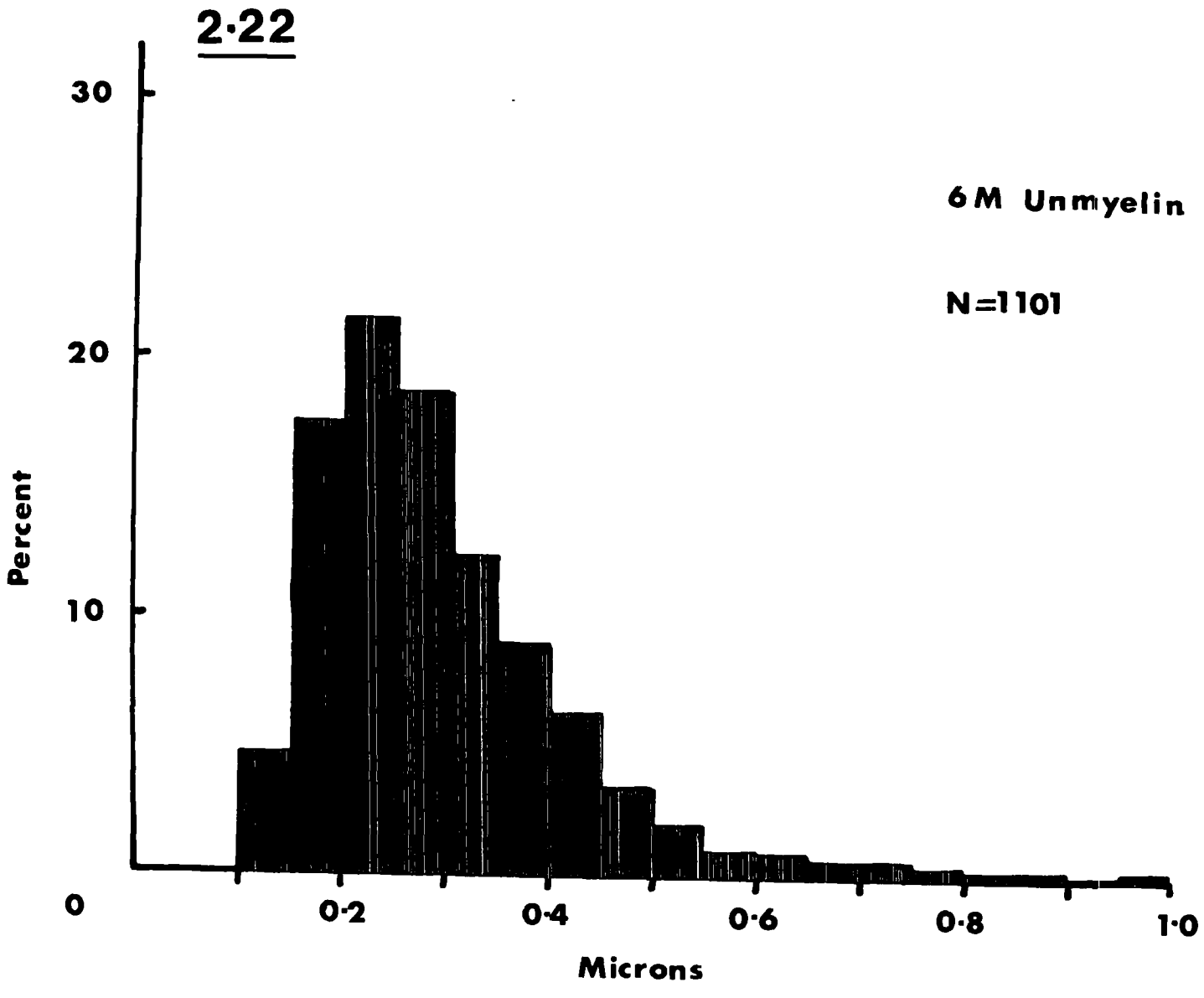
2·22
30
20
10
0
Percent
6M Unmyelin
N=1101
0·2
0·4
0·6
0·8
1·0
Microns

bution has decreased. These two facts indicate that there is a relative increase in the number of smaller unmyelinated fibres in this nerve, although their effects on the distribution are partially compensated by an increase in the number of larger diameter fibres.

The shape of the diameter distribution histogram of unmyelinated axons in the adult (fig. 2:23) is derived from the measurement of 2,113 fibres. The distribution changes slightly compared to those derived from optic nerves at other stages of development. The distribution is less skewed and the peak is much broader. This is reflected by the increase in mean value to 0.357 μm. Very few large unmyelinated axons were found. The modal value has increased from that at Stage 66 to 0.275 μm.

Newly myelinating fibres

One hundred and ninety-eight unmyelinated fibres which were encircled completely by glial processes were measured in the Stage 66, 60 and two Stage 58 nerves to produce the combined histogram in figure 2:24. The distribution has a slight positive skew and the base is fairly broad with a mode at 1.05 μm and a mean at 1.12 μm. No completely encircled axons were found below 0.5 μm in diameter and only two were above 2.00 μm, at 2.05 μm and 3.05 μm.

Fig. 2:23 Fibre diameter distribution of unmyelinated axons in a sample of 2113 fibres from an adult toad. The sample mean was found to be 0.357 μm ± 0.0034. A significant difference ($P < 1\%$) between the means of the six month old adult and the mature adult was indicated by a 'Students' t-test ($t = 16.38$).

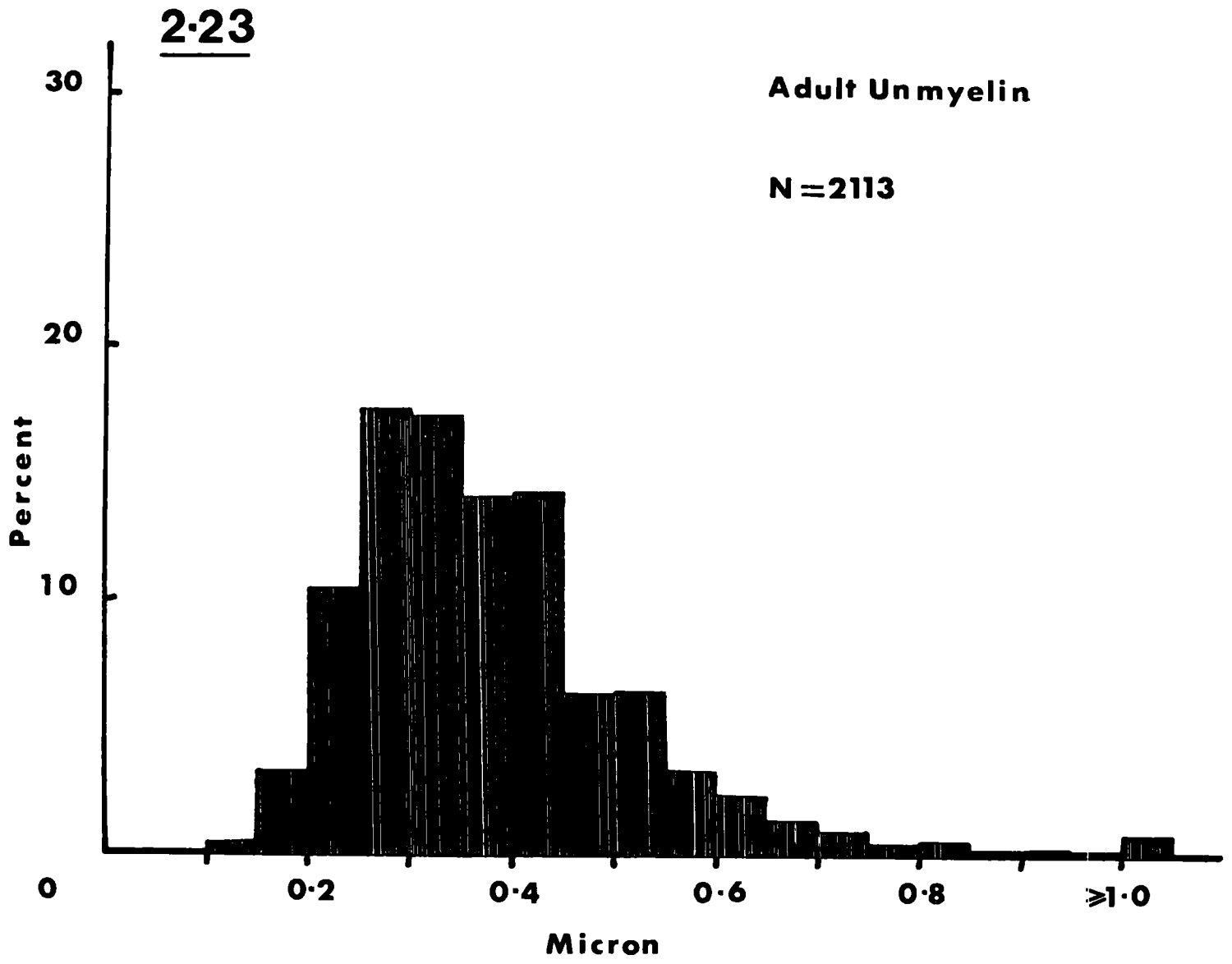
2·23
Adult Unmyelin
N=2113
30
20
10
0
Percent
0·2
0·4
0·6
0·8
≥1·0
Micron

Fig. 2:24 Fibre diameter distribution of unmyelinated fibres that were completely encircled by glial cell processes. This distribution is based on the pooled samples (total number 196) of fibres measured in Stages 58, 60 and 66 animals. The mode and mean for this distribution are 1.05 μm and 1.12 μm respectively.

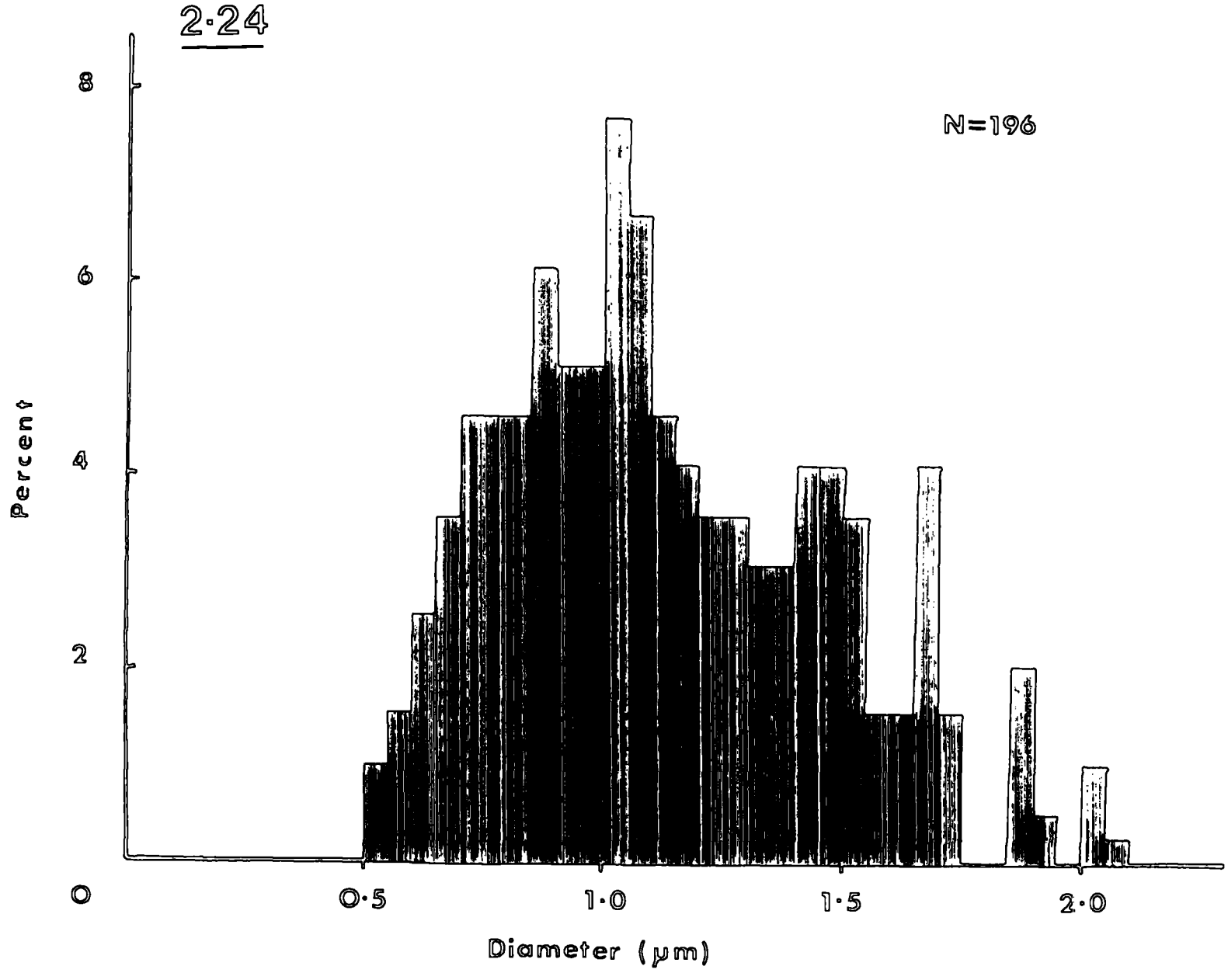
2·24
N=196
Percent
8
6
4
2
0
0·5
1·0
1·5
2·0
Diameter (μm)

DISCUSSION

The fibre diameter distributions of ganglion cell axons in the optic nerve of Xenopus have been studied previously by Gaze and Peters (1961) and Wilson (1971). This more recent study appears to be more thorough and accurate. Both investigations were concerned with the study of a range of optic nerves from tadpoles at different stages of development in comparison with the adult nerve. However, both investigations avoided study of the period of metamorphosis.

Numbers of ganglion cell axons

The absolute numbers of myelinated fibres obtained from tadpole nerves correspond quite closely to those of Wilson (1971), although for postmetamorphic animals the discrepancy is quite large. At Stage 66, the number of myelinated fibres was found to be approximately one quarter lower than the result obtained by Wilson. In older animals the differences were even greater, the numbers reported here for myelinated fibres being only two-thirds, and three-eighths of those reported by Wilson, for six month and adult toads respectively. The difference in results from the six month animal may be due to variability inherent

within the Xenopus laevis species. Alternatively, the difference may reflect rearing conditions. In the case of the adult, the individual used in this study was obtained from the wild, whereas the one used by Wilson was bred in the laboratory. The greater number of myelinated fibres in the optic nerve of the laboratory-raised animal may indicate that under such conditions there are very few constraints on the developing system and the animal realises a greater developmental potential. Wilson suggests that the discrepancy of 15% between her results and those of Gaze and Peters (1961) may be accounted for by degeneration of fibres in older animals. However, it is unlikely that this explanation would account for a 5/8 reduction in the numbers of myelinated fibres from the results of Wilson to those of the present study.

The total number of unmyelinated fibres was not determined in the present work since Wilson (1971) obtained total numbers which were in good agreement with the total number of ganglion cells present in the eye. However, her results differ markedly from those of Gaze and Peters (1961), since the total number of fibres determined by her was more than twice that calculated in the earlier study of Gaze and Peters (1961). Wilson (1971) has shown that the numbers of fibres increase linearly with age.

Unmyelinated fibres

Once the first ganglion cells have been produced in the retina, unmyelinated axons can be found in the optic nerve of Xenopus tadpoles by Stage 35 and are ubiquitous throughout life (Wilson, 1971).

In young tadpoles (Stage 50) the mean and the mode of the unmyelinated fibre diameter histogram are low compared to all other stages, except for the nerve obtained from a six months old toad. At Stage 50, many ganglion cells are being produced (Jacobson, 1976; Straznicky and Tay, 1977) and it would be expected that the axons growing along the optic nerve at this time would be quite small in comparison to similar fibres which had made synaptic connexions in the brain. However, Wilson (1971) showed that throughout tadpole and adult life the mode of the unmyelinated fibre distribution remained at 0.2 μm, except for the fibre distribution from a Stage 38 animal, where the mode was 0.3 μm. When the evidence of Jacobson (1976) that the addition of new ganglion cells is most rapid between Stages 53 and 66 is viewed in conjunction with the results obtained in this study that the means and modes of the distributions studied at Stage 58 are much higher than those of the distribution studied at Stage 50, the conclusion to be drawn is that as fibres enter the nerve not only do they increase in length, but also in width. If such an increase in width did not occur, the means and modes

of the population would be much lower. This growth is not surprising since the animal itself is growing rapidly during this phase of development.

After Stage 58, the populations of unmyelinated fibres from Stages 60 and 66 nerves remain stable. When these points are viewed in the light of the knowledge that ganglion cells are still in the most rapid phase of growth (Jacobson, 1976) and that the numbers of unmyelinated fibres are increasing linearly (Wilson, 1971) two alternatives are possible. The first is that as unmyelinated fibres are added to the population they grow rapidly and replace fibres which have been myelinated. The second alternative is that as fibres become part of the population growth occurs to the extent that their axon diameters do not alter the population distribution from that found prior to the axons' development. The first alternative is unlikely since if ganglion cells are being added to the eye at the rate of 500 per day (Jacobson, 1976) 2,000 myelinated fibres would be produced in four days, whereas this number is produced in six months (fig. 2:8).

After metamorphosis has been completed the rate of production of ganglion cells decreases to 120 cells per day (Jacobson, 1976). Although the total number of ganglion cells, and hence axons, increases daily and has doubled by six months of age (Wilson, 1971), the growth is purely in length since both the mean and the mode of

the population of unmyelinated fibres decrease. A suggestion of this trend occurs at Stage 66 when, although the mode remains constant, the mean value decreases. It is only after this period, when ganglion cell addition is minimal, that the mean and mode increase in value again, indicating an increased diameter. These findings are in contrast to those of Wilson (1971) who reports that the mode of the unmyelinated fibre distribution remained at 0.2 μm throughout life. This fact, in conjunction with the observation that the numbers of unmyelinated fibres increase continually, suggests that fibres are added continuously to the whole population of fibre diameters.

Myelinated fibres

In all nervous systems, signal transfer usually comprises two or more components which have fast and slow conduction velocities. The fast transmitting sensory pathway is usually involved with escape or avoidance patterns of behaviour, whereas the slow transmitting sensory pathway is usually associated with feeding and awareness of the surroundings. The speed of conduction of the fibres may be increased by one of two strategies; either by increasing the calibre of the axon, or by investing the axon in myelin and inducing saltatory conduction. Invertebrates have adopted the former method and vertebrates

have tended towards the latter. However, even in the case of the myelinated fibre, the conduction velocity is still dependent to some degree on the diameter of the axon, since this determines the thickness of the myelin and the length of the internode.

In Xenopus, by the time tadpoles have developed to Stage 54 the number of myelinated fibres is roughly 3% of the total number of fibres present. This ratio is maintained approximately throughout life, such that even in a mature adult the number of myelinated fibres is not greater than 5% of the total number of fibres present.

Rager (1976 a), Moore et al (1976) and Skoff et al (1976 a, b) show that myelination has started just prior to the onset of vision at hatching in the chick or eye opening in the kitten or rat. At two weeks postnatally approximately 25% of the total number of fibres were myelinated and virtually all were myelinated after eleven or twelve weeks. This is quite different to the situation found in Xenopus optic nerve, where only a small proportion of the fibres became myelinated and myelination continues into adulthood.

(i) Development of myelinated fibres

Smith and Koles (1970) have shown that a myelinated axon with a particular diameter conducts impulses at a maximal velocity when it is invested by a given thickness of myelin. Therefore, it would be expected that during development myelination continues until a favourable thickness is obtained.

It is believed (Friede and Samorajski, 1967; Matthews, 1968) that myelination occurs when an axon reaches a certain "critical" diameter. Contrary to this view, Matthews and Duncan (1971) found that myelination first occurs with large fibres and then with progressively smaller ones. Similarly, Fraher (1972) concluded that, for the ventral roots of the rat spinal cord, neither a critical axon circumference nor even a critical range of circumferences appears to be important for the initiation of myelogenesis. Moore et al (1976) found that, while all the optic tract axons in the cat had received a myelin sheath by 12 weeks of age, the sheaths were not of a mature thickness and at some stage after 12 weeks they grow slowly to maturity. These results together with the present results from Xenopus suggest that myelination is not triggered by the attainment of a critical axon size, although there may be a minimum diameter below which axons will not become myelinated. Since the mode of the myelinated axon population in a mature adult is within a range of values at which only very few fibres are myelinated in the tadpole, this indicates that the possible lower limit of the axon diameter for myelination decreases with age.

The finding of Rager (1976 a) that in the chick the values of ρ remain within the range of 0.6 to 0.8 indicates that the process of myelination is intimately linked with axonal growth. A similar finding was obtained by Peters

(1964) in the optic nerves of rats and mice. He found that whenever an axon was surrounded by four or more myelin lamellae there was a tendency for the internal and external mesaxons to lie in the same quadrant.

According to Peters, the most reasonable explanation for this finding is that myelin sheath growth is a phasic process. Similarly, in the cat optic nerve Moore et al (1976) suggest that the initiation of myelin synthesis is associated closely with an almost stepwise growth of an unmyelinated axon. They continue that, during the most active period of myelination, newly myelinating fibres are drawn continuously and uniformily from the entire distribution of unmyelinated fibres. They are rapidly added to the myelinated population by growing by about 0.6 μm in diameter. Their basis for this conclusion is that the means of the two fibre populations remain at the same values.

As in the cat, new fibres for myelination in Xenopus are drawn from the whole population and increase in size, but with postmetamorphic age the growth is limited and the mode of the distribution is less than 1 μm. However, with maturity fibres increase in size, but it is difficult to determine if this is the same in Xenopus as in the cat because of the relative numbers of fibres involved. Many myelinated fibres are less than 1 μm and the mode is

0.87 μm in the six months old toad and 1.11 μm in the adult. This represents a downward shift relative to the tadpole and indicates that smaller fibres are being myelinated, although these increase in diameter in the adult. Therefore, myelination is not due to a stepwise growth. Further weight to this idea is provided by the fact that $^{d}/_{D}$ decreases with age, which shows that myelin is being added to the sheaths to bring more fibres within the physiologically efficient range. Determination of whether myelination is a stepwise process or not would require the study of many nerves, since in the tadpole less than a hundred fibres are being myelinated at any one time and this figure is even lower in the adult.

During development of tadpole and adult Xenopus the means and modes of the myelinated fibre diameter distributions change. During tadpole life only the largest fibres are myelinated and then only sparsely. Large axons and the presence of a myelin sheath are usually indicative of a faster conduction velocity. The trend of decreasing means and modes and increasing numbers of myelinated fibres with age indicates that small fibres become myelinated with increasing juvenile age. However, during maturity there is a general increase in the size of the fibres in the population, hence producing a higher mean and mode than found at six months of age. The irregular shape of the Stage 60 myelinated fibre histo-

gram (fig. 2:4) may be partly due to the shortening of the nerve causing fibres to alter shape or to the degradation of particular myelin sheaths. At Stage 66, the decrease in the mean and the mode may be due to shrinkage of the larger fibres or to their selective loss and replacement by smaller fibres.

(ii) The relationship of myelin thickness to axon diameter during development

The literature concerning the optimal thickness of myelin for a given size of axon is discussed in detail by Rager (1976 a). From a theoretical point of view, Smith and Koles (1970) have calculated that the ratio of axon diameter (d) to fibre diameter (D), $^{d}/_{D}$, at which the myelin sheath has a maximum effect of increasing the conduction velocity is when the value of ρ falls within the range 0.6 to 0.8.

Very few studies have been carried out on the relationship between myelin thickness and axon diameter in the optic nerve during development. The two known studies are both from endothermic animals, the chick (Rager, 1976 a) and the kitten (Moore et al, 1976). The results of Rager indicate that the value of ρ for a variety of axon diameters remains within theoretically favourable limits of Smith and Koles through-

out development up to 80 days post-hatching. In comparison the results of Moore et al indicate that generally the values of ρ for the three sizes of fibres (2 μm, 4 μm and 6 μm in circumference) have mean values which are at or above the upper limit of the theoretical values of Smith and Koles. However, sometime between the 12th week of life and adulthood, the thickness of the myelin increases, and mean ρ values of 0.68 to 0.74 can be calculated. This is a similar situation to that found here in Xenopus. Initial myelination is poor, but with time the thickness increases until in a mature adult the mean value is at an optimum. However, mean values must be used with caution since the population may be dispersed over a wide range or concentrated within a small range and these features of the distribution cannot be determined from the mean alone. Mean values become misleading when the populations are skewed. Tapp (1974) found in the optic nerve of the teleost Eugerres that the mean value of ρ was 0.67 but that more than half of the population fell outside the theoretical limits of Smith and Koles. With respect to these two points, neither Rager (1976 a) nor Moore et al (1976) publish the histograms of the relationship of myelin thickness to axon diameter, but in both cases these are represented by mean values. Moore et al (1976) show that the degree of myelination is proportional to the size of the axon although the diameter of the fibre indicates that the axon is probably physiologically inefficient.

In the case of a Stage 58 tadpole the mean value of is high, which indicates that, relative to the axon size, the amount of myelin is small. In tadpoles mature myelin comprises only six or seven lamellae. The mean values of ρ are 0.845 and 0.858 for the two nerves at Stage 58 and 0.833 at Stage 60. The conclusion to be drawn is that the myelinated fibres are not minimizing their conduction time effectively in these nerves. It is interesting to note that during the period of myelin degradation at Stage 66, the mean value of ρ falls to 0.768. This may be explained in terms of an increase in the thickness of the myelin sheaths already present, although this seems unlikely in the light of the myelin degradation occurring at this time. Since the numbers of myelinated fibres vary little at this time, the decrease in the value of ρ cannot result from an increase in the number of smaller myelinated fibres. Alternatively, the myelinated fibres are decreasing in diameter, a possibility which is supported by a decrease of one third in the mean diameter. In this case, the myelin sheath will have increased in thickness relative to the axon diameter, and the mean value of ρ falls within the optimal physiological range of Smith and Koles. After metamorphosis has been completed the mean value of the ratio $^{d}/_{D}$ continues to decrease and the distribution becomes more dispersed. In the adult a mean of 0.702 and a mode of 0.725 are realised, with the majority of fibres having ρ values which indicate physiological efficiency in terms of conduction velocity.

The high value of $^{d}/_{D}$ may be an indication that in the tadpole there is competition for the lipid precursors which are required for myelin formation. This may also be evidenced by the high values of ρ in the kitten (Moore et al, 1976). On the other hand, the values of ρ in the chick (Rager, 1976 a) may be maintained in the most efficient range by the large amounts of fat within the egg, which continue to be used as a food source after hatching. The myelinated fibres at Stage 58 may act as a lipid store for the myelination of other fibres during and shortly after metamorphosis. On the other hand, the factors which initiate myelin degradation may have an earlier effect on the glial cells to prevent myelin sheath production.

Growth of axons

It is interesting to note that during development the fibre diameter distributions change, although this change is not a result of straightforward growth. In tadpole life the axons have small diameters when they are first produced but have grown to a large diameter by Stage 58 (figs. 2:18 and 2:19). During and after metamorphosis the increase in the smaller diameter fibres can be attributed to the influx of many axons which originate from newly developed ganglion cells.

Since throughout life the animal is growing continually, and the eye becomes further and further removed from the brain, any temporal relationships between the eye and the brain would change, unless

the axons in the optic nerve alter their conduction velocities to compensate for this change. Temporal relationships are present not only between the afferent ganglion cell axons (Maturana et al 1960) but also possibly between the brain and the eye, since efferents to the retina are known to occur in birds (Cowan, 1971; Sohal, 1975) and in snakes (Halpern et al, 1976). There is also some evidence, both structural (Maturana, 1958) and physiological (Ewert and Borchers, 1974 a) for the presence of efferents in the toad (Bufo bufo) optic nerve. This change to an increased conduction velocity is most applicable to myelinated fibres, which have been associated with the Class III and Class IV ganglion cell responses. Ewert and Borchers (1974 a) have shown that the responses of these two ganglion cell classes were inhibited during blinking. It is not only myelinated fibres which are affected since the signals carried by unmyelinated fibres will have a different temporal relationship relative to each other and to the myelinated fibres. This difference will not affect the relative temporal spacing of afferent signals, but could have a drastic effect on the absolute temporal spacing of signals.

This change in the absolute timing of afferent impulses is reduced by myelinated fibres increasing not only in diameter but also the amount of myelin surrounding the axon, so that many fibres fall within the physiologically

efficient range of values of ρ of 0.6 - 0.8 (Smith and Koles, 1970). Unmyelinated fibres also increase in diameter in adulthood (see figs. 2:16, 2:22 and 2:23). These points should be viewed in conjunction with the facts that when the ganglion cell axons are large in the tadpole, the nerve is long; when the nerve is short, after metamorphosis, the diameters of the fibre populations are small (figs. 2:1 and 2:16).

Reconstructions of compound action potentials

Since physical factors are intimately involved in the conduction of action potentials it is possible to reconstruct the compound action potentials of nerves providing the fibre diameter distributions are known (Gasser and Erlanger, 1927). Reconstructions of the compound action potentials during development of the optic nerves were attempted. The complex geometric reconstruction of Gasser and Erlanger (1927) was used for the adult optic nerve, but was found to be inapplicable. The more pragmatic method of Landau et al (1968) was also used since favourable results had been obtained for the optic nerve of the cat (Landau et al, 1968; Hughes and Wässle, 1976), duck (O'Flaherty, 1971) and teleost Eugerres (Tapp, 1974) and for the optic tracts of the cat (Bishop et al, 1969). The method was found to be inapplicable to the optic nerves of tadpole and adult Xenopus. This may be because

the nerve contains a mixture of both myelinated and unmyelinated fibres, although the latter are predominant. However, Vaney and Hughes (1976), in their study of the rabbit optic nerve, also were unable to obtain satisfactory results using the method of Landau et al, even though the nerve contains predominantly (98%) myelinated fibres.

Overall comparison of the development of the optic nerve of Xenopus with that of other animals

In other studies on the development of the visual system of other animals Rager (1976 a, b) finds for the chick that the connexions have been made and could possibly be functioning prior to hatching. However, it has been reported that growth of the chick retina may continue post-natally (Morris et al, 1976). Similar studies on the rat have shown that, although the visual system is still immature at the time of eye opening, the connexions have been made and are functioning (Weidman and Kuwabara, 1968; Caley et al, 1972; Lund and Bunt, 1976). Similar results have been obtained for the cat, although in this case it is known that development proceeds at an explosive rate after eye opening (Hubel and Wiesel, 1963; Donovan, 1966; Glendenning and Norton, 1973; Stein et al, 1973; Norton, 1974; Pettigrew, 1974; Cragg, 1975) and that the system is especially vulnerable to deprivation (Hubel and Wiesel, 1970; Hubel et al, 1977) and is probably sensitive

to modified visual experience (Blakemore, 1974, 1977). However, in Xenopus and other amphibia and some teleost fish, the situation is somewhat different since the eye is functional during the period of its growth which continues into adulthood (Hollyfield, 1968, 1971; Straznicky and Gaze, 1971; Jacobson, 1976; Easter, 1977; Straznicky and Tay, 1977).

CHAPTER III

Electrophysiology of the developing optic nerves

INTRODUCTION

Two previous studies have been carried out on the size classes of axons in the optic nerve of adult and tadpole Xenopus (Gaze and Peters, 1961; Wilson, 1971). Including the findings presented here (Chapter 2), all three reports indicate a small but substantial myelinated fibre component in the tadpole nerve. Physiological evidence (Chung, Keating and Bliss, 1974) suggests that postsynaptic activity from fast conducting myelinated axons is absent from the optic tectum prior to Stage 59. This raises the question of whether the myelinated fibres are functional in the tadpole optic nerve. This was investigated by attempting to record the responses of these fibres to an electrical stimulus applied to the nerve.

Since there is some discrepancy in the literature concerning the conduction velocities of fibre groups in the optic nerve of anurans (all species of Rana, see Grüsser and Grüsser-Cornehls, 1976) an attempt to determine the conduction velocities of fibres in Xenopus optic nerve would be useful for comparison. The results from both adult and tadpole were also correlated with the postsynaptic evoked potentials in the optic tectum (see Chapter 5).

METHOD

Two approaches were used to study the physiology of the optic nerves; one to record compound action potentials (CAPs) *in situ*, and another to measure CAPs in isolated preparations.

A. *IN SITU* RECORDINGS

(i) Two months of age and older

The brains were exposed as described in section 'B' of the General Methods. The brain rostral to the cerebellum was removed by suction and the lateral edges of the skull were cut away. A small hole was made in the sclera of the eye to facilitate entry of a stimulating electrode. The animals were immobilized by an injection of 2-12 mg of succinyl choline in aqueous solution into the dorsal lymph sac. Electrophysiological recordings from the optic nerves of toads were made with the animals in air and at room temperature. All exposed surfaces were covered with paraffin oil.

(ii) Tadpoles and postmetamorphic toads up to two months of age

The brains were exposed according to the procedure given in section 'B' of the General Methods. The brain was removed and a small hole was made in the eye. These individuals were immobilized with 0.02 - 0.05 mg of d-tubocurarine (Duncan, Flockhart and Co. Ltd., London) administered by injection into the leg in young toads and behind the non-experimental eye in tadpoles (Gaze et al, 1974). CAPs were recorded from tadpoles under Niu-Twitty solution.

In animals of all ages the cranium was filled with Niu-Twitty solution and the severed optic nerve was drawn up into a recording suction electrode. A steel micro-electrode, insulated to within 5-10 μms of the tip, was introduced into the eye through the hole in the sclera. The electrode was advanced in 5 μm steps towards the region of the optic nerve head until a maximal response to a 20 V 0.1 msec pulse could be recorded with the suction electrode. The indifferent electrode was placed on the cornea in toads and near to the eye in tadpoles.

B. RECORDINGS FROM ISOLATED NERVES

Recordings were made from isolated nerves from animals up to a postmetamorphic age of two months. After this time,

it is too difficult to isolate the nerve intact. The brains were exposed and removed under Niu-Twitty solution as described in 'A' above. The optic nerve and the eye were freed from all the surrounding tissue and the nerve sheath was loosened with sharpened steel pins to enable the nerve to be withdrawn. A desheathed preparation was necessary to prevent fouling of the suction electrodes. For ease of handling the eye remained attached to the nerve until the latter was introduced into the electrodes.

The diameter of the isolated nerve was measured using a calibrated eyepiece graticule. Suction electrodes were produced by breaking the tip from a glass microelectrode and flame polishing the end. These electrodes were filled by injection of Niu-Twitty solution and were inserted into the holder which contained a silver/silver chloride wire. Each end of the nerve was then introduced into a separate suction electrode by reduced pressure. The second stimulating electrode was placed adjacent to where the nerve emerged from the suction electrode. The indifferent electrode for recording was positioned so as to reduce the stimulus artefact to a minimum.

Pulses were generated by a C.F. Palmer 8128 stimulator and were used to drive a Devices Isolated Stimulator Mark III, with a delay. This produced pulses of up to 90 V. The width of the stimulating pulse was usually maintained at 50 μsecs, although occasionally a width of 100 μsecs

was used. The CAP signals were amplified by 1,000 using a high input impedance amplifier with an input time constant of two seconds. For display and recording the output was passed to a Tektronix 502A oscilloscope which was triggered by the C.F. Palmer stimulator. Single frame photographs were taken on Kodak 2495 RAR film, with a Nihon-Kohden PC-2A oscilloscope camera.

The length of each optic nerve was measured *in vivo* and *in vitro* using a calibrated eye piece graticule in an Olympus stereomicroscope. The length of the nerves, or distance between the electrodes, could be measured to within an accuracy of 50 μm in all preparations except those involving adults.

Latency and hence conduction velocity were determined and stimulus/response graphs were compiled from the photographs.

C. HISTOLOGY

A number of nerves were prepared for electron microscopy in order to correlate the nerve fibre size distribution with the recorded CAP. For this, nerves from which recordings had been made *in situ* were fixed *in situ* by immersion and were left in the same fixative overnight. The nerves were then dissected from the animal and were left in fixative for a further twelve hours, after which they were transferred to a dextrose/phosphate wash.

Isolated nerves were fixed in the recording apparatus for 30 minutes with cold fixative, after which they were released from the suction electrodes. The nerves were kept in the same fixative for 24 hours and were then transferred to the dextrose/phosphate wash.

All nerves were stored in this wash solution until a number had accumulated over a period of one week. They were then processed and embedded for electron microscopy as detailed in section 'E' of the General Methods. Measurements of myelinated and unmyelinated fibres were carried out as described in Chapter 1.

RESULTS

A. PHYSIOLOGICAL RECORDINGS

Compound action potentials (CAP's) were recorded in response to electrical stimulation in 76 optic nerves. In the case of 13 individuals, responses were obtained from both optic nerves. The results from *in situ* and isolated preparations were found to be similar in animals of the same stage. Fourteen of the nerves from which the CAP was recorded were fixed for electron microscopy. Detailed analysis of the fibre diameter distribution of five of these nerves were carried out.

The length of the nerve between stimulating and recording electrodes was taken to be the conduction distance. Measurements of latencies were taken from oscilloscope traces photographed at high sweep speeds. Photographs of responses were taken at low sweep speeds for illustrative purposes. Latency measurements were always taken from the maximal response evoked, and measured with respect to the peak of the wave, since

Fig. 3.1: Compound action potentials recorded in an adult Xenopus optic nerve.

(a) Sequence of compound action wave forms recorded from the adult optic nerve to two levels of stimulating voltage. The first record (10 V stimulus) reveals the short latency m_1 potential at stimulus levels that do not stimulate the slower conducting fibres. The second record, at a higher stimulus voltage (60 V) reveals three additional conduction velocity groups, labelled m_2, u_1, and u_2 (the m_1 wave is obscured by the stimulus artifact). The calibration scales apply to both records.

(b) Stimulus voltage - amplitude plot for the four compound action waves. The waves, in order of increasing threshold, are m_1 wave (curve 1), m_2 wave (curve 2), u_1 wave (curve 3) and u_2 wave (curve 4).

3·1

a

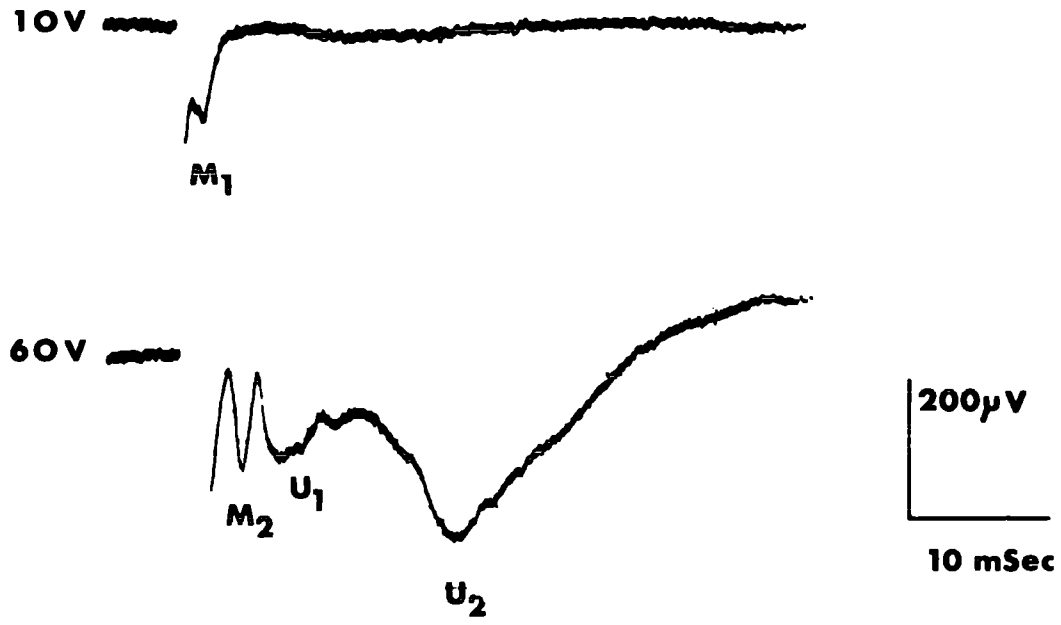
10V
M1
60V
M2
U1
U2
200μV
10 mSec

b

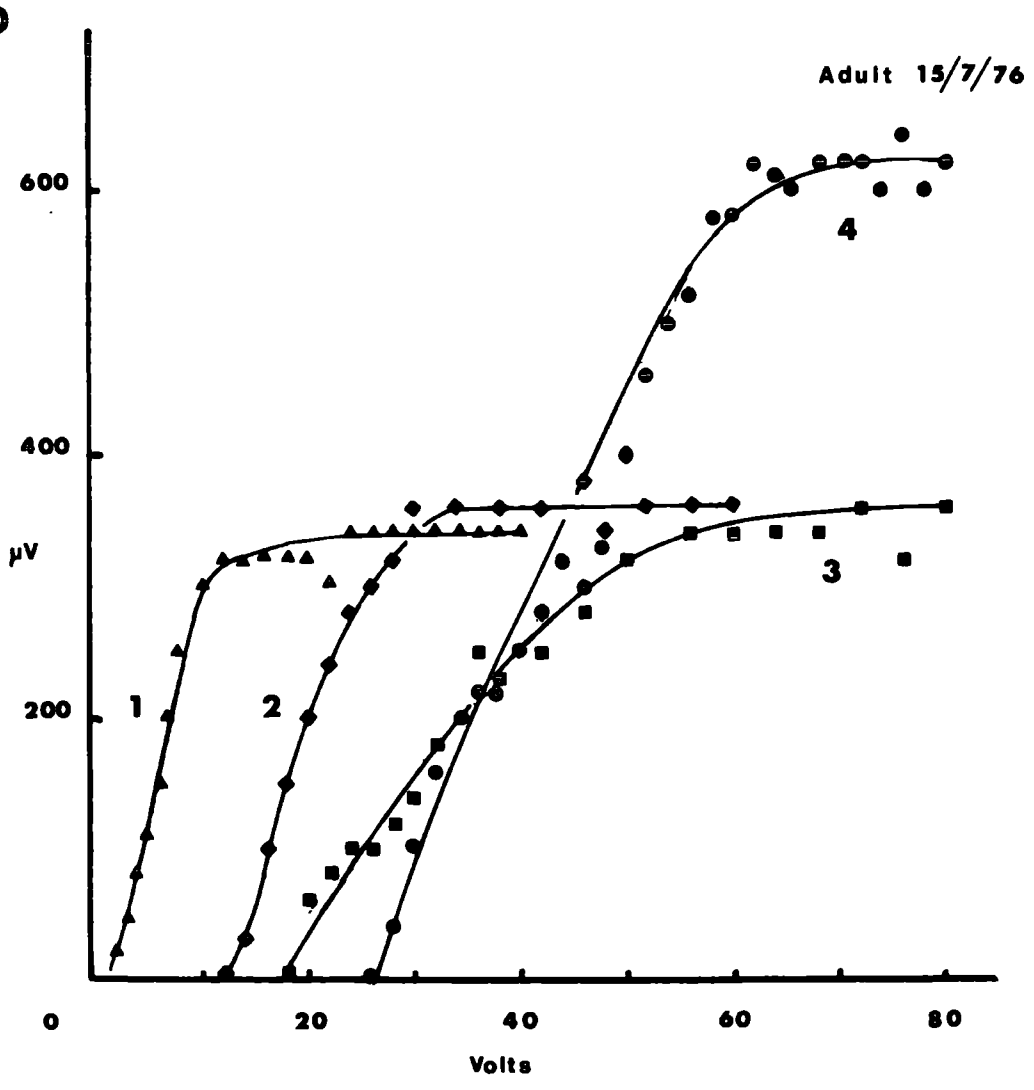
Adult 15/7/76
600
400
200
μV
1
2
3
4
0
20
40
60
80
Volts

the beginning of a particular wave was often obscured by another wave or the stimulus artifact. Conduction velocities were calculated from the measured conduction distance divided by the measured latency.

Adult

The compound action potential recorded from the adult Xenopus optic nerve in response to a low intensity stimulus (10 V) comprises a small negative deflection of short latency which is partially obscured by the stimulus artifact (fig. 3:1 a, 10 V). At a much higher stimulus intensity (60 V), the first wave is completely obscured by the stimulus artifact, and three waves with longer latencies are apparent (fig. 3:1 a) at this higher stimulus intensity. The four waves have conduction velocities of 2.75, 1.2, 0.78 and 0.25 m/sec^{-1} and have been termed m_1, m_2, u_1 and u_2 respectively, in accordance with a study of the conduction velocities in the optic nerve of Rana pipiens (Chung, Bliss and Keating, 1974).

The responses of the four waves of the CAP to increasing stimulus voltages are given in figure 3:1 b. From this it can be seen that the four waves appear sequentially as the stimulus voltage is increased. The first wave (m_1) appears at a stimulus voltage of 2 V and very rapidly reaches a maximum amplitude at 12 V. The second wave (m_2) appears at 14 V and the maximum response is reached at 30 V. The third wave (u_1) appears at 20 V and increases very slowly

to a maximum at 66 V. The fourth wave (u_2) appears in response to a 24 V stimulus and becomes maximal at 70 V. It was possible to stimulate all four groups maximally with the 90 V available using pulses of 50 or 100 μsec only.

These stimulus-response recordings demonstrate that the m_1 wave has the lowest threshold and the fastest conduction velocity, which suggest that the fibres producing this wave are the largest fibres within the optic nerve. The threshold values for the second, third and fourth waves are progressively higher and the latencies progressively longer. This indicates that the responses are recorded from groups of fibres of decreasing diameter, the fourth wave being derived from the smallest fibres.

Tadpoles

Stage 48

At Stage 48, only one CAP wave can be evoked in the optic nerve (fig. 3:2 a). The stimulus-response characteristics are essentially linear up to a stimulus of 8 V, and a maximal response is obtained at 12 V (fig. 3:2 b). The latency to the peak of the wave indicates a conduction velocity of 0.19 m/sec^{-1}.

Fig. 3.2: Compound action potentials in a stage 48 tadpole optic nerve.

(a) Compound action potentials recorded in a stage 48 tadpole optic nerve to increasing stimulus voltage (stimulus voltage indicated below each record). Only one wave is present in all records. The conduction velocity of this compound action potential was 0.19 m/sec.$^{-1}$ In all records the time of application of the stimulus is marked by a small spot above the records.

(b) Stimulus voltage - compound action potential amplitude plot for the stage 48 optic nerve illustrated in a.

3·2

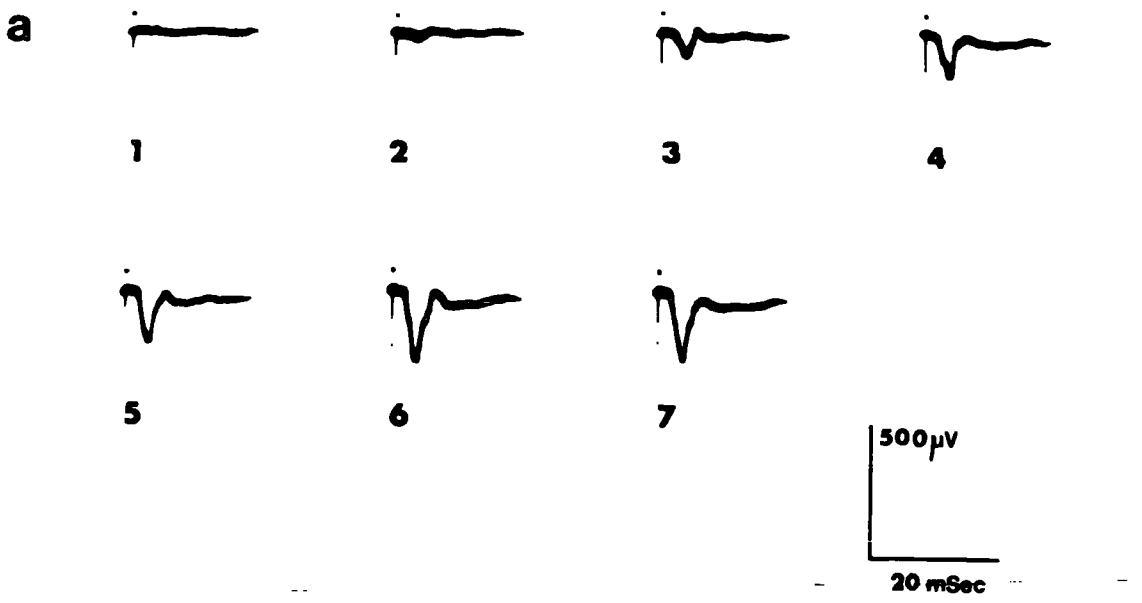
a
1
2
3
4
5
6
7
500μV
20 mSec

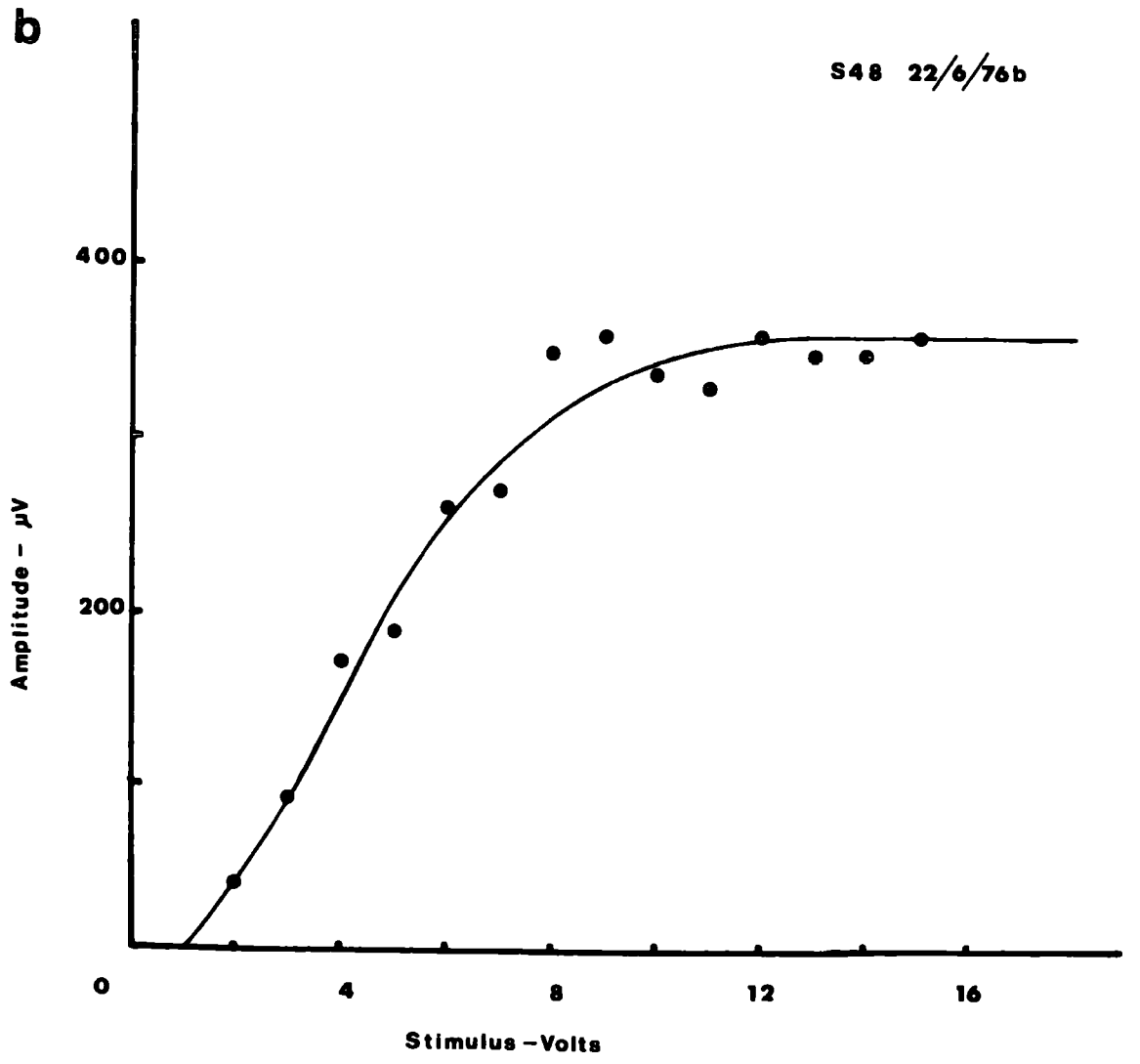
b
S48 22/6/76b
400
200
0
4
8
12
16
Amplitude – μV
Stimulus – Volts

Stage 50

At Stage 50, either one or two waves are evoked. Figure 3:3 a shows a stimulus-response series with the CAP consisting of one wave only. This is represented graphically in figure 3:3 b which shows the stimulus-response relationship to be asymptotic. The latency to the peak of the wave gives a conduction velocity of 0.14 $m/sec.^{-1}$ Figure 3:4 a is an example of the CAP consisting of two waves. The wave with the lowest threshold has the shortest latency. Both waves show an asymptotic relationship between the stimulus voltage and the response (fig. 3:4 b). The conduction velocities of the two waves are 0.2 - 0.25 m/sec^{-1} and 0.14 $m/sec.^{-1}$ This second wave has the same conduction velocity as the single wave recorded in preparations of the same stage in which only one wave could be elicited.

Stage 54

At Stage 54, the evoked CAP is more complex (figs. 3:5 a, b). The first wave to be evoked occurs in response to a 4 V stimulus and the amplitude of the response shows an initial rapid increase with increasing intensity and reaches asymptote at 30 V. The second wave also has a low threshold, appearing at a stimulus intensity of 6 V. The response amplitude increases rapidly and levels off at 40 V. The third wave, which

Fig. 3.3: Compound action potentials in a stage 50 tadpole optic nerve.

(a) Records of compound action potentials in a stage 50 tadpole nerve to increasing values of stimulus voltage (indicated beneath each record). In this series only a single compound action potential is recorded, whose conduction velocity is 0.14 $m/sec.^{-1}$

(b) Stimulus voltage - compound action potential amplitude graph for the records illustrated in a.

3·3

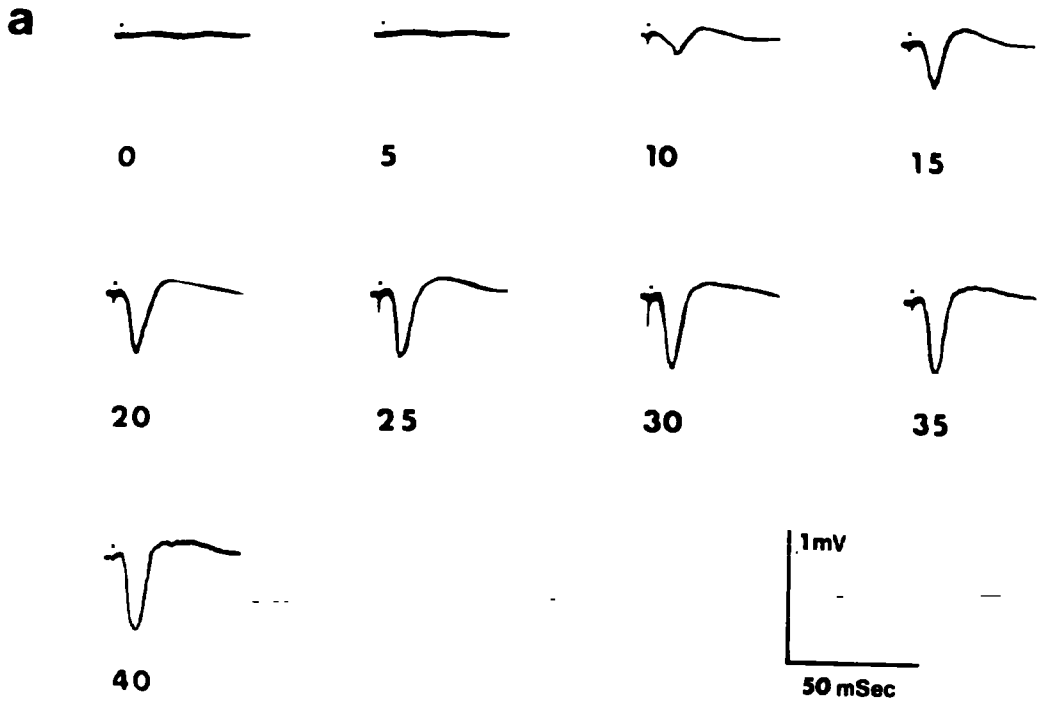
a
0
5
10
15
20
25
30
35
40
1mV
50 mSec

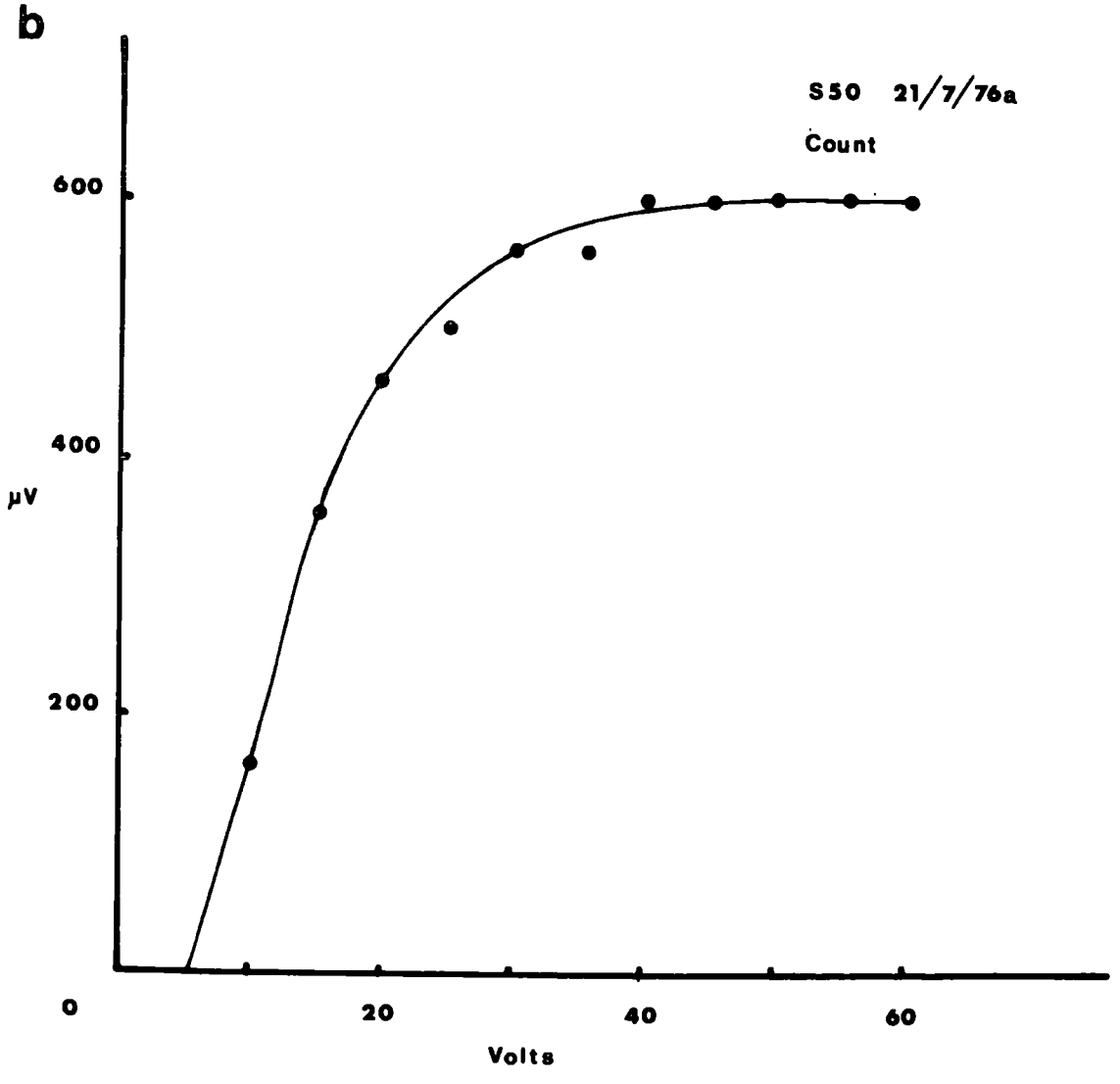
b
S50 21/7/76a
Count
600
400
200
0
µV
20
40
60
Volts

Fig. 3.4: Compound action potentials in a stage 50 tadpole optic nerve.

(a) Records of compound action potentials in a stage 50 tadpole nerve to increasing values of stimulus voltage (indicated beneath each record). In this series the compound action potential fractionates into two conduction velocity groups (0.25 m/sec^{-1} and 0.14 m/sec^{-1}).

(b) Stimulus voltage - compound action potential amplitude graph for the two potential components illustrated in a. The lowest threshold group (labelled $\overline{1}$) corresponds to the wave with the shortest latency, (plotted as filled circles). The longer latency wave B labelled 2 (solid squares).

3-4

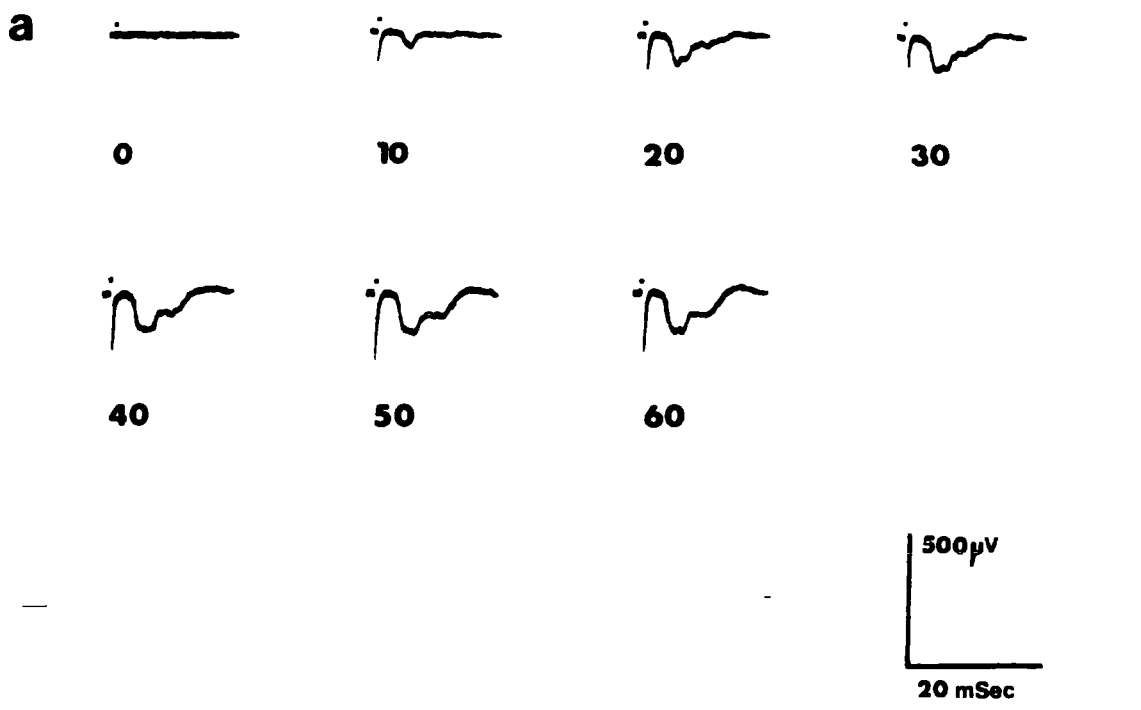
a
0
10
20
30
40
50
60
500μV
20 mSec

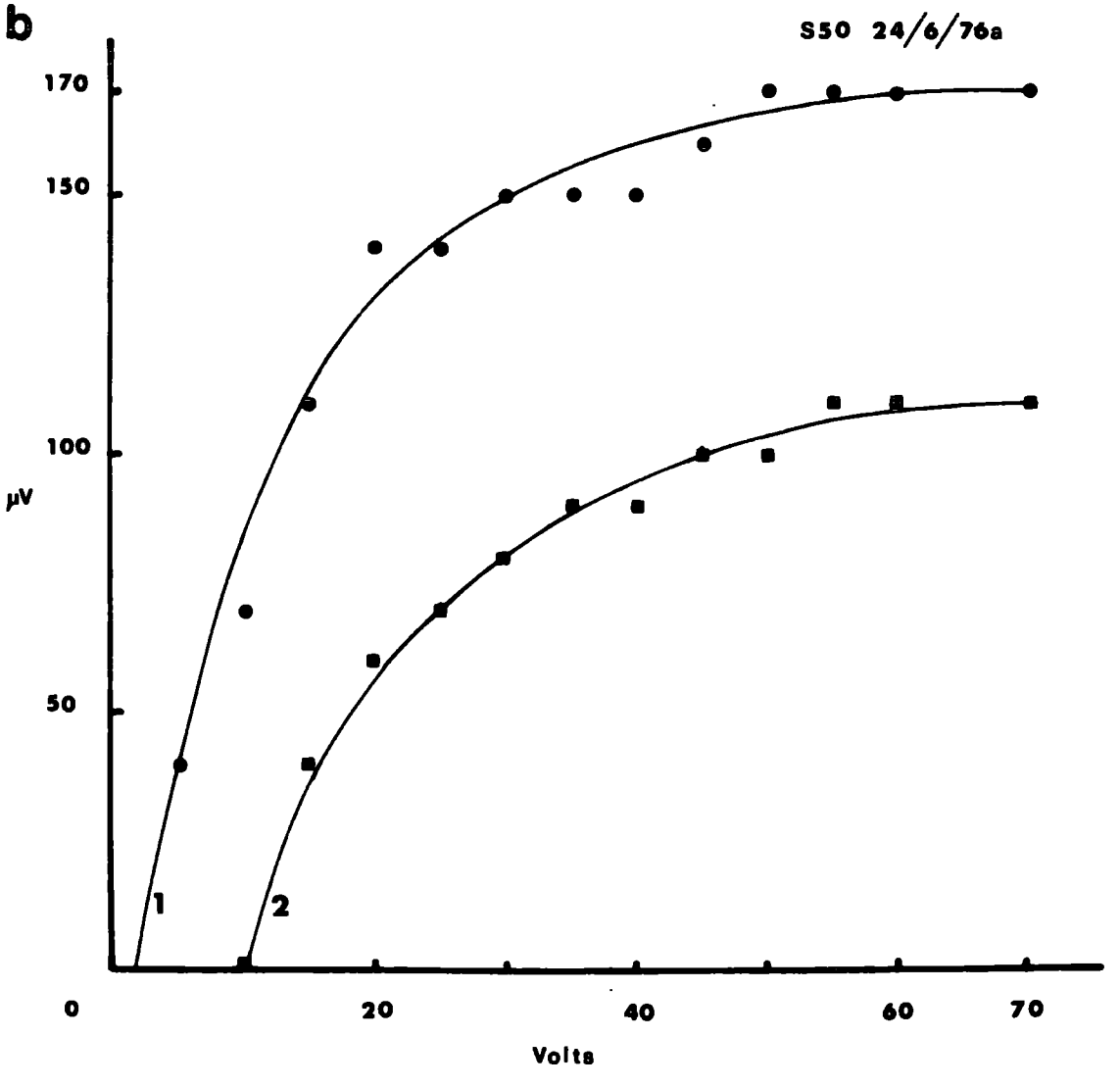
b
S50 24/6/76a
170
150
100
μV
50
1
2
0
20
40
60
70
Volts

Fig. 3.5: Compound action potentials in a stage 54 tadpole optic nerve.

(a) Compound action potentials recorded in a stage 54 optic nerve at different levels of stimulus voltage (indicated below each record). At this stage three compound action potential groups, separated by their different time courses and latencies, can be observed. The conduction velocities of the waves are 1.13, 0.25 and 0.15 m/sec^{-1}.

(b) Stimulus voltage - compound action potential amplitude graph for the three waves recorded in the series in a. The curves labelled 1 (solid triangles), 2 (solid circles) and 3 (solid squares) are the stimulus voltage-amplitude relationships for the groups with conduction velocities of 1.13, 0.25 and 0.15 m/sec^{-1} respectively.

3·5

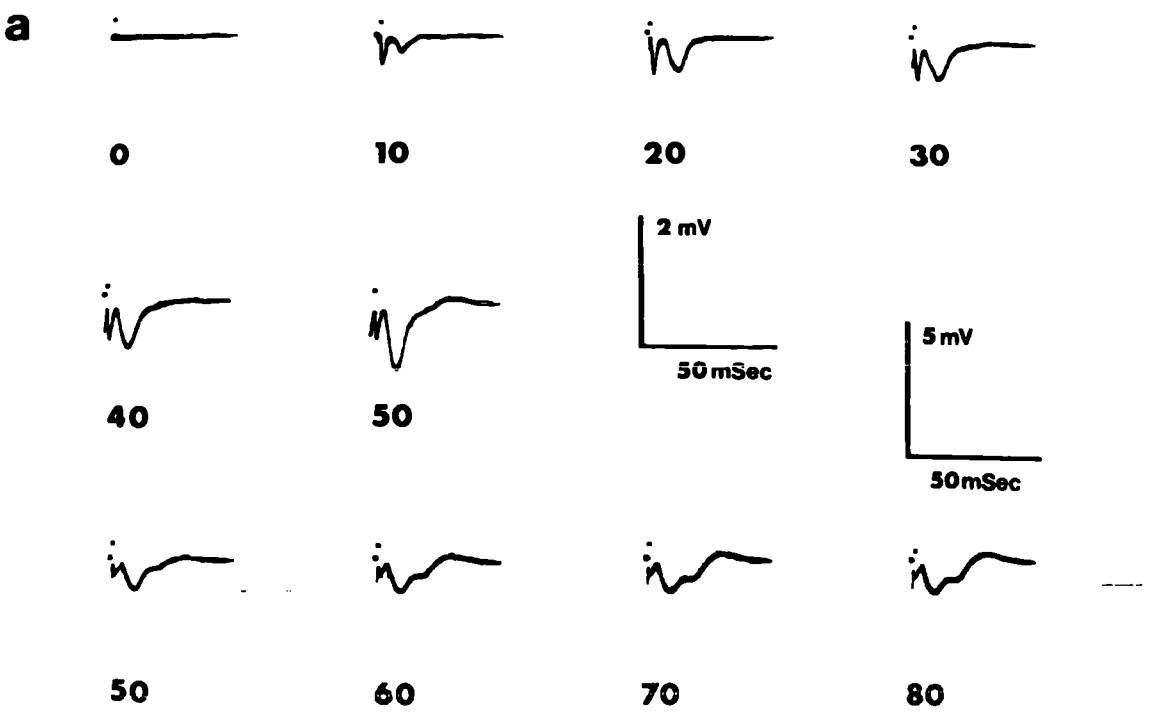
a
0
10
20
30
2 mV
50 mSec
40
50
5 mV
50 mSec
50
60
70
80

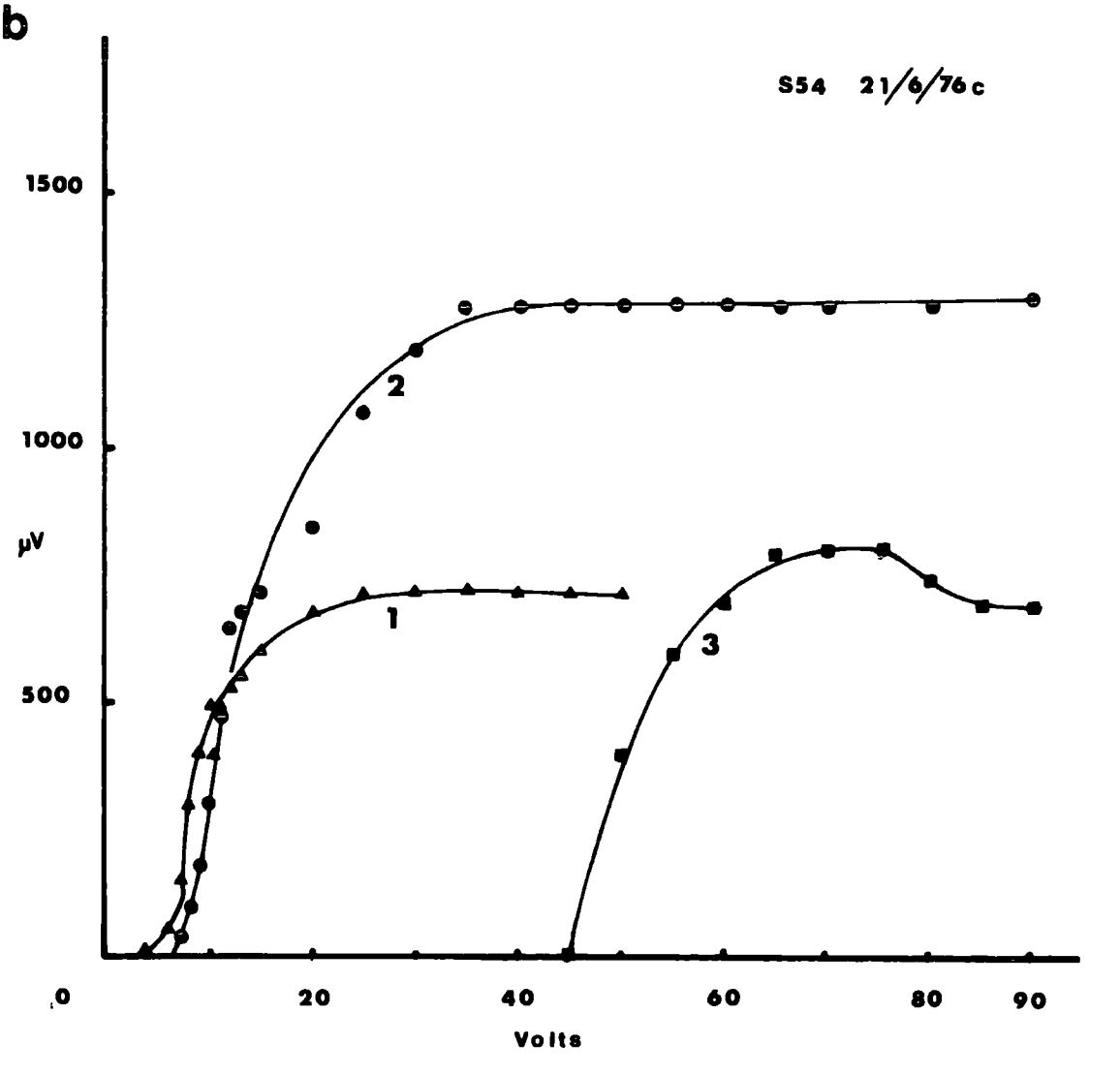
b
S54 21/6/76 c
1500
1000
µV
500
1
2
3
0
20
40
60
80
90
Volts

is partially obscured by the second wave, slowly increases in amplitude and is evoked maximally at about 70 V. At higher stimulus voltages the amplitude of the wave decreases. The conduction velocities of the three waves are 1.13, 0.25 and 0.15 m/sec.$^{-1}$ The very short latency wave is possibly comparable to the m_2 wave of the adult. If this is the case, Stage 54 is the earliest age at which myelinated fibre activity can be detected in the tadpole optic nerve.

Figure 3:6 shows the CAP's recorded from both optic nerves obtained from a Stage 54 animal. The responses obtained were slightly sub-maximal, but similar waveforms are produced in the two nerves. Two prominent waves are present in each response, a fast conducting group (wave 1) with conduction velocities of 1.33 m/sec^{-1} for nerve 'a' and 1.2 m/sec^{-1} for nerve 'b', and a slower group (wave 2) with conduction velocities of 0.3 m/sec^{-1} for nerve 'a' and 0.28 m/sec^{-1} for nerve 'b'. A third long latency wave (wave 3) with a conduction velocity of 0.1 m/sec^{-1} is indicated in the recordings from both nerves.

Stage 56

At Stage 56, similar responses to those obtained from the Stage 54 nerves can be evoked. The m_2 wave can be evoked at a very low stimulus intensity (fig. 3:7 a, b). Typically, the response amplitude rises rapidly with small increments of the stimulus intensity,

Fig. 3.6: Compound action potentials in both optic nerves of a single stage 54 tadpole.

(a) Compound action potential waves recorded from one nerve of a stage 54 animal compared with the records obtained from the optic nerve on the opposite side (b). The calibration bars apply to both records. Labels 1, 2 and 3 identify the m_2, u_1 and u_2 waves respectively.

3·6

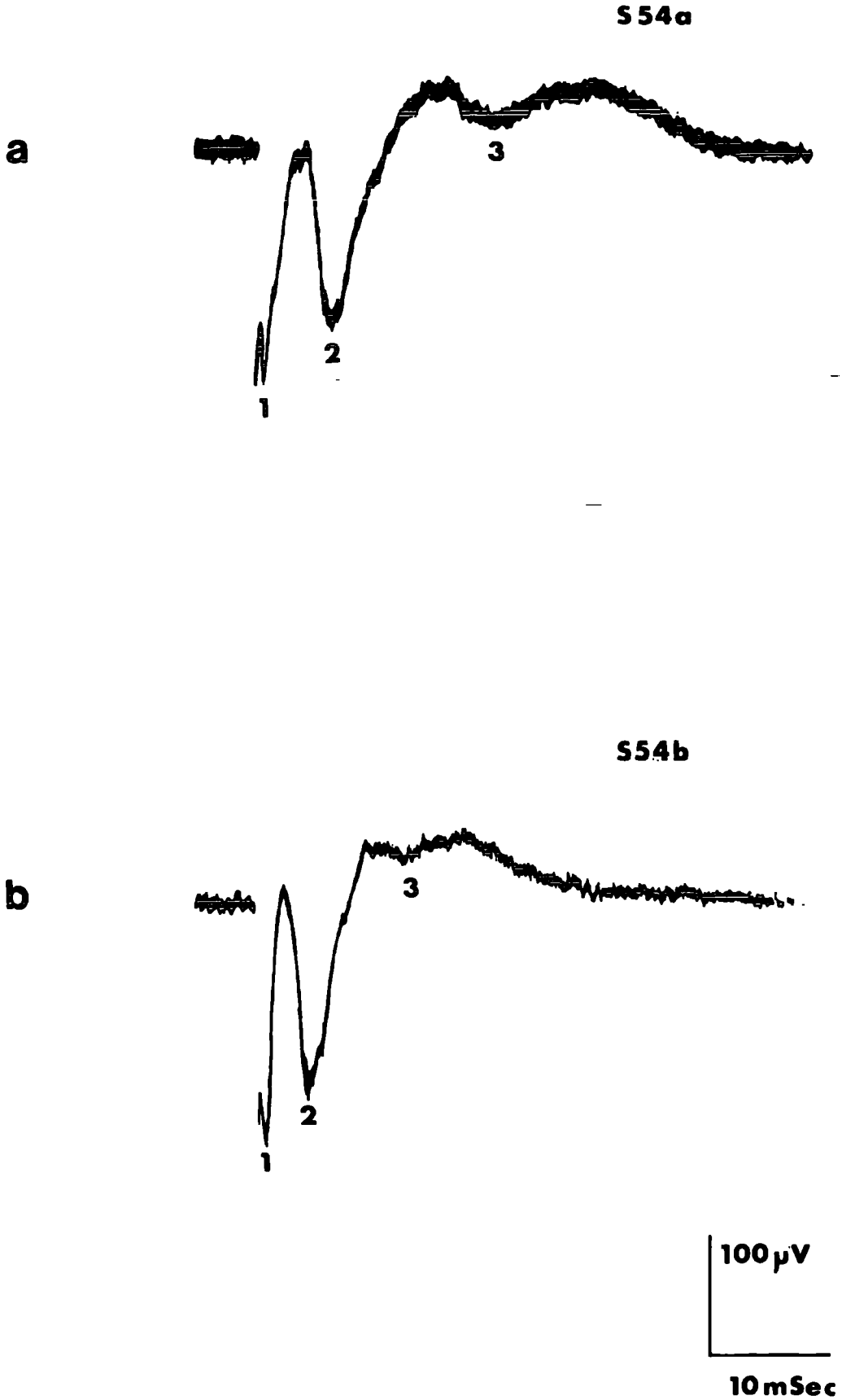

Fig. 3.7: Compound action potentials in a stage 56 tadpole optic nerve.

(a) Records of compound action potential responses in a stage 56 tadpole optic nerve to increasing values of stimulus voltage (indicated beneath each record). In this series it is clear that three distinct conduction velocity groups are present. (Conduction velocities 1.27, 0.22 and 0.16 m/sec^{-1}).

(b) Stimulus voltage - compound action potential amplitude plot for the three waves illustrated in a. The lowest threshold group (solid triangle is labelled 1) corresponds to the wave with the shortest latency (conduction velocity 1.27 m/sec^{-1}). The curve labelled 2 (solid circles) corresponds to the wave with a conduction velocity of 0.22 m/sec.$^{-1}$ The curve labelled 3 (solid squares) represents the long latency wave with a conduction velocity of 0.16 m/sec.$^{-1}$ This nerve was fixed after recordings and fibre diameters and numbers were counted. The structure is illustrated in figure 3.12.

3·7

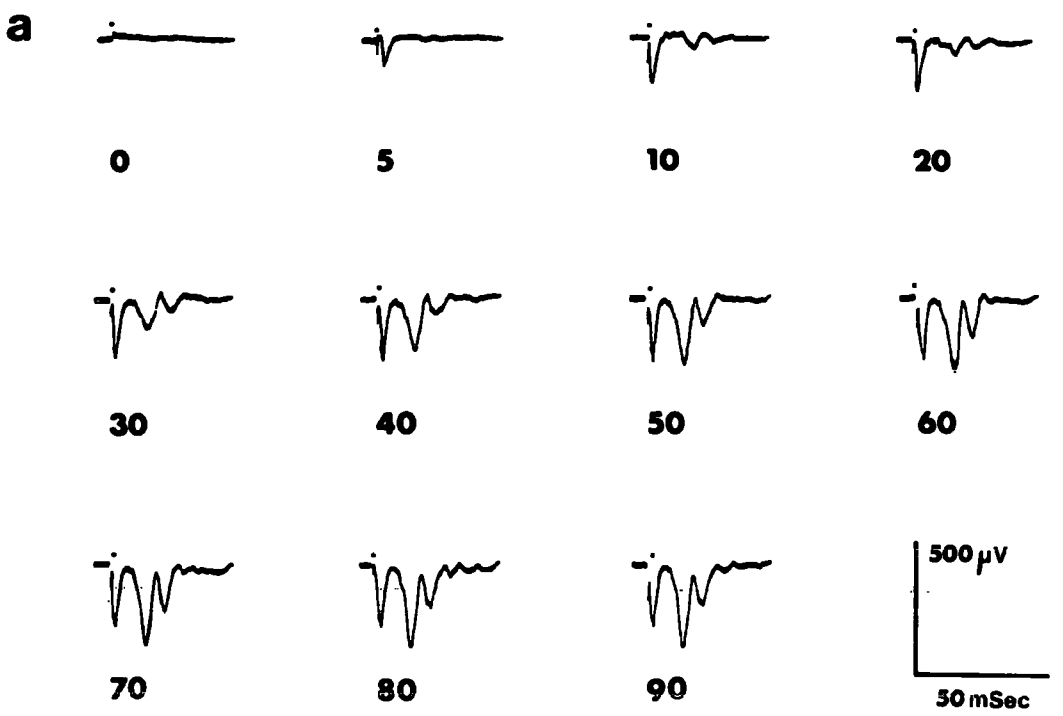
a
0
5
10
20
30
40
50
60
70
80
90
500 µV
50 mSec

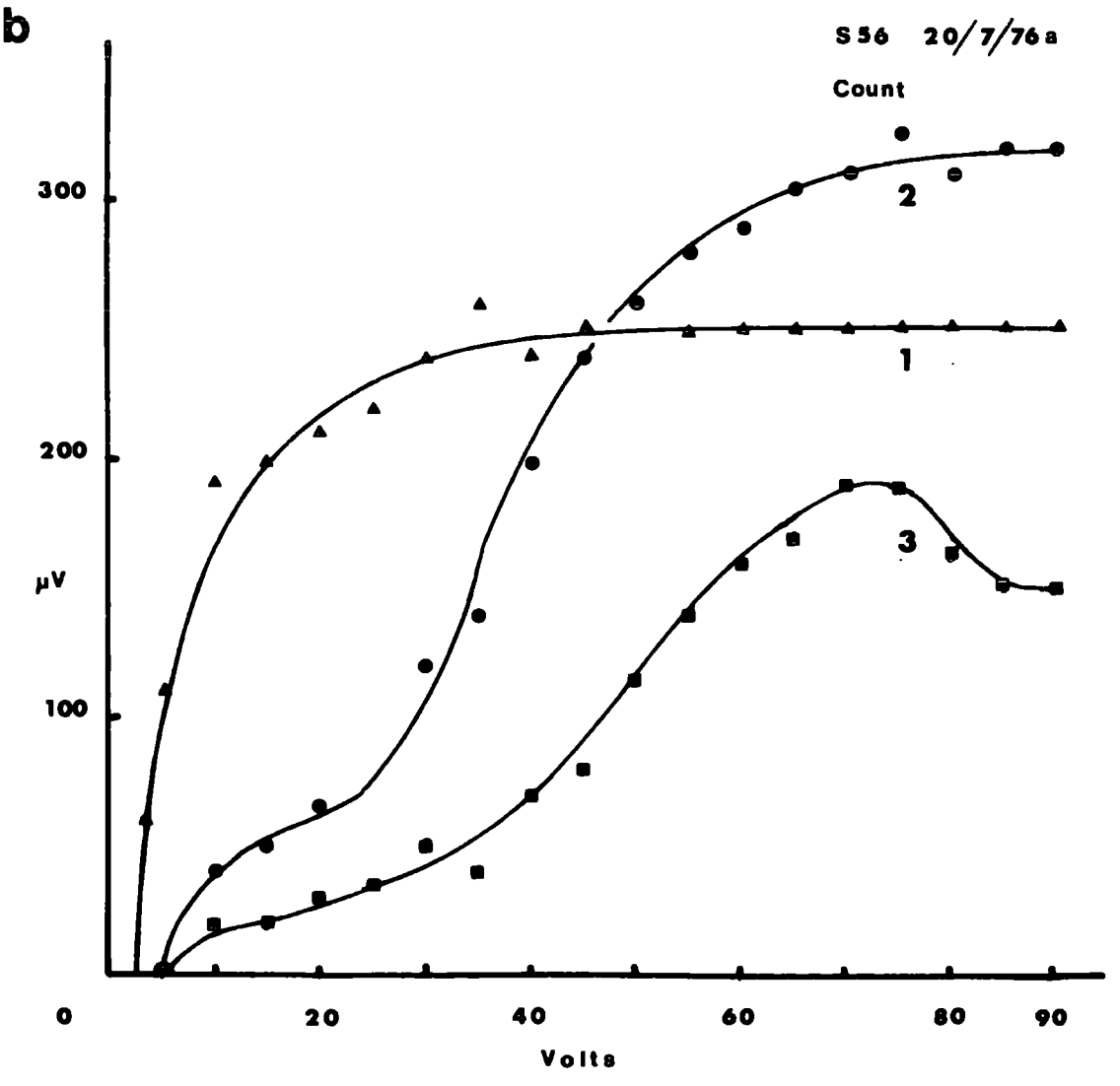
b
S 56 20/7/76 a
Count
300
200
100
µV
1
2
3
0
20
40
60
80
90
Volts

but no further increase can be produced by stimuli greater than about 40 V. At a stimulus of 10 V, the second wave appears. The responses of these two waves initially increase and then level off. At higher stimulus intensities (e.g. 30 V) a third longer latency wave is present, which at even higher intensities (greater than 75 Volts) decreases, as in the Stage 54 nerve (fig. 3:6). There is a possible indication of a very long latency fourth wave in the CAP's produced by 80 V and 90 V stimuli (fig. 3:7 a), the conduction velocity of which is 0.1 $m/sec.^{-1}$ The latencies of the three prominent waves indicate conduction velocities of 1.27, 0.22 and 0.16 $m/sec.^{-1}$

Stage 58

The CAP recorded from a Stage 58 tadpole comprises four waves (fig. 3:8 a). The first wave has a conduction velocity of 1.43 m/sec^{-1}, and the amplitude rises quickly in response to increased stimuli up to 10 V. Thereafter the amplitude of the response appears to increase for all increments in stimulus intensity. This however is a consequence of the increasing stimulus artifact which is superimposed on this wave (fig. 3:8 a, b). The second wave is the most prominent and first appears in response to a 20 V stimulus. Its amplitude steadily increases with increasing stimulus intensity. The third wave first appears at a stimulus of 30 V, and the fourth wave at 50 V. The second

Fig. 3.8: Compound action potentials in a stage 58 tadpole optic nerve.

(a) Representative waveforms produced with increasing stimulus voltages (values beneath each record). At this stage of development four waves are present, separated in time by their differing conduction velocities and hence latencies. The conduction velocities of these four waves are 1.43, 0.29, 0.2, and 0.1 m/sec.$^{-1}$

(b) Stimulus voltage - compound action potential amplitude graphs for the four waves illustrated in the records of a. The numbers refer to descending conduction velocity groups i.e. curve 1 is the group with the fastest conduction velocity (1.43 m/sec^{-1}), curve 4 is the group with the slowest conduction velocity (0.1 m/sec^{-1}).

3·8

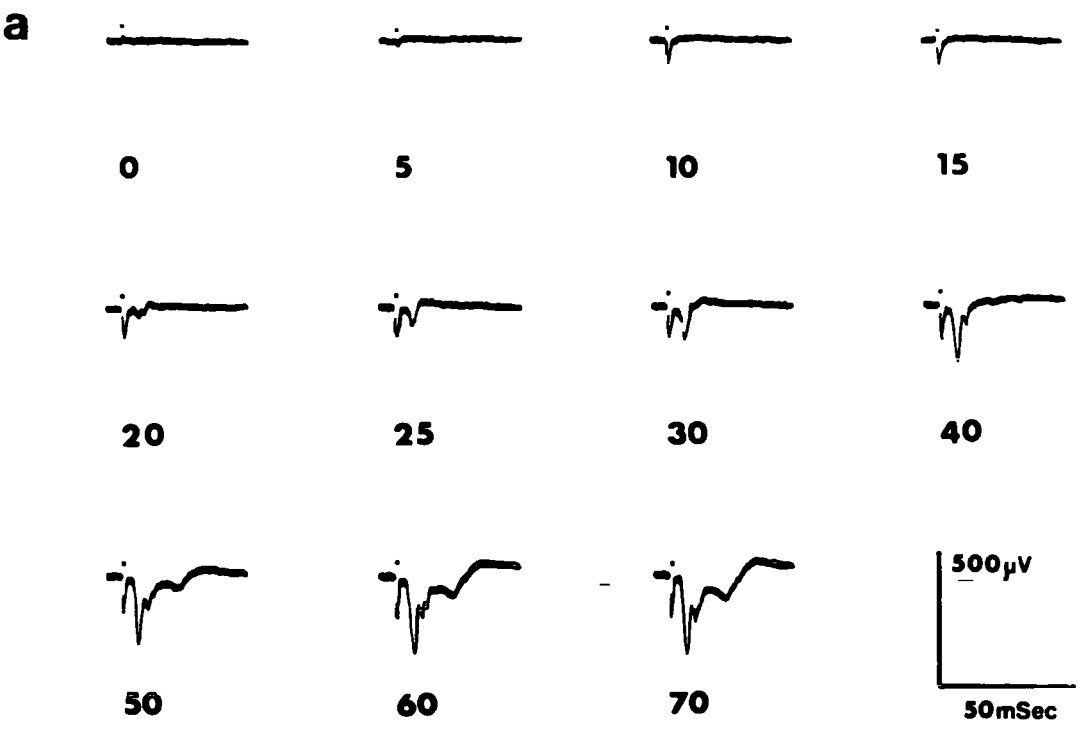
a
0
5
10
15
20
25
30
40
50
60
70
500μV
50mSec

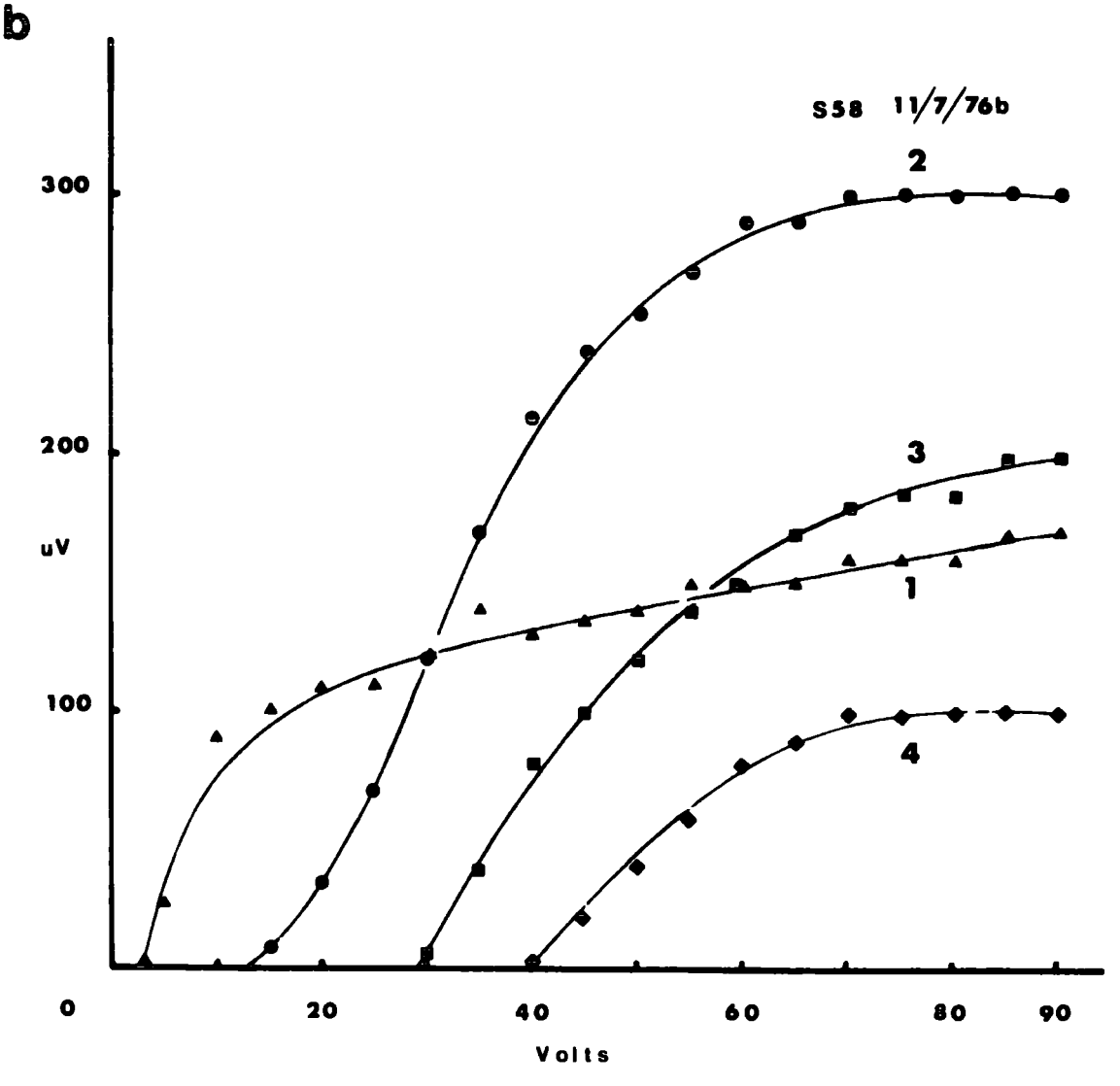
b
S58 11/7/76b
2
3
1
4
300
200
100
uV
0
20
40
60
80
90
Volts

and fourth waves produce maximal responses to a 75 V stimulus, whereas the maximal response of the third wave occurs at about 85 V. The conduction velocities of the second, third and fourth waves are 0.29, 0.2 and 0.1 m/sec^{-1} respectively. The fourth wave may be identified with the fourth wave from the Stage 56 tadpole CAP. The conduction velocity (0.1 m/sec^{-1}) is very low for a vertebrate axon, and it is difficult to ascribe it to a particular group of fibres.

Stage 60

The responses recorded from a Stage 60 (fig. 3:9 a) optic nerve are less complex than those recorded from a Stage 58 nerve (fig. 3:8 a). At Stage 60, two principal waves are present, with an inflexion on the second of these waves. The first wave has typical response characteristics to a low stimulus intensity (fig. 3:9 b) with a stimulus of 1 V being sufficient to evoke a response. Typically, on further increase of the stimulus intensity the response rises sharply to become maximal at about 10 V (fig. 3:9 a, b). The second wave is evoked by a stimulus of 12 V and increases in amplitude up to an intensity of 35 V when it becomes maximal. However, at 20 V a small inflexion is observed on the falling phase of the second wave which increases with increasing stimulus intensity and becomes maximal at about 40 V. The conduction velocities of these three waves, calculated from their latencies are 1.63, 0.27 and 0.19 m/sec^{-1} respectively.

Fig. 3.9: Compound action potentials in a stage 60 tadpole optic nerve.

(a) Representative waveforms evoked by a series of increasing stimulus voltages (stimulus voltage beneath each record). In this nerve only three clearly distinct conduction velocity groups are present (1.63, 0.27 and 0.19 m/sec).

(b) Stimulus voltage - compound action potential amplitude curves of the waves illustrated in a. The curves are numbered in order of their latencies (curve 1 is the shortest latency wave, curve 3 is the longest latency wave). This nerve was fixed after the records were taken and used for fibre diameter and number counts.

3·9

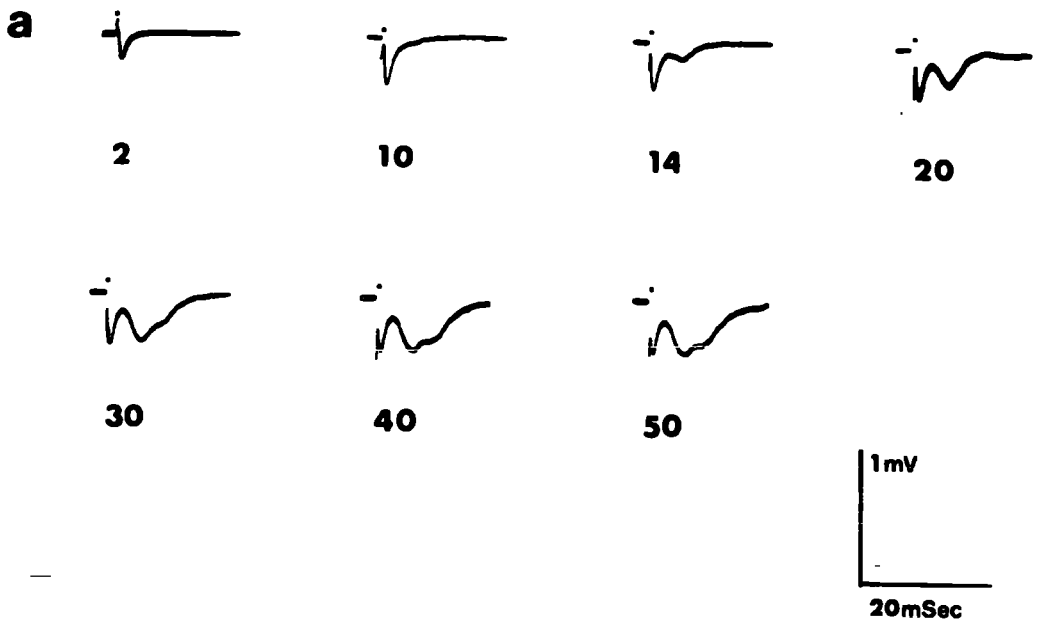
a
2
10
14
20
30
40
50
1mV
20mSec

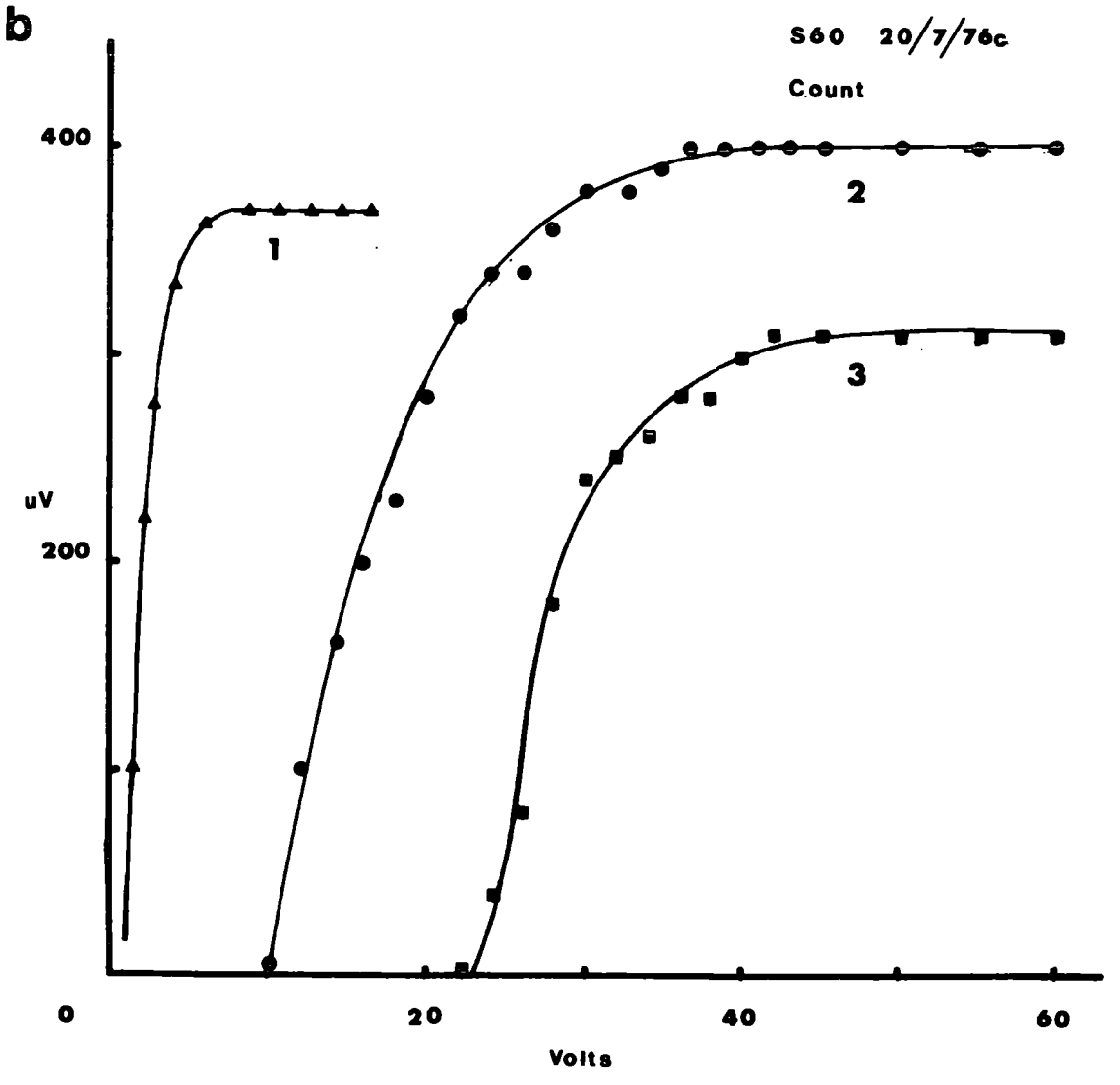
b
S60 20/7/76c
Count
400
uV
200
0
20
40
60
Volts
1
2
3

Stage 66

At the end of metamorphic climax (Stage 66), the CAP consists of two waves (fig. 3:10 a). The shortest latency wave appears at a stimulus intensity of 4 V. For small increments in stimulus intensity, the amplitude of the wave rises dramatically to become maximal at 15 V (fig. 3:10 a, b). At 13 V, a second wave, which is the more prominent of the two waves, emerges and initially the incremental increase in amplitude, with increasing stimulus intensity, is small. However, above an intensity of 20 V the amplitude of the evoked wave increases rapidly until it becomes maximal at 50 V. The conduction velocities are 1.13 m/sec^{-1} and 0.25 m/sec^{-1} for the two waves. It should be noted that in figure 3:10 a the first evoked wave becomes increasingly affected by the artifact above a 20 V stimulus and is completely lost at 40 V.

Juvenile Toads

The optic nerves of toads, up to the age of two months postmetamorphosis, produce essentially the same pattern of responses depicted for a Stage 66 individual (fig. 3:10). After the age of six months responses are typically adult. However, between these two ages either two or three waves can be evoked in response to electrical stimulation.

Fig. 3.10: Compound action potentials in a stage 66 optic nerve.

(a) Representative waveforms recorded in response to a series of increasing stimulus voltages (stimulus voltage indicated beneath each record). In this metamorphic animal only two waves were evoked in the optic nerve. The conduction velocities of these two waves are 1.13 and 0.25 m/sec.$^{-1}$

(b) Stimulus voltage - compound action potential amplitude curves of the two waves illustrated in a. Curve 1 (solid triangles) is the short latency, low amplitude wave whose conduction velocity is 1.13 m/sec.$^{-1}$ Curve 2 (solid circles) is the longer latency, greater amplitude wave whose conduction velocity is 0.25 m/sec.$^{-1}$

3·10

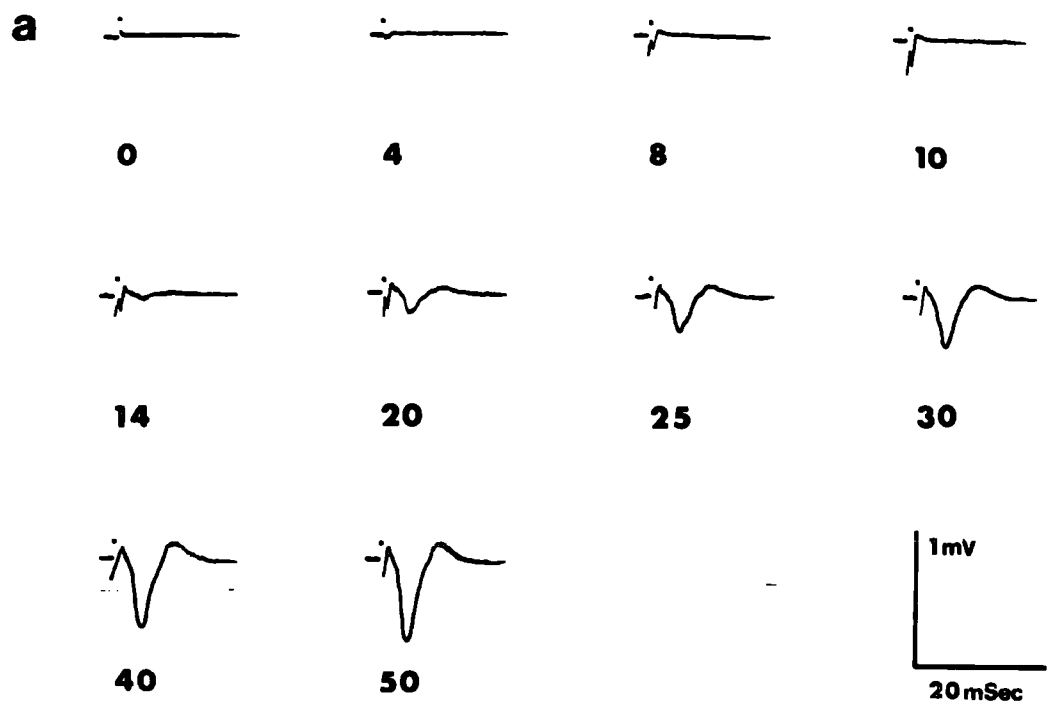
a
0
4
8
10
14
20
25
30
40
50
1mV
20mSec

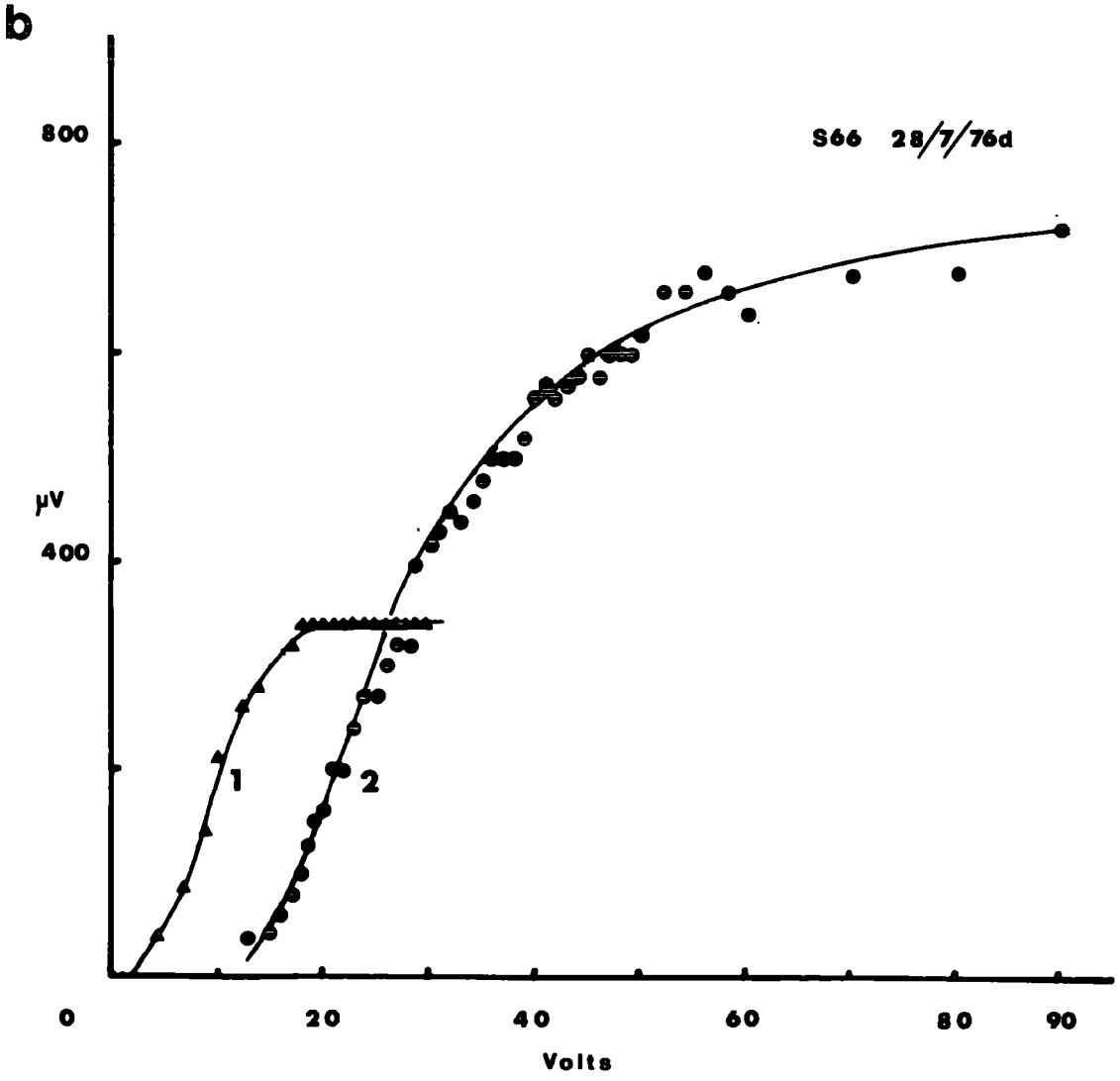
b
S66 28/7/76d
800
μV
400
0
20
40
60
80
90
Volts
1
2

The results obtained from all the physiological experiments carried out on the optic nerves of tadpole and adult Xenopus are shown diagrammatically in figure 3:11. It is apparent that there are two groups of conduction velocities which can be recorded in tadpole nerves. The responses in the lower group can be recorded from the youngest animals studied and are present throughout life. This group is continuous with the u_2 wave of the adult, with conduction velocities falling typically in the range 0.15 - 0.3 m/sec.$^{-1}$

The group with conduction velocities of about 1.2 m/sec is probably homologous with the m_2 fibre group of the adult. It is interesting to note that the CAP wave with a conduction velocity of 1.2 m/sec^{-1} appears at Stage 54 although there is no evidence for conduction velocities between 0.2 and 1.2 m/sec.$^{-1}$

At Stage 66, a group with conduction velocities about 0.6 m/sec^{-1} appears, which can probably be identified with the group in the adult nerve whose conduction velocity is 0.71 m/sec.$^{-1}$

It is clear from figure 3:10 that in the tadpole optic nerve there are no values which are comparable to the mean conduction velocity of 2.68 m/sec^{-1} found in the adult Xenopus nerve. In the two nerves from a Stage 55

Fig. 3.11: Collected data for the conduction velocity groups present in various stages of developing optic nerves. In tadpoles younger than stage 54 only one low conduction velocity group is present (0.15 -0.3 m/sec^{-1} solid circles). This low conduction velocity group can be recorded in the optic nerve throughout tadpole and adult life. At stage 54 a second group of fibres (solid triangles) with a conduction velocity of 1.2 m/sec^{-1} appears. In subsequent tadpole stages and in adults this group of fibres is a constant feature. In stage 66, and adult animals a third conduction velocity group is present (conduction velocity 0.6-0.7 m/sec^{-1} open circles). In the adult animal, in addition to the three groups mentioned above, a fourth short latency group can be recorded (conduction velocity 2.68 m/sec^{-1}). At stage 55 an intermediate conduction velocity of 2.68 m/sec^{-1} (open circle) is present, whereas the conduction velocity group (1.2 m/sec^{-1}) common to ages 54 to adult animals is absent. The arrows at stages 56 and 57 indicate that two values for the low conduction velocity group have been measured, this is a reflection of the fact that in the nerves from these stages a number of independent waves with similar long latencies can be measured (see text).

3·11

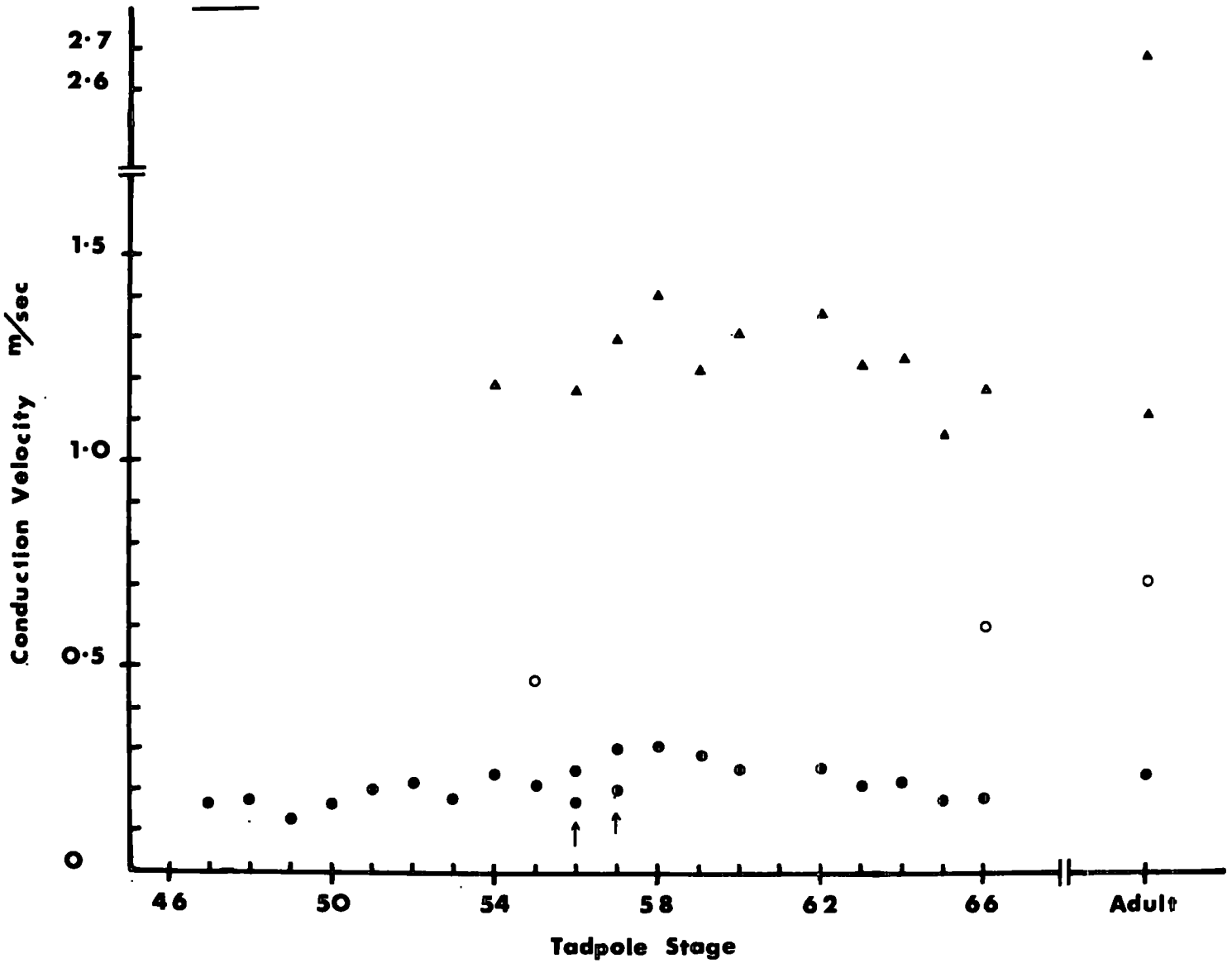
2·7
2·6
1·5
1·0
0·5
0
Conduction Velocity m/sec
46
50
54
58
62
66
Adult
Tadpole Stage

tadpole an intermediate mean conduction velocity of 0.47 m/sec^{-1} was obtained. At Stages 56 and 57 two velocities are plotted for the fibre group (fig. 3:11) since at this time a number of independent waves could be differentiated and these waves fell into two groups having conduction velocities of about 0.2 and 0.3 $m/sec.^{-1}$

B. ELECTRON MICROSCOPY OF EXPERIMENTAL NERVES

After physiological experiments, 28 of the nerves used were prepared for electron microscopy, 14 of which were studied, five in detail. The general quality of the preservation was good, especially of the axons which could be seen to contain microtubules and microfilaments (fig. 3:12). Glial cell processes were absent in many cases and the extracellular space had increased. The glial cell illustrated (fig. 3:12) is an astrocyte, and although slightly damaged, its general appearance is normal, with an intact nucleus and processes containing microfilaments. Summarized in Table 3:1 are the morphological findings of the Stage 50, 56 and 60 optic nerves from which the electrophysiological results are given in section A above.

Fig. 3.12: Electron micrograph of a stage 56 tadpole experimental optic nerve.

The electron micrograph shows unmyelinated (U) and myelinated (A) fibres which contain microfilaments and microtubules. The myelinated fibres are surrounded by normal myelin (m). An astrocyte (AST) is evident. All these features appear to be essentially normal when compared with non-experimental nerves (e.g. Fig. 1.15), although in this figure the extracellular (ex) spaces have increased.

3·12

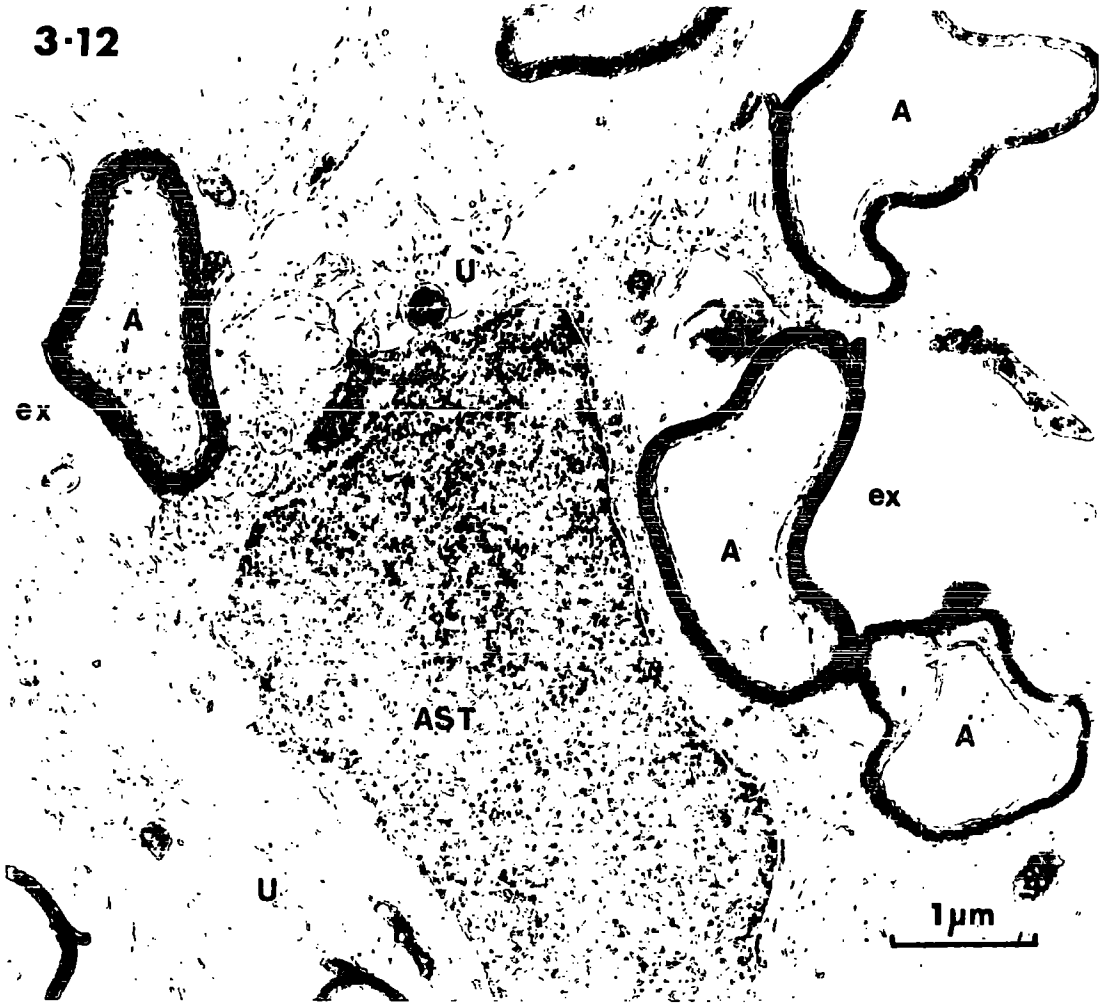

TABLE 3:1

A summary of the conduction velocities and the respective mean and modal diameters for both myelinated and unmyelinated fibres. The tabulated results are derived from three tadpole optic nerves at Stages 50, 56 and 60. The quality of the preservation of the Stage 56 nerve can be observed in figure 3:12.

TABLE 3:1

	Myelinated fibres			Unmyelinated fibres		
	Cv	Mean Diameter (μm)	Mode Diameter (μm)	Cv	Mean Diameter (μm)	Mode Diameter (μm)
Stage 50	-	n= 1.47 (97)	1.35	0.14	0.15	0.175
Stage 56	1.27	n= 1.61 (363)	1.35	0.22 0.16	0.20	0.15
Stage 60	1.63	n= 2.11 (367)	1.35	0.27 0.19	0.22	0.23

Myelinated fibres

All myelinated fibres from the three nerves shown in Table 3:1 have similar fibre diameter distributions with the modal values the same at 1.35 μm. However, the mean values are somewhat different, being 1.47 μm at Stage 50, 1.61 μm at Stage 56 and 2.11 μm at Stage 60. These values indicate that, while the populations have similar distributions, the size of the myelinated fibres increases with age. Compound action potentials attributable to the myelinated fibres could not be recorded in the nerve from a Stage 50 tadpole. However, waves elicited from myelinated fibres were evident in the recordings from the optic nerve of Stage 56 and Stage 60 animals and the latency of the peaks of these waves indicate conduction velocities of 1.27 and 1.63 m/sec^{-1} respectively.

Unmyelinated fibres

Table 3:1 also contains data concerning the unmyelinated fibres in the same Stage 50, 56 and 60 nerves mentioned above. The modes of the fibre diameter distributions are variable, with values of 0.175 μm at Stage 50, 0.15 μm at Stage 56 and 0.23 μm at Stage 60. The mean values of the fibre populations are less erratic, being 0.15 μm at Stage 50, 0.20 μm at Stage 56 and 0.22 μm at Stage 60, which indicate a trend of increasing fibre size during development.

The conduction velocities of the unmyelinated fibre groups in the developmental series were somewhat more variable. At Stage 50, there is a single wave and the latency of the peak indicates a conduction velocity of 0.14 $m/sec.^{-1}$ At Stages 56 and 60, two clearly discernable waves are present, the peaks of which indicate conduction velocities of 0.22 and 0.16 m/sec^{-1} for the Stage 56 nerve and 0.27 and 0.19 m/sec^{-1} for the Stage 60 nerve.

DISCUSSION

Similar results were obtained in response to electrical stimulation of the optic nerve of a particular aged individual, whether the stimulus was applied intraocularly and recorded intracranially, or whether the nerve was an isolated preparation. The variations observed between preparations were not associated with one particular recording situation, and may be due to a number of reasons. Inaccuracies may occur in the measurement of the length of the optic nerve, although for tadpole nerves the interelectrode distance could be measured to within an accuracy of 50 μm. In some cases a shift in the latency of the peak of the CAP was observed with increasing stimulus intensities. It is unknown whether this is due to differential excitability characteristics of the population of fibres under study or whether it indicates a shift in the site of action potential initiation. If it is the latter case, the conduction distance will be less than the interelectrode distance and hence the conduction velocity will be overestimated. Inaccuracies of this nature diminish with increasing lengths of the nerves used for study.

Inaccuracies may arise after the nerve has been cut to permit entry into the suction electrodes. After cutting, the nerve may shorten or there could be a possible retraction of fibres, especially if they are held under a slight tension in the animal. If this is the case, the conduction velocity will be underestimated. One obvious disadvantage encountered in Xenopus tadpoles was the naturally occurring change in length of the nerve during maturation. At Stage 47, the nerve is of the order of 2 to 2.5 mm in length and may increase to 7 mm at Stages 57 to 58, after which it shortens again. Although a complete description of the CAP can be given at all stages of development, comparison between different stages is difficult. The increased length at Stages 57 to 58, in comparison to Stages 47 and 66, enables greater temporal segregation of the CAP into a number of waves. On account of this it is not known whether the presence of small minor peaks at Stages 56 and 58 (figs. 2:6 a and 2:7 a) are due to morphological changes occurring in the nerve at that time or due to the more evident temporal separation of the components.

It is very difficult to compare stimulus strength/response characteristics quantitatively because the stimulating and recording situations differ slightly between preparations. However, it is possible to compare them qualitatively on the basis of the order in which the waves appear, their relative prominance and conduction velocities.

There is much confusion in the literature concerning the conduction velocities of ganglion cell axons in the anuran optic nerve, and this confusion is compounded by the different criteria set for latencies, the different methods of measurement and the different species used (see Grüsser and Grüsser-Cornehls, 1976). A variety of findings have been made with values ranging from 12 to 0.2 m/sec^{-1} in four ranid anurans. The results which are most similar to the present ones are those of Tasaki (1970) who quotes conduction velocities of 3.3, 1.4 and 0.24 m/sec^{-1} for Rana catesbeiana. However, Chung, Bliss and Keating (1974) quote minimum values of 6, 2, 0.5 and 0.2 m/sec^{-1} for the four waves in the optic nerve of Rana pipiens.

From tadpole Stage 54, two main conduction velocity groups are present in Xenopus, with values of about 0.2 and 1.2 m/sec^{-1}. Correlating the data from the CAP's and the fibre diameter distributions is not easy, except in that the two groups of conduction velocities at 1.2 and 0.2 m/sec^{-1} can be associated with the myelinated and unmyelinated fibres respectively. The fibres which are excited by the lowest stimulus intensity and also have the shortest latency would be expected to be myelinated, since these are the largest fibres present (Katz, 1966). The fact that the fibres which have a conduction velocity of 1.2 m/sec^{-1} in the adult are myelinated (Chapter 5) also gives grounds for surmising that the fastest conducting group in the tadpole after Stage 54 is myelinated.

Vertebrate unmyelinated fibres commonly conduct impulses at 0.2 to 0.5 m/sec.$^{-1}$ Eccles et al (1966), Freeman (1969), Kitae et al (1969), Nicholson and Llinas (1971), Shepherd (1974), Vanegas and Williams (1977) and other workers studying the optic nerve of anurans have encountered conduction velocities which fall within these values (Peretz, 1961; ter Keurs, 1970; Tasaki, 1970; Chung, Bliss and Keating, 1974). Comparisons are made more difficult by the presence of the four conduction velocity groups obtained from an adult optic nerve, but of only two population fibre sizes of myelinated and unmyelinated fibres. In the two populations of over 1,000 and 2,000 measurements, no subpopulations were apparent morphologically (see Chapter 2). The only possibility which remains is that, within these two groups, four groups of fibres with different excitability and conduction characteristics are present.

From figure 3:11, it is clear that the myelinated fibre response starts at Stage 54. The fast component of the CAP was recorded from all five Stage 54 nerves studied. In the Stage 50 nerve, which was studied by electron microscopy, 97 myelinated fibres were present although no response could be recorded from them. It is possible that these fibres are not capable of supporting action potential propagation, although this is unlikely, since much smaller unmyelinated fibres carry action

potentials readily. Alternatively, there are not enough myelinated fibres present to register a response with the present experimental methods. It is unlikely that the numbers of myelinated fibres present in this nerve are unusually high, since a count on another Stage 50 optic nerve produced 11 myelinated fibres, and Wilson (1971) in her study counted 30 and 72 myelinated fibres in two Stage 52 nerves. The recording of responses from Stage 54 myelinated fibres may be due to one of two possibilities, that it is at this stage that they start to conduct action potentials, or that they are present in sufficient numbers to register a response. The latter is the more probable, since myelinated fibres usually function as unmyelinated fibres before developing a myelin sheath (Rager, 1976 a, b). However, this does not take into account the absence of a fast conducting group in the Stage 55 optic nerve studied. The responses recorded at this stage included a wave with an intermediate conduction velocity of 0.47 $m/sec.^{-1}$ The two Stage 55 nerves used for recording CAP's were obtained from the same animal. It is unlikely that this velocity is artificially low because of shrinkage of the nerve, because the unmyelinated fibre conduction velocities were as expected at 0.21 and 0.22 $m/sec.^{-1}$ Alternatively, the wave represents a genuine class of fibres which are possibly in the process of forming myelin or are only myelinated for a part of their

length, which would produce a mixture of saltatory and continuous conduction. From Stage 56 onwards, conduction velocity groups of about 1.2 m/sec^{-1} were present in all preparations studied.

At Stage 66, a response can occasionally be recorded whose conduction velocity is 0.6 m/sec^{-1}, although this response is absent in figure 3:9 a. This group may be a class of fibre which "matures" physiologically from the other fibres of the u_2 group at this time, by developing lower threshold excitability and increased conduction velocity characteristics. This group is probably homologous with the u_1 group found in the adult optic nerve which has a conduction velocity of 0.71 m/sec^{-1}. The fast (m_1) conduction velocity group (2.75 m/sec^{-1}) of the adult optic nerve can only be recorded in animals of six months of age or more. However, its absence in recordings from tadpoles is not necessarily an indication that the fibres contributing to the wave are only present in the adult. In recording CAP's, occasionally very fast responses (up to about 3 m/sec^{-1}) could be recorded, but could not be maintained for a sufficient length of time to study them in detail. The shortness of the nerves from which recordings were taken, especially in animals just prior to and just after metamorphosis, precluded the recording of fast conducting fibres. For example the length of some nerves from metamorphic animals from which recordings were made was only 800 μm.

The presence of waves with long latencies which indicate conduction velocities below 0.2 m/sec^{-1} at Stages 54, 56 and 58 for example (figs. 3:5 a, 3:7 a and 3:8 a), suggest that these fibres may be small and immature. Evidence for this was obtained by using repetitive stimuli. Whilst the u_2 group of the adult and most tadpoles could sustain a response at a stimulus frequency of up to 10 to 50 Hz, these long latency groups could only be stimulated to give comparable responses each time at a frequency of 0.5 to 1 Hz. The long latency and susceptibility of impulse propagation suggest that these fibres are of very small diameter.

When the fibre diameter data for the Stage 50 and Stage 60 nerves are compared with their non-experimental counterparts, it can be seen that the myelinated fibres have similar mean values, whereas the unmyelinated fibres are approximately one third smaller in the case of the experimental nerves.

The shrinkage effects obtained with the material prepared for electron microscopy may cause some anxiety about the effects of using preparations in Niu-Twitty solution. However, it is more likely that the shrinkage of the unmyelinated fibres is caused by the fixation and dehydration of the tissue for electron microscopy. Since the results of experiments carried out on <u>in situ</u> and isolated preparations were similar, and the Niu-Twitty solution only came into contact with the intracranial

portion of the optic nerve in the *in situ* preparations, it is justified to regard the Niu-Twitty solution as having no effect on the physiology of the nerve.

However, no rigorous control experiments were carried out to explore this possibility further.

The ability of myelinated fibres in the optic nerve to conduct impulses at Stage 54 is of particular interest since a postsynaptic component derived from myelinated fibres cannot be recorded in the optic tectum prior to Stage 59 (Chapter 5; Chung, Keating and Bliss (1974)). This implies that these fibres either project elsewhere in the brain or are synaptically non-functional (see general discussion). Another interesting finding was the absence of any overt effect of the aberrant myelin reported to be present at metamorphosis in Chapter 1.